



International Agreement Report

Assessment of RELAP5/MOD2 Using LOCE Large Break Loss-of-Coolant Experiment L2-5

Prepared by
Lainsu Kao, Kuo-Shing Liang, Jeng-Lang Chiou,
Lih-Yih Liao, Song-Feng Wang, Yi-Bin Chen

Institute of Nuclear Energy Research
P.O. Box 3, Lung-Tan 32500
Taiwan, Republic of China

Office of Nuclear Regulatory Research
U.S. Nuclear Regulatory Commission
Washington, DC 20555

April 1992

Prepared as part of
The Agreement on Research Participation and Technical Exchange
under the International Thermal-Hydraulic Code Assessment
and Application Program (ICAP)

Published by
U.S. Nuclear Regulatory Commission

920605C059 920430
PDR NUREG
IA-0045 R PDR

NOTICE

This report was prepared under an international cooperative agreement for the exchange of technical information.* Neither the United States Government nor any agency thereof, or any of their employees, makes any warranty, expressed or implied, or assumes any legal liability or responsibility for any third party's use, or the results of such use, of any information, apparatus product or process disclosed in this report, or represents that its use by such third party would not infringe privately owned rights.

Available from

Superintendent of Documents
U.S. Government Printing Office
P.O. Box 37082
Washington, D.C. 20013-7082

and

National Technical Information Service
Springfield, VA 22161



International Agreement Report

Assessment of RELAP5/MOD2 Using LOCE Large Break Loss-of-Coolant Experiment L2-5

Prepared by
Lainsu Kao, Kuo-Shing Liang, Jeng-Lang Chiou,
Lih-Yih Liao, Song-Feng Wang, Yi-Bin Chen

Institute of Nuclear Energy Research
P.O. Box 3, Lung-Tan 32500
Taiwan, Republic of China

Office of Nuclear Regulatory Research
U.S. Nuclear Regulatory Commission
Washington, DC 20555

April 1992

Prepared as part of
The Agreement on Research Participation and Technical Exchange
under the International Thermal-Hydraulic Code Assessment
and Application Program (ICAP)

Published by
U.S. Nuclear Regulatory Commission

NOTICE

This report documents work performed under the sponsorship of the Institute of Nuclear Energy Research of Taiwan. The information in this report has been provided to the USNRC under the terms of an information exchange agreement, Cooperative Program on Thermal-Hydraulic Code Assessment between the Coordination Council for North American Affairs (CCNAA) and the American Institute in Taiwan (AIT), March 22, 1986. Taiwan has consented to the publication of this report as a USNRC document in order that it may receive the widest possible circulation among the reactor safety community. Neither the United States Government nor Taiwan or any agency thereof, or any of their employees, makes any warranty, expressed or implied, or assumes any legal liability of responsibility for any third party's use, or the results of such use, or any information, apparatus, product or process disclosed in this report, or represents that its use by such third party would not infringe privately owned rights.

ABSTRACT

Comprehensive analysis with RELAP5/MOD2 is performed to predict the LOFT transient thermal-hydraulic responses for the LOCE L2-5 test. Experiment L2-5 is planned to simulate a hypothetical LOCA which results from a 200% double-ended offset shear break in a cold-leg of a typical pressurized water reactor. The test simulation begins with break initiation and subsequent blowdown, and continues through lower plenum refill, core reflood, and terminates with corewide quench. The nominal best estimate calculation results indicate that the cladding temperature continuously increases during blowdown phase without an early fuel-rod rewet (blowdown quench). A peak cladding temperature of 1,112 K, which is very close to the experimental data, is calculated at 7.0 s, and fuel rods are predicted to be quenched at 57 s after the break initiation. Sensitivity analyses of the test simulation with respect to various code input uncertainties, including broken loop initial temperature, cross-flow junction, discharge coefficient, accumulator condition, reflood fine mesh number, form loss coefficient, fuel gap dimension, and reflood option are performed to investigate their impacts on the calculation results. Scenario study on the pump behavior is analyzed to see whether the blowdown quench could be resulted from the RELAP5/MOD2 model. The effect of the uncertainty of Biasi CHF on the cladding temperature response is also studied.

SUMMARY

This report documents the results and conclusions of the RELAP5/MOD2 code assessment in the analysis of LOCE test L2-5. Sensitivity studies of the L2-5 simulation with respect to various modeling options are performed as well to investigate their impacts on the calculation results.

LOCE L2-5 is performed to simulate a hypothetical LOCA which results from a 200% double-ended offset shear break in the cold-leg of a typical pressurized water reactor. A specific purpose of L2-5 test is to establish conditions which will result in a large break blowdown without early quench that occurred during previous large break LOCA tests. RELAP5/MOD2 is an advanced, one-dimensional, two fluid, six-equation, thermal nonequilibrium reactor transient and accident analysis program. The objective of this assessment study is to provide systematic assessment of the RELAP5/MOD2 code relative to code development, code improvement, and the enhancement of user guidelines.

In this study, the test simulations using RELAP5/MOD2 begin with break initiation and subsequent blowdown, and continue through lower plenum refill, core reflood, and terminate with corewide quench. Major events and their timings of the large break LOCA test L2-5 are well predicted by the RELAP5/MOD2 model. According to the hydraulic process (pump behavior) set up in L2-5, the RELAP5/MOD2 calculation gives no early quench phenomenon. Important parameters, such as pressure, break flow,

and cladding temperature, are calculated with reasonable agreement in the comparison to the test data. Noticed differences between the calculation results and the test data including hot-leg break flow at initial period, cladding temperature during reflood, pressurizer pressure response, cladding temperature responses at upper and lower elevations of the fuel rod, fuel quench temperature etc., are discussed with possible reasons in this report. On the other hand, the calculated peak cladding temperature (the most critical parameter concerned in a large break LOCA) of 1,112 K is in excellent agreement with the test data of 1,077 K.

Sensitivity analyses of the test simulation with respect to various code input uncertainties, including broken loop initial temperature, cross-flow junction, discharge coefficient, accumulator condition, reflood fine mesh number, form loss coefficient, fuel gap dimension, and reflood option are performed to investigate their impacts on the calculation results. Scenario study on the pump behavior is analyzed to see whether the blowdown quench could be resulted from the RELAP5/MOD2 model. The effect of the uncertainty of Biasi CHF on the cladding temperature response is also studied.

Calculated PCTs are quite insensitive to the selected parameters and their variations in the sensitivity studies except in the cases of the fuel gap dimension and the CHF correlation. With the doubled fuel gap dimension used in the code calculation,

the resulted PCT is increased by 130 K in the comparison to that of the base case. In the sensitivity study of the Biasi CHF correlation, the reduction of the CHF does not yield improvement in the cladding temperature predictions at upper and lower elevations of the fuel rod. At the hottest location, significant reduction of the time-to-CHF is calculated with the reduction of the CHF, which leads to an overestimation of the PCT by more than 500 K.

From the results of the scenario study, it is learned that the present RELAP5/MOD2 model does not calculate the blowdown quench phenomena even at the assumption of connected flywheel system during the pump coastdown.

Excessive precursory cooling of the fuel rod is calculated during the reflood period. It is seen that discontinuities of the cladding surface heat flux and the vapor temperature are calculated at the moment of the reflood model actuation. Without using the reflood model in RELAP5/MOD2, the calculated cladding temperatures during the reflood period are in good agreement with the test data. These results may indicate that either the criteria used in RELAP5/MOD2 for the actuation of the reflood model calculation are inadequate or the heat transfer package in the reflood model is improper.

CONTENT

ABSTRACT	iii
SUMMARY	v
1. INTRODUCTION	1
2. FACILITY AND TEST DESCRIPTIONS	2
2.1 LOFT Facility	2
2.2 Experiment L2-5	9
3. CODE AND MODEL DESCRIPTIONS	10
3.1 Computer Code	10
3.2 Model Descriptions	11
3.3 Initialization Process	16
4. RESULTS AND DISCUSSIONS	17
4.1 Base Case Analysis	18
4.2 Sensitivity Studies	33
5. RUN STATISTICS	42
6. CONCLUSIONS	43
REFERENCE	133
APPENDIX	A-1

LIST OF TABLES

	<u>Page</u>
Table 3.1 Initial Conditions of LOCE Test L2-5	48
Table 4.1 Sequence of Events in LOCE Test L2-5	49
Table 4.2 Cases Analyzed in the Sensitivity Study of the LOCE Test L2-5 Simulation	50
Table 5.1 Run Statistics of the LOCE Test L2-5 Simulation	51

LIST OF FIGURES

	<u>Page</u>	
Figure 1.1	LOFT Facility Major Components	52
Figure 1.2	LOFT Facility Core Arrangement	53
Figure 3.1	RELAP5/MOD2-LOFT Large Break Model Nodalization for Experiment L2-5	54
Figure 4.1	Comparison between the Calculated and Measured Broken Loop Cold-Leg Pressures of Test L2-5	55
Figure 4.2	Comparison between the Calculated and Measured Pressurizer Pressures of Test L2-5	56
Figure 4.3	Comparison between the Calculated and Measured Pressurizer Water Levels of Test L2-5	57
Figure 4.4	Calculated Water Levels in Reactor Vessel of Test L2-5 Simulation	58
Figure 4.5	Calculated ECC Flow Rates of Test L2-5 Simulation	59
Figure 4.6	Comparison between the Calculated and Measured Cold-Leg Break Flow Rates of Test L2-5	60
Figure 4.7	Comparison between the Calculated and Measured Hot-Leg Break Flow Rates of Test L2-5	61
Figure 4.8	Calculated Void Fractions Upstream the Break Junctions of Test L2-5 Simulation	62
Figure 4.9	Comparison between the Calculated and Measured Intact Loop Cold-Leg Flow Rates of Test L2-5	63
Figure 4.10	Comparison between the Calculated and Measured Intact Loop Hot-Leg Flow Rates of Test L2-5	64

LIST OF FIGURES (Cont.)

		<u>Page</u>
Figure 4.11	Comparison between the Calculated and Measured Intact Loop Hot-Leg Flow Rates During the Blowdown Period of Test L2-5	65
Figure 4.12	Calculated Core Flow Rates During the Blowdown Period of Test L2-5 Simulation	66
Figure 4.13	Calculated Core Flow Rates of Test L2-5 Simulation	67
Figure 4.14	Calculated Cladding Temperatures at Hot Channel Hot Rod of Test L2-5 Simulation	68
Figure 4.15	Comparison between the Calculated and Measured Cladding Temperatures of Test L2-5	69
Figure 4.16	Comparison between the Calculated and Measured Upper Plenum Fluid Temperatures of Test L2-5	70
Figure 4.17	Comparison between the Calculated and Measured Intact Loop Hot-Leg Fluid Temperatures of Test L2-5	71
Figure 4.18	Comparison between the Calculated and Measured Broken Loop Hot-Leg Fluid Temperatures of Test L2-5	72
Figure 4.19	Comparison between the Calculated and Measured Intact Loop Cold-Leg Fluid Temperatures of Test L2-5	73
Figure 4.20	Calculated Fluid Temperatures in Upper Downcomer of Test L2-5 Simulation	74
Figure 4.21	Calculated Fluid Temperatures in Lower Downcomer of Test L2-5 Simulation	75
Figure 4.22	Comparison between the Calculated and Measured Downcomer (4.8 m from RV Bottom) Fluid Temperatures of Test L2-5	76
Figure 4.23	Comparison between the Calculated and Measured Downcomer (2.98 m from RV Bottom) Fluid Temperatures of Test L2-5	77

LIST OF FIGURES (Cont.)

		<u>Page</u>
Figure 4.24	Comparison between the Calculated and Measured Downcomer (0.74 m from RV Bottom) Fluid Temperatures of Test L2-5	78
Figure 4.25	Comparison between the Calculated and Measured Downcomer (0.54 m from RV Bottom) Fluid Temperatures of Test L2-5	79
Figure 4.26	Comparison between the Calculated and Measured Broken Loop Cold-Leg Fluid Temperatures of Test L2-5	80
Figure 4.27	Comparison between the Calculated and Measured Intact Loop Cold-Leg Densities of Test L2-5	81
Figure 4.28	Comparison between the Calculated and Measured Intact Loop Cold-Leg Densities of Test L2-5	82
Figure 4.29	Comparison between the Calculated and Measured Broken Loop Cold-Leg Densities of Test L2-5	83
Figure 4.30	Calculated Flow Rates in Broken Loop Cold-Leg of Test L2-5 Simulation	84
Figure 4.31	Calculated Flow Rates in Reactor Vessel Near Broken Loop Cold-Leg of Test L2-5 Simulation	85
Figure 4.32	Comparison between Calculated Accumulator Flow Rates of the BASE and ACCUM50 Cases	86
Figure 4.33	Comparison between Calculated Water Levels in Core Region of the BASE and ACCUM50 Cases	87
Figure 4.34	Comparison between Calculated Water Levels in Downcomer Near Intact Loop of the BASE and ACCUM50 Cases	88
Figure 4.35	Comparison between Calculated Water Levels in Downcomer Near Broken Loop of the BASE and ACCUM50 Cases	89

LIST OF FIGURES (Cont.)

	<u>Page</u>
Figure 4.36 Comparison between Calculated Cold-Leg Break Flow Rates of the BASE and ACCUM50 Cases	90
Figure 4.37 Comparison between Calculated Broken Loop Cold-Leg Densities of the BASE and ACCUM50 Cases	91
Figure 4.38 Comparison between Calculated Cladding Temperatures at Various Axial Locations of the BASE and ACCUM50 Cases	92
Figure 4.39 Comparison between Calculated Cladding Temperatures at Hottest Location of the BASE and ACCUM50 Cases	93
Figure 4.40 Comparison between Calculated Hot-Leg Break Flow Rates of the BASE and BLHL-HT Cases	94
Figure 4.41 Comparison between Calculated Cold-Leg Break Flow Rates of the BASE and BLHL-HT Cases	95
Figure 4.42 Comparison between Calculated Cladding Temperatures at Various Axial Locations of the BASE and BLHL-HT Cases	96
Figure 4.43 Comparison between Calculated Cladding Temperatures at Hottest Location of the BASE and BLHL-HT Cases	97
Figure 4.44 Comparison between Calculated Hot-Leg Break Flow Rates of the BASE and BLHL-DC Cases	98
Figure 4.45 Comparison between Calculated Broken Loop Cold-Leg Pressures of the BASE and BLHL-DC Cases	99
Figure 4.46 Comparison between Calculated Cold-Leg Break Flow Rates of the BASE and BLHL-DC Cases	100
Figure 4.47 Comparison between Calculated Cladding Temperatures at Various Axial Locations of the BASE and BLHL-DC Cases	101

LIST OF FIGURES (Cont.)

	<u>Page</u>
Figure 4.60 Comparison between Calculated Cold-Leg Break Flow Rates of the BASE and MESH#32 Cases	114
Figure 4.61 Comparison between Calculated Cladding Temperatures at Various Axial Locations of the BASE and MESH#32 Cases	115
Figure 4.62 Comparison between Calculated Cladding Temperatures at Hottest Location of the BASE and MESH#32 Cases	116
Figure 4.63 Comparison between Calculated Radial Temperature Distributions in Fuel Rod of the BASE and FUEL-GAP Cases	117
Figure 4.64 Comparison between Calculated Cladding Temperatures at Various Axial Locations of the BASE and FUEL-GAP Cases	118
Figure 4.65 Comparison between Calculated Cladding Temperatures at Hottest Location of the BASE and FUEL-GAP Cases	119
Figure 4.66 Comparison between Calculated Hot-Leg Break Flow Rates of the BASE and FUEL-GAP Cases	120
Figure 4.67 Comparison between Calculated Cold-Leg Break Flow Rates of the BASE and FUEL-Gap Cases	121
Figure 4.68 Comparison between Calculated Intact Loop Cold-Leg Flow Rates of the BASE and PUMP-FW Cases	122
Figure 4.69 Comparison between Calculated Core Inlet Flow Rates of the BASE and PUMP-FW Cases	123
Figure 4.70 Comparison between Calculated Cladding Temperatures at Hottest Location of the BASE and PUMP-FW Cases	124
Figure 4.71 Comparison between Calculated Hot-Leg Brak Flow Rates of the BASE and PUMP-FW Cases	125
Figure 4.72 Comparison between Calculated Cold-Leg Break Flow Rates of the BASE and PUMP-FW Cases	126

LIST OF FIGURES (Cont.)

		<u>Page</u>
Figure 4.48	Comparison between Calculated Cladding Temperatures at Hottest Location of the BASE and BLHL-DC Cases	102
Figure 4.49	Comparison between Calculated Broken Loop Cold-Leg Pressures of the BASE and BLHL-5K Cases	103
Figure 4.50	Comparison between Calculated Pressurizer Pressures of the BASE and BLHL-5K Cases	104
Figure 4.51	Comparison between Calculated Hot-Leg Break Flow Rates of the BASE and BLHL-5K Cases	105
Figure 4.52	Comparison between Calculated Cold-Leg Break Flow Rates of the BASE and BLHL-5K Cases	106
Figure 4.53	Comparison between Calculated Cladding Temperatures at Various Axial Locations of the BASE and BLHL-5K Cases	107
Figure 4.54	Comparison between Calculated Cladding Temperatures at Hottest Location of the BASE and BLHL-5K Cases	108
Figure 4.55	Comparison between Calculated Hot-Leg Break Flow Rates of the BASE and PV-X-BL Cases	109
Figure 4.56	Comparison between Calculated Cold-Leg Break Flow Rates of the BASE and PV-X-BL Cases	110
Figure 4.57	Comparison between Cladding Temperatures at Various Axial Locations of the BASE and PV-X-BL Cases	111
Figure 4.58	Comparison between Cladding Temperatures at Hottest Location of the BASE and PV-X-BL Cases	112
Figure 4.59	Comparison between Calculated Hot-Leg Break Flow of the BASE and MESH#32 Cases	113

LIST OF FIGURES (Cont.)

		<u>Page</u>
Figure 4.73	Comparison between Calculated Cladding Temperatures at Axial Level 3 of the BASE and CHF*0.6 Cases	127
Figure 4.74	Comparison between Calculated Cladding Temperatures at Axial Level 4 of the BASE and CHF*0.6 Cases	128
Figure 4.75	Comparison between Calculated Cladding Temperatures at Axial Level 5 of the BASE and CHF*0.6 Cases	129
Figure 4.76	Comparison between Calculated Voids in Core Region of the BASE and NORFLOD Cases	130
Figure 4.77	Calculated Cladding Temperatures at Hot Channel Hot Rod of the NORFLOD Case	131
Figure 4.78	Comparison between Calculated Cladding Surface Heat Fluxes of the BASE and NORFLOD Cases	132
Figure 4.79	Comparison between Calculated Vapor Temperatures in Core Region of the BASE and NORFLOD Cases	133
Figure 4.80	Comparison between Calculated Cladding Temperatures at Axial Level 2 of the BASE and NORFLOD Cases	134
Figure 4.81	Comparison between Calculated Cladding Temperatures at Axial Level 4 of the BASE and NORFLOD Cases	135
Figure 4.82	Comparison between Calculated Cladding Temperatures at Axial Level 5 of the BASE and NORFLOD Cases	136

1. INTRODUCTION

The assessment study documented in this report contributes to the overall code assessment effort, which is coordinated within the International Code Assessment and Applications Program (ICAP) sponsored by the U.S. Nuclear Regulatory Commission (NRC). The objective of the ICAP is to provide qualitative assessment of the major thermal-hydraulic computer codes relative to code development, code improvement, and the enhancement of user guidelines. This report contains results from the best estimate experiment prediction analysis performed using the RELAP5/MOD2[1] Version 36.04 computer code to simulate the system thermal-hydraulic responses of the Loss-of-Fluid Test (LOFT) during Loss-of-Coolant Experiment (LOCE) L2-5.

LOCE L2-5, in conjunction with previously conducted LOCE L2-2 and L2-3, is intended to evaluate the system responses during a large break loss-of-coolant accident (LOCA). These tests are conducted to address conservatisms in licensing criteria defined in the U.S. code of Federal Regulations (10CFR50 Appendix K). Current licensing criteria limit fuel rod cladding temperatures to 1,477 K (2,200 F). For most plants limited by this criteria, the peak cladding temperature occurs during reflood portion of the licensing calculation. While there are other limits that determine the maximum power a plant can operate at, the majority of plants are limited by the LOCA analysis.

Experiment L2-5 uses nominally the same system configuration as the previously performed Experiment L2-3. The essential differences between L2-5 and L2-3 are the post-break pump operation and ECCS actuation times. Experiment L2-2 and L2-3 unexpectedly show that during blowdown phase (with pump left running), a surge of coolant through the core occurs when flow from the pumps exceeds flow out of the cold-leg break. This coolant surge caused an "early rewet" of the nuclear fuel rods, effectively halting the rapid increase in cladding temperature that is typically predicted to occur in large break LOCAs. One purpose of Experiment L2-5 is to establish conditions which will result in a large break blowdown without "rewet". Therefore, in Experiment L2-5, the primary coolant pumps (PCPs) are unpowered quickly and then coast down while disconnected from their flywheel system. Such a coastdown during Experiment L2-5 is nontypical since the LOFT pumps would normally coast down while connected to their flywheel system to simulate the normal coastdown of the PCPs in a commercial PWR. The reason of having this nontypical PCP coastdown is the intention of producing core hydraulic conditions which would most likely prevent the early fuel-rod rewet that occurred during Experiment L2-3.

A RELAP5/MOD2 model used in the simulation of Experiment L2-5 is developed for the base case study according to the information provided by the Idaho National Engineering Laboratory (INEL). These information include description of the LOFT

facility [2], L2-5 test conditions [3], RELAP5/MOD1 input deck [4], and data report [5]. Except the base case study, sensitivity analyses with respect to various code input uncertainties are also performed to investigate their impacts on the calculation results, and to provide information in setting user guidelines of the RELAP5/MOD2 code. Scenario study on the pump coastdown behavior and simple modification of the CHF correlation in the code are made as well. In these studies, the experiment simulations using RELAP5/MOD2 begin with break initiation and subsequent blowdown, and continue through lower plenum refill, core reflood, and terminate with corewide quench.

This report is organized as follows: section 2 gives brief descriptions of the test facility and conditions. The RELAP5/MOD2 model used to simulate the experiment is described in section 3. In section 4 the calculation results compared to the test data are presented and discussed. Computational efficiency of RELAP5/MOD2 is given in section 5. Finally, some conclusions obtained from this study are drawn in section 6. A listing of the RELAP5/MOD2 input deck for the Experiment L2-5 simulation is provided in Appendix A.

2. FACILITY AND TEST DESCRIPTIONS

2.1 LOFT Facility

The LOFT facility is a 50-MWt pressurized water reactor system with instruments that measure and provide data on the

system thermal-hydraulic and nuclear core behavior during postulated LOCAs and anomalous transients. The LOFT facility consists of five major systems: reactor system, primary coolant system, blowdown suppression system, emergency core cooling system, and secondary coolant system.

The LOFT primary-coolant-system (PCS), shown in Figure 1.1, is volume-scaled to a typical four-loop commercial PWR. The general philosophy in scaling coolant volumes and flow areas in LOFT is to use the ratio of the LOFT core power (50 MWt) to a PWR core power (3,000 MWt).

The nuclear core of the LOFT facility is 1.68 m high and 0.6 m in diameter and contains 1,300 fuel rods and 4 control assemblies. A top view of the core arrangement is shown in Figure 1.2. The postulated broken loop and three unbroken loops of a four-loop PWR are simulated by a single broken loop and intact loop, respectively. The broken loop is connected to a suppression tank that holds the effluent and simulates the back pressure in a PWR containment building. The ECCS is designed functionally the same as commercial plant system but has additional flexibility in injection flow rates and locations.

The LOFT system response may not be identical to that of any specific commercial plant for a LOCA or operational transient. However, the LOFT design incorporates the same physical processes and general boundary conditions important to the transient so that results can be used to qualify the accuracy of the

analytical models used for predicting accident behavior. The safety of commercial plants can then be assessed by these qualified models.

2.2 Experiment L2-5

LOCE L2-5 is the third experiment conducted in LOFT Power Ascension Experiment Series L2. The purpose of the LOFT L2 experiment series is to provide thermal-hydraulic and fuel behavior data during double-ended cold-leg break experiments at various ECCS conditions. These data are to be used to evaluate and verify models in computer codes to predict large PWR LOCA response.

The major conditions achieved in Experiment L2-5 are: (1) the reactor has been operating at steady state power long enough to establish near equilibrium fission product concentrations; (2) there has been a loss of offsite power coincident with the LOCA, thus the primary coolant pump will be tripped off at break initiation and ECC injection will be delayed for a period of time corresponding to the delay until the commercial plant's emergency diesel is delivering power; (3) the minimum ECC action takes place, which requires that the High Pressure Injection System (HPIS), and Low Pressure Injection System (LPIS) flow rates be scaled to represent only one of the two pumps available for each system; and (4) The PCP will coast down without connection to its flywheel system in order to establish hydraulic condition which would prevent the occurrence of early rewet for this experiment.

2.2.1 Initial conditions Initial reactor criticality occurred about 54 hours prior to experiment initiation. The power level reached 36.0 ± 2.0 MW 28 hours prior to Experiment L2-5 initiation, and was maintained at approximately that level until the experiment began. Prior to blowdown, the conditions in the intact loop were established to provide a flow of 192.4 ± 7.8 kg/s, with temperature and pressure in the hot-leg of 589.7 ± 1.6 K and 14.94 ± 0.06 MPa, respectively.

2.2.2 Experiment procedure The experiment was initiated by opening the Quick Opening Blowdown Valves (QOBVs) in the broken loop hot-leg and cold-leg. The reactor scrambled on low pressure at 0.24 ± 0.01 s. Following the reactor scram, the operators tripped the PCPs at 0.94 ± 0.01 s. Accumulator injection was actuated when the system pressure dropped below 4.2 MPa. Delayed ECC injection from the HPIS and LPIS were actuated at 23.90 ± 0.02 and 37.32 ± 0.02 s, respectively. The LPIS injection was stopped at 107.1 ± 0.4 s, after the experiment was considered complete.

3. CODE AND MODEL DESCRIPTIONS

3.1 Computer Code

The RELAP5/MOD2 Version 36.04 computer code is used to simulate the transient thermal-hydraulic response of the LOFT system during Experiment L2-5. RELAP5/MOD2 is a one-dimensional, two fluid, six-equation, thermal nonequilibrium reactor transient

and accident analysis program. This computer code is developed at the INEL for the U.S. Nuclear Regulatory Commission. Specific application of the code to the Experiment L2-5 simulation is discussed in the following sections.

3.2 Model Descriptions

The RELAP5/MOD2 model of the L2-5 simulation is shown in Figure 3.1. The nodalization used in this study is based on the nodalization presented in Reference 4 with changes where necessary to convert the RELAP5/MOD1 model into the RELAP5/MOD2 model and to make simplifications based on experience obtained in using the code. This model consists of 128 volumes, 145 junctions, and 77 heat structures to describe the LOFT systems including reactor vessel, broken loop, intact loop, pressurizer, steam generator, and ECCS. Brief descriptions of the RELAP5/MOD2 model of the LOFT facility are presented as follows.

3.2.1 Reactor vessel The reactor core is represented by two parallel six-volume channels --- hot and average channels. The geometry of the hot channel represents that of the center fuel assembly in the LOFT core; the average channel is used to simulate the remaining eight fuel assemblies. Crossflow junctions with appropriate flow areas and resistances between volumes are employed to represent the interconnections of these assemblies. A three-section pipe in parallel with fuel channels is used in modeling the bypass channel.

Modeling of the reactor vessel downcomer is one area of major importance in a large-break LOCA analysis because of ECC water injection phenomena. Conventionally, the downcomer was modelled by a single series of vertically stacked control volumes. The inadequacy of this model was demonstrated in the LOFT large-break LOCA simulations in which strong azimuthal asymmetries were measured, especially during ECC injection. The conventional downcomer model apparently is unable to calculate these phenomena. This deficiency can be improved by modeling the downcomer as a two-channel downcomer interconnected with crossflow junction. In this study, the downcomer is split into two equal parts (with equal flow area and volume) associated with the intact loop and broken loop, respectively. Each part is represented by six stacked annulus components. The connections between the parallel downcomers are represented by crossflow junctions.

The lower plenum and upper plenum are divided into several control volumes and simulated by branch or single-volume components in the RELAP5/MOD2 model.

Cylindrical heat structures are included to represent high-powered fuel rods (4 rods in the core center) and average fuel rods in the hot channel, and average fuel rods in the average channel. These heat structures representing the fuel rods are each divided vertically into six geometrical structures to allow different radial nodalization dimensions of the fuel rods at

different axial locations associated with different power levels. The best estimate values of the dimensions of the fuel pellet, gap, and cladding corresponding to the Experiment L2-5 power levels are used in order to obtain the best estimate initial stored energy. Reflood option is chosen for the fuel rod heat structures, and reflood calculation will be turned on when the connected hydrodynamic volume is nearly empty. A maximum number of axial fine mesh intervals of 8 is specified for axial length of 0.28 m during reflood calculation.

Other heat structures representing the flow ducts and reactor vessel are also modelled to describe the appropriate heat transfer between different flow channels, and ambient.

3.2.2 Broken loop Modeling of the broken loop deserves careful attention since the accuracy of the break flow calculation is of major importance in the predictions of the system responses of a large break LOCA. In this study, the broken loops (hot-leg and cold-leg) are simulated by a series of branch and pipe components, and the QOBVs are represented by trip valves to simulate the break junctions. Downstream of the break junctions, the broken loops are connected to time-dependent volumes where the pressure boundary conditions of the blowdown suppression tank (BST) are provided. Flow areas and flow resistances of the junctions along the broken loops are specified to simulate the pump simulator, steam generator simulator, and broken loop piping. Choked-flow

model is applied to the junctions wherever the junction flow area is restricted.

Definition of the break geometry is also of importance in accurately calculating the break flow. A discharge coefficient is required to account for multi-dimensional effects at the break that cannot be calculated using one-dimensional computer codes. A recommended discharge coefficient of 0.84 [6,7] is applied in the broken loop cold-leg break for both subcooled and saturated choked flow. However, a discharge coefficient of 1.0 is used for the broken loop hot-leg break.

3.2.3 Intact loop The intact loop modeling includes the hot-leg, loop seal, PCP, and cold-leg which are simulated by branch, single-volume, pipe, and pump components. Pump characteristics (head curves and torque curves) are provided for single-phase conditions. A set of two-phase difference curves are input, in conjunction with the single-phase curves to calculate the two phase pump performance. The moment of inertia of the pump rotor shaft (1.43 kg-m²) is used to characterize the coastdown behavior of the PCP.

3.2.4 Pressurizer The pressurizer model is not expected to be sensitive to the calculated peak cladding temperature in a large break LOCA analysis, therefore, simplification with neglecting the water spray and heater is made in order to save computation effort. The pressurizer surge line is nodalized with three control volumes and related junctions. The pressurizer tank is

represented by a seven-section pipe with PORV simulated by a trip valve connecting to a time-dependent volume with atmospheric pressure at the top.

3.2.5 Steam generator The steam generator primary side is represented by two branch components in modeling of the inlet and outlet plena, and an eight-section pipe (with four sections direct vertically upward and four sections direct downward) in simulating the steam generator U-tubes. In the secondary side, it is represented by a series of feedwater system, downcomer, boiler, separator, riser, and mist extractor simulations based on various components available in the RELAP5/MOD2 code. At the exit of the secondary side, a time-dependent volume is used to provide the pressure boundary conditions of the air-cooled condenser. Cylindrical heat structures representing the tubes are added to permit the heat exchange between the primary and the secondary sides of the steam generator. Additional heat structures are also used to simulate the heat loss to the environment.

3.2.6 ECCS The emergency core cooling systems, including the accumulator, HPIS and LPIS are simulated in the RELAP5/MOD2 model. The accumulator is represented by an ACCUMTOR component with back pressure of 4.2 MPa. The HPIS and LPIS are modelled by time-dependent junctions with injected coolant flow controlled by the system pressure. In order to simulate delayed HPIS and LPIS established in L2-5 test, the HPIS and LPIS are initiated in the calculation model at given times (23.9 and 37.32 s, respective-

ly). The accumulator flow is, however, actuated when the calculated system pressure drops below its back pressure, and the accumulator flow rate is determined by the pressure difference and given flow resistance. All emergency coolant injections are conducted to a common volume (volume 600) before being injected to the intact loop cold-leg.

Downstream of the accumulator, a TRPVLV component (junction 603) is used in simulating the accumulator check valve. This component will be used to shutoff nitrogen injection after the accumulator is empty in order to avoid the numerical problem of the RELAP5/MOD2 calculation.

3.3 Initialization Process

The RELAP5/MOD2 model of the L2-5 experiment simulation is initialized to a steady-state corresponding to the test initial conditions before it is utilized for the large break LOCA transient analysis. During initialization, the following processes are taken:

- (1) In order to achieve pressure condition, a time-dependent volume with system initial pressure (14.94 MPa) is connected to the top of the pressurizer tank.
- (2) In order to obtain correct pressurizer water level (i.e. primary water inventory), a time-dependent volume is connected to the bottom of the pressurizer tank by a time-dependent junction. The flow rate (including both insurge and outsurge flows) of the time-dependent junction is controlled by the difference between

the calculated water level and desired water level. Thermodynamic properties of the water inventory provided by the time-dependent volume are specified according to the properties of the water in the pressurizer tank.

(3) In the primary coolant system, minor adjustments of the flow resistances at certain locations are made in order to achieve the flow condition and core T.

(4) At the steam generator secondary side, a pressure lower than the measurement is used in the RELAP5/MOD2 model in order to obtain the primary coolant temperature closing to the test data. This requirement shows a possible deficiency of RELAP5/MOD2 in describing heat transfer between the primary and the secondary sides. However, the conditions of the steam generator secondary side is not sensitive in determining the system response of a large break LOCA type of transient, minor adjustment of the secondary side pressure is acceptable.

The initial conditions of the RELAP5/MOD2 model obtained by the initialization process are listed in Table 3.1 in comparison to the test data.

4. RESULTS AND DISCUSSIONS

Results of the experimental simulation of the thermal-hydraulic responses of L2-5 test are assessed through comparison of experimental data. The comparisons presented in this report

are representative key parameters of the L2-5 large break LOCA transient.

4.1 Base Case Analysis

Following the test procedure in L2-5 simulation with transient calculation initiated by the opening of break valves, the timings of major events calculated by RELAP5/MOD2 compared to the test data are listed in Table 3.1. There is no significant difference between the calculated transient scenario and the test result.

The calculated pressure response upstream of the cold-leg break (volume 345) compared to the test data are shown in Figure 4.1. An extremely rapid system depressurization commences with the opening of the QOBVs. Figure 4.1 shows that both the calculated and measured pressures drop from 14.94 MPa to 10.0 MPa immediately after the test initiation. As the pressure decreases, the temperature of the liquid in the vessel reaches saturation and flashing phenomenon occurs. Consequently, the depressurization rate is reduced by the voiding in the vessel as shown in both the calculation result and test data. The calculated pressure closely follows the test data at the first five seconds. After that, the pressure is underpredicted by RELAP5/MOD2 with little difference to the measurement. In Figure 4.2, the comparison of the pressurizer pressure is shown. It can be seen that the differences between the calculated and measured pressures are large with lower pressurizer pressure being

calculated by RELAP5/ MOD2. This could be resulted from the overprediction of the outsurge flow and the neglect of the pressurizer heat structure in the calculation model. The inflection point of the pressurizer pressure response at the moment of pressurizer empty occurs earlier in the calculation than that of measurement. According to the pressurizer water level response shown in Figure 4.3, the calculated pressurizer empty occurs at 10.0 s after the test initiation, which is about four seconds earlier than the test data.

In Figure 4.4, calculated interfacial water levels of the core region, the downcomer region near intact loop, and the downcomer region near broken loop are shown with level zero referring to the bottom of the reactor vessel. Based on the calculated water level in the core region, the L2-5 large break LOCA transient is divided into three periods: blowdown phase (0 to 21 s), refill phase (21 to 30 s), and reflood phase (30 to 54 s). According to the void measurements of L2-5 test, lower plenum refill starts at 22 s and ends with the beginning of core reflood at 31 s; and core reflood sequentially completes at 55 s. These events and their timings are well predicted by RELAP5/MOD2. During the blowdown phase, the calculated water level at the downcomer near broken loop declines much faster than that of the downcomer near intact loop. This result emphasizes the necessity of the downcomer modeling used in this study. In the core region, an even faster water level decrease is calculated with minimum

water level reaching 0.623 m below the bottom of the active fuel at 21.3 s. At this time, the blowdown phase of the transient ends and the refill phase begins as liquid from the accumulator reaches the lower plenum. The lower plenum is then refilled when the calculated water level reaches the bottom of the active fuel at 30.5 s. The end of the core reflood is calculated when the water level reaches the top of active fuel at 54.0 s. During the reflood period, the calculated water level rises with a rate of 70 mm/s.

Figure 4.5 shows calculated mass flow rates from the accumulator, HPIS, and LPIS. Calculated HPIS and LPIS flow rates shown in this figure are 1.585 kg/s and 6.42 kg/s, respectively. Compared to the test data, calculated HPIS and LPIS flow rates are overpredicted (measured HPIS and LPIS flow rates are 0.75 kg/s and 6.0 kg/s, respectively) because of the underprediction of the system pressure by RELAP5/MOD2. Since the major portion of the ECC flow is provided by the accumulator, the differences found in HPIS and LPIS flow rates can be neglected. The calculated accumulator flow initiated at 15.7 s goes up to 50.0 kg/s at 27.7 s, and then decreases linearly to 30.0 kg/s at the end of the calculation (90.0 s). However, the accumulator flow is, unfortunately, failed to be measured in L2-5 test. After the actuation of the accumulator recorded at 16.8 s, the only available measurement regarding to the accumulator is the accumulator water level, which gives an indication that the

accumulator flow ends at 50.0 s because the water level drops below the inlet of the variable standpipe at that time. In L2-5 test, the inlet of the variable standpipe is located at 0.95 m above the bottom of the accumulator tank. Therefore, certain amount of water (about 1,200 kg) stored below the variable standpipe inlet would not be injected into the reactor vessel. This condition is not included properly in the calculation model of the base case study which consequently leads to a continuous accumulator flow after 50.0 s in the calculation result. This error may not be significant in calculating the L2-5 transient since major events are almost complete at that time. A sensitivity study with accumulator tripped off at 50.0 s will be performed to investigate whether it is important or not in calculating the L2-5 transient.

According to the test data, single-phase blowdown ends and two-phase blowdown begins at the cold-leg break 3.4 s after the experiment initiation. While in the calculation, break flow transition from subcooled to saturated condition occurs at 2.0 s. Calculate² cold-leg break flow rates compared to the test data are shown in Figure 4.6. It is seen that RELAP5/MOD2 gives good result in the prediction of the cold-leg break flow during the blowdown period. In general, subcooled break flow is slightly underpredicted while saturated break flow is overestimated by the RELAP5/MOD2 model. During the refill and reflood periods, RELAP5/MOD2 calculates an almost zero break flow while the test

data shows a bunch of water slugs periodically rush out of the cold-leg break. The cold-leg break flow observed during the refill and reflood periods of L2-5 test may be attributed to the ECC bypass which is not calculated by the RELAP5/MOD2 model. Certainly, the underprediction of the system pressure shown in Figure 4.1 could be the reason of the underestimation of the break flow during these periods. After 70.0 seconds, increased cold-leg break flow rates are calculated because the calculated downcomer water level increases to the level of the cold-leg break by the excessive accumulator flow.

For the hot-leg break flow comparison shown in Figure 4.7, significant differences are found during the blowdown period. However, the calculated break flow shows excellent agreement with the test data later on. During blowdown, the measured flow rate shows a hump shape response while the calculated break flow monotonically decreases from its initial peak value. It is seen that the measured flow rate drops from an initial flow of 210 kg/s to a minimum flow of 30 kg/s at 4.0 s, and then increases to a maximum flow of 70.0 kg/s at 8.0 s. During this period, the break flow is significantly overpredicted by the RELAP5/MOD2 model. In the test data, the reason for the break flow to increase during system depressurization is very difficult to identify without other detailed measurements. The break flow can be increased with the increasing density (or with the decreasing void fraction) near the break. Probably, the break flow increase

as observed in L2-5 is due to "loop clearance" occurred at the top of the steam generator simulator. During the blowdown period, bubbles are generated by flashing flow upward along the U-tube (0.367 m ID pipe) of the steam generator simulator. Because the broken loop flow is restricted by the critical discharge at the break, the flowing bubbles could be momentarily accumulated in the region of the U-tube bend which results in a vertical stratification pattern in the U-tube pipe. At the moment when the broken loop cold-leg starts voiding, the cold-leg break flow rate is suddenly reduced which produces a perturbation to push the upstream liquid in the broken loop hot-leg over the U-tube bend. This liquid push over will yield consequently a syphon phenomenon which leads to void reduction near the break and therefore the hot-leg break flow increases. Calculated void fractions near the breaks are shown in Figure 4.8. From this figure, it is noted that the broken loop hot-leg starts voiding immediately after the break initiation. Small oscillation of the hot-leg void are calculated during the period of 4.0 to 8.0 s resulted from the occurrence of significant void in the broken loop cold-leg. The hot-leg void oscillation leads to oscillation of the hot-leg break flow without having flow increase in the calculation results. The failure in the prediction of the hot-leg break flow increase during blowdown with the RELAP5/MOD2 code could refer to its capability in the modeling of the phase separation and loop clearance phenomena.

The mass flow rate of the intact loop cold-leg is shown in Figure 4.9. Before the accumulator flow initiation, the cold-leg flow calculated by RELAP5/MOD2 agrees reasonably well with the test data. Flow oscillation observed in L2-5 after ECC injection due to direct contact condensation is also calculated by RELAP5/MOD2 with smaller oscillation magnitude than the test data.

The comparison between calculated and measured results of the intact loop hot-leg flow is shown in Figure 4.10. Significant discrepancies of the flow rates during the blowdown period are found in this figure. In order to understand the differences, a more detailed comparison of the hot-leg flow during the blowdown period is presented in Figure 4.11 with zero flow indication. It clearly shows that calculated flow rates are lower than the test data at the first few seconds of the initial period. After four seconds of the transient, negative flow rates (water runback) caused by the PCP stop are calculated with similar magnitudes of the positive flow rates shown by the test data. It is known [5] that as the result of partial failure of the flow measurement in test L2-5, the test data provides only the magnitude of the intact loop hot-leg flow without indication of the flow direction. However, the differential pressure measurement across the intact loop hot-leg indicates the existence of reverse flow during the blowdown period because the measured differential pressure changes sign from an initial

positive value to a negative value at 5.0 s, and maintains negative pressure difference to the end of the blowdown period.

Calculated core flow rates during the blowdown period are shown in Figure 4.12. It shows that the core inlet flow changes direction immediately after the break initiation from a positive (upward) flow of 195 kg/s to a negative (downward) flow of 250 kg/s, while a positive flow is sustained at the core outlet for 0.5 s. This bidirectional flow configuration results in the reducing of water inventory in the core region, flow stagnation somewhere in the core, and the occurrence of transient CHF. Core flow oscillation induced by direct condensation during ECC injection is also calculated and presented in Figure 4.13.

Calculated cladding temperatures of the hot channel hot rod at different axial elevations (with level 1 corresponding to the bottom node) are shown in Figure 4.14. It is seen that significant temperature rises are calculated for the fuel rod cladding at levels 2, 3, and 4 when CHF conditions are predicted at 0.3 s. At the level 1 position, temperature spikes occur with relatively small magnitudes during the blowdown and refill periods. At higher portions of the fuel rod (levels 5 and 6), calculated cladding temperatures keep going down without departure from saturation temperature during the whole transient. However, the cladding temperature measurements located at various axial positions from the bottom to the top of the hottest fuel rods indicate that the whole fuel rods experience CHF during L2-5

test. Inaccurate predictions of the cladding temperature responses at the upper and lower parts of the fuel rod could be resulted from inaccurate prediction of the CHF. The present model used in RELAPS/MOD2 for CHF calculation is the Biasi correlation which overpredicts the CHF by 60% in the comparison to the dryout experiment conducted at the Royal Institute of Technology in Sweden [8]. A sensitivity study with reduced Biasi CHF will be performed to see whether the cladding temperature prediction can be improved.

In test L2-5, a peak cladding temperature (PCT) is recorded at one third of the full length of the fuel rod from the bottom which corresponds to the elevation at the middle of the level 2 and level 3 positions in the calculation model. However, differences in calculated cladding temperatures between the level 2 and level 3 positions are small. Therefore, calculated cladding temperatures of the level 3 elevation shown in Figure 4.15 are used in the comparison to the test data. According to the calculated cladding temperature response, the CHF occurrence is predicted at 0.3 s after the break initiation. The calculated cladding temperature reaches a peak value of 1,112 K at 7.0 s and sustains at that level to the end of the blowdown period without the occurrence of the early fuel rod rewet. An enhanced cooling is calculated after the reflood model is turned on at 26.0 s, which depresses the cladding temperature to a calculated quench temperature (T) of 530 K at 57.2 s. In test L2-5, the cladding

temperature drops before the CHF occurs at 0.9 s. After that, a severe heatup of the fuel rod cladding is detected, and the cladding temperature increases from 600 K to 1,000 K in six seconds. A slower temperature increase is then measured to the end of the refill period with the PCT of 1,077 K reached at 28.5 s after the experiment initiation. Early quenching phenomena observed in test L2-3 does not occur in test L2-5 because different hydraulic conditions achieved in these tests. At the beginning of the reflood period, the measured cladding temperature starts declining with slower decreasing rate than that of the calculated temperature. Fuel rod quench occurred at 54.0 s is detected when the cladding temperature drops to 820 K which is about 300 K higher than the RELAP5/MOD2 calculation. The underestimation of the fuel rod quench temperature by RELAP5/MOD2 is also found in the comparison to FLECHT-SEASET data [9]. It is caused by a simplified formula in computing quench temperature currently used in the reflood heat transfer package which gives an almost constant quench temperature of 520 K [1]. Based on the observation of the quench temperature in test L2-5, the calculation model should be reexamined.

The underprediction of the cladding temperature before quench caused by an excessive cooling is calculated with the reflood model of RELAP5/MOD2. Currently, the reflood model uses a correlation for the dispersed-flow film boiling heat transfer based on Dougall and Rohsenow's modifications to the single phase

flow Dittus-Boelter correlation. It is known that the correlation does not account for nonequilibrium effect, therefore, tends to overpredict the film boiling heat transfer coefficients [10,11].

The excessive precursory cooling of the fuel cladding by the RELAP5/MOD2 calculation could also be caused by excessive interfacial drag with its present model [12,13]. Too much liquid is entrained from the lower plenum to the core region. In the hydraulic volumes next to the fuel where post-dryout condition occurs, the flow regimes predicted by RELAP5/MOD2 are mist (dispersed) flow during the refill and reflood periods. Increased liquid droplet entrainment will increase interface heat transfer area between the liquid and vapor, which in turn will reduce the degree of vapor superheating in rod bundles and lead to a higher driving potential for energy removal. In addition, the vapor superheating could be also underpredicted by RELAP5/MOD2 with its present interfacial heat transfer model at high void flow conditions [14,15]. Moreover, steep increase of the wall heat flux is calculated at the moment of the reflood model actuation, which contributes also to the excessive precursory cooling. Detailed discussions of the reflood model calculation can be seen in the following section.

Evidence of RELAP5/MOD2 underpredicting the vapor superheating can be observed from the comparison of fluid temperatures at the upper plenum and hot-leg. Calculated fluid temperatures at the upper plenum (volume 240) compared to the test data are shown

in Figure 4.16. The temperature measurements indicate the existence of superheated steam while calculated temperatures show that both the liquid and vapor stay saturated during the refill and reflood periods. At the end of the reflood period, subcooled ECC water reaching the upper plenum region is calculated. Superheated vapor is also observed in the hot-leg region during L2-5 test. Fluid temperature responses at the intact loop and broken loop are shown in Figures 4.17 and 4.18, respectively. Again, the comparison clearly indicates that RELAP5/MOD2 fails in calculating the extent of vapor superheating of the L2-5 transient.

In the intact loop cold-leg, near the ECC injection point, subcooled liquid temperatures are calculated at the moment of the accumulator flow initiation. According to the measurements shown in Figure 4.19, the thermocouple could be surrounded by vapor space at the initial period of the accumulator injection, subcooled temperature is detected with several seconds delay. Temperature oscillation measured during the accumulator injection can be caused by the alternate contact of the liquid and vapor phases with the thermocouple. However, measured fluid temperature in the intact loop cold-leg is higher than the RELAP5/MOD2 prediction. The underprediction of the liquid temperature could be resulted from underestimation of the condensation with the RELAP5/MOD2 model.

In the downcomer region, calculated liquid temperatures of the upper portion (volume 202 and 282) and the lower portion

(volume 210 and 290) are shown in Figures 4.20 and 4.21, respectively. It is seen that calculated temperatures near the intact loop where ECC water is injected are different from that near the broken loop. At the intact side, the delivery of the subcooled ECC water to the downcomer is calculated with few seconds delay after the accumulator flow initiation. At the broken side, subcooled liquid temperature is calculated in the downcomer when the liquid level increases during the refill and reflood periods. In test L2-5, downcomer fluid temperature measurements are located at an azimuthal angle of 155 away from the intact loop cold-leg. The fluid temperature responses measured at various axial locations in the downcomer region are shown from Figures 4.22 to 4.25 for the comparison to the calculated temperatures in the downcomer near the broken loop. The temperature underprediction shown in these figures could be caused by the underprediction of the heat transfer between the vessel hot wall and the ECC liquid. Of course, the downcomer liquid temperature could be also underpredicted if the ECC condensation is underestimated with the RELAP5/MOD2 model.

The comparison of the fluid temperatures of the broken loop hot-leg is shown in Figure 4.26. Significant differences found after 60.0 s are caused by the excessive accumulator injection in the calculation model.

The comparisons of the fluid densities of the intact loop cold-leg, intact loop hot-leg, and broken loop cold-leg are

presented in Figures 4.27, 4.28 and 4.29, respectively. Calculated fluid densities in the intact loop cold-leg agree well with the measurements before the actuation of the accumulator. Increased densities with ECC injection are noted in the test data with significant variations resulted from local measurement. In the calculation results, the volume-averaged densities are shown with smooth changes. Density overprediction in the RELAP5/MOD2 calculation after 60.0 s is due to overflow of the downcomer by excessive accumulator flow. Excessive carryover of the core liquid to the intact loop hot-leg is illustrated by the high density fluid present after 45.0 s (see Figure 4.28). The cause of this carryover lies in the interfacial drag model used in the RELAP5/MOD2 code. In the broken loop cold-leg (volume 345), calculated densities shown in Figure 4.29 are in good agreement with the test data during early period of the transient. After about 10.0 s, calculated densities in general are higher than the measurements. It is interesting to note that the calculated density in the broken loop cold-leg is high while the calculated cold-leg break flow shown in Figure 4.6 is almost zero during the ECC injection period. The questions turn out to be where the high density fluid comes from and where it goes during the refill and reflood periods. In Figure 4.30, calculated mass flow rates of the BLCL junction (vessel outlet junction from volume 282 to volume 335) and the cold-leg break junction are shown. From this figure, it is seen that fluid periodically flows into the broken

loop cold-leg and back to the reactor vessel without exiting flow through the break during 25.0 to 42.0 s. However, whether the flow is provided by the carryover from the downcomer or resulted from the ECC bypass phenomena in the calculation model remains unknown. Calculated flow rates of the BLCL junction are compared to that of junction 272 and junction 283 in Figure 4.31. A positive flow of the junction 272 represents bypass flow from the intact side (volume 202) to the broken side (volume 282); while a negative flow of the junction 283 indicates the amount of carryover from downcomer to the broken loop. It is seen from Figure 4.31 that in general the junction 272 flow is less than zero, i.e. reverse flow is calculated on the flow path of the ECC bypass. It is known that the ECC bypass phenomena will occur when the ECC water can flow downward the annulus downcomer by gravity and be swept out through the break by the escaping upward steam flow, that is, due to the counter-current flow limitation (CCFL) phenomenon. However, there is no direct modeling of the CCFL in RELAP5/MOD2, and the existing model of the interfacial drag is not good enough in retarding the downflow of the ECC water [16]. Therefore, it can be concluded that the RELAP5/MOD2 model does not calculate ECC bypass in the L2-5 simulation. High density fluid of the broken loop cold-leg during ECC injection is resulted from excessive carryover with the present RELAP5/MOD2 models.

4.2 Sensitivity Studies

In addition to the base case calculation, sensitivity studies are performed to explore the effects of input modeling and code options. Scenario study and simple model modification, specifically speaking, the pump coastdown behavior and the Biasi CHF correlation are also analyzed in elucidating the code performance. The identifications of the cases analyzed in this study are listed in Table 4.2 with the conditions which are different from that of the base case. The purpose and the results of the sensitivity studies are discussed in the following sections.

4.2.1 ACCUM50 This case study is used to identify the influences of the thermal-hydraulic response predictions resulted from the excessive accumulator flow of the base case. Calculated accumulator flows compared to the base case are shown in Figure 4.32. The water level comparisons are presented from Figure 4.33 to 4.35. Major differences of the water level responses can be seen when the accumulator flow is tripped off at 50.0 s in the ACCUM50 case. The cold-leg break flow shown in Figure 4.36 indicates similar results except some flow spikes after 70.0 s are calculated. Calculated fluid densities of the broken loop cold-leg are compared in Figure 4.37. Simulation with correct accumulator flow stop can improve the prediction of the density at later period. However, the calculated density of the ACCUM50 case is still higher than the test data. In Figures 4.38 and

4.39, calculated cladding temperatures are shown. It is seen that there is no significant difference in the cladding temperature prediction resulted from the difference in the accumulator simulation. With lower accumulator flow simulated in the ACCUM50 case, the fuel rod quench is delayed by 2.0 seconds compared to the base case.

4.2.2 BLHL-HT In the base case study, it is found that the hot-leg break flow is overpredicted during the blowdown phase. Considering the possible uncertainties in the temperature measurements, higher initial temperatures of the broken loop hot-leg are used in the BLHL-HT case to see if the hot-leg break flow prediction can be improved.

Reduced hot-leg break flow with the increasing of the initial temperature is shown in Figure 4.40. However, the hump shape of the break flow response shown by the test data is still failed to be calculated. With reduced hot-leg break flow, increasing of the cold-leg break is expected. Figure 4.41 shows that the calculated cold-leg break flow of the BLHL-HT case is higher than the base case in the first two seconds. Cladding temperature responses at various axial locations are compared in Figure 4.42. Significant difference is seen in the cladding temperature at level 2 position. This could be resulted from the relocation of the stagnation point. Higher flow resistance can be induced by the higher initial temperature in the broken loop hot leg, which moves the stagnation point upward in the core

region and introduces an increased reverse flow in the level 2 node immediately after the opening of the QOBVs. The increased reverse flow will then prevent the deviation from saturation at that location. However, the calculated PCT at the hottest location (level 3) of the BLHL-HT case is only 20 K lower than that of the base case (see Figure 4.43).

4.2.3 BLHL-DC The calculated flow can be reduced with reducing of the discharge coefficient specified in the RELAP5/MOD2 input. In the BLHL-DC case, the hot-leg break discharge coefficient is reduced from 1.0 in the base case to 0.8.

It is seen from Figure 4.44 that the calculated hot-leg break flow is decreased by this input change, but with limited difference from the base case. The other parameters, including the pressure, cold-leg break flow, and cladding temperature responses, shown in Figures 4.45 to 4.48 indicate minor effects of the hot-leg break discharge coefficient on the L2-5 simulation.

4.2.4 BLHL-5K Regarding the uncertainty of the form loss coefficient during flow transient condition, a sensitivity study is needed to investigate the possible impacts in the large break LOCA calculation. In the BLHL-5K case, the form loss coefficients of the junctions in the broken loop hot-leg specified in the RELAP5/MOD2 input are five times of the base case.

Calculated pressures of the broken loop cold-leg and pressurizer compared to the test data are shown in Figures 4.49 and 4.45, respectively. It is seen that the system pressure

increases with increased form loss coefficient in the broken loop hot-leg. During the blowdown period, the calculated pressure of the broken loop cold-leg is higher than the test data with increased form loss coefficient, however, the calculated pressure of the pressurizer is still much lower than the test data. Significant reduction of the hot-leg break flow is seen in the BLHL-5K case (see Figure 4.51). In general, better agreement on the hot-leg break flow is seen in the BLHL-5K case, but the initial break flow is apparently underestimated. Because of the increasing of the system pressure, the calculated cold-leg break flow shown in Figure 4.52 is increased with the increasing of the form loss coefficient. The comparisons of the cladding temperatures are presented in Figures 4.53 and 4.54. The major difference is found in the temperature response of the level 2 position as resulted from the relocation of the stagnation point. The fuel quench time is delayed by 8.0 seconds while the PCT is compatible in the comparison to the base case.

4.2.5 PV-X-PL The RELAP5/MOD2 numerical scheme is generally formulated using one-dimensional elements. However, there are several applications where an approximate treatment of crossflow provides an improved physical simulation. One major application of the crossflow junction is to provide a tee model. In the L2-5 base deck, the pressure vessel outflow junctions connecting to broken loops are considered to be normal junctions. In reality, the momentum flux in the reactor vessel is perpendicular to the

momentum flux in the broken loop. Therefore, crossflow junctions instead are chosen in the PV-X-BL case to identify the difference with this option in the L2-5 simulation.

Important parameters with respect to the large break LOCA transient, including the break flows and cladding temperatures, are shown in Figures 4.55 to 4.58. It is interesting to see the calculated break flows, both in the hot-leg break and the cold-leg break, with crossflow junction modeling are equal to the base case. The effects of the crossflow option on the cladding temperature responses are calculated with limited differences. The PCT calculated in the PV-X-BL case is the same as that of the base case.

4.2.6 MESH#32 A fine mesh-rezoning scheme is implemented to efficiently use the two-dimensional conduction solution for reflood calculations. It is suggested in the RELAP5/MOD2 manual that appropriate user-specified maximum number of axial fine mesh intervals is 8 to 32 with the length of hydrodynamic volumes ranged from 0.15 m to 0.6 m. In the analysis of the MESH#32 case, the number of fine mesh intervals increases from 8 used in the base case to 32.

The results of this study are presented in Figures 4.59 to 4.62. It is seen that important parameters calculated with increased number of fine mesh intervals are identical to those in the base case, except a little difference of the fuel quench time.

4.2.7 FUEL-GAP It is well known that fuel gap distance (or gap conductance) is an extremely important parameter in determining the PCT during a large break LOCA. In the L2-5 base deck, varied fuel gap distances are used for various axial and radial locations of the fuel rods in accordance with different power levels. At the hottest section, the fuel gap distance specified in the base deck is 0.04944 mm. In the FUEL-GAP case, a nominal fuel gap distance of 0.0953 mm [2] is universally used for fuel rod modeling at various locations. The increase of the fuel gap distance will reduce the gap conductance and, consequently, increase the initial rod temperature and the initial stored energy.

Radial profiles of calculated rod temperatures at the hottest location are presented in Figure 4.63. It is seen that the initial fuel rod centerline temperature of the FUEL-GAP case is 270 K higher than the base case. The effect of the increased stored energy on the cladding surface temperature can be seen in Figures 4.64 and 4.65. The PCT calculated for the FUEL-GAP case is 130 K higher than that of the base case in the L2-5 simulation. This disparity emphasizes the importance of fuel-rod modeling for the large break LOCA transient analysis. Calculated break flows presented in Figures 4.66 and 4.67 are, however, not affected by the increasing of the fuel gap distance.

4.2.8 PUMP-FW The major difference observed between the LOCE L2-3 and L2-5 tests is the early rewet phenomena as a result of

different operations of the primary coolant pumps during the transients. In the base case study, no early rewet of the fuel rod is calculated according to the pump operation of L2-5. In a sensitivity study [4] performed with earlier version RELAP5/MOD1, it is found that the early rewet of the fuel rod can be predicted in the L2-5 simulation if the pumps coast down with their flywheel system. In this study, the same assumption on the pump behavior is used to see whether the RELAP5/MOD2 code can predict early quenching.

Figure 4.68 shows the coolant mass flow rate of the intact loop cold-leg provided by the surge flow from the coastdown pump. It is seen that with the assistance of the flywheel system the cold-leg flow of the PUMP-FW case is sustained for a longer period than the base case. Because of the higher coolant flow in the intact loop cold-leg of the PUMP-FW case, a positive core flow is re-established at earlier time and results in a higher core flow between 5.0 to 10.0 s in the comparison to the base case (see Figure 4.69). However, calculated cladding temperature shown in Figure 4.70 indicates no early rewet even though the pumps coastdown with their flywheel is assumed in the calculation. Calculated cladding temperatures of the PUMP-FW case deviate from the base case after 7.0 s with small difference. The calculated PCT of the PUMP-FW case is almost the same as that of the base case. Calculated break flows shown in Figures 4.71 and 4.72 can be used to illustrate the insignificant

effect of the pump coastdown behavior on the break flow calculation in the L2-5 simulation.

4.2.9 CHF*0.6 Regarding the failure of the cladding temperature predictions at the upper and lower portions of the hottest fuel rods in the base case study, the accuracy of the Biasi CHF correlation used in RELAP5/MOD2 is questioned. This sensitivity study is performed with a modified Biasi correlation (simply multiply by a factor of 0.6) to see whether the cladding temperature prediction can be improved.

Results of the cladding temperatures are shown in Figures 4.73 to 4.75. It is learned that the discrepancies of the cladding temperature responses at the upper portion of the fuel rod found in the base case still exist in the CHF*0.6 case. The calculation model still fails in predicting CHF at low power sections. Moreover, the predictions of the cladding temperatures of the hottest portion are even worse with the CHF reduction. In Figure 4.73, it is seen that the time-to-CHF is reduced from 0.3 s in the base case to almost time zero with the reduction of the CHF, and the associated PCT is calculated to be 500 K higher than the test data. Therefore, a solid statement on the Biasi correlation can not be made, and the reason for the failure of the cladding temperature prediction is unknown.

4.2.10 NORFLOD Different heat transfer correlations are used in RELAP5/MOD2 for post-dryout condition between the calculations with and without reflood model option [1]. The reflood model

calculation is actuated when the system pressure is lower than 1.0 MPa, when the mass flux is less than 200 kg/m s, and when the connected hydrodynamic volume is nearly empty. In view of the failure of the cladding temperature prediction resulted from the excessive precursor cooling during the reflood period of the base case analysis, an experimental simulation is performed without the actuation of the reflood model in the RELAP5/MOD2 calculation.

Calculated void fractions in the hot channel of the NORFLOD case compared to the base case are shown in Figure 4.76. In general, the calculated void fraction without using reflood model is a little higher than that of calculation with reflood model. In Figure 4.77, calculated cladding temperatures at various axial elevations of the NORFLOD case are shown. It is seen that high cladding temperatures are sustained for the rest of the reflood period without significant precursory cooling before quench because lower heat fluxes are calculated for the NORFLOD case in the comparison to the base case (see Figure 4.78). Discontinuity of the heat flux calculation is exhibited in the base case at the moment of the reflood model actuation. The calculated vapor temperature comparison shown in Figure 4.79 indicates also a significant vapor temperature increase with the heat transfer package switching. These discontinuities should be further studied to see whether they are real situations.

The comparisons of the cladding temperatures are shown in Figures 4.80, 4.81, and 4.82 for various axial elevations. Significant improvement in the cladding temperature prediction at the hottest section results in the NORFL 3 case study. In Figure 4.80, it is seen that not only the cladding temperatures before quench but also the fuel rod quench temperature and its timing calculated without the reflood model are in good agreement with the test data. These results may indicate that either the criteria used in RELAP5/MOD2 for the actuation of the reflood model calculation are inadequate or the heat transfer package in the reflood model is improper. However, the suggestion of not using reflood model in the L2-5 simulation can not be justified because the accuracy of the RELAP5/MOD2 model in predicting local hydraulic conditions (quality, droplet size, interfacial area, and two phase velocities' is still an open question. It would be almost impossible to evaluate separately the heat transfer correlations and hydraulic models in calculating the cladding temperature response during post-dryout dispersed flow conditions.

5. RUN STATISTICS

The computational efficiency of the RELAP5/MOD2 simulations are summarized in Table 5.1. The simulations are conducted on a FACOM M200 computer which is compatible to an IBM MVS system.

6. CONCLUSIONS

In this study, the large break LOCA test L2-5 is analyzed by the RELAP5/MOD2 model. The test simulations begin with break initiation and subsequent blowdown, and continue through lower plenum refill, core reflood, and terminate with corewide quench. Major events and their timings of the large break test L2-5 are well predicted by the RELAP5/MOD2 model. Important parameters, such as pressure, break flow, and cladding temperature, are calculated with reasonable agreement in the comparison to the test data. Especially, the most critical parameter in the large break LOCA, the peak cladding temperature, is very well calculated by the RELAP5/MOD2 model. Noticed differences and code deficiencies found in the L2-5 test simulation and various major findings of the sensitivity studies are described in the following:

1. The broken loop pressure is well predicted (slightly underestimated) while the pressurizer pressure is significantly underpredicted. The underprediction of the pressurizer pressure is caused by the overprediction of the outsurge flow during blowdown.
2. Significant differences in the water level responses between the downcomer near the intact loop and the downcomer near the broken loop are calculated. It indicates that the downcomer modeling employed in this study is quite important in a large break LOCA analysis.

3. The effect of the excessive accumulator injection after 50.0 s found in the base case calculation is insignificant in determining the transient behaviors of the L2-5 simulation. Since L2-5 failed to measure the accumulator flow rate, the calculated result according to the accumulator model used in the RELAP5/MOD2 calculation can not be verified. However, according to the comparison of the major event timing, the calculated accumulator flow rate could be a close resemblance to the test condition.
4. The hot-leg break flow is overpredicted by RELAP5/MOD2 during early stages of the transient. The measured hot-leg break flow rate shows a hump shape response while the calculated break flow monotonically decreases from its initial peak value during the blowdown period. The break flow increase during blowdown observed in L2-5 could be resulted from momentarily accumulation of the bubbles in the U-tube bend and sequentially the occurrence of the "loop clearance" by the liquid push over. These phenomena could be out of the RELAP5/MOD2 calculation capability. In the sensitivity studies, no improvement in the hot-leg break flow is calculated with various input modifications.
5. Flow oscillation observed in L2-5 after ECC injection due to direct contact condensation is calculated by RELAP5/MOD2 with smaller oscillation magnitude than the test data. In the comparison of the fluid temperatures in both the cold-leg and

the downcomer regions, it is found that RELAP5/MOD2 underpredicts the fluid temperature during ECC injection period. These differences indicate a possible deficiency in the condensation model of the present RELAP5/MOD2 code.

6. During ECC injection, high density fluid is calculated in the broken loop cold-leg. However, the high density liquid in the calculation is provided by the carryover from the downcomer region instead of the ECC bypass. Compared to the measured density, it is found that the carryover is overpredicted with the interfacial drag model of RELAP5/MOD2.
7. According to the cladding temperature measurements located at various axial elevations, the hottest fuel rods from the bottom to the top experience CHF conditions during L2-5 test. The RELAP5/MOD2 calculation, however, shows that only the middle high power portions of the fuel rods suffer from dryout while the lower and upper elevations of the fuel rods stay cooled in the transient analysis. In the sensitivity study with the reduction of the Biasi CHF by a factor of 0.6, the calculation results do not give better predictions of the cladding temperatures at the low power elevations. Moreover, the calculated cladding temperatures at the high power elevations significantly deviate from the test data with the reduction of the CHF.
8. With the reflood model calculation, excessive precursor cooling of the fuel rod results which leads to the underesti-

mation of the cladding temperature during the reflood period. Calculation without using the reflood model, not only the calculated cladding temperatures but also the quench temperature and its timing are in very good agreements with the test data. However, the exciting results of this special calculation could be caused by wrong reasons, because the accuracy of the RELAP5/MOD2 model in predicting local hydraulic conditions is still an open question. However, the results may indicate that either the criteria used in RELAP5/MOD2 for the actuation of the reflood model calculation are inadequate or the heat transfer package in the reflood model is improper. In any case, the discontinuities of the calculated rod surface heat flux and vapor temperature indicate a discontinuous heat transfer coefficient before and after the actuation of the reflood model. Further review is required for these discontinuity.

9. In the sensitivity studies of the large break LOCA test L2-5, the calculated PCTs of various cases are obtained during the blowdown period. The calculated PCTs are quite insensitive to different input modifications including (1) adjusted accumulator modeling; (2) initial temperature distributions in the broken loop hot-leg; (3) flow resistances of the broken loop hot-leg; (4) discharge coefficient of the critical flow at the hot-leg break; (5) cross-flow junction used for the linkage between the broken loop and the reactor

vessel. However, significant differences in the PCT calculations are found in the studies of the fuel gap dimension and the CHF correlation.

10. With the assumption of having flywheel connected during pump coastdown, the calculation results show that the present RELAP5/MOD2 model does not yield blowdown quench phenomena.

Table 3.1 Initial Conditions of LOCE Test L2-5

<u>Parameter</u>	<u>L2-5</u>	<u>RELAP5/MOD2</u>
Power level (MW)	36.0 ± 1.2	36.0
Primary colant system mass flow (kg/s)	192.4 ± 7.8	194.97
Hot-leg pressure (MPa)	14.94 ± 0.06	14.935
Intact loop hot-leg temperature (K)	589.7 ± 1.6	589.71
Intact loop cold-leg temperature (K)	556.6 ± 4.0	556.24
Core Δ T (K)	33.1 ± 4.3	33.47
Broken loop hot-leg temperature (K)	561.9 ± 4.3	565.44
Broken loop cold-leg temperature (K)	554.3 ± 4.2	554.31
S.G. secondary side pressure (MPa)	5.85 ± 0.06	5.548
S.G. secondary side flow (kg/s)	19.1 ± 0.4	18.86
Pressurizer water level (m)	1.14 ± 0.03	1.14

Table 4.1 Sequence of Events in LOCE Test L2-5

Event	Time (s)	
	L2-5	RELAP5/MOD2
Experiment initiation	0.0	0.0*
CHF occurred	0.9	0.3
Primary coolant pump trip	0.94	0.94*
Liquid level drops below top of core	3.2 [#]	1.7
Liquid level drops below bottom of core	5.4 [#]	5.0
Peak cladding temperature reached	30.0	7.0
Pressurizer empty	14.0	10.0
Accumulator flow initiation	16.8	15.7
End of blowdown	22.0 [#]	21.3
HPIS flow initiation	23.9	23.9*
Lower plenum refill	31.0 [#]	30.5
LPIS flow initiation	37.3	37.3*
Core reflood	55.0 [#]	54.0
Final core quench	62.0	57.2
Transient ended	120.0	90.0

* Boundary conditions

Rough estimate from void measurements in the core region

Table 4.2 Cases Analyzed in the Sensitivity Study
of the LOCE Test L2-5 Simulation

Case	Conditions different from the base case
ACCUM50	Smaller accumulator volume (67% of the base case) and accumulator flow tripped-off at 50.0 s
*BLHL-HT	Initial temperature of 590 K (25 K higher than the base case) is specified in the broken loop hot-leg
BLHL-DC	Discharge coefficient of 0.8 (instead of 1.0 in the base case) is used in the hot-leg break
BCHL-5K	Junction form loss coefficients used in the broken loop hot-leg are five times of the base case
PV-X-BL	Cross-flow junction is used in connecting the broken loop to the pressure vessel
MESH#32	Number of reflood fine mesh intervals increases from 8 to 32
*FUEL-GAP	Nominal fuel gap distance of 0.0953 mm (about twice larger than the base case) is assumed without considering possible fuel swelling effect
PUMP-FW	Pump coastdown with 316.04 kg-m ² inertia (instead of 1.431 kg-m ² in the base case) produced by its flywheel system
CHF*0.6	CHF calculated by the Biasi correlation is reduced by a factor of 0.6
NORFLOD	Calculation without the actuation of the reflood heat transfer model

*Initialization process is performed before transient calculation

Table 5.1 Run Statistics of the LOCE Test L2-5 Simulation

Case	Transient Time(s)	CPU(s)	Number of Time Step	Number of Volume Cell	* Performance Number
BASE	90	3277.13	6284	128	4.074
BLHL-HT	60	2301.99	4394	128	4.093
BLHL-DC	60	2280.81	4335	128	4.110
BLHL-5K	90	2761.04	5220	128	4.132
PV-X-BL	60	2310.41	4436	128	4.069
MESH#32	60	2423.19	4494	128	4.213
FUEL-GAP	80	2969.44	5825	128	3.983
PUMP-FW	60	2330.01	4452	128	4.089
CHF*0.6	90	3068.71	5992	128	4.001
NORFLOD	80	2685.07	5503	128	3.812

*Performance Number=

$$\text{CPU} \times 10^3 / [\text{Number of Time Step}] / [\text{Number of Volume Cell}]$$

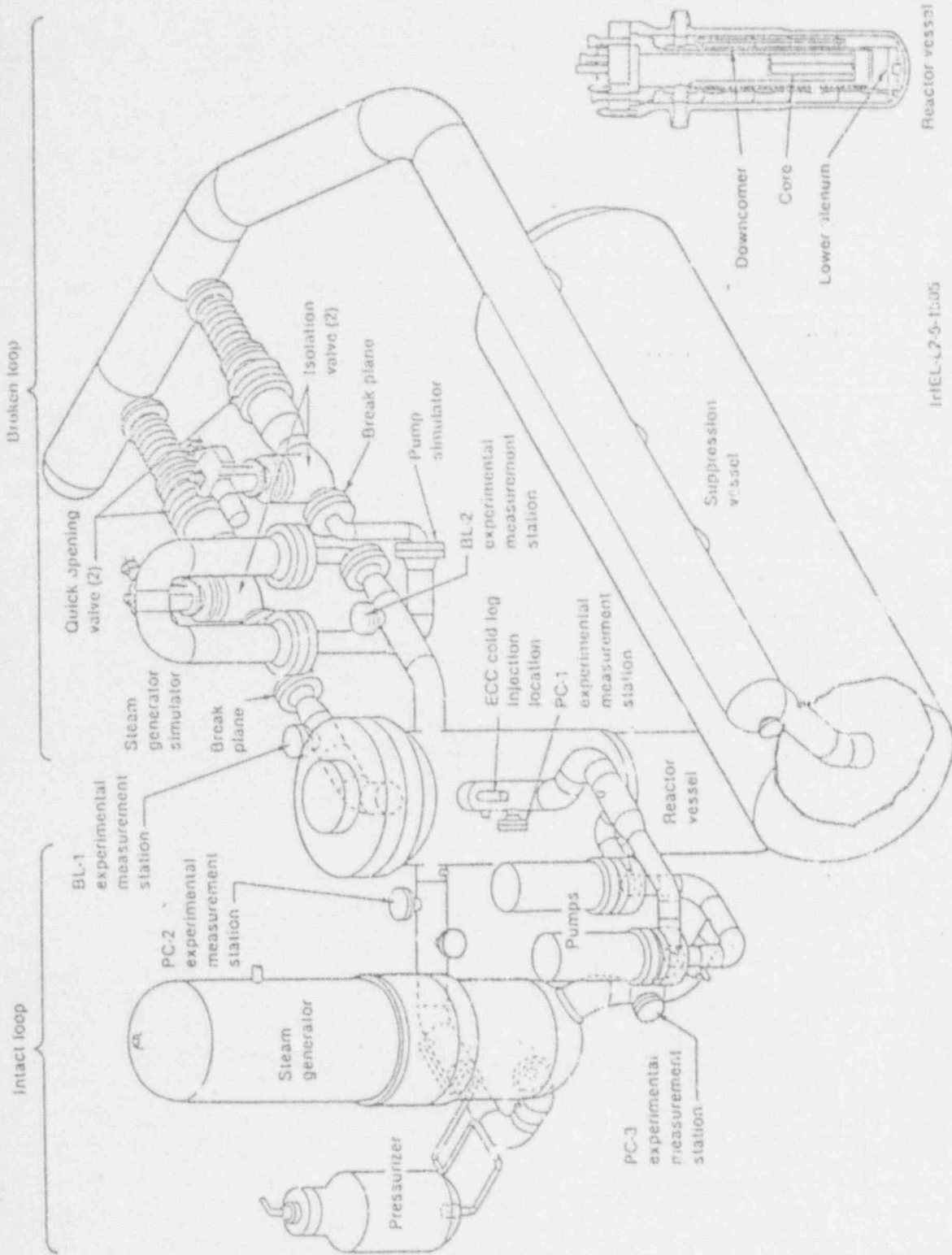
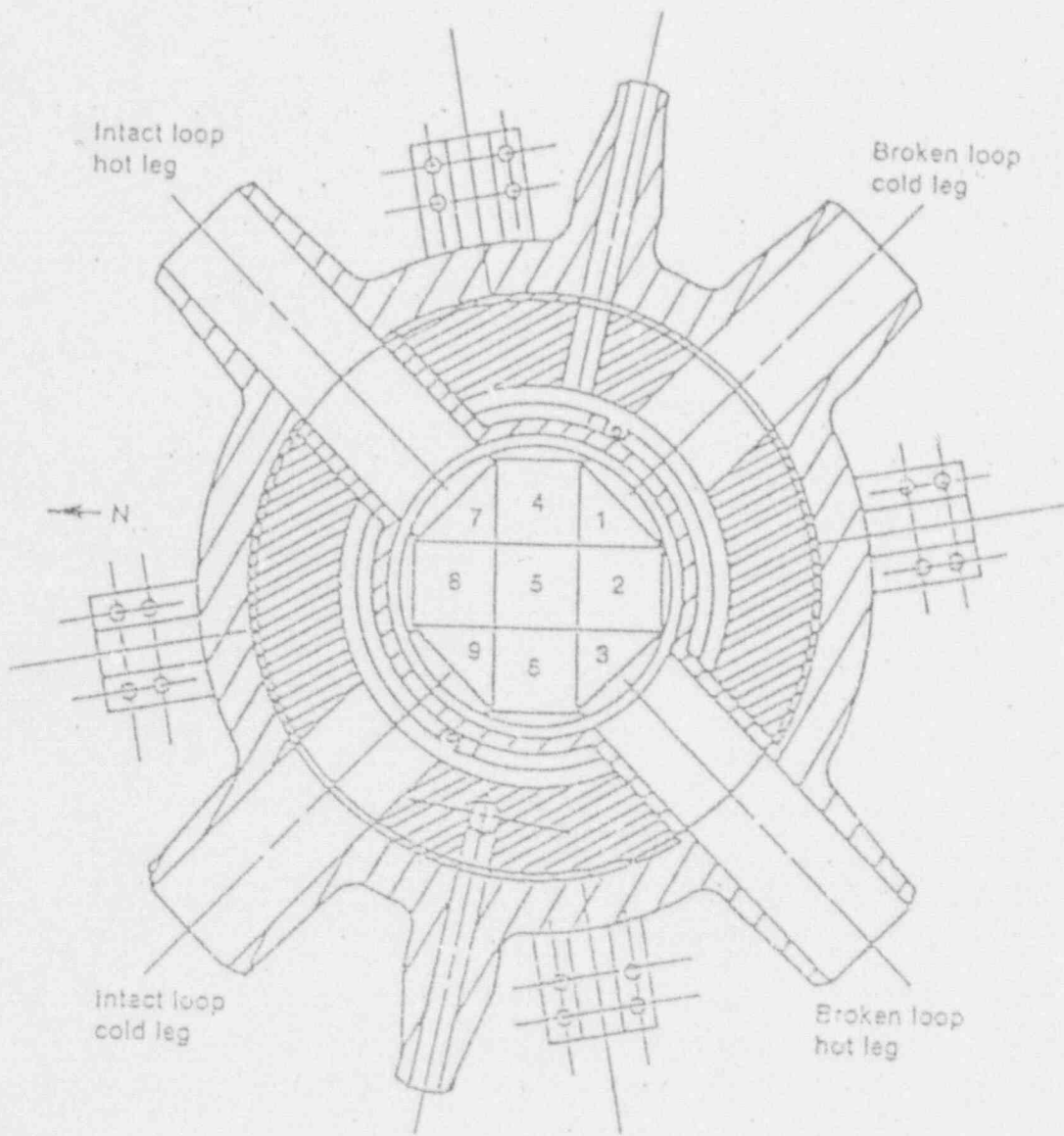


Figure 1.1 LOFT Facility Major Components



INEL-A-5339

Figure 1.2 LOFT Facility Core Arrangement

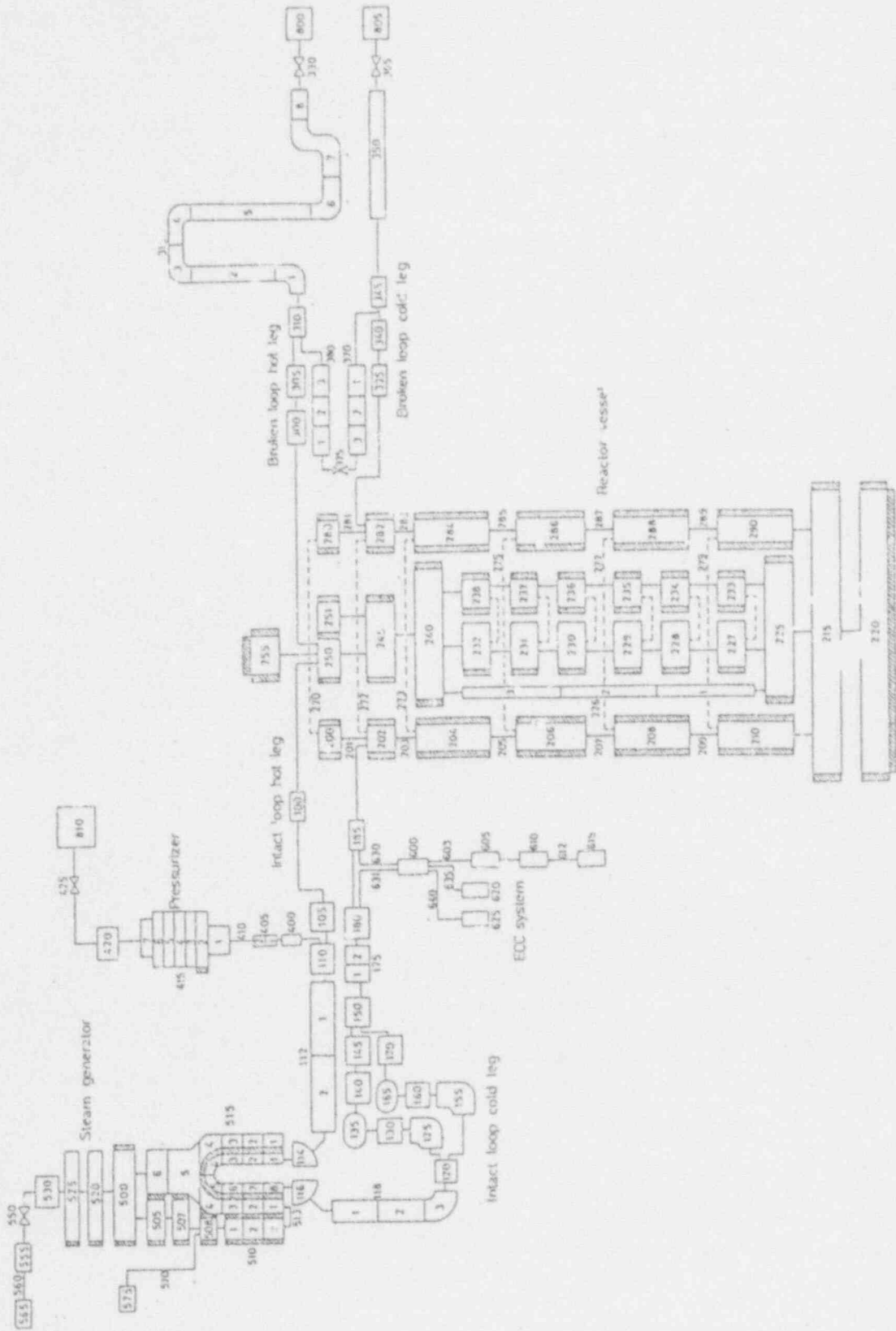


Figure 3.1 RELAP5/MOD2-LOFT Large Break Model Nodalization for Experiment L2-5

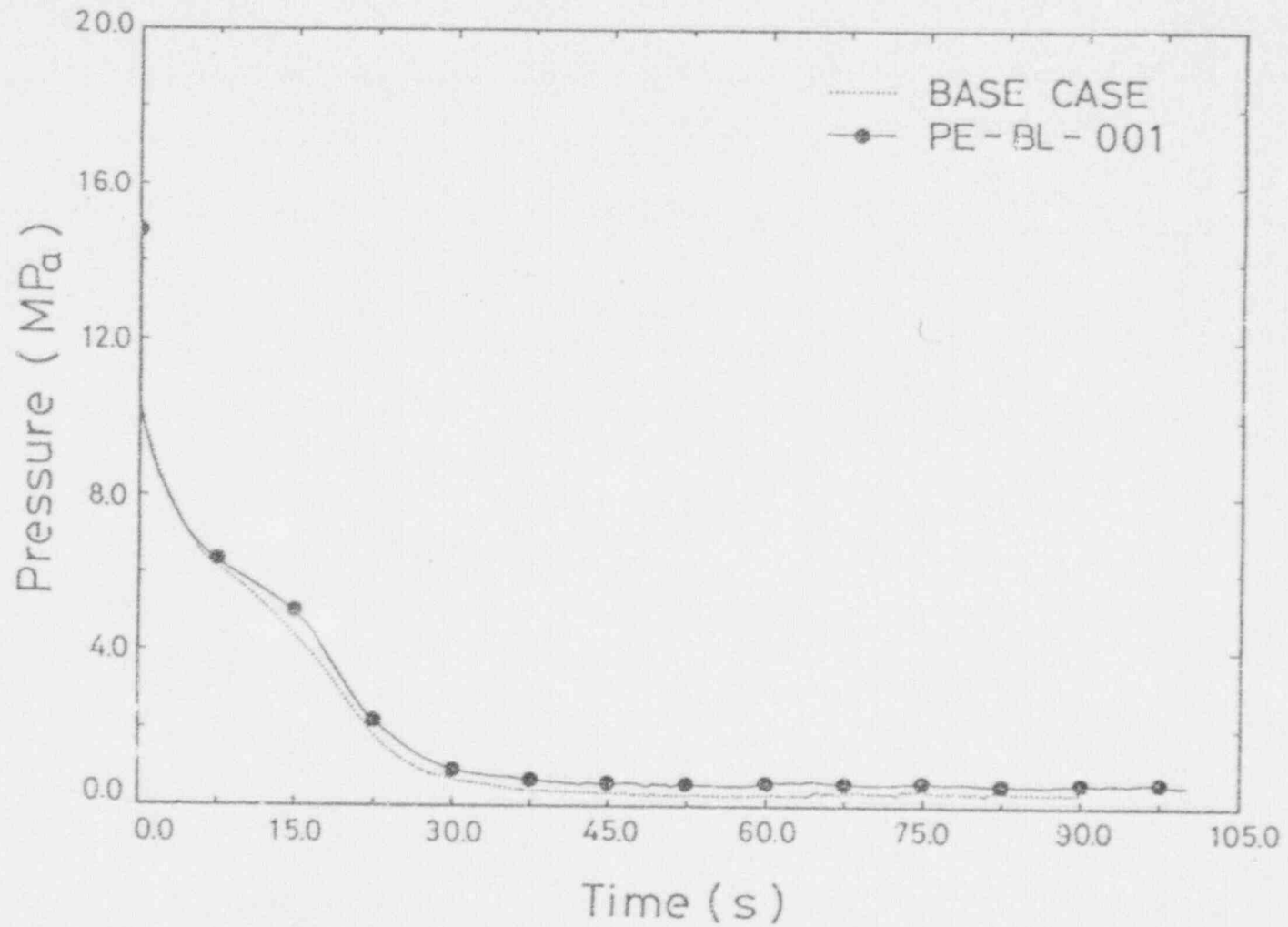


Figure 4.1 Comparison between the Calculated and Measured Broken Loop Cold-Leg Pressures of Test L2-5

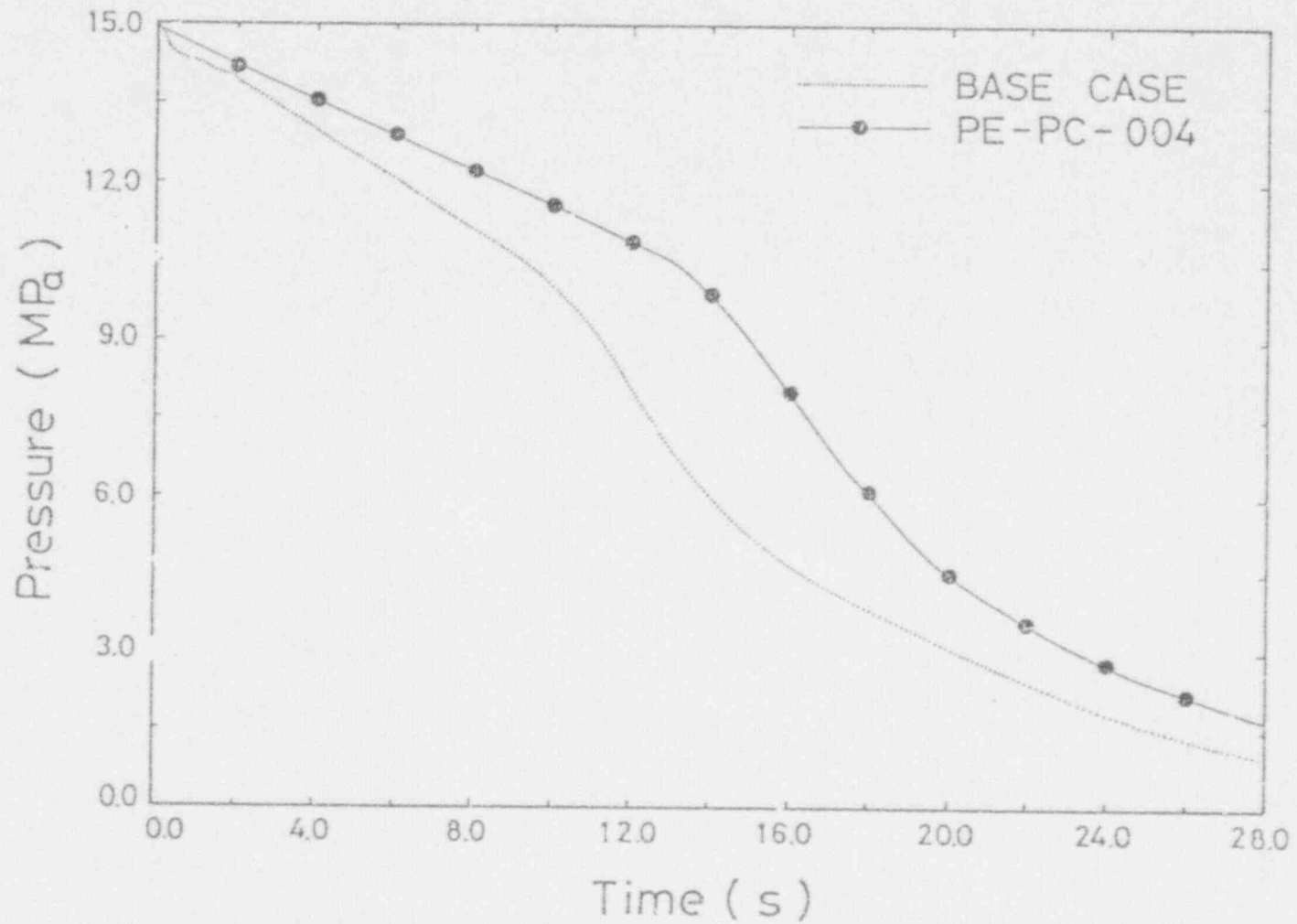


Figure 4.2 Comparison between the Calculated and Measured Pressurizer Pressures of Test L2-5.

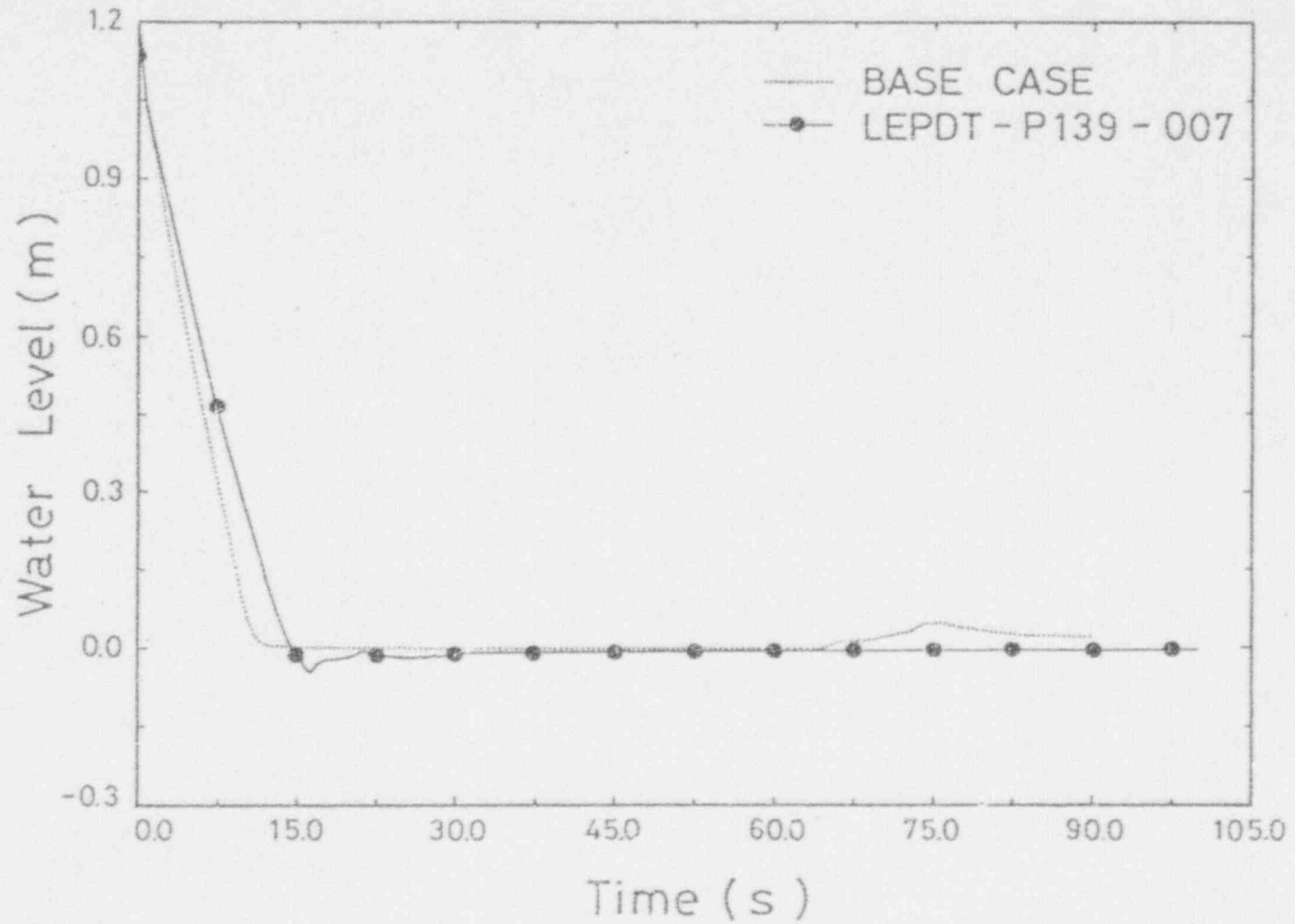


Figure 4.3 Comparison between the Calculated and Measured Pressurizer Water Levels of Test L2-5

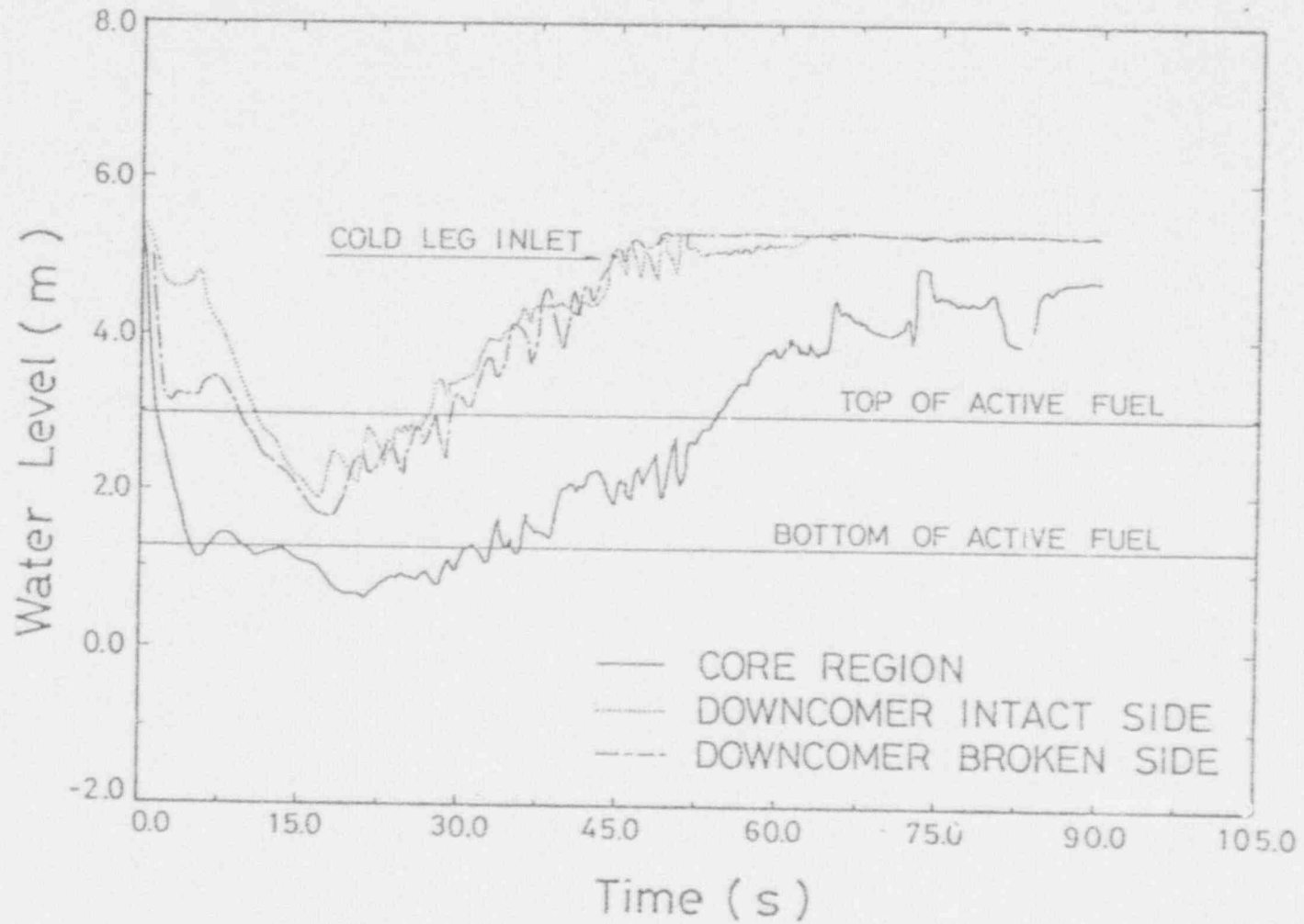


Figure 4.4 Calculated Water Levels in Reactor Vessel of Test L2-5 Simulation

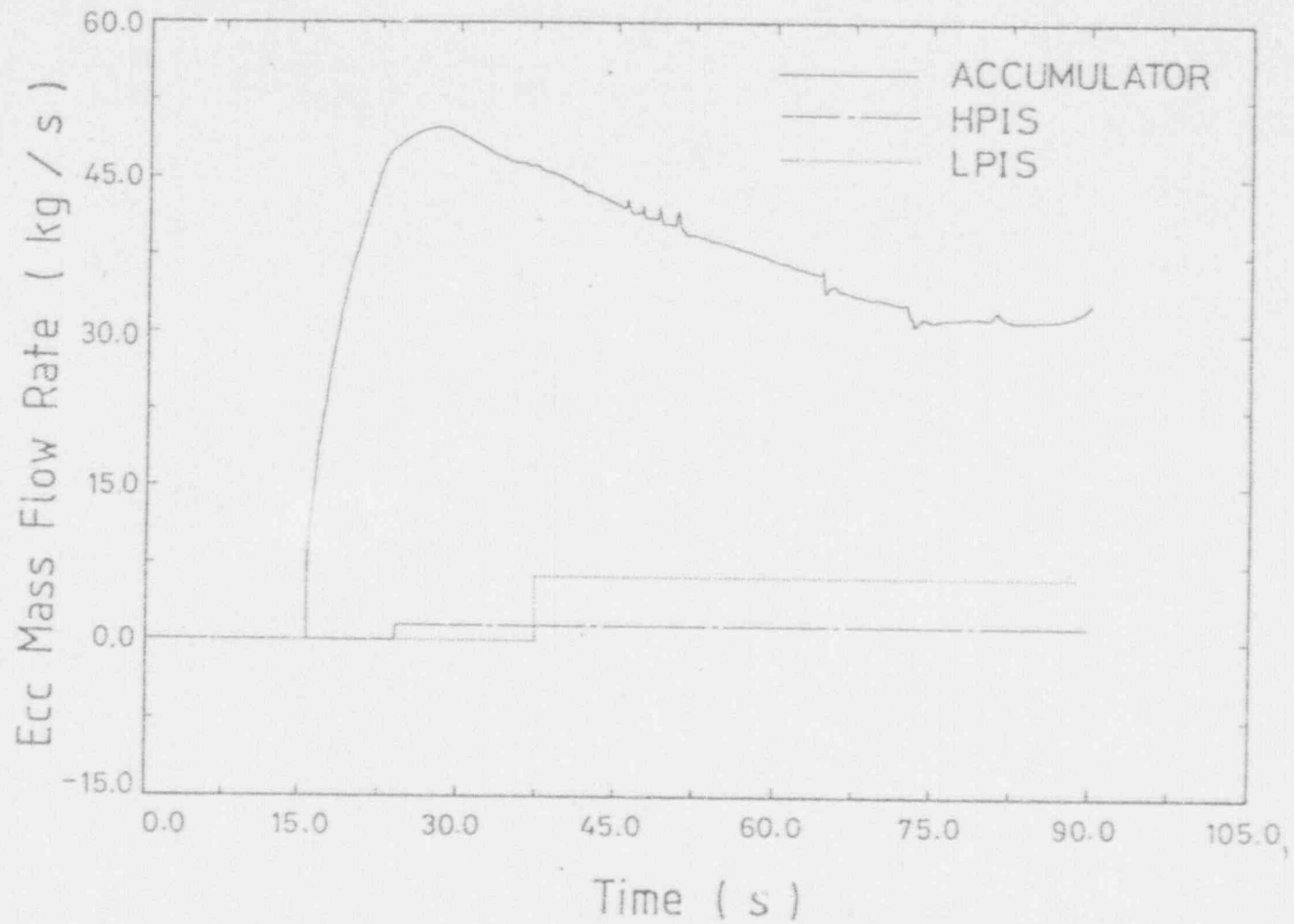


Figure 4.5 Calculated ECC Flow Rates of Test L2-5 Simulation

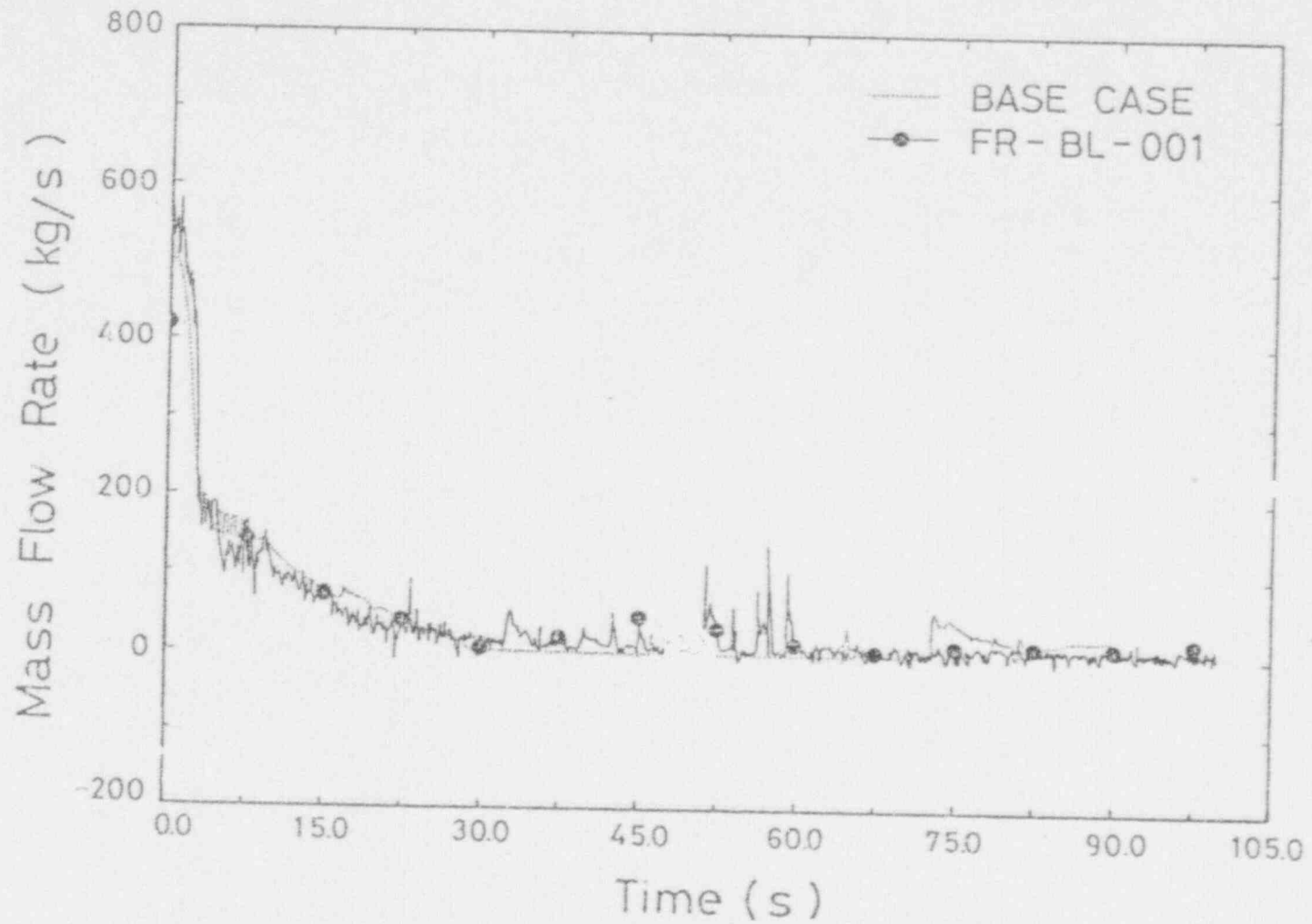


Figure 4.6 Comparison between the Calculated and Measured Cold-Leg Break Flow Rates of Test L2-5

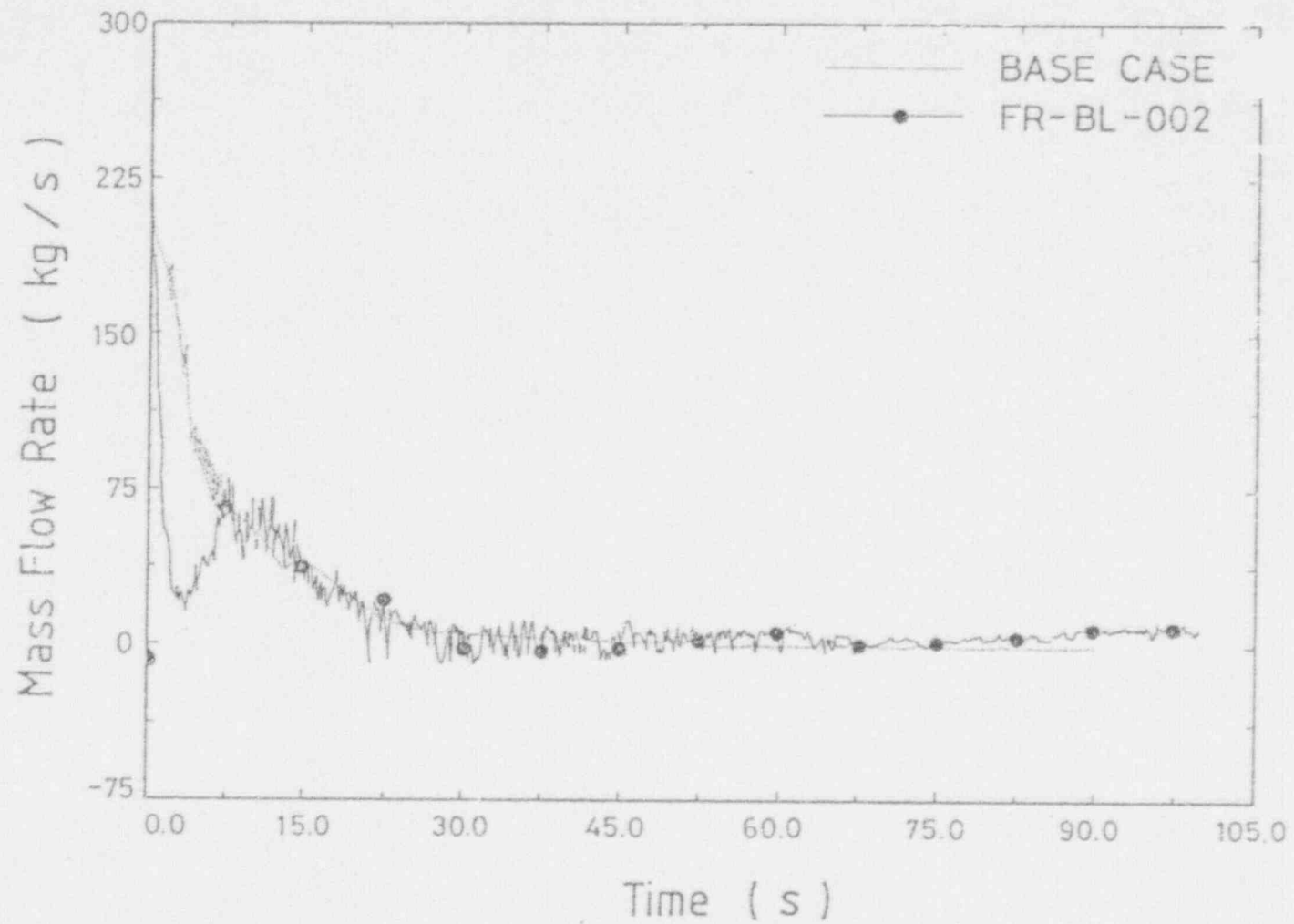


Figure 4.7 Comparison between the Calculated and Measured Hot-Leg Break Flow Rates of Test L2-5

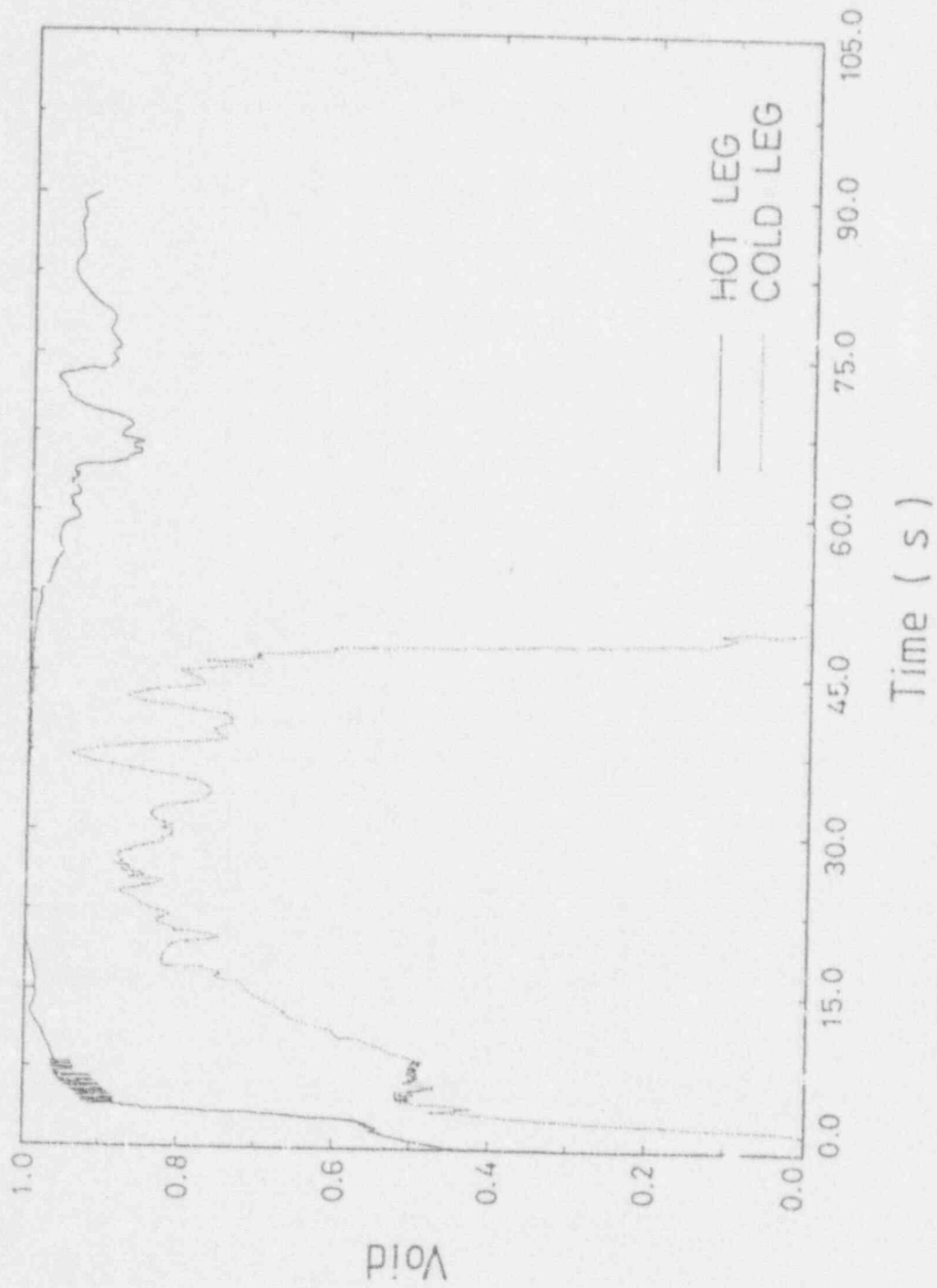


Figure 4.8 Calculated Void Fractions Upstream the Break Junctions of Test L2-5 Simulation

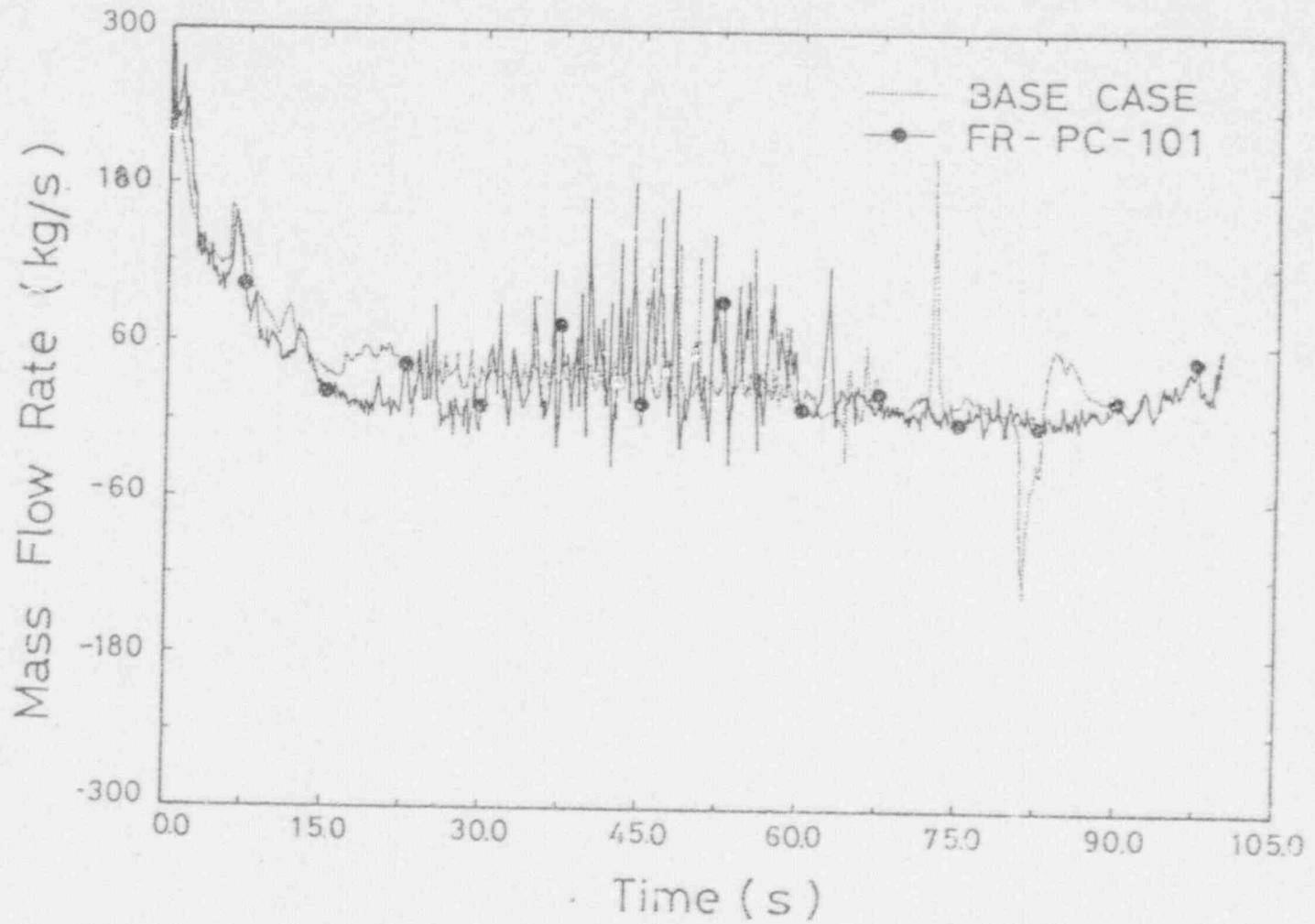


Figure 4.9 Comparison between the Calculated and Measured Intact Loop Cold-Leg Flow Rates of Test L2-5

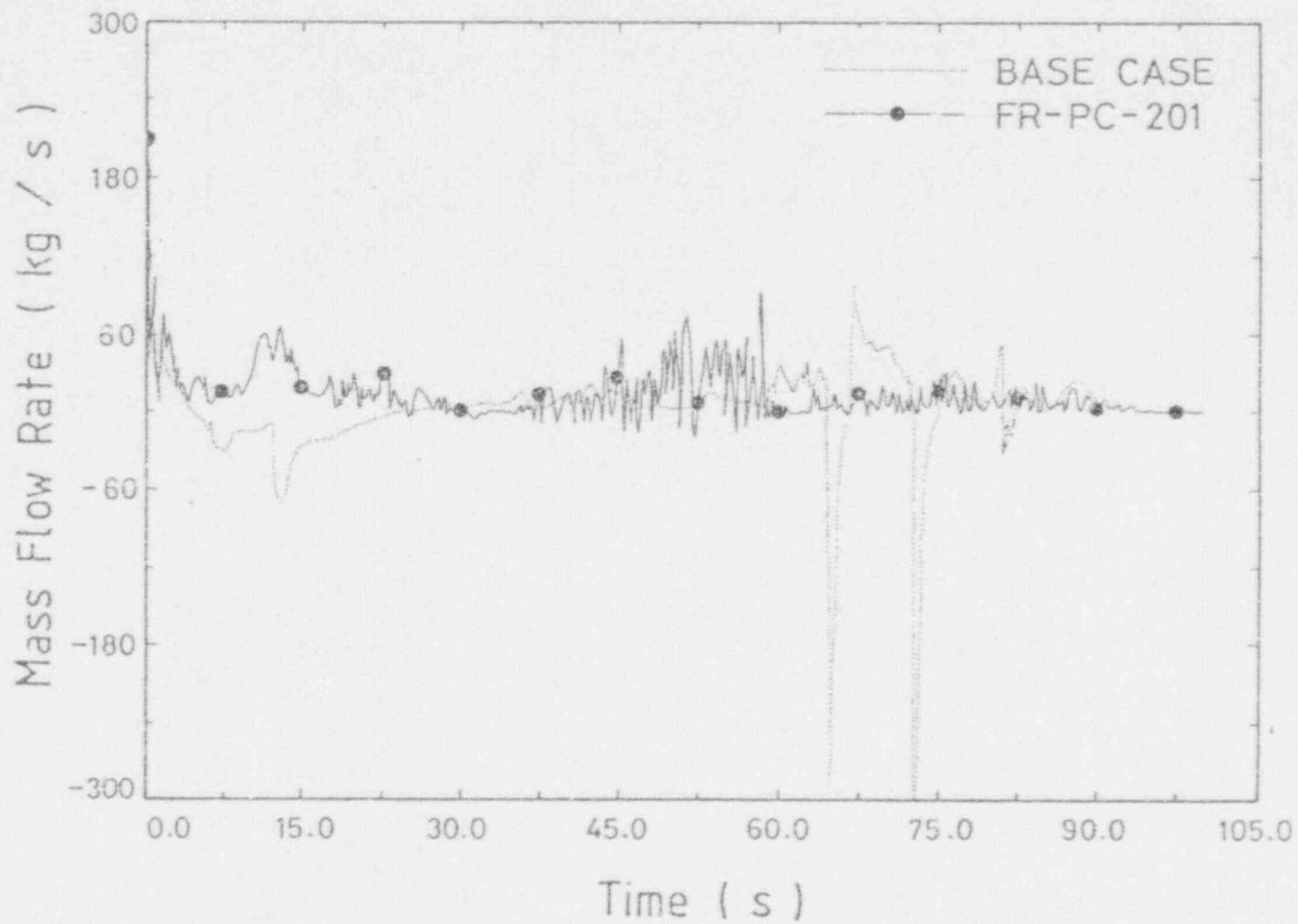


Figure 4.10 Comparison between the Calculated and Measured Intact Loop Hot-Leg Flow Rates of Test L2-5

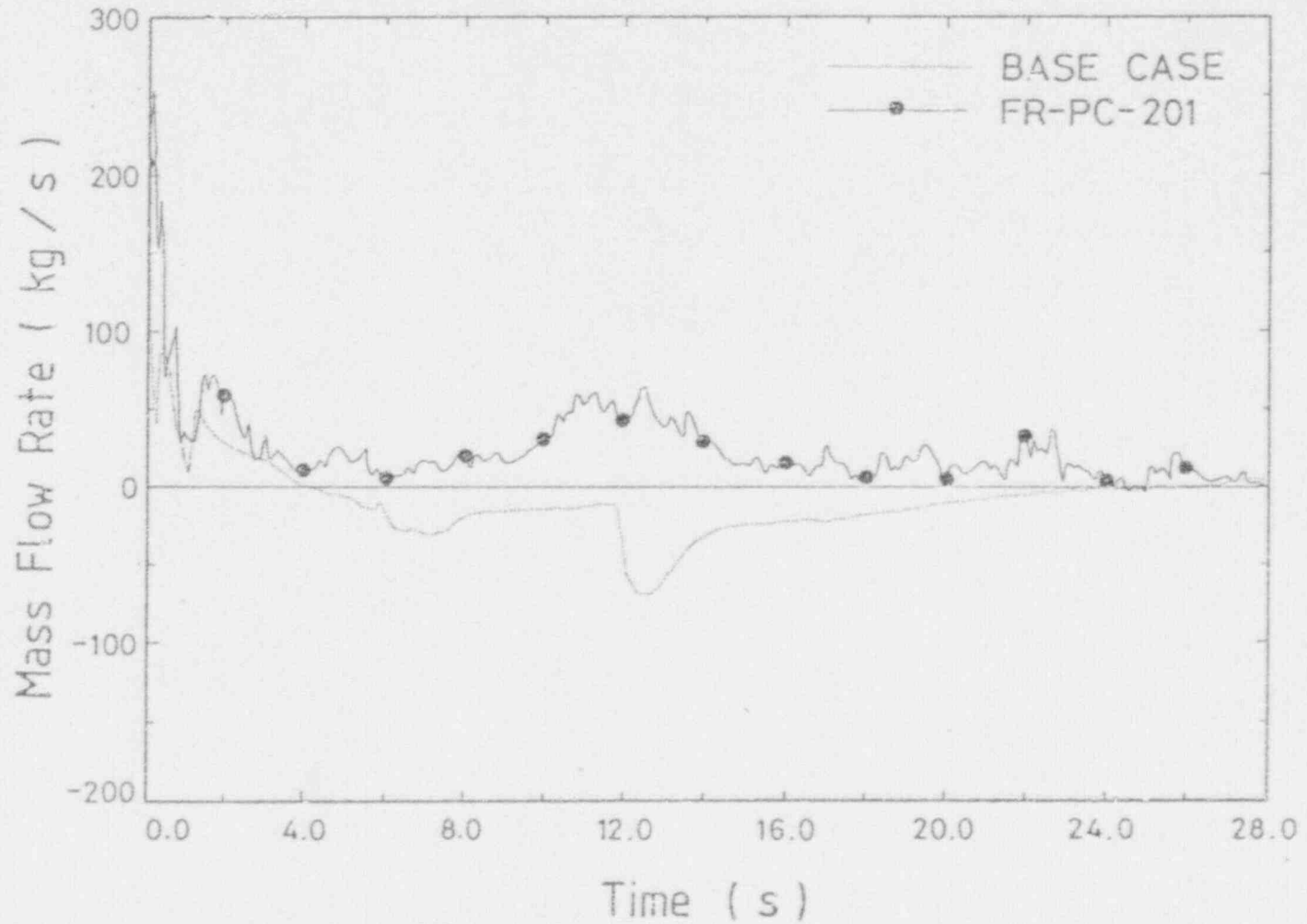


Figure 4.11 Comparison between the Calculated and Measured Intact Loop Hot-Leg Flow Rates During the Blowdown Period of Test L2-5

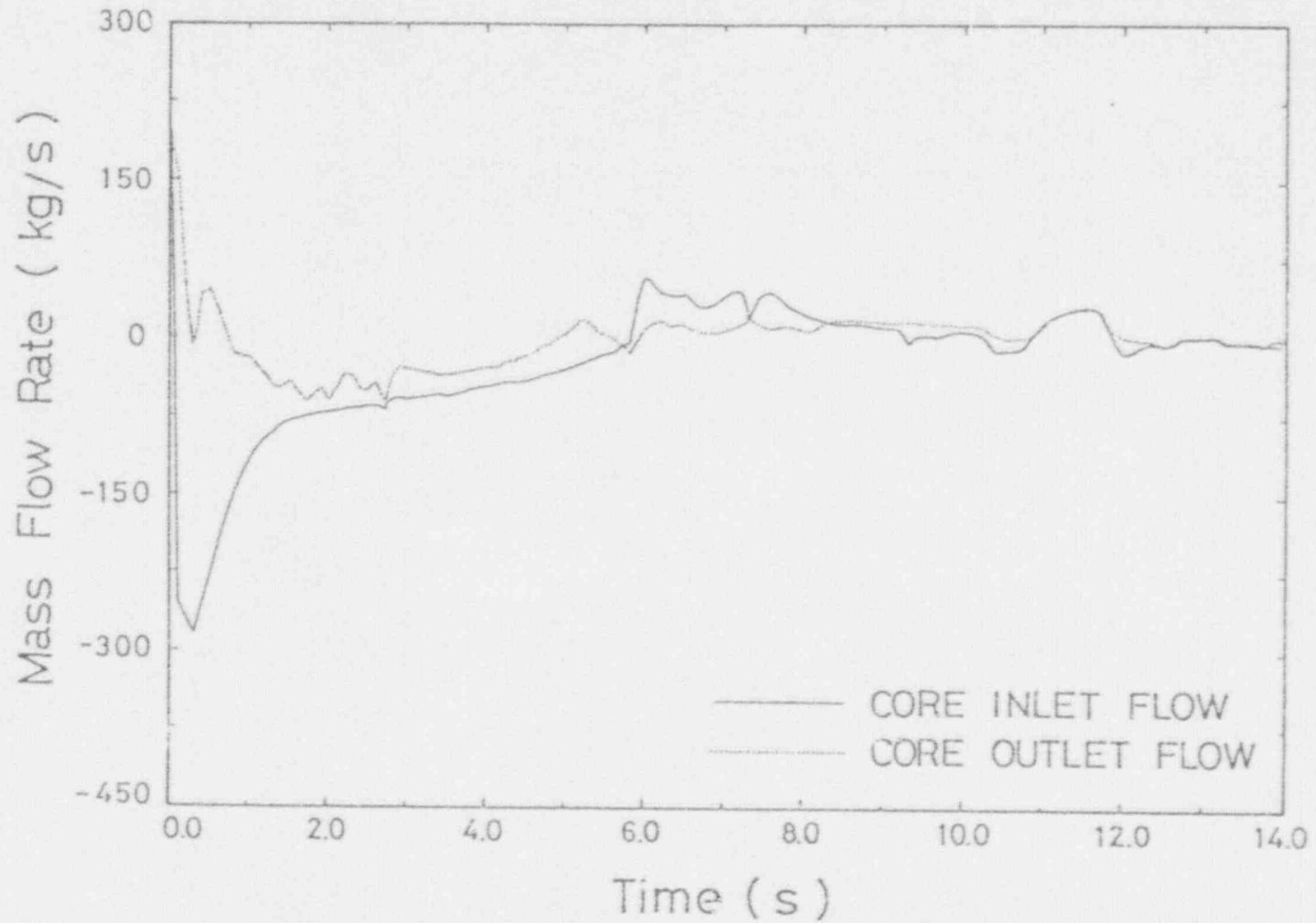


Figure 4.12 Calculated Core Flow Rates During the Blowdown Period of Test L2-5 Simulation

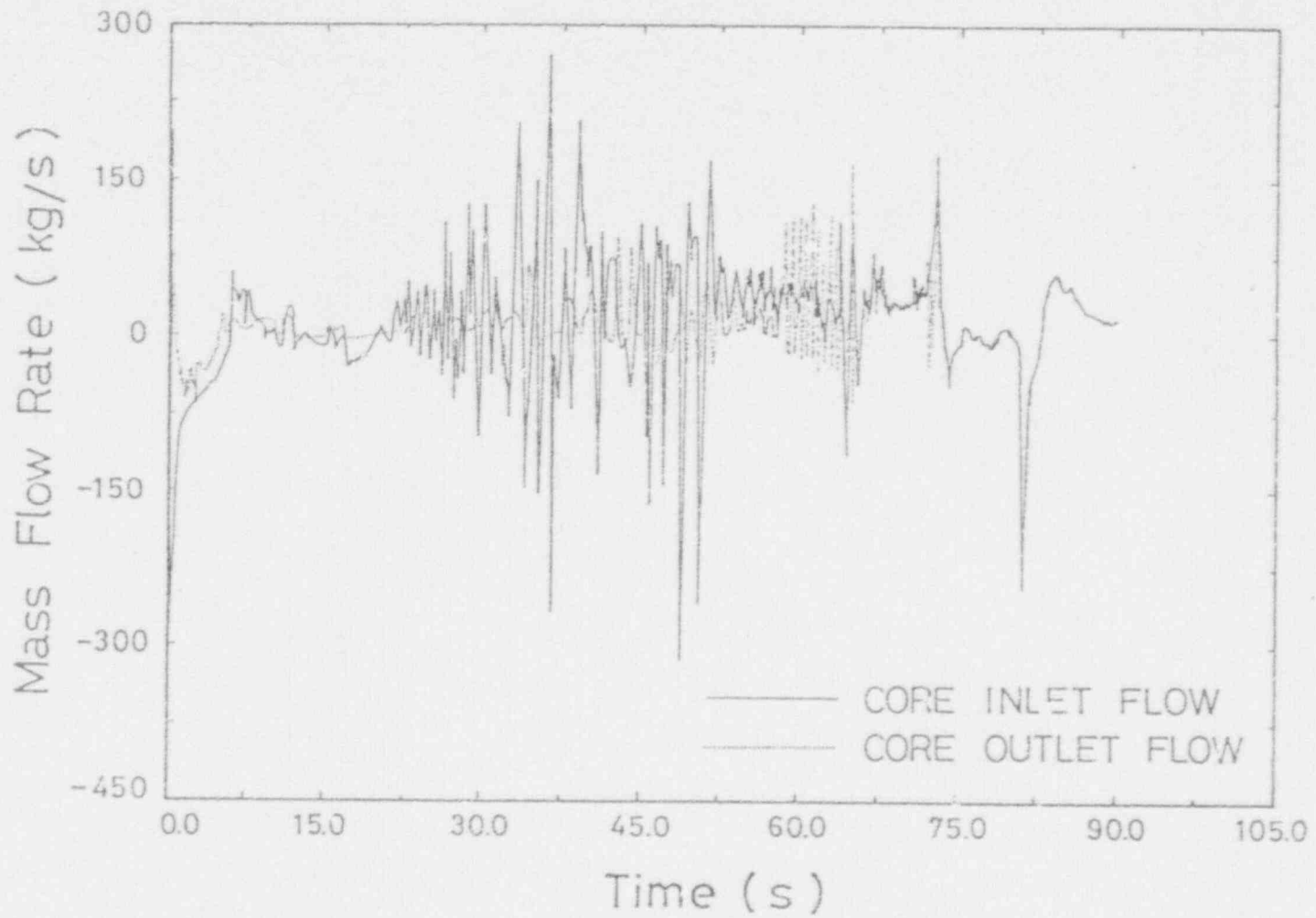


Figure 4.13 Calculated Core Flow Rates of Test L2-5 Simulation

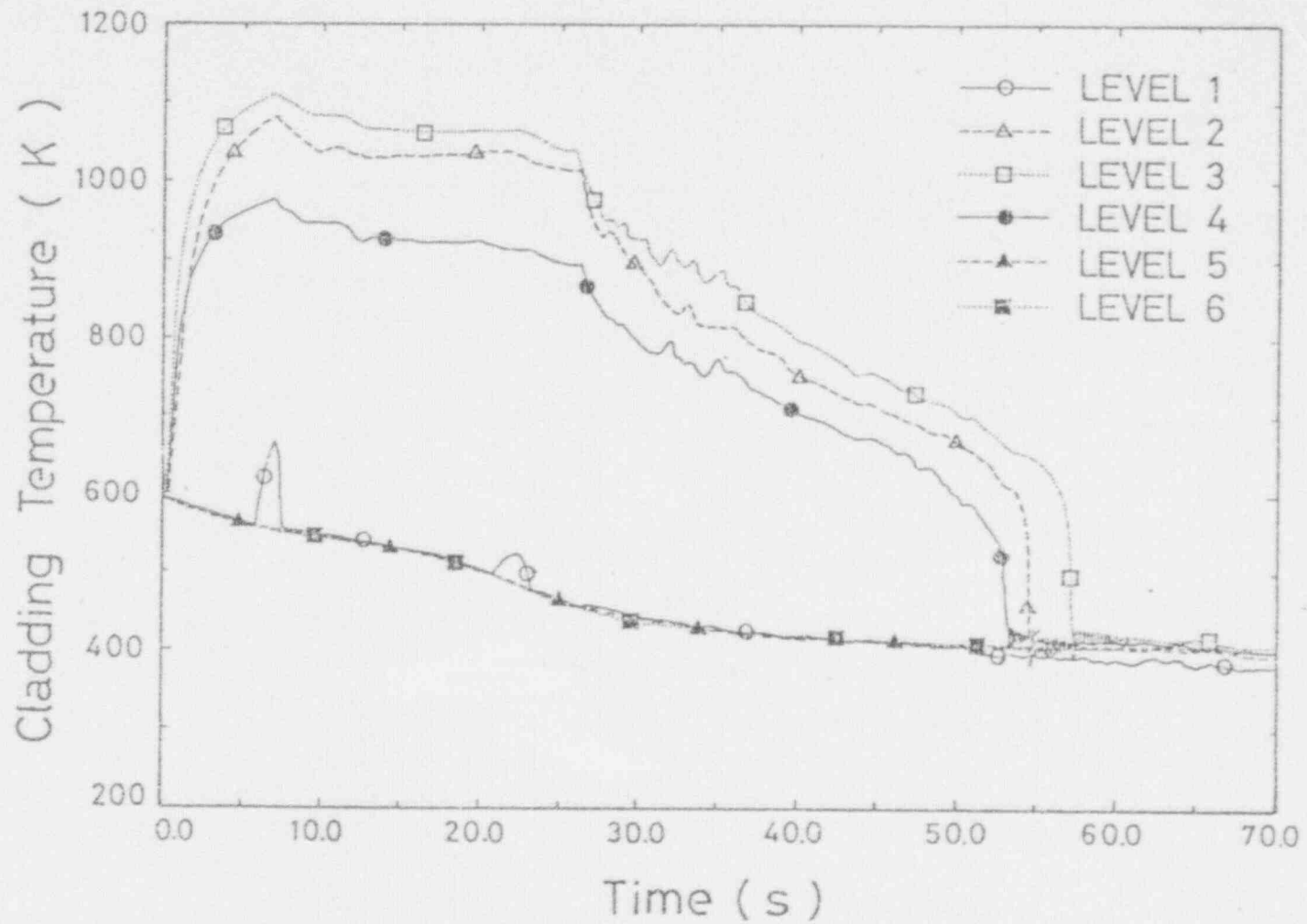


Figure 4.14 Calculated Cladding Temperatures at Hot Channel Hot Rod of Test L2-5 Simulation

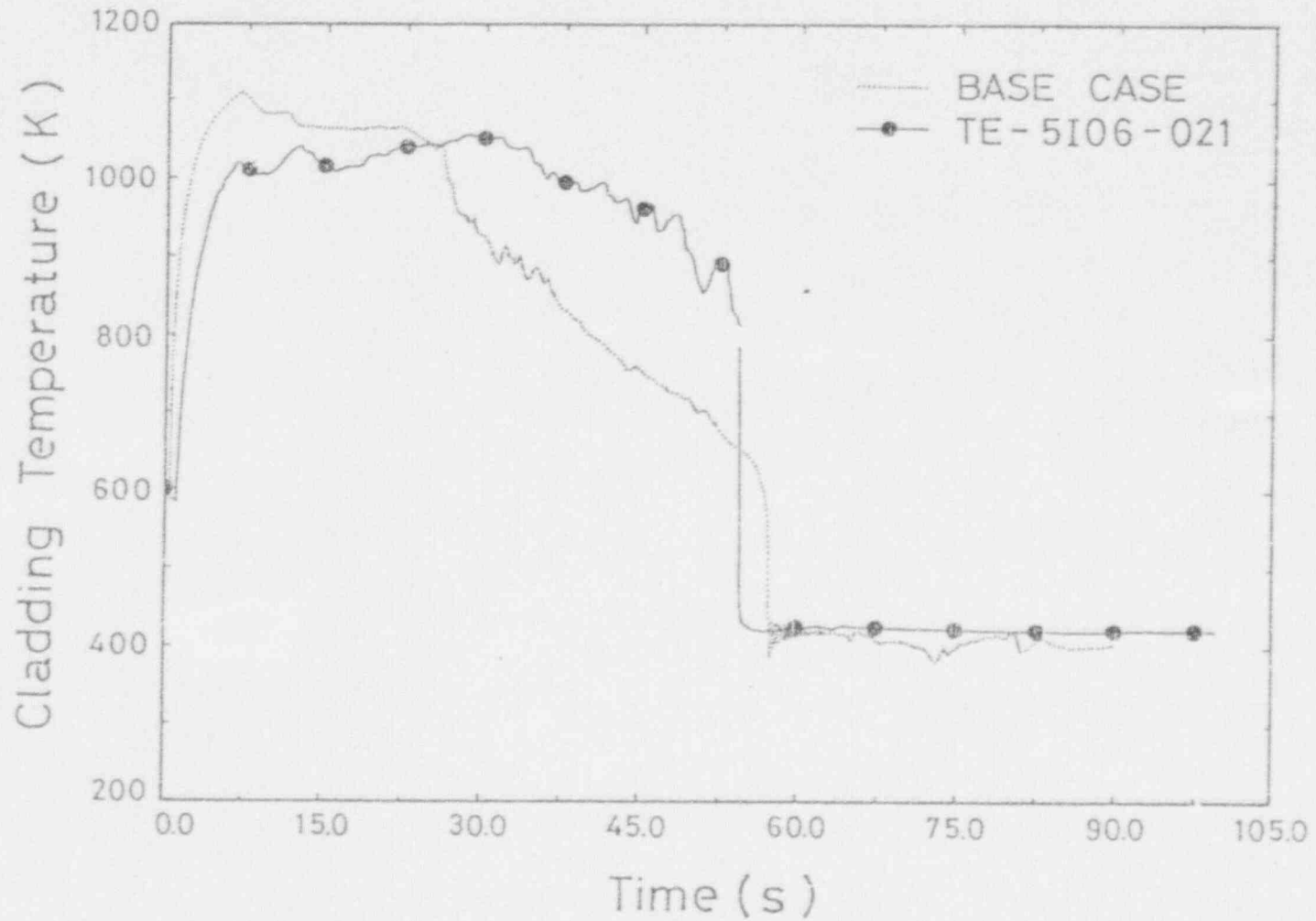


Figure 4.15 Comparison between the Calculated and Measured Cladding Temperatures of Test L2-5

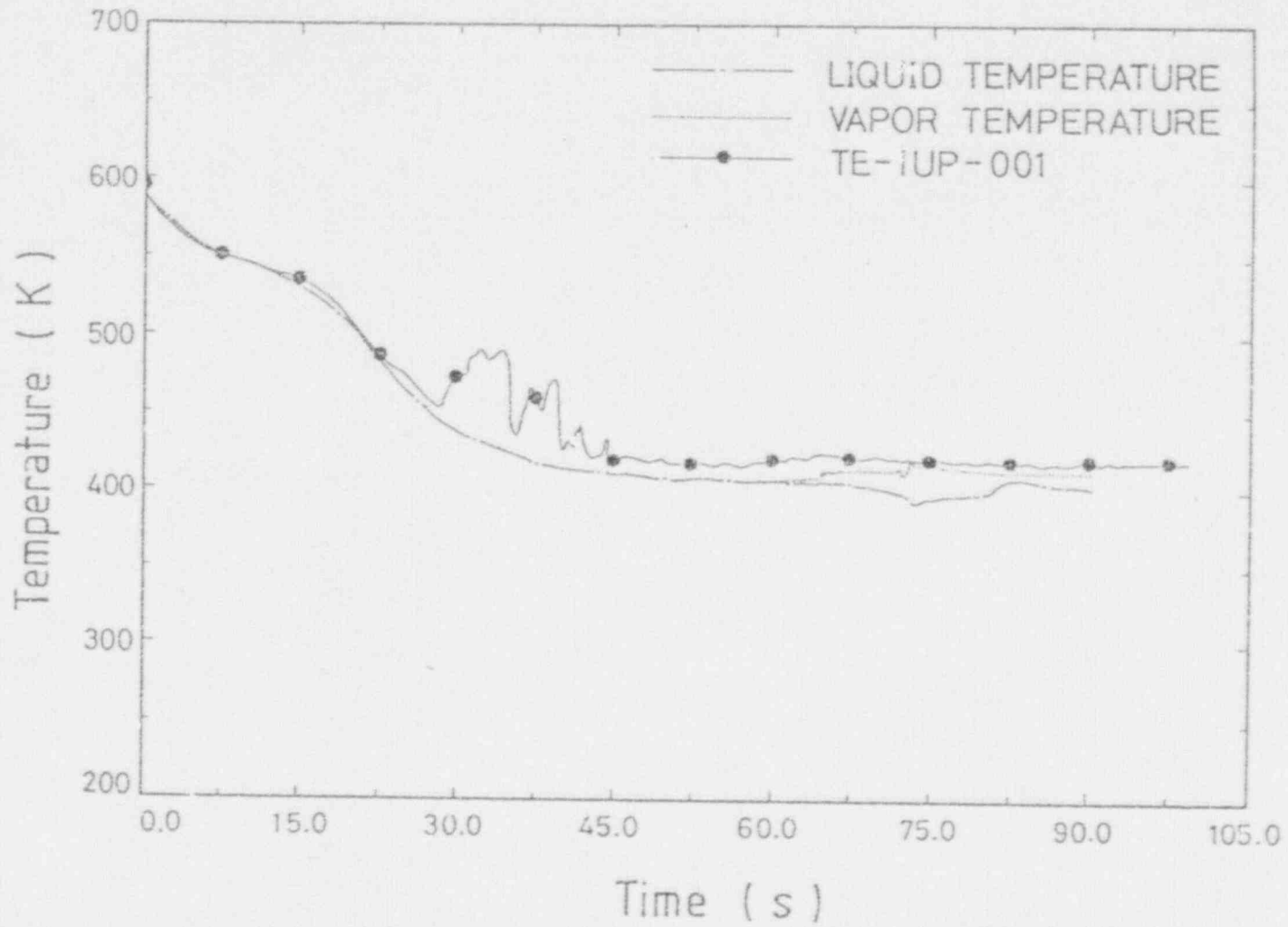


Figure 4.16 Comparison between the Calculated and Measured Upper Plenum Fluid Temperatures of Test L2-5

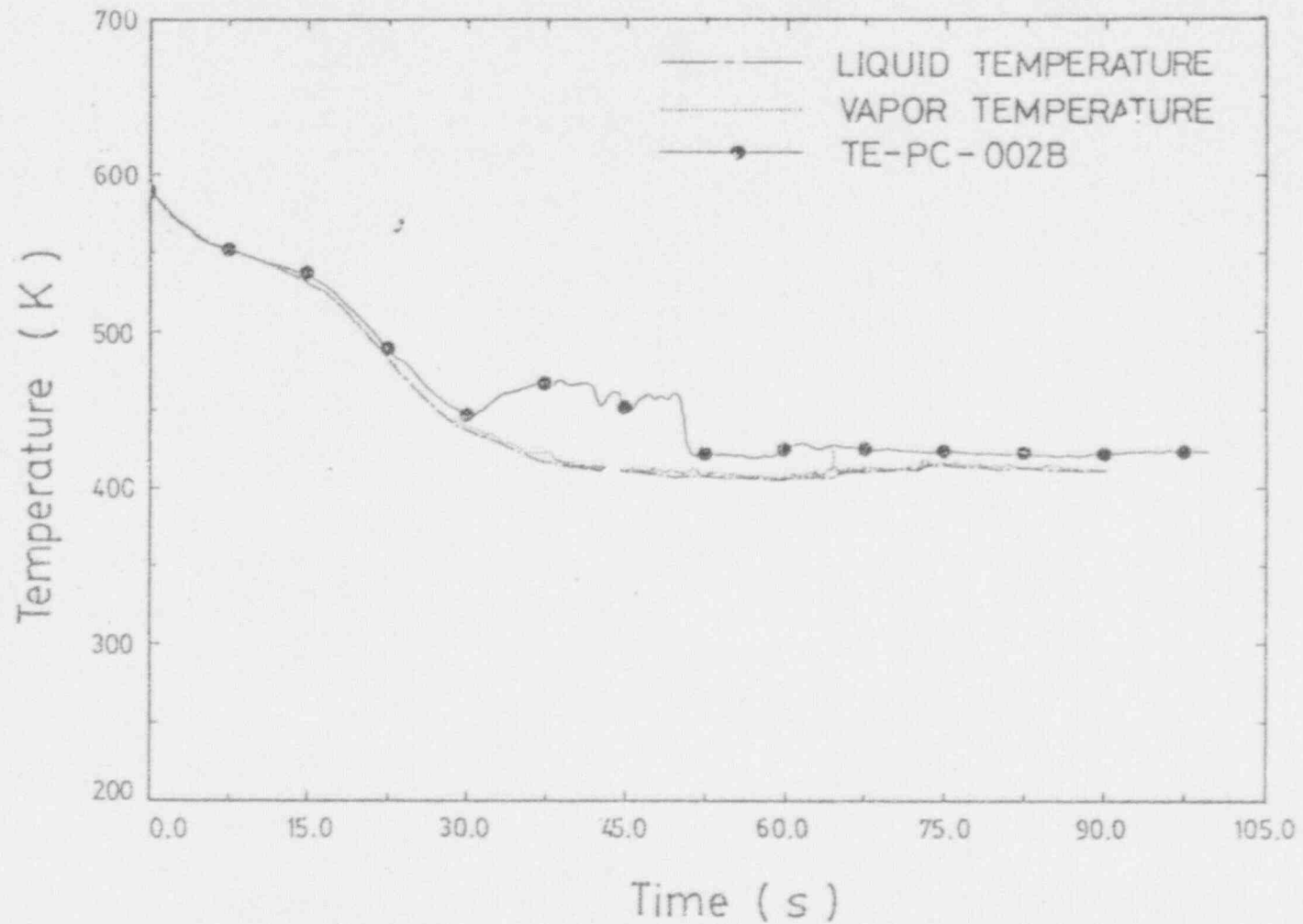


Figure 4.17 Comparison between the Calculated and Measured Intact Loop Hot-Leg Fluid Temperatures of Test L2-5

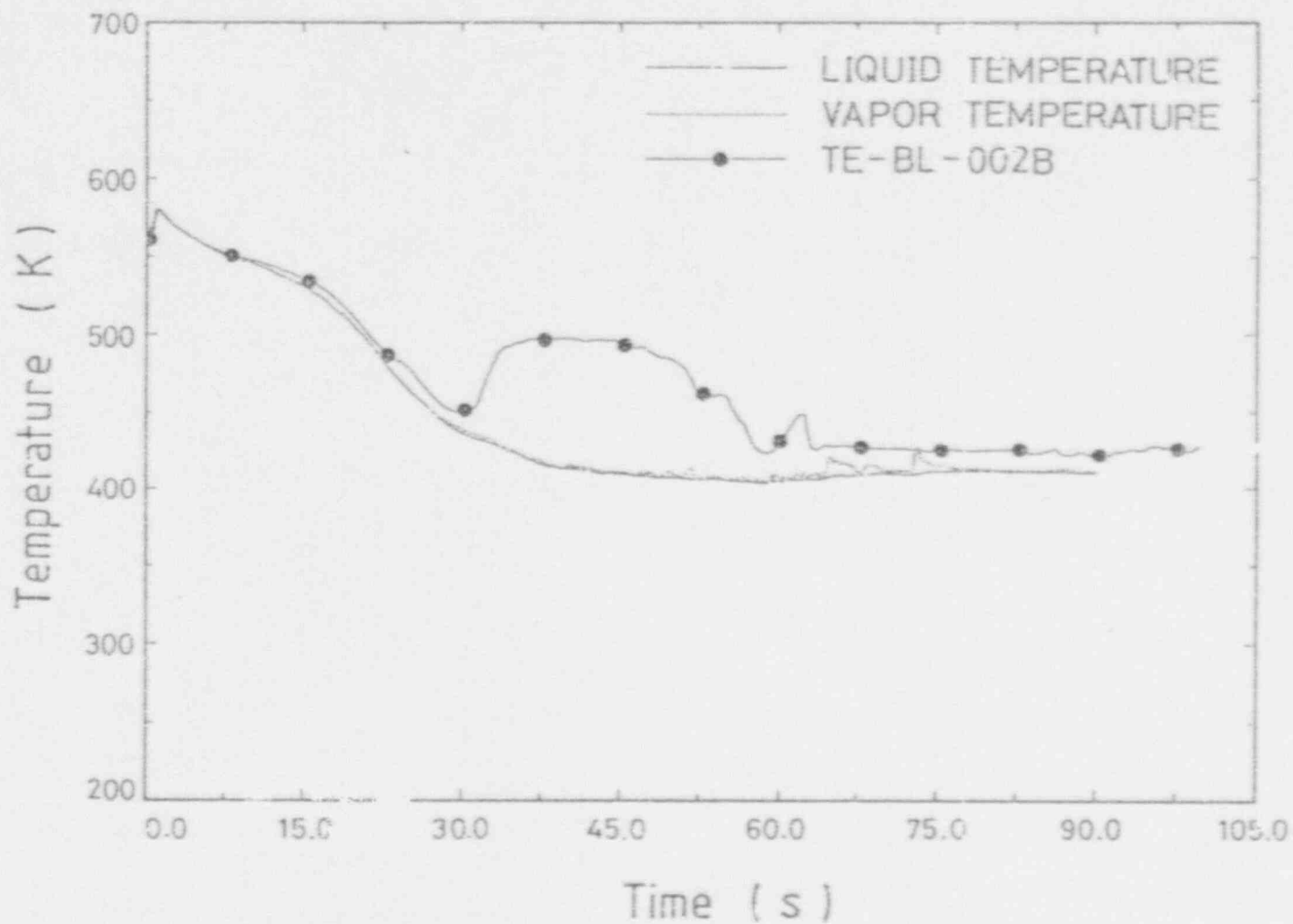


Figure 4.18 Comparison between the Calculated and Measured Broken Loop Hot-Leg Fluid Temperatures of Test L2-5

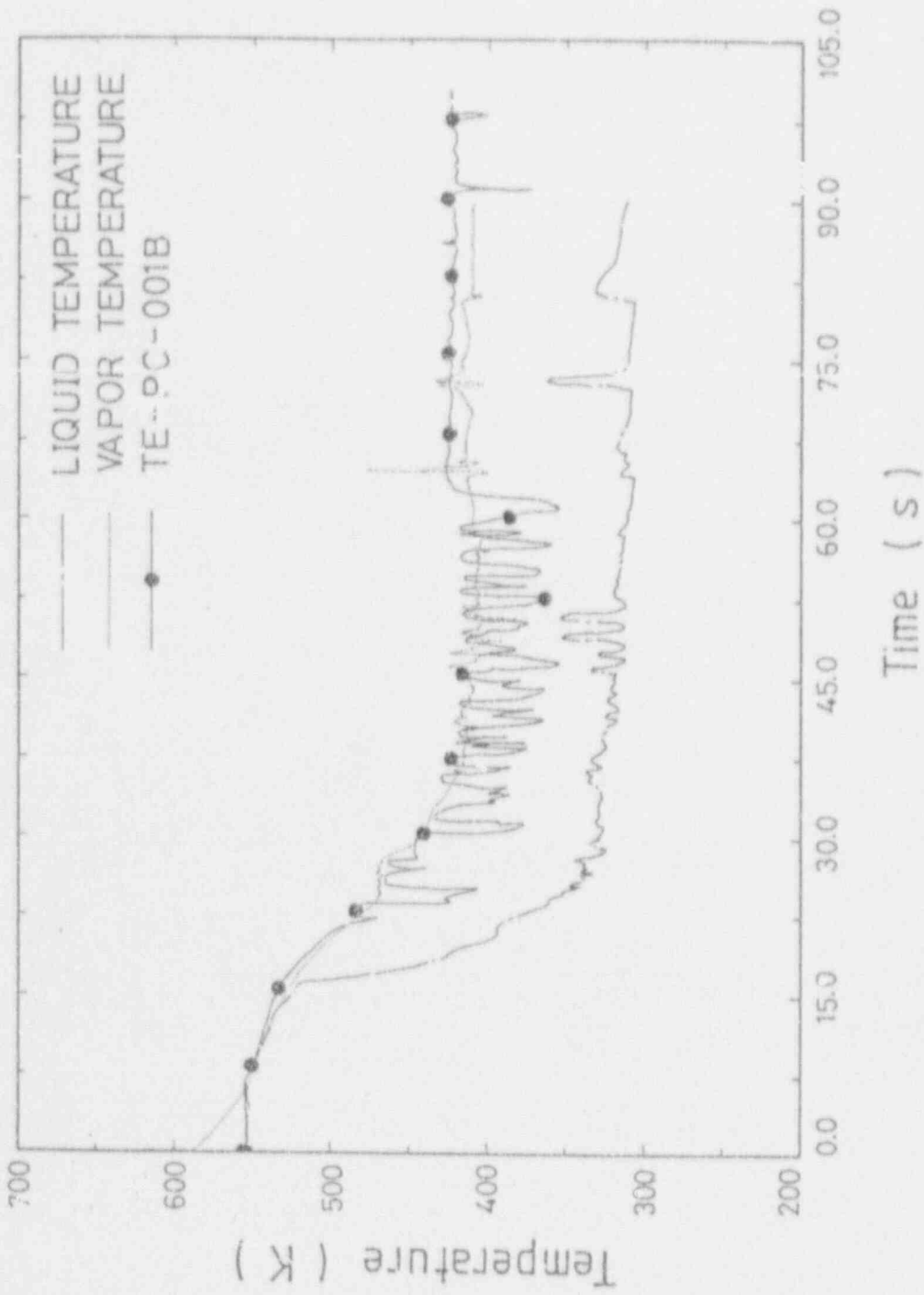


Figure 4.19 Comparison between the Calculated and Measured Intact Loop Cold-Leg Fluid Temperatures of Test L2-5

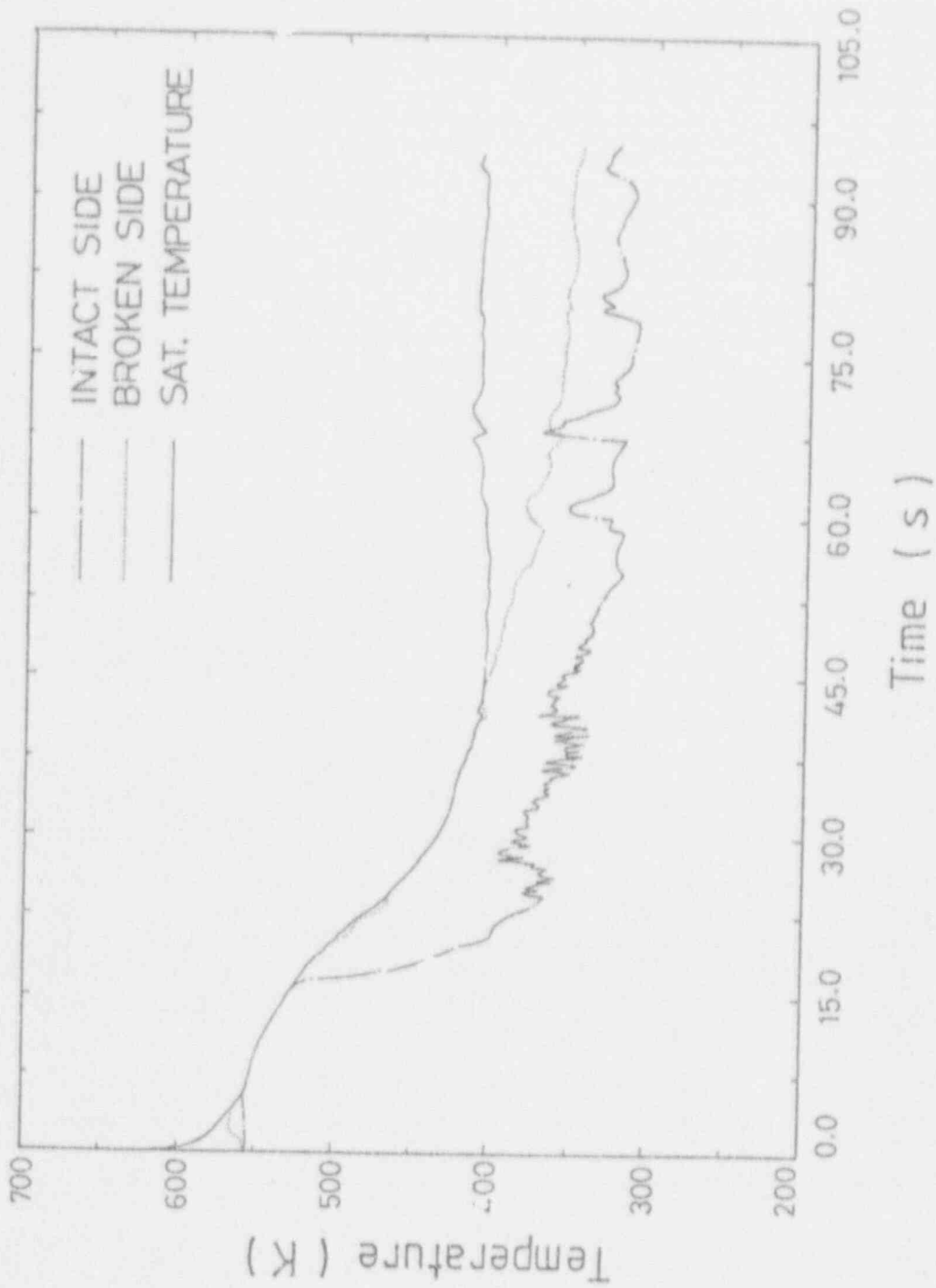


Figure 4.20 Calculated Fluid Temperatures in Upper downcomer of Test L2-5 Simulation

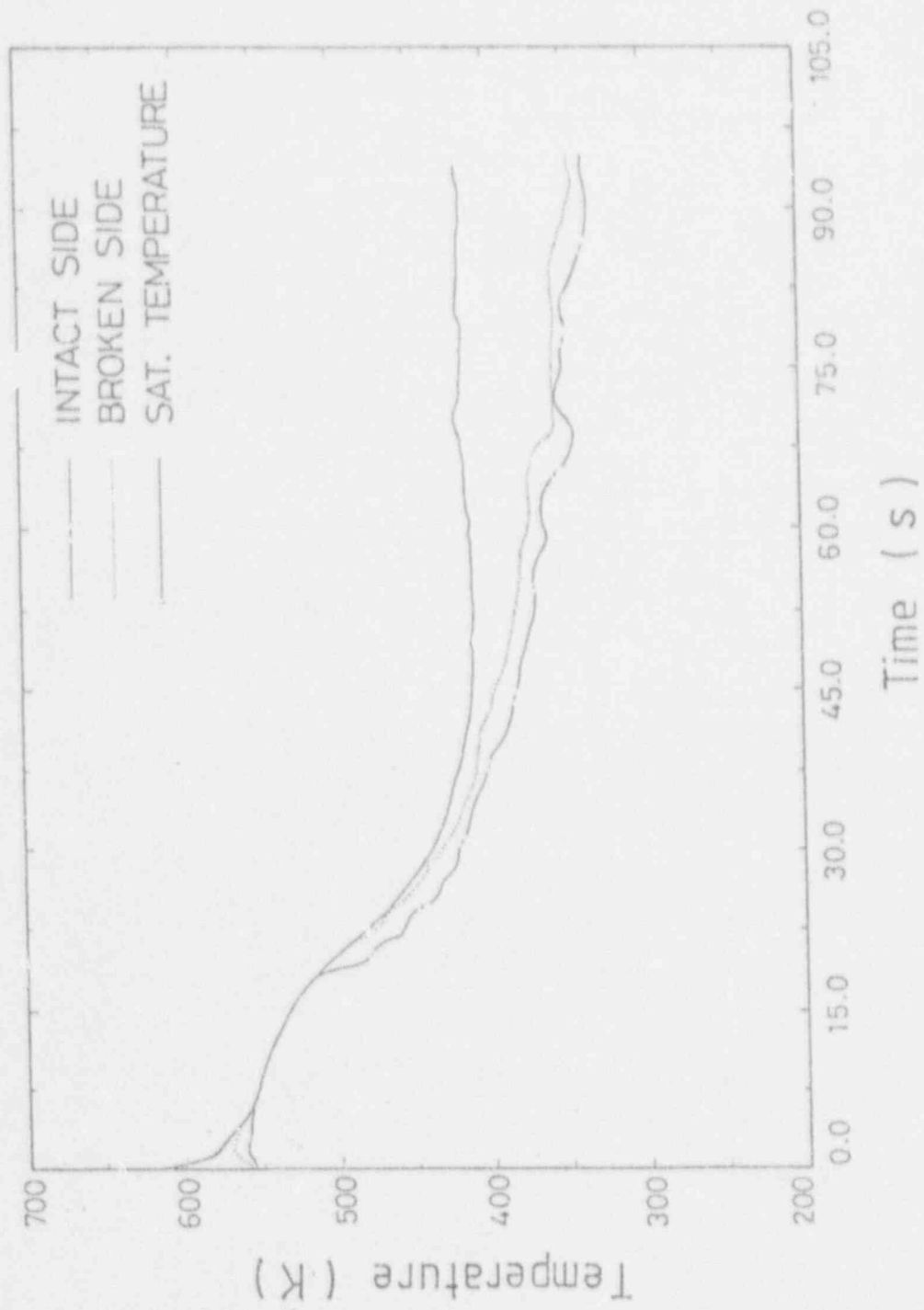


Figure 4.21 Calculated Fluid Temperatures in Lower Downcomer of Test L2-5 Simulation

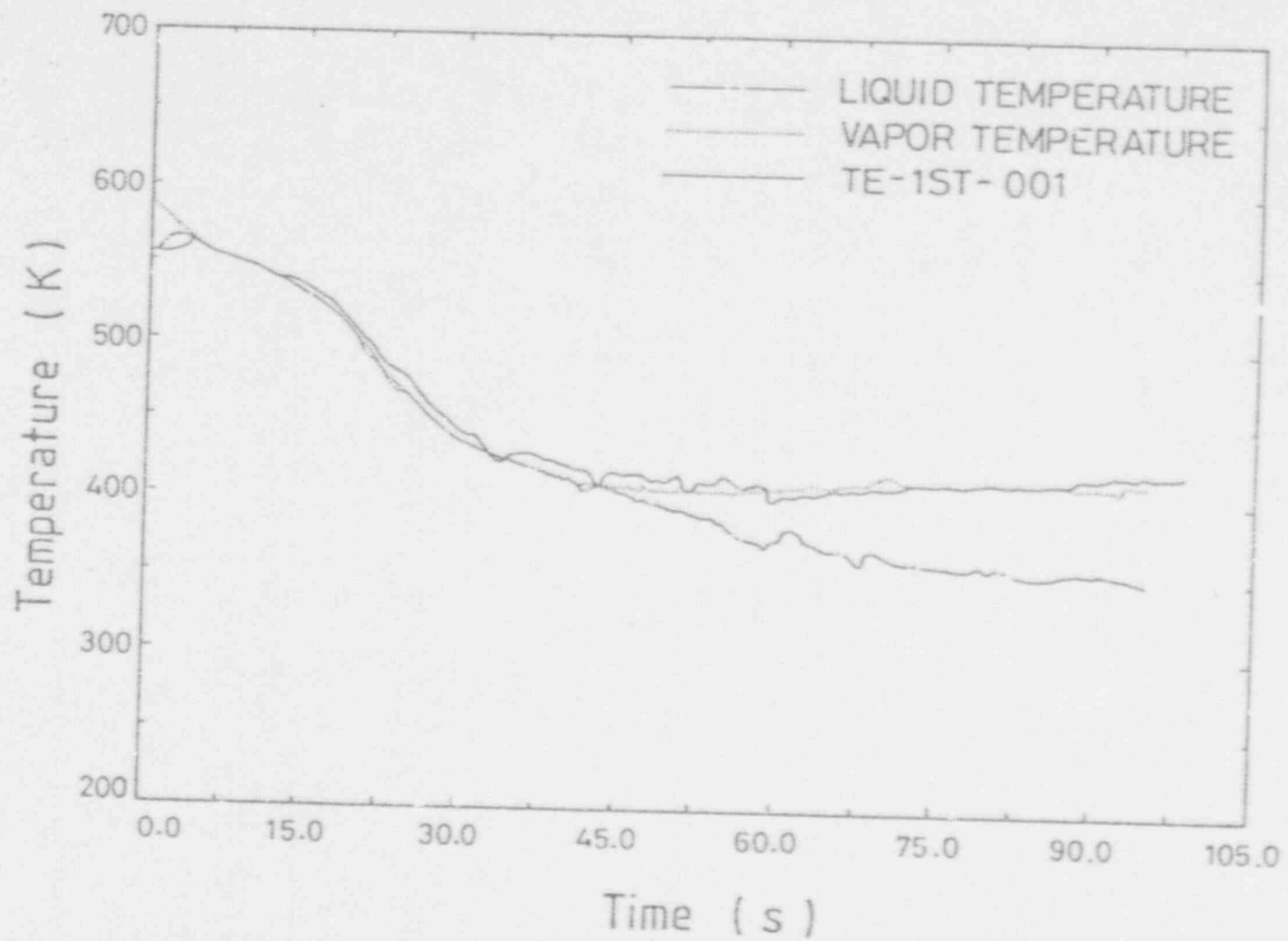


Figure 4.22 Comparison between the Calculated and Measured Downcomer (4.8 m from RV Bottom) Fluid Temperatures of Test L2-5

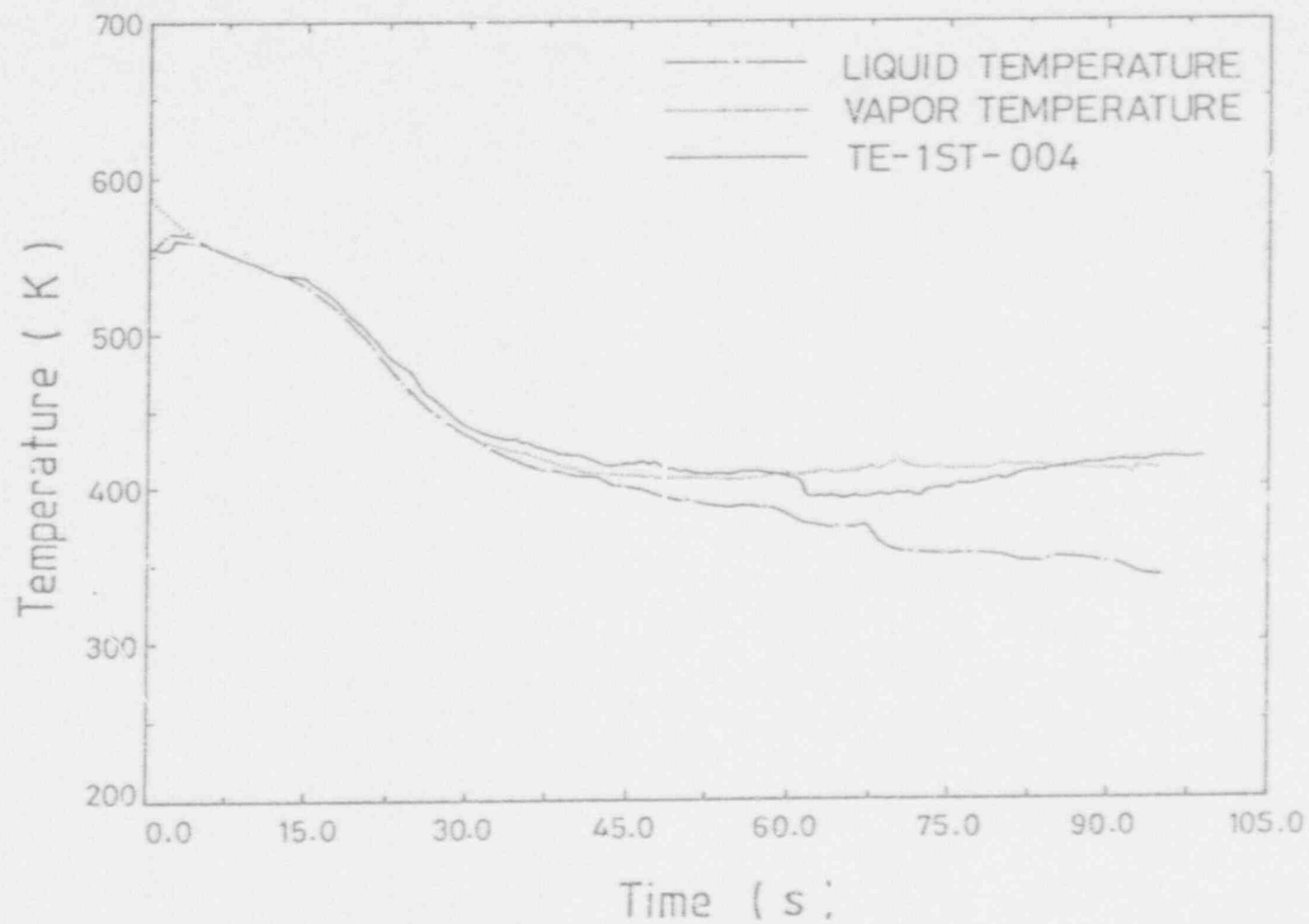


Figure 4.23 Comparison between the Calculated and Measured Downcomer (2.98 m from RV Bottom) Fluid Temperatures of Test L2-5

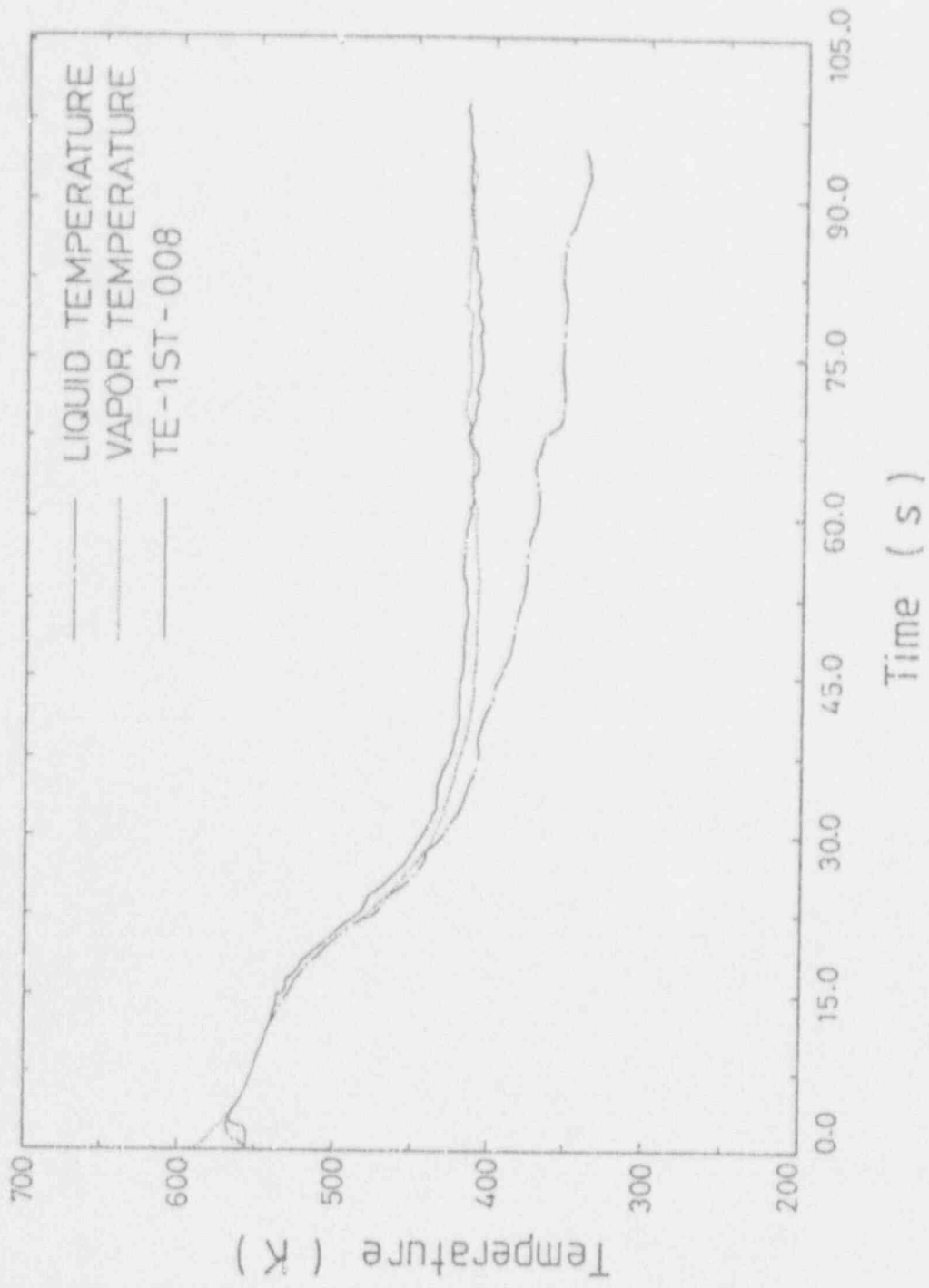


Figure 4.24 Comparison between the Calculated and Measured Downcomer (0.74 m from RV Bottom) Fluid Temperatures of Test L2-5

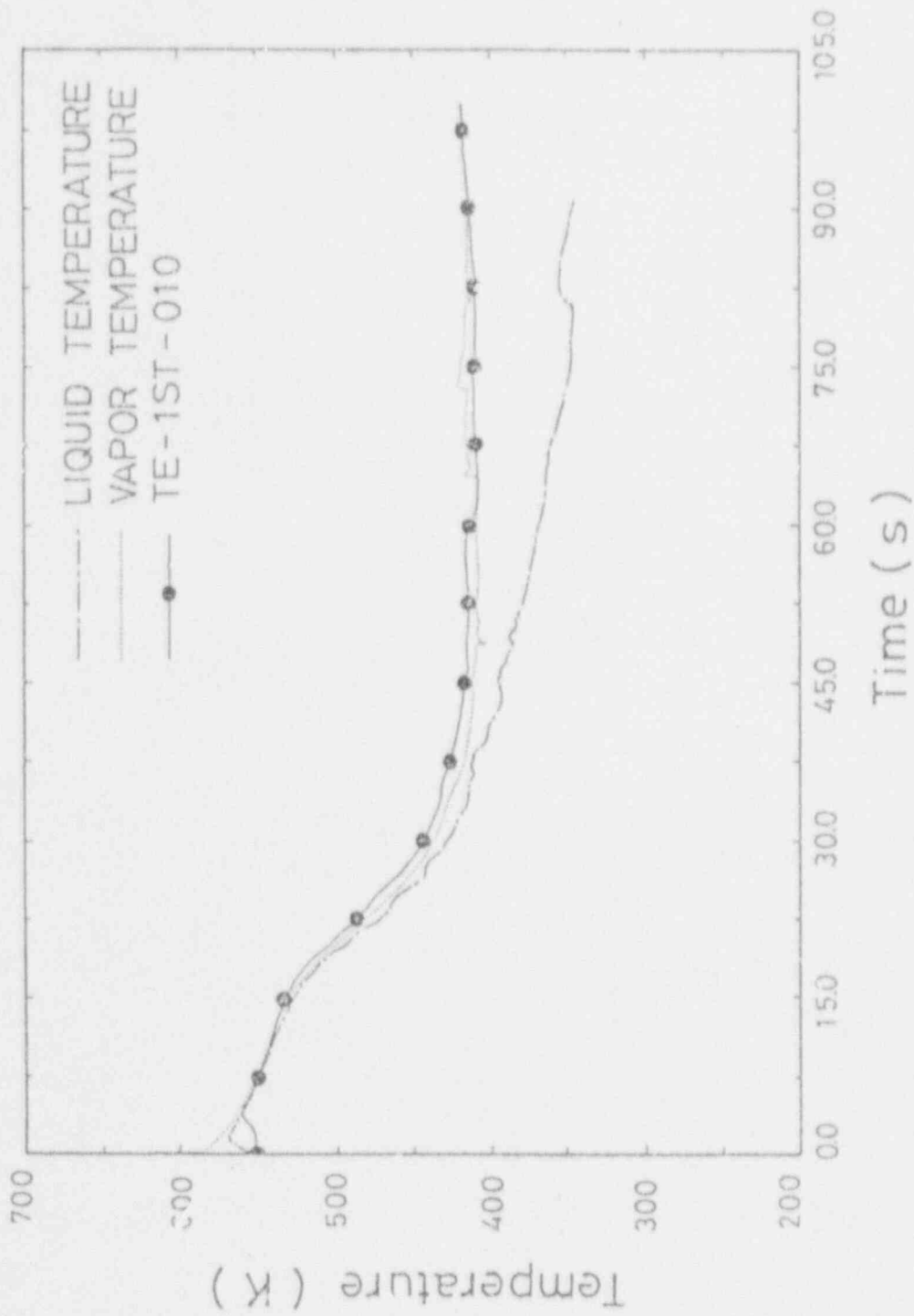


Figure 4.25 Comparison between the Calculated and Measured Downcomer (0.54 m from RV Bottom) Fluid Temperatures of Test L2-5

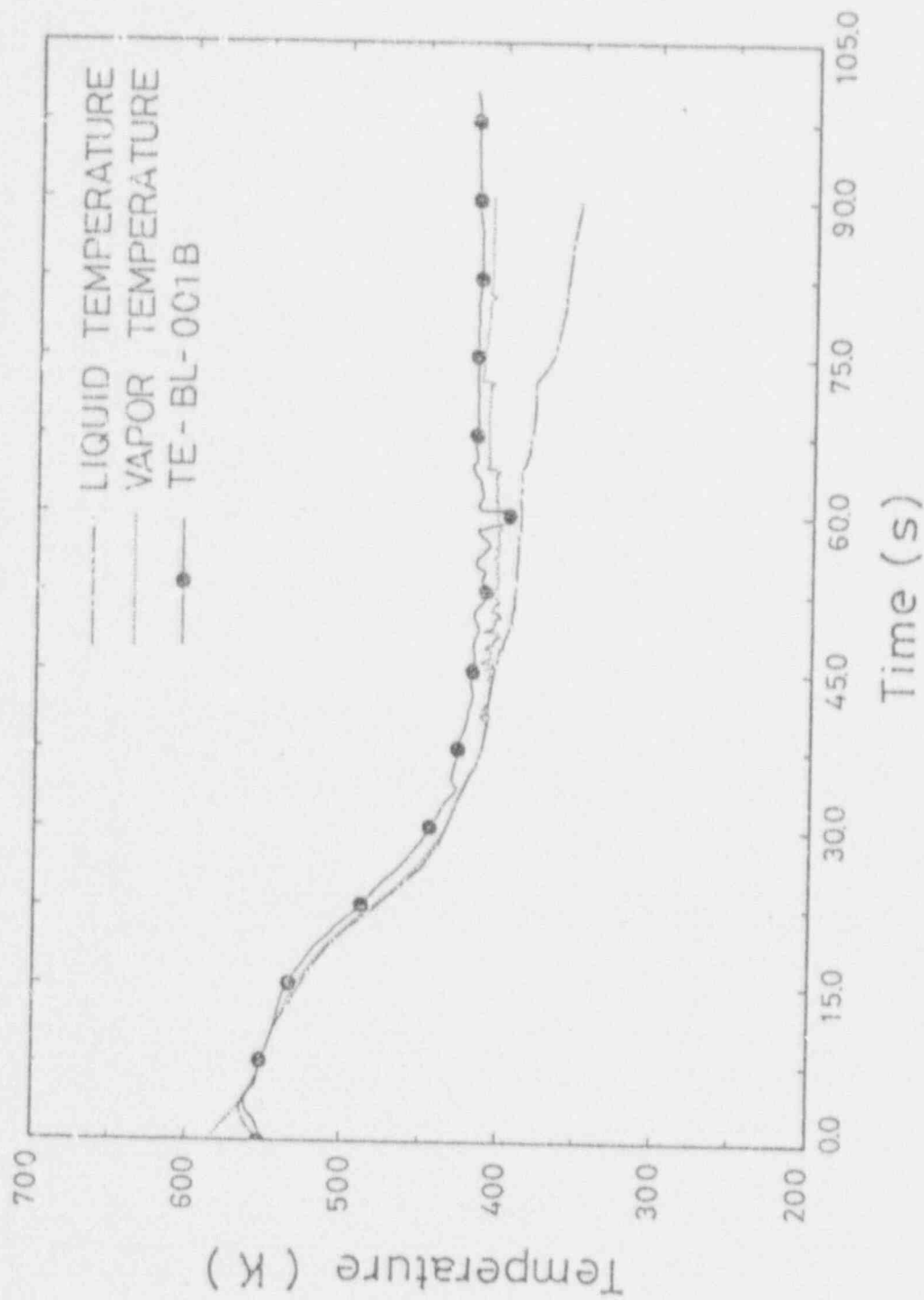


Figure 4.26 Comparison between the Calculated and Measured Broken Loop Cold-Leg Fluid Temperatures of Test L2-5

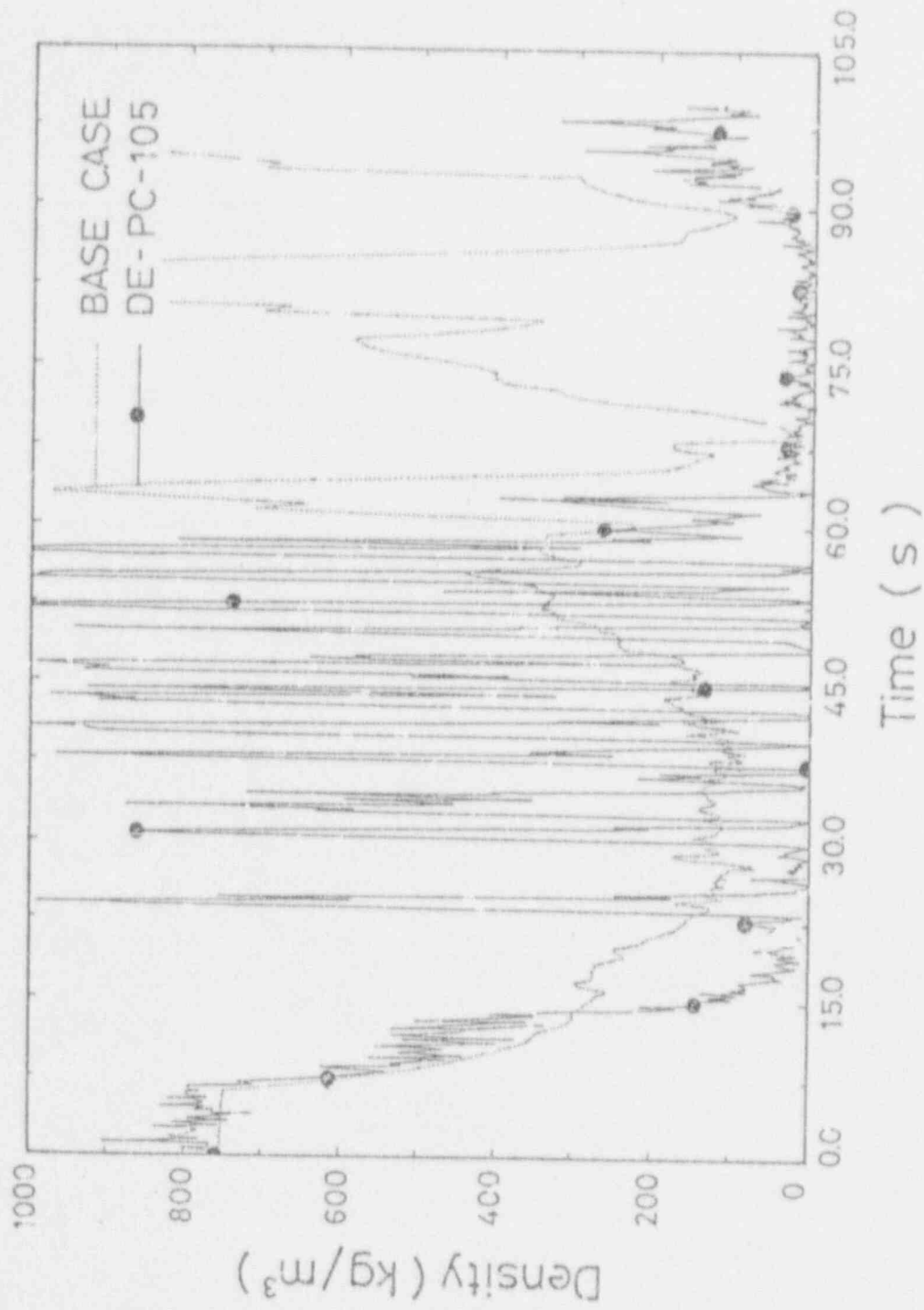


Figure 4.27 Comparison between the Calculated and Measured Intact Loop Cold-Leg Densities of Test L2-5

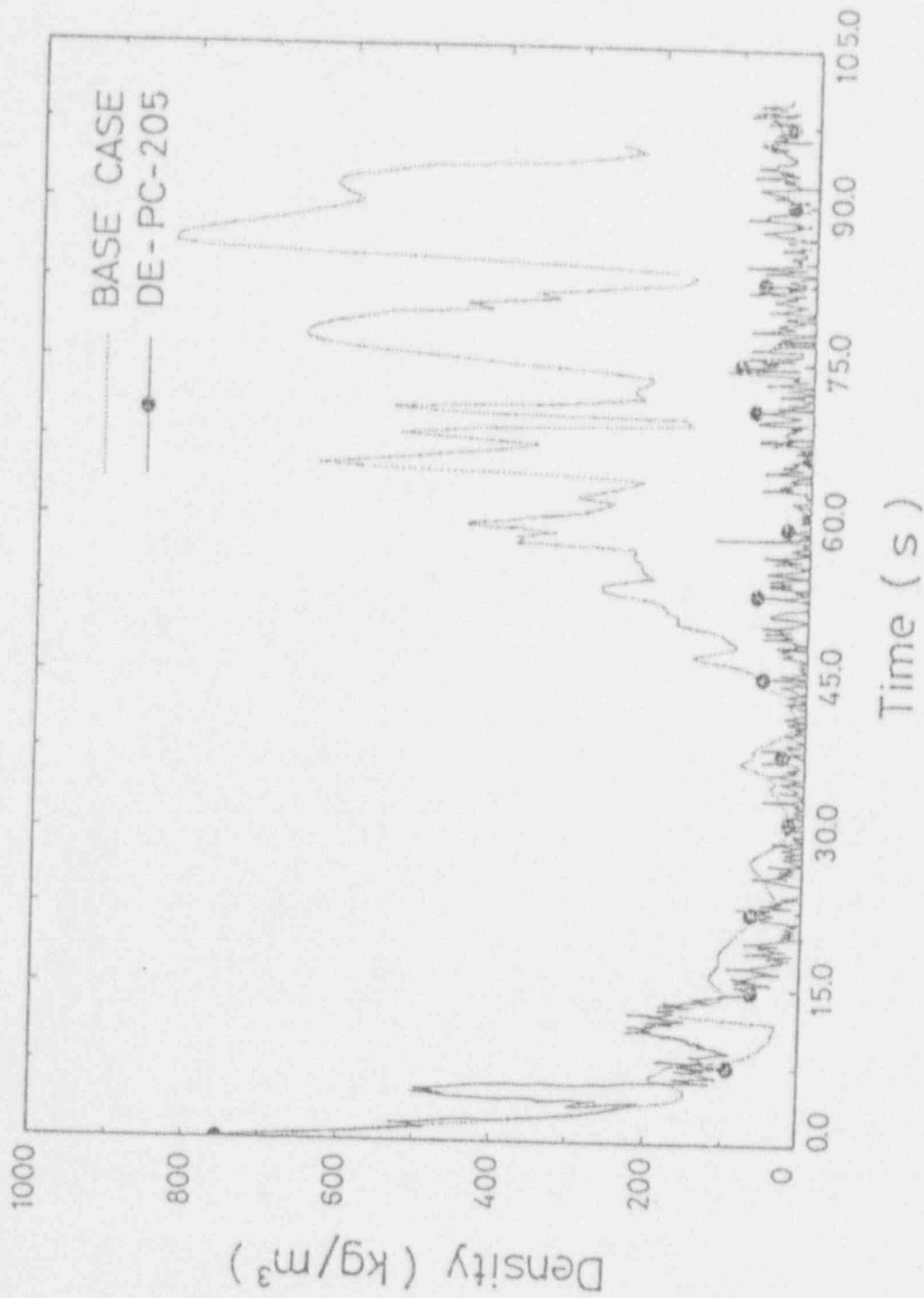


Figure 4.28 Comparison between the Calculated and Measured Intact Loop Hot-Leg Densities of Test L2-5

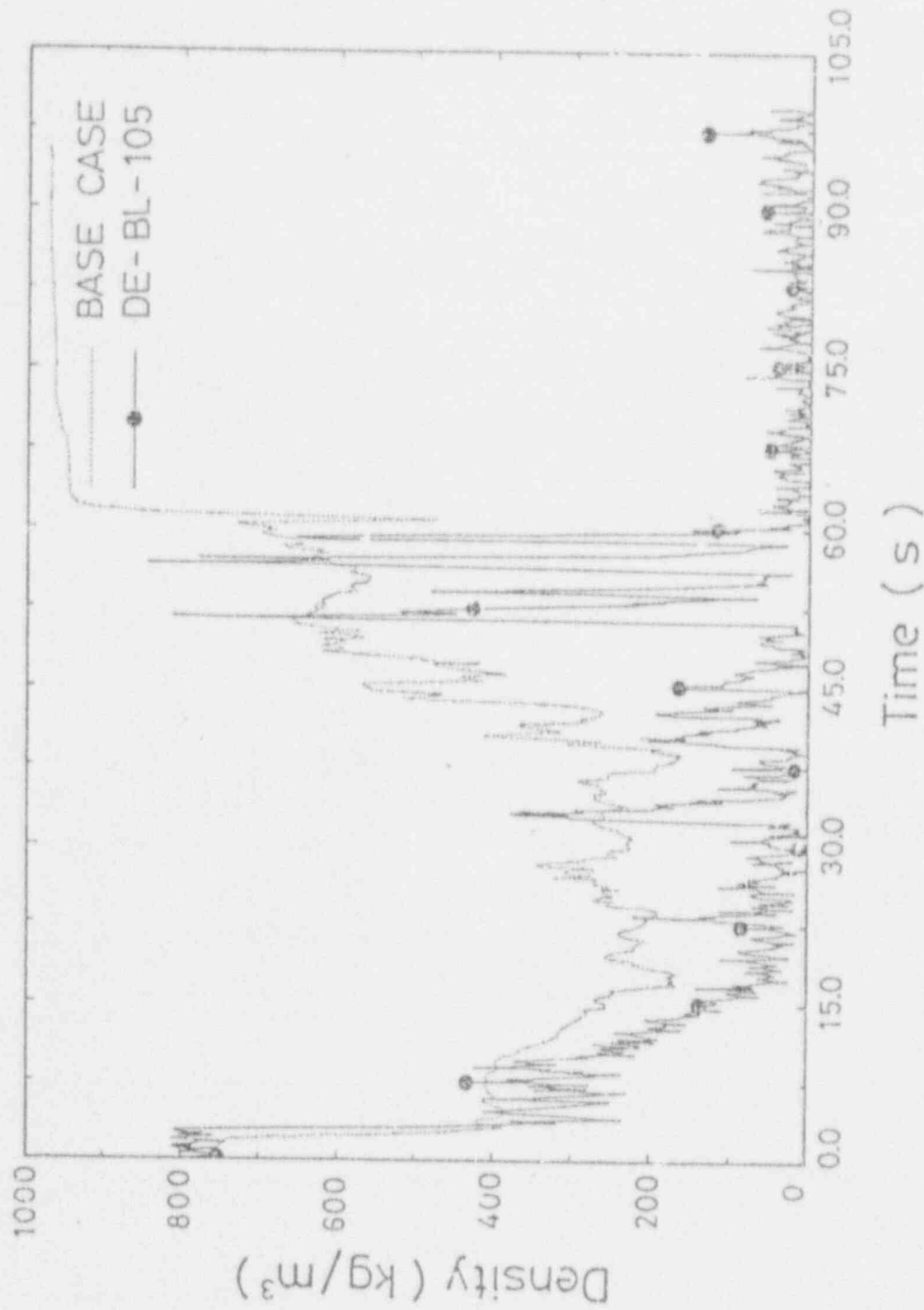


Figure 4.25 Comparison between the Calculated and Measured Broken Loop Cold-Leg Densities of Test L2-5

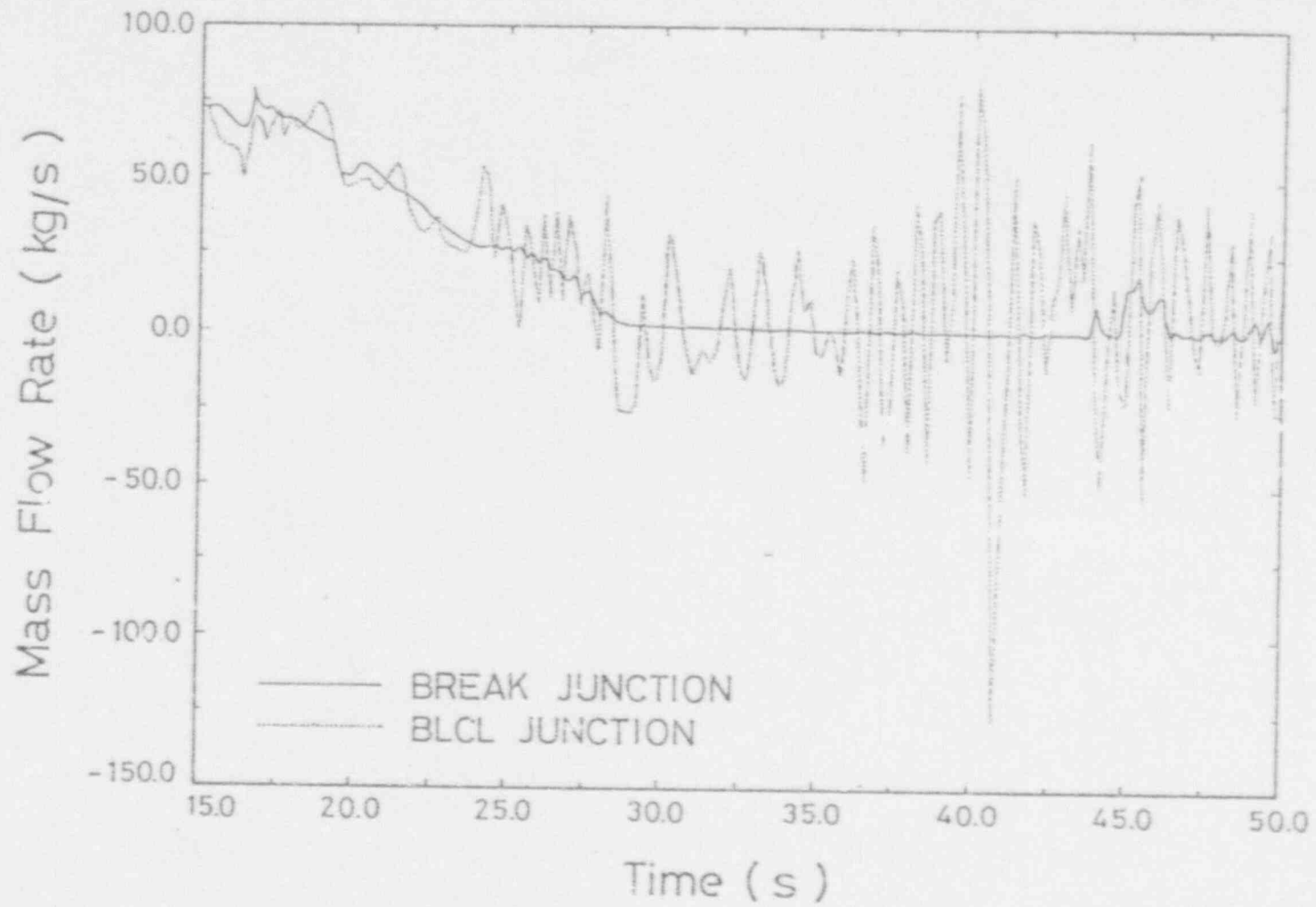


Figure 4.30 Calculated Flow Rates in Broken Loop Cold-Leg of Test L2-5 Simulation

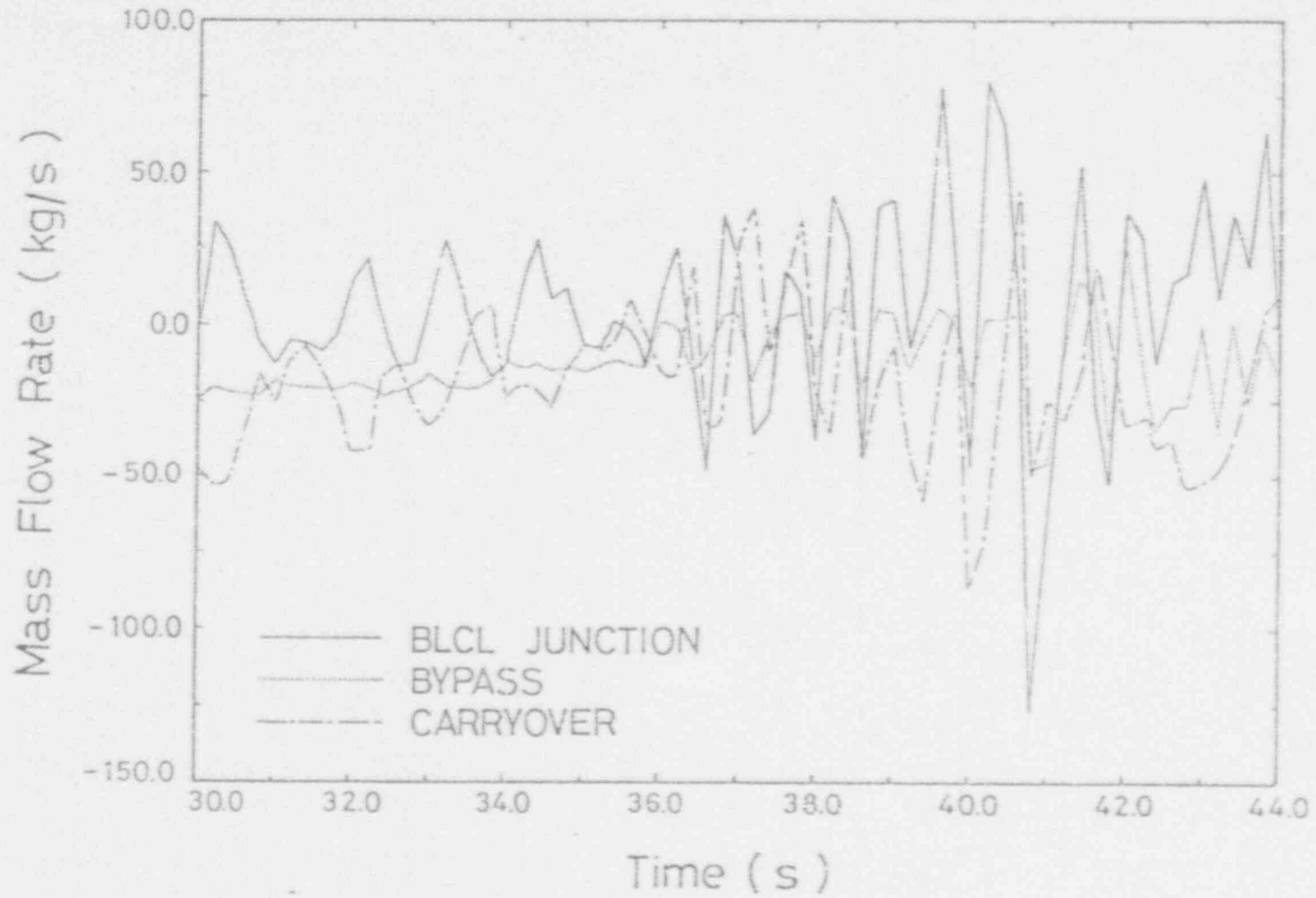


Figure 4.31 Calculated Flow Rates in Reactor Vessel Near Broken Loop Cold-Leg of Test L2-5 Simulation

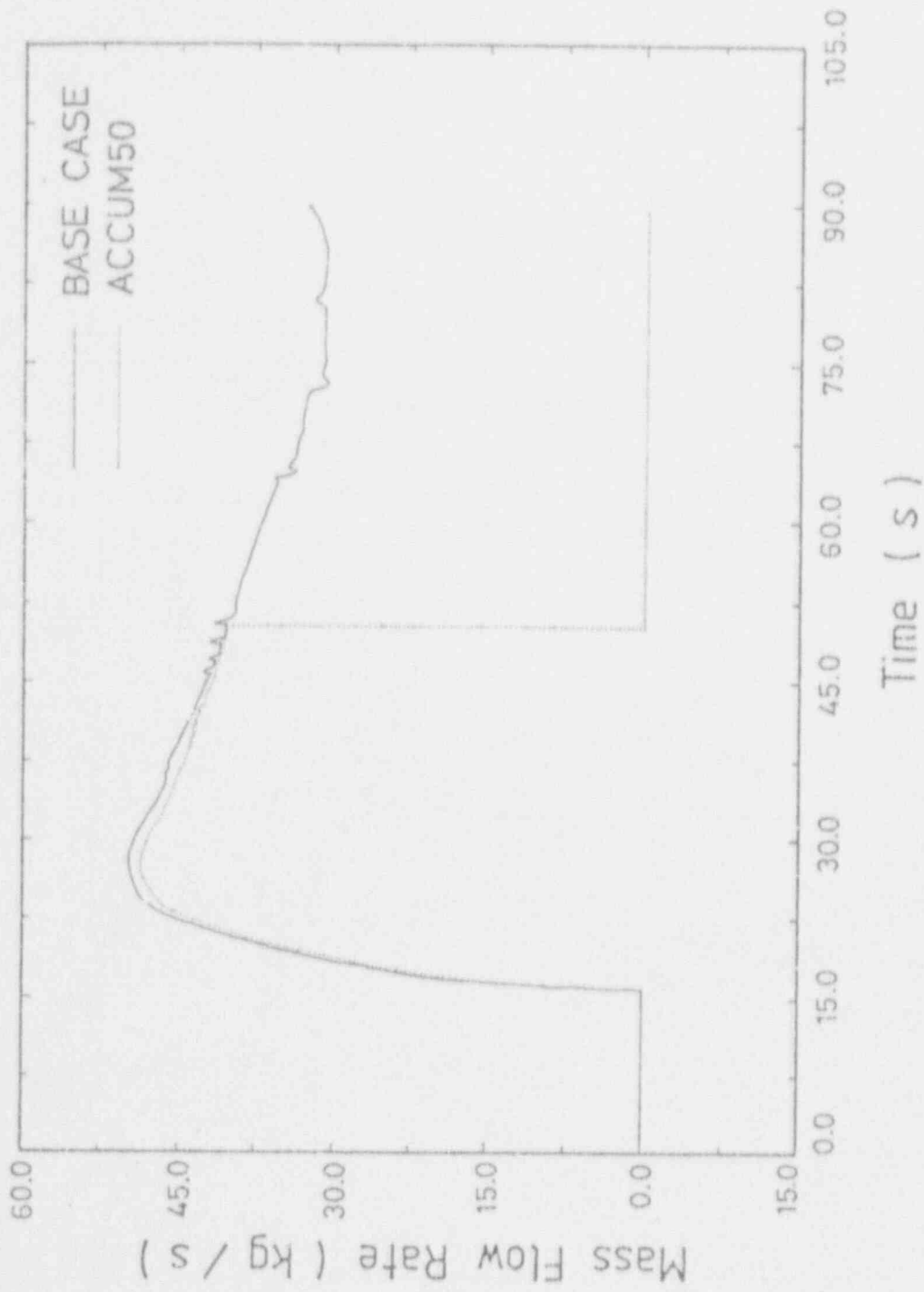


Figure 4.37 Comparison between Calculated Accumulator Flow Rates of the BASE and ACCUM50 Cases

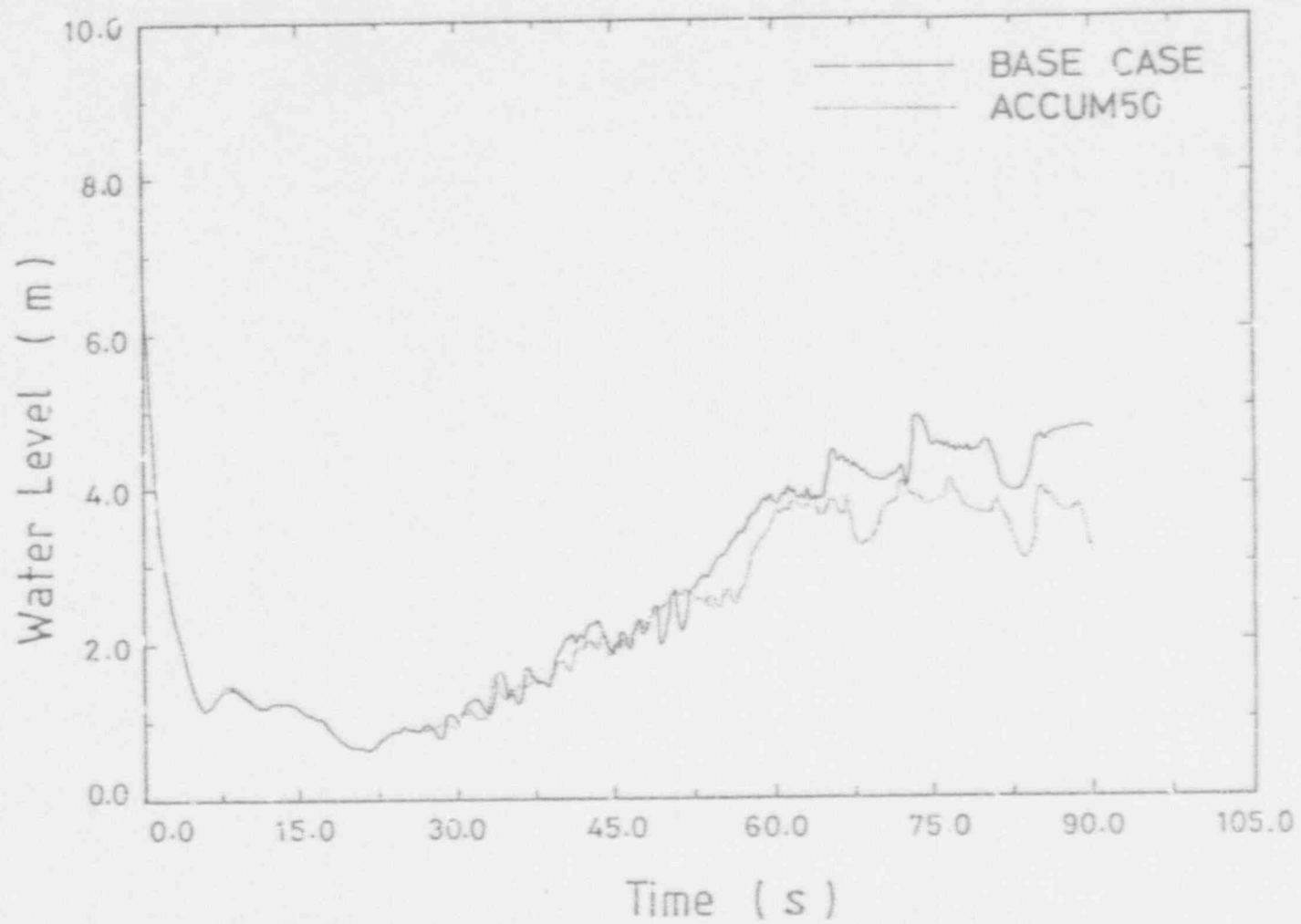


Figure 4.33 Comparison between Calculated Water Levels in Core Region of the BASE and ACCUM50 Cases

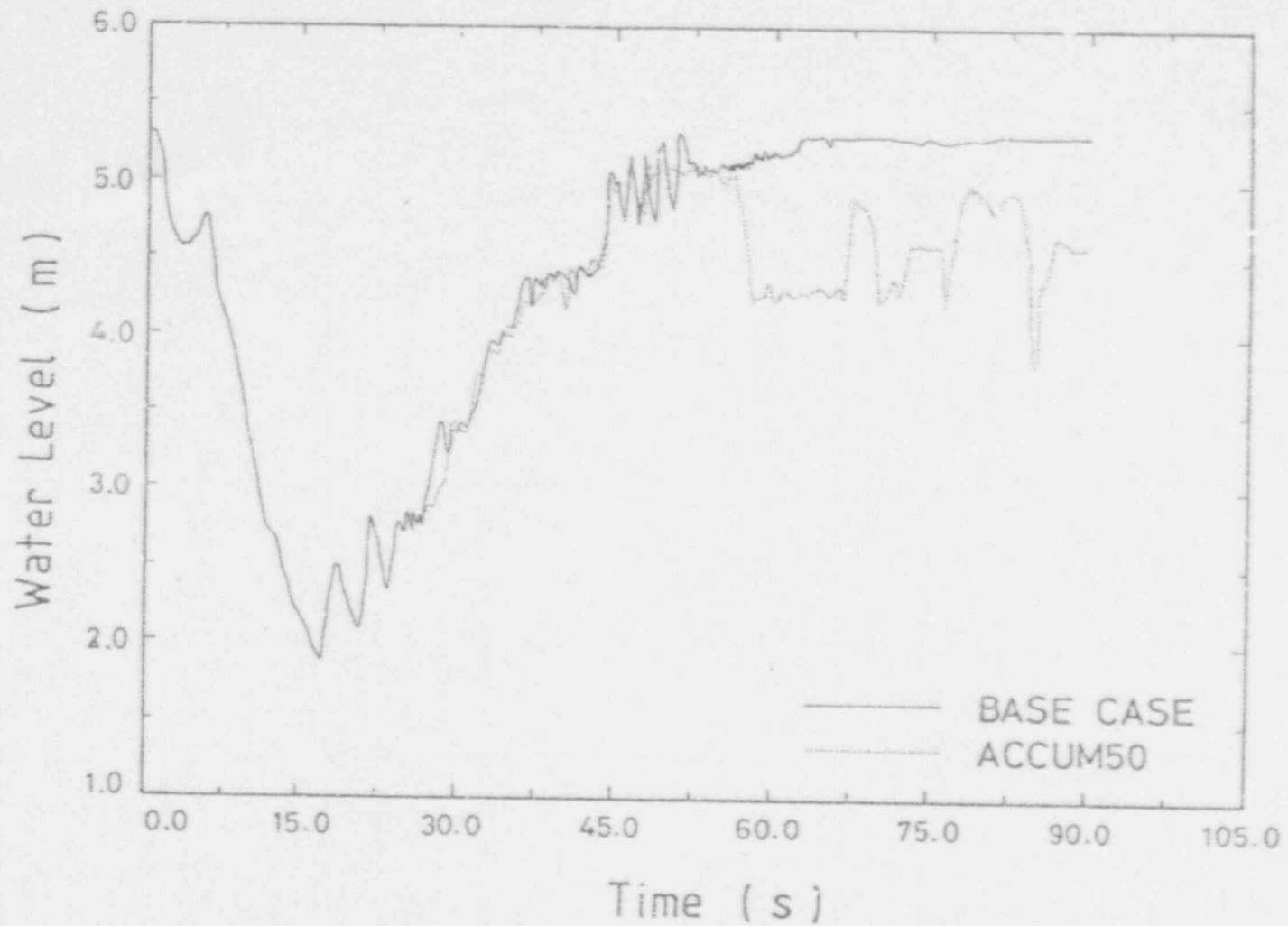


Figure 4.34 Comparison between Calculated Water Levels in Downcomer Near Intact Loop of the BASE and ACCUM50 Cases

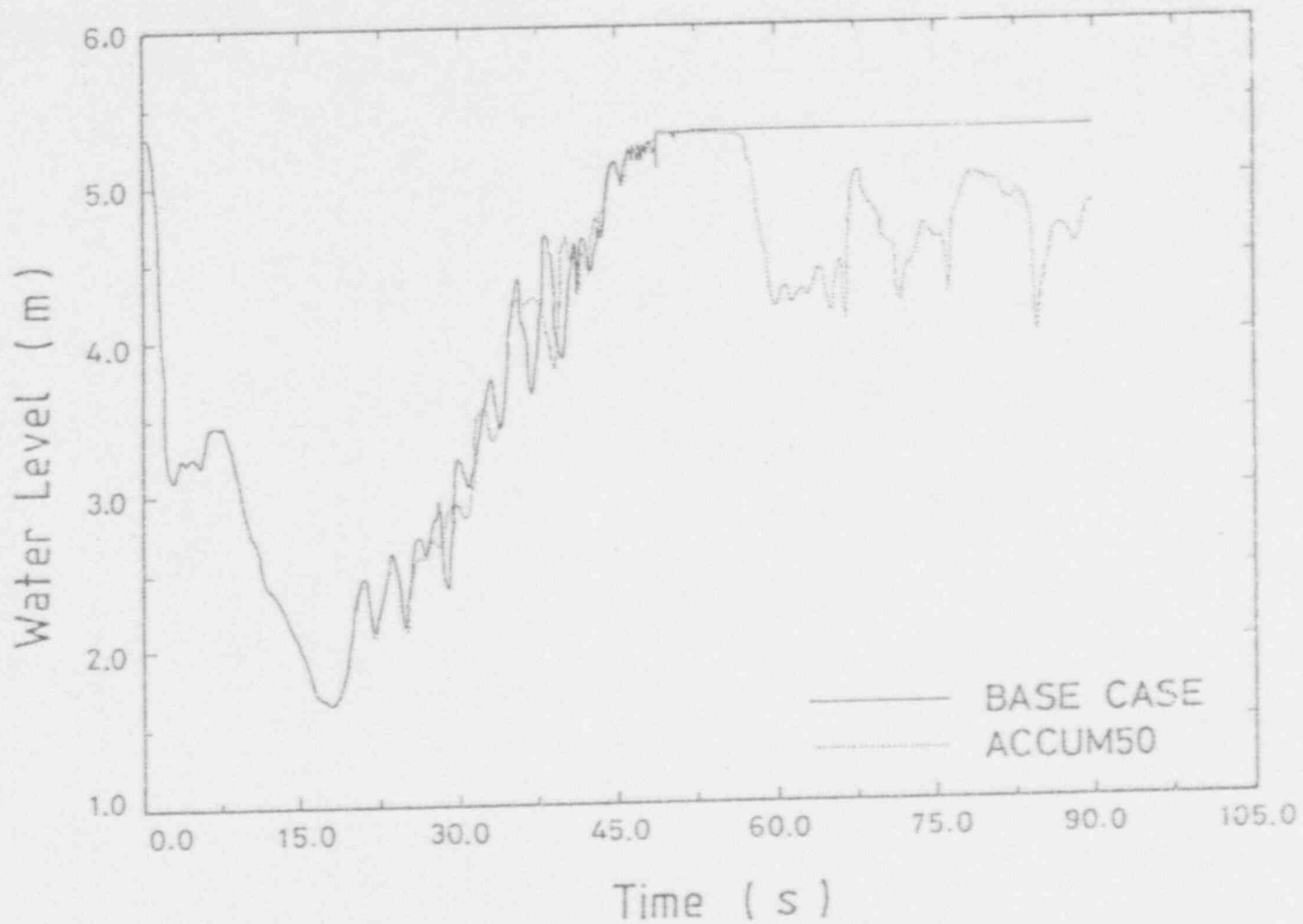


Figure 4.35 Comparison between Calculated Water Levels in Downcomer Near Broken Loop of the BASE and ACCUM50 Cases

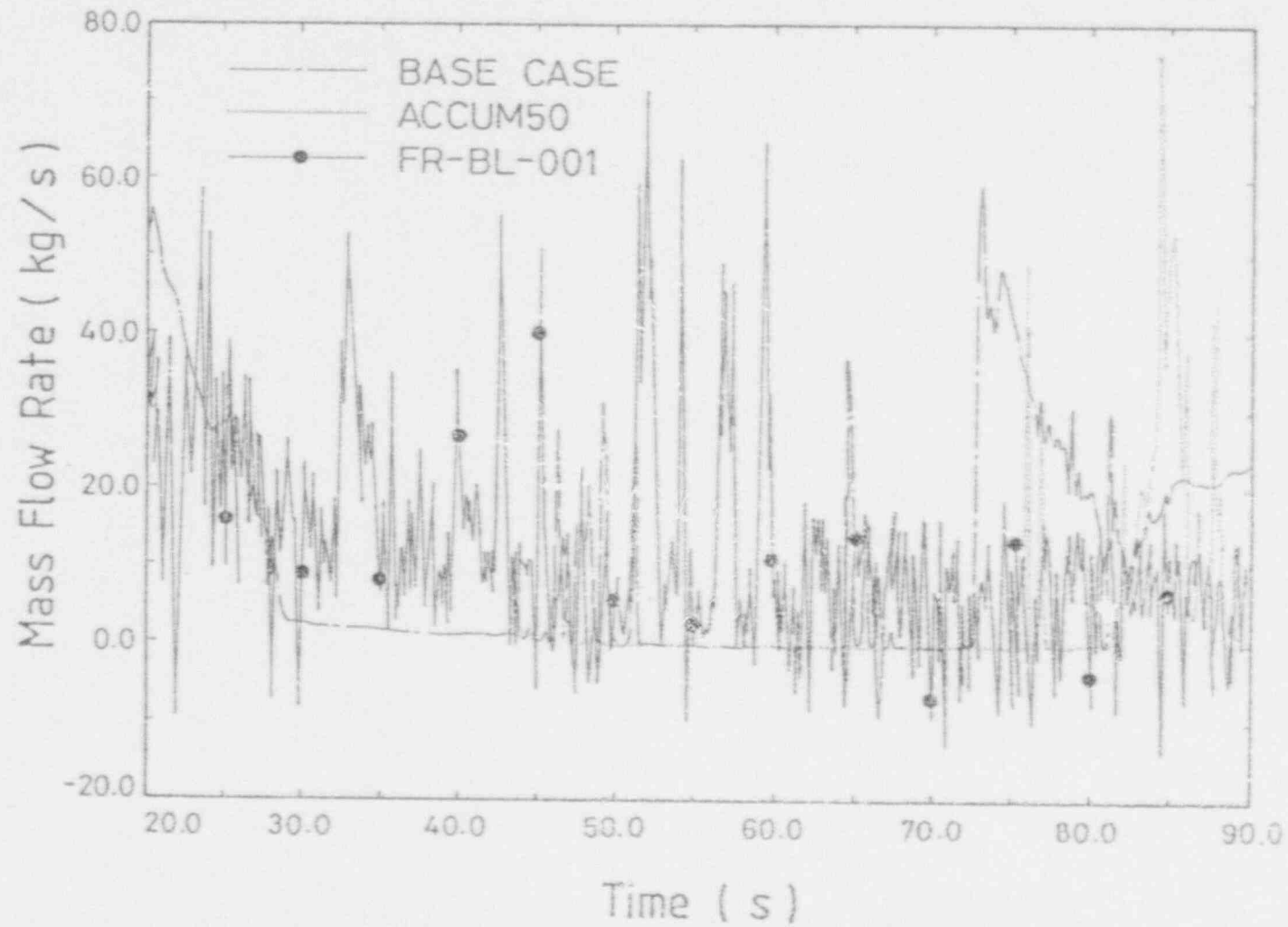


Figure 4.36 Comparison between Calculated Cold-Leg Break Flow Rates of the BASE and ACCUM50 Cases

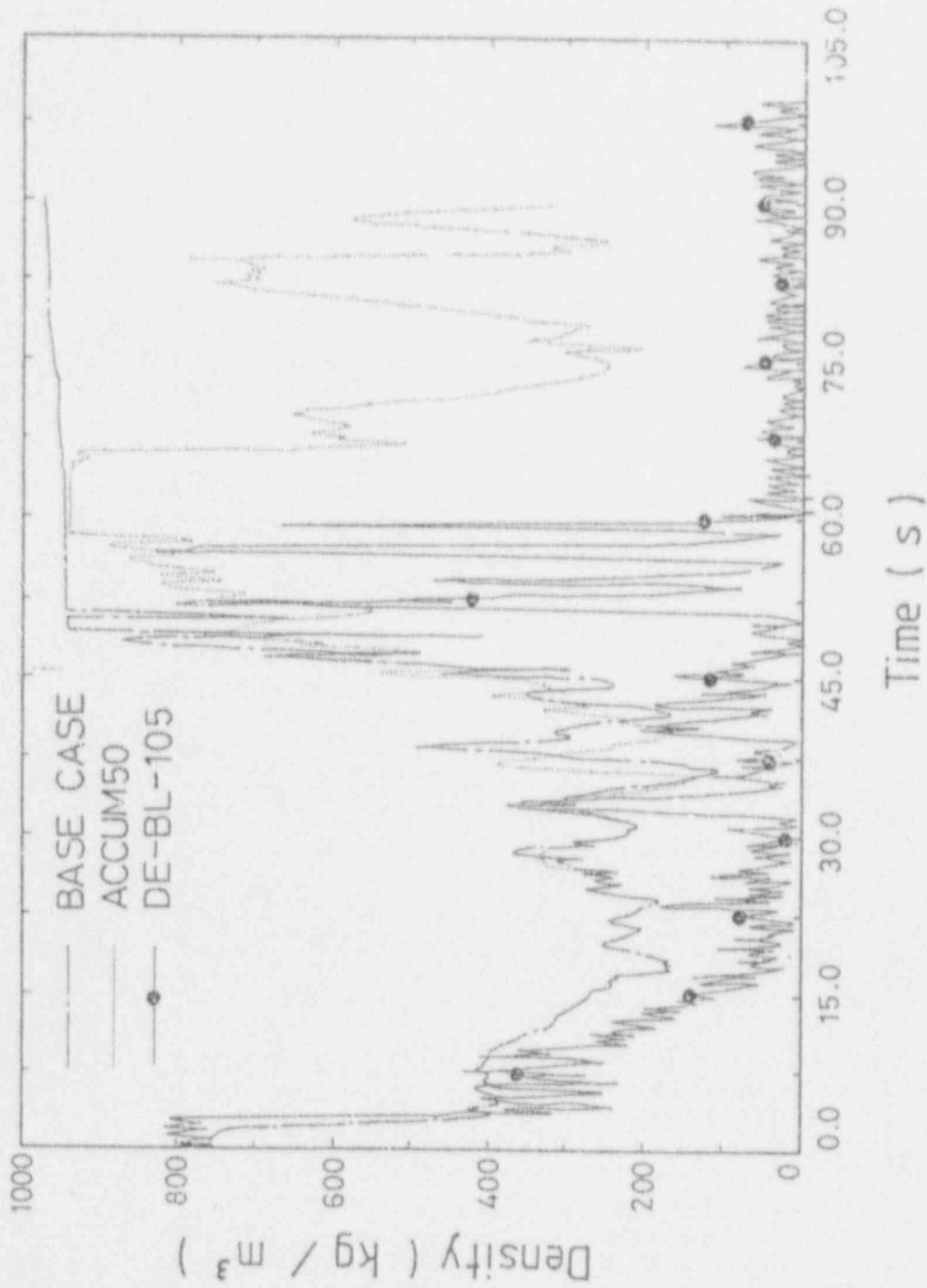


Figure 4.37 Comparison between Calculated Broken Loop Cold-Leg Densities of the BASE and ACCUM50 Cases

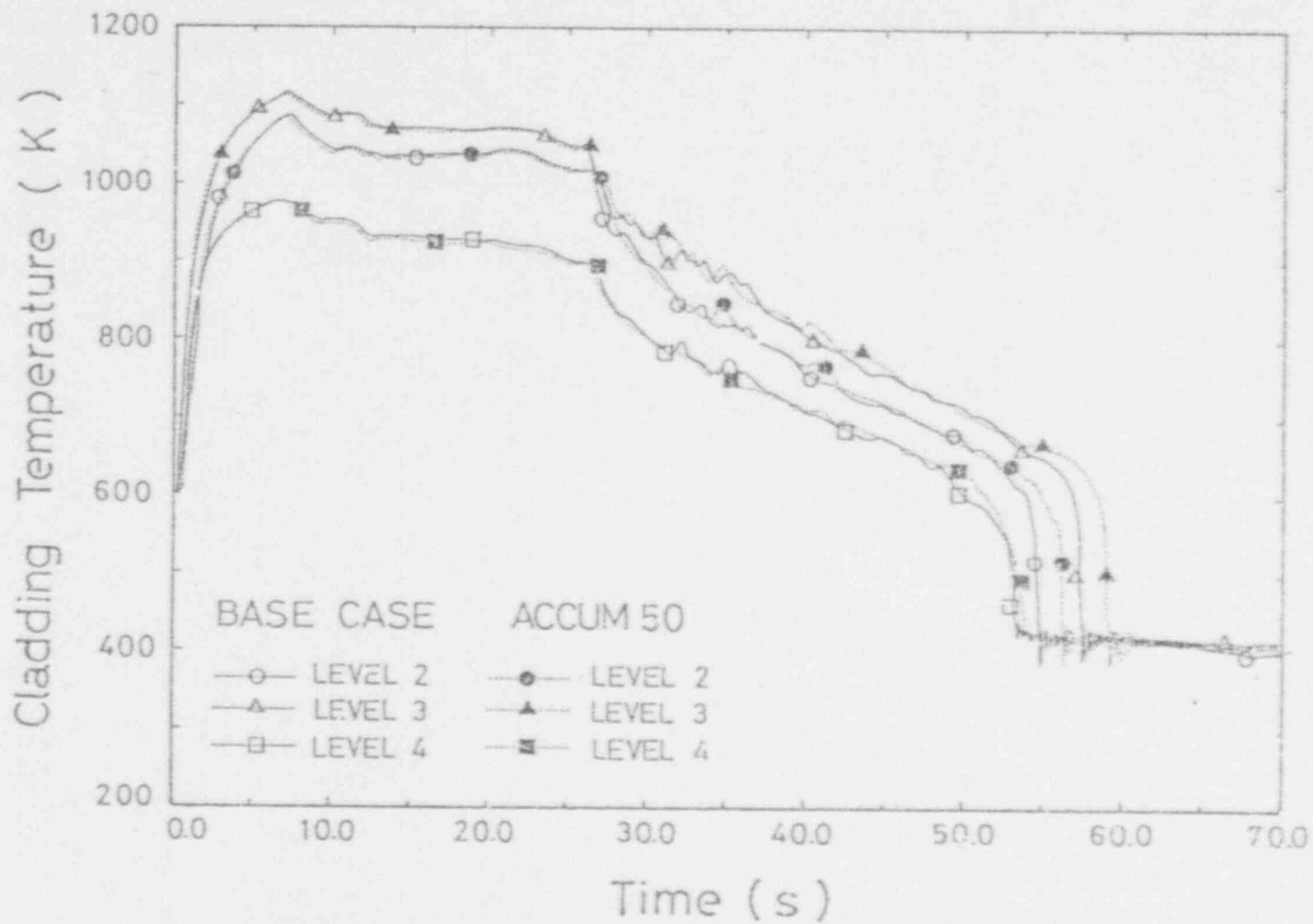


Figure 4.38 Comparison between Calculated Cladding Temperatures at Various Axial Locations of the BASE and ACCUM50 Cases

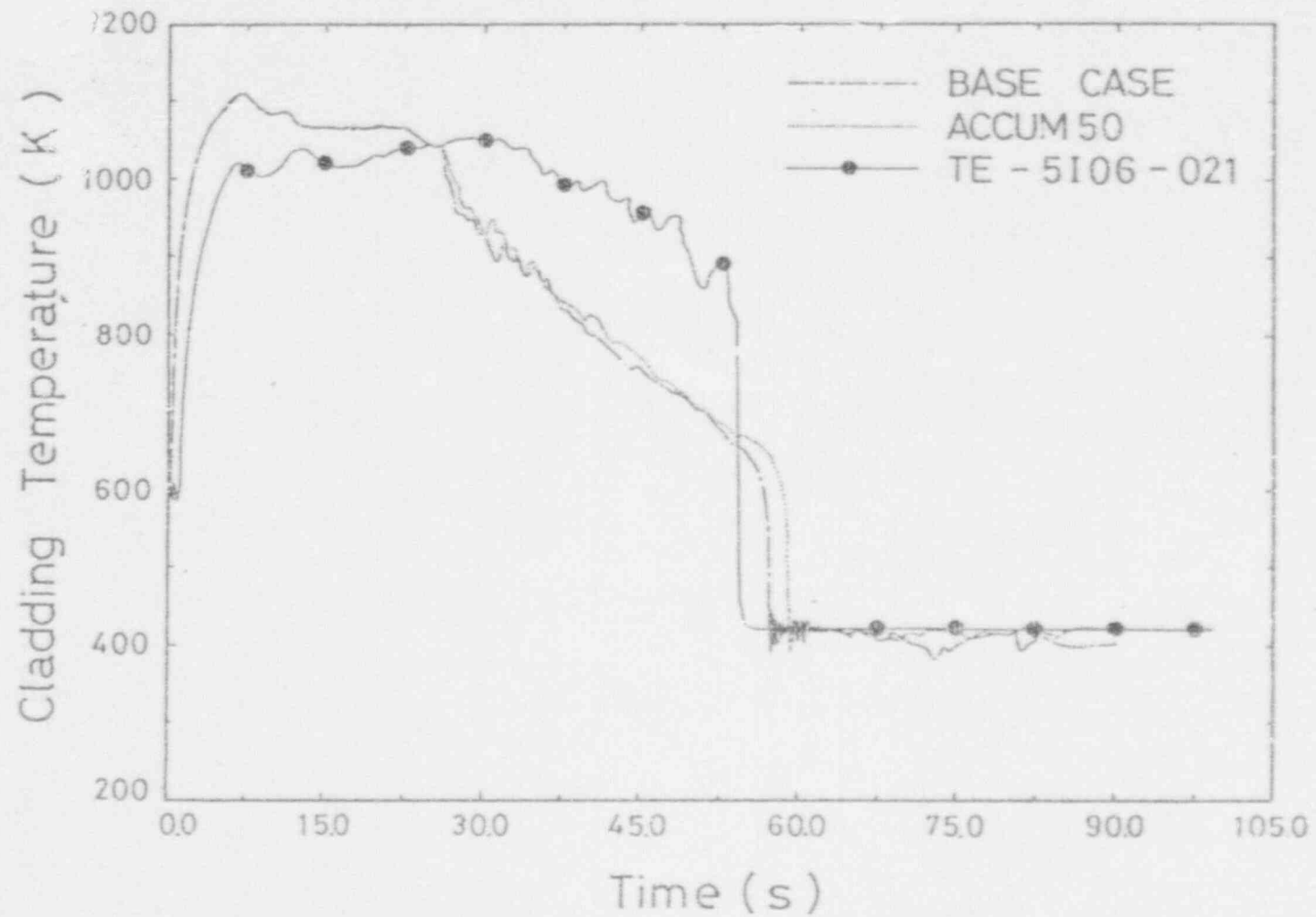


Figure 4.39 Comparison between Calculated Cladding Temperatures at Hottest Location of the BASE and ACCUM50 Cases

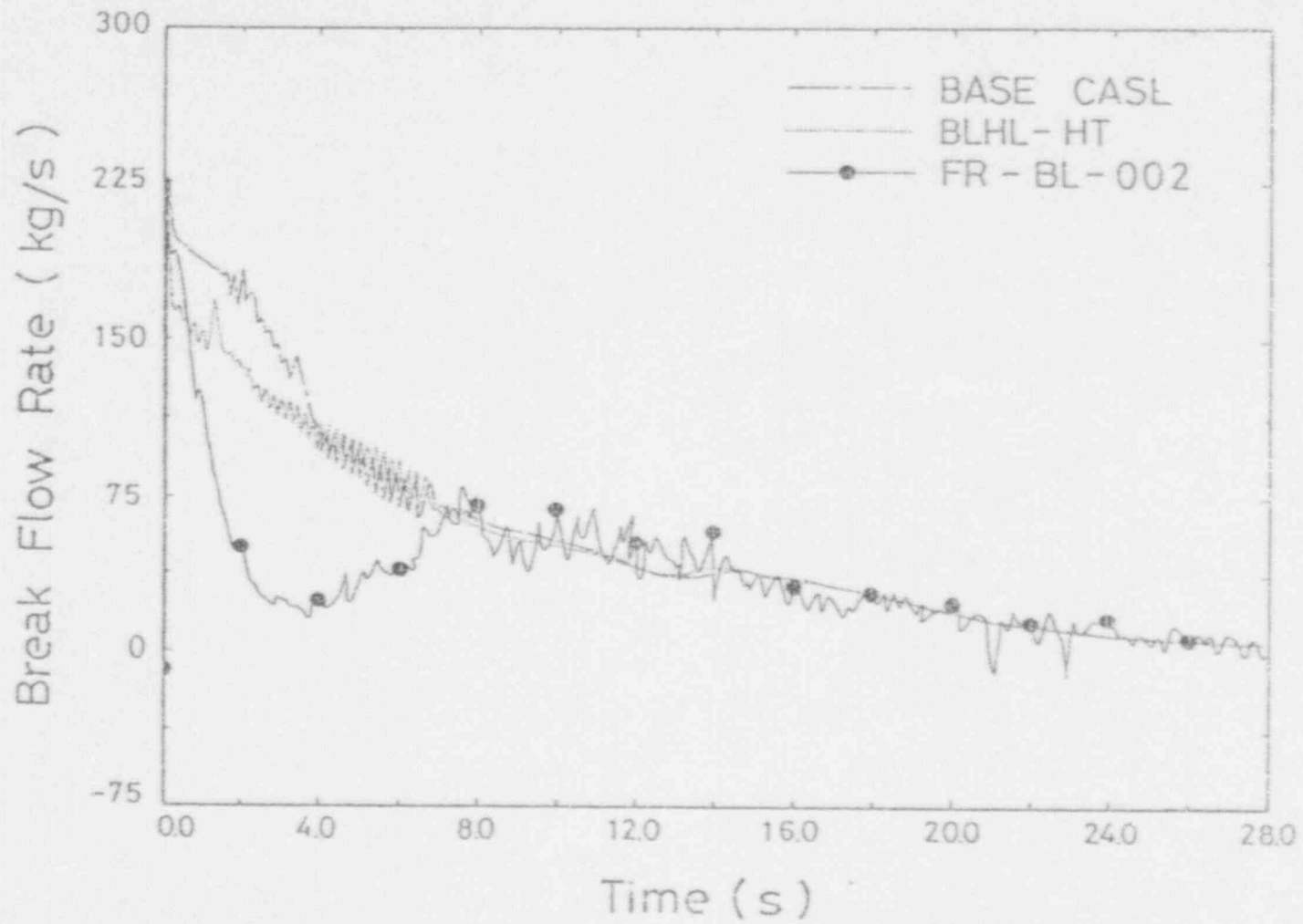


Figure 4.40 Comparison between Calculated Hot-Leg Break Flow Rates of the BASE and BLHL-HT Cases

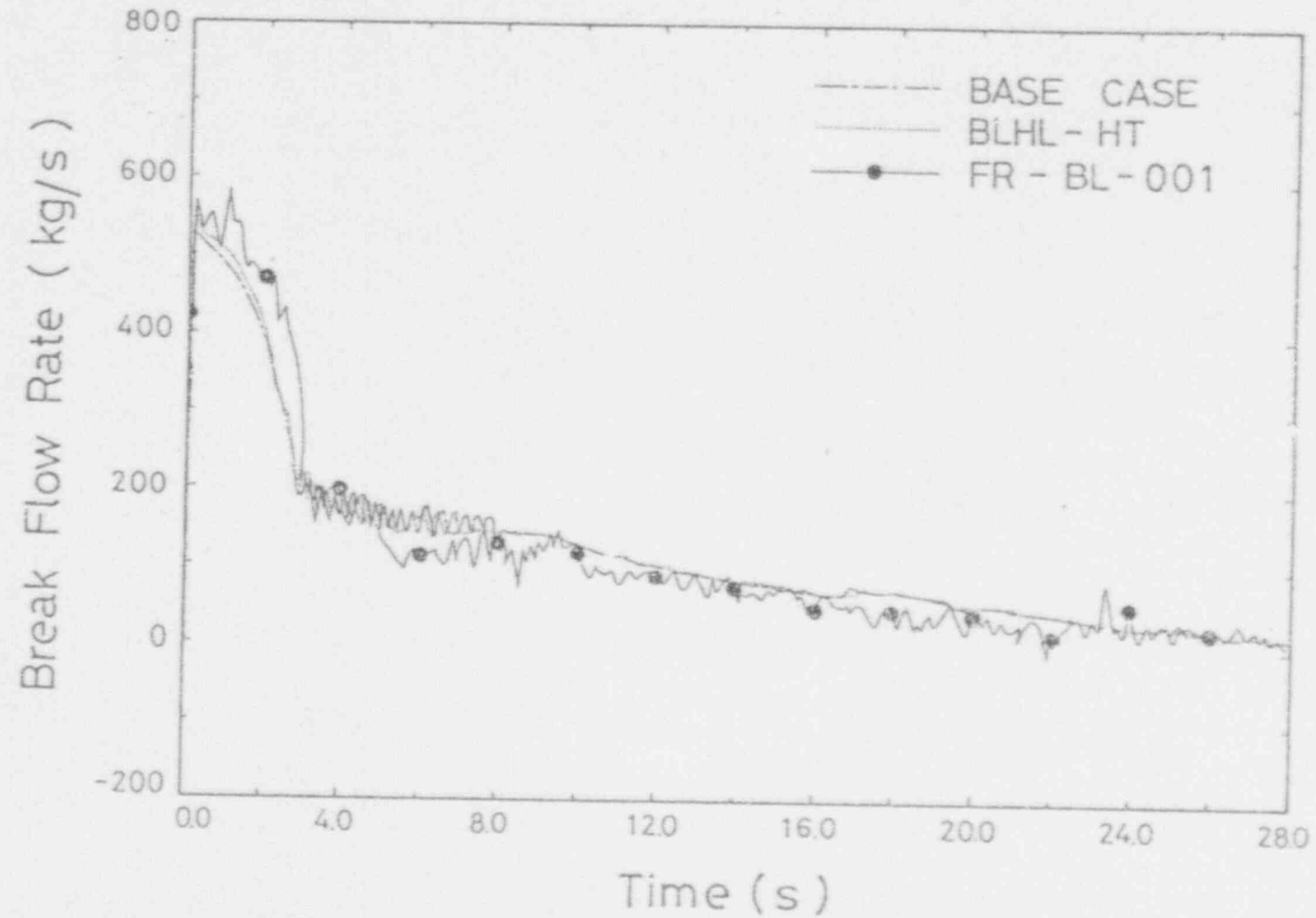


Figure 4.41 Comparison between Calculated Cold-Leg Break Flow Rates of the BASE and BLHL-HT Cases

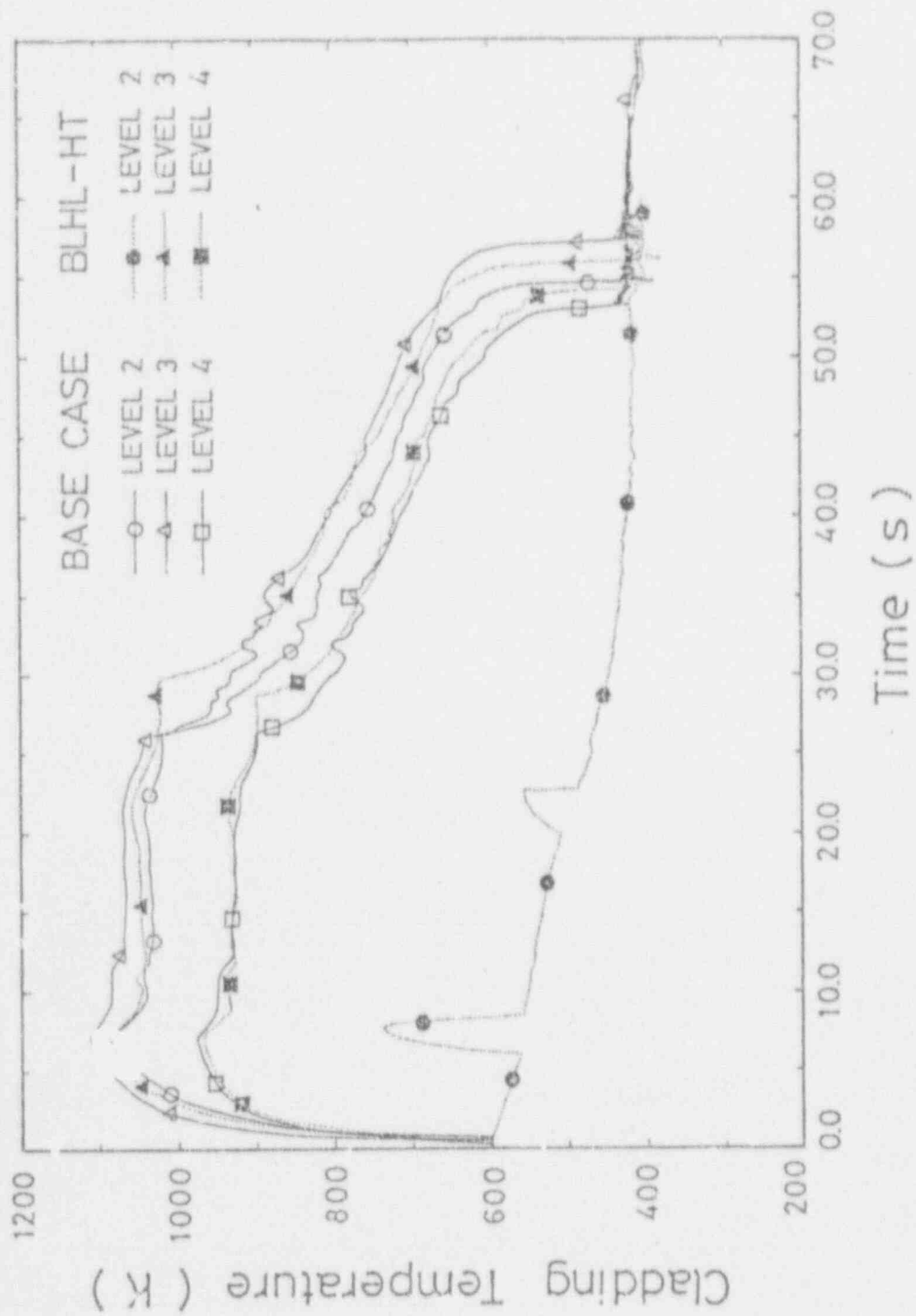


Figure 4.42 Comparison between Calculated Cladding Temperatures at Various Axial Locations of the BASE and BLHL-HT Cases

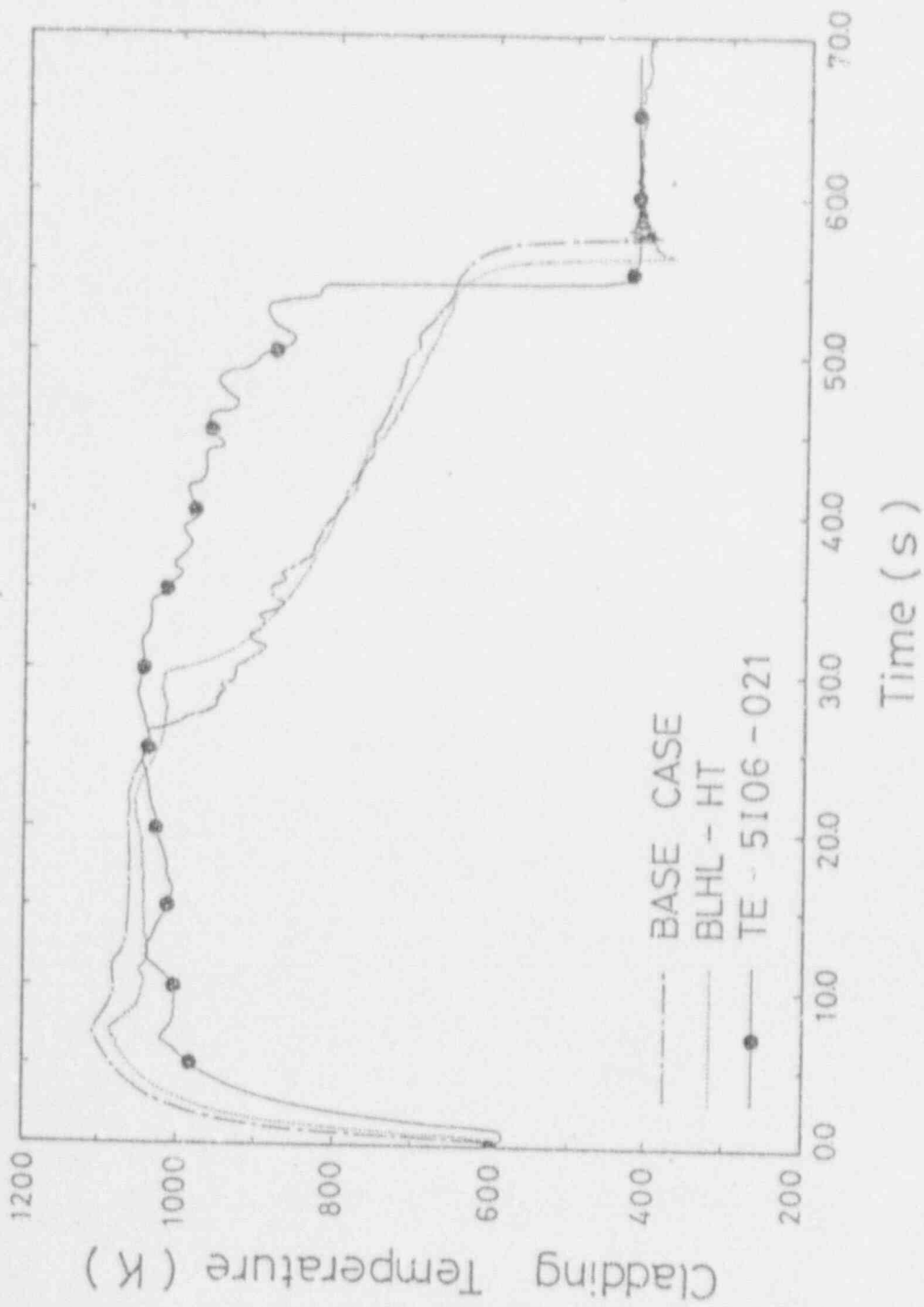


Figure 4.43 Comparison between Calculated Cladding Temperatures at Hottest Location of the BASE and BLHL-HT Cases

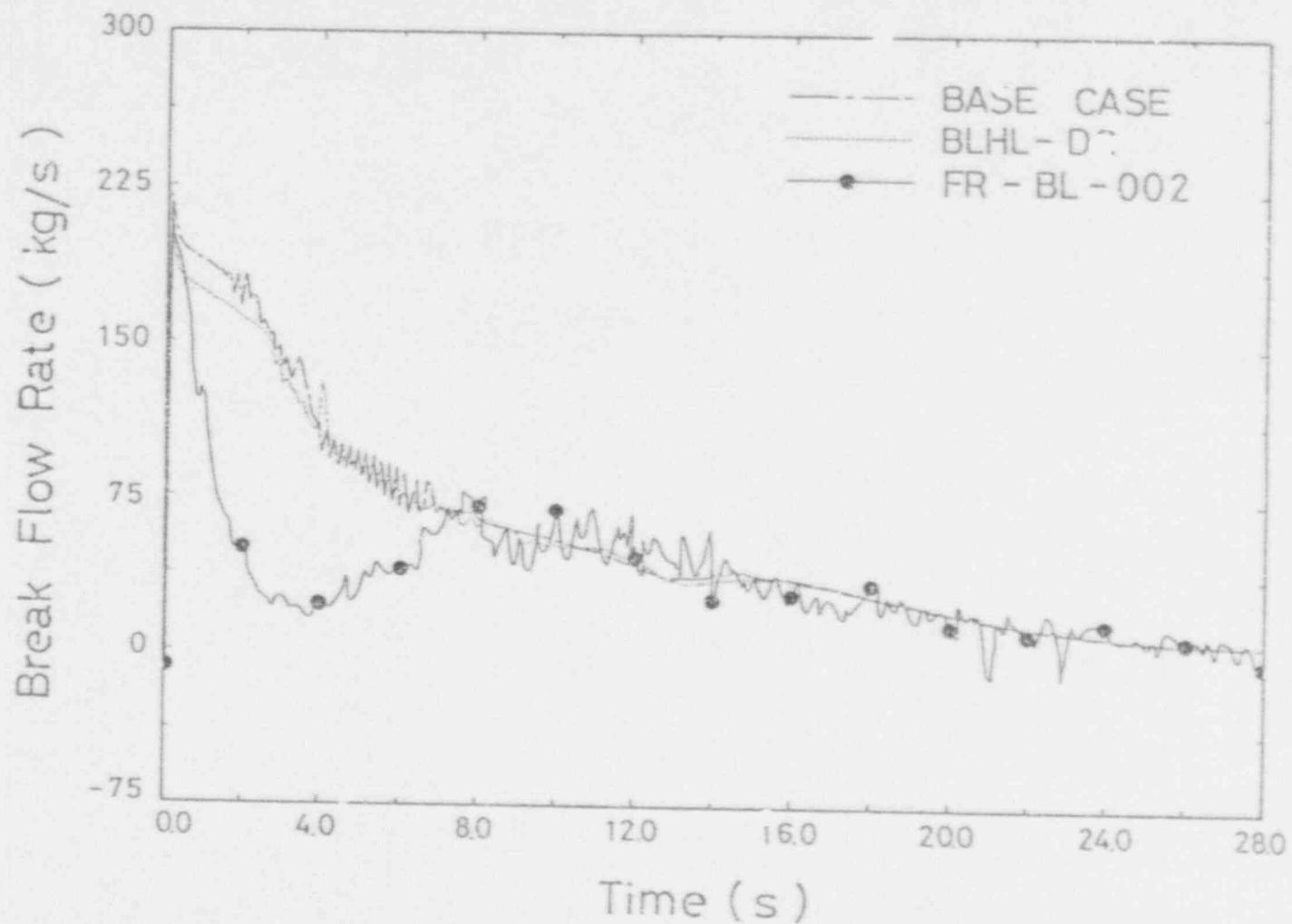


Figure 4.44 Comparison between Calculated Hot-Leg Break Flow Rates of the BASE and BLHL-DC Cases

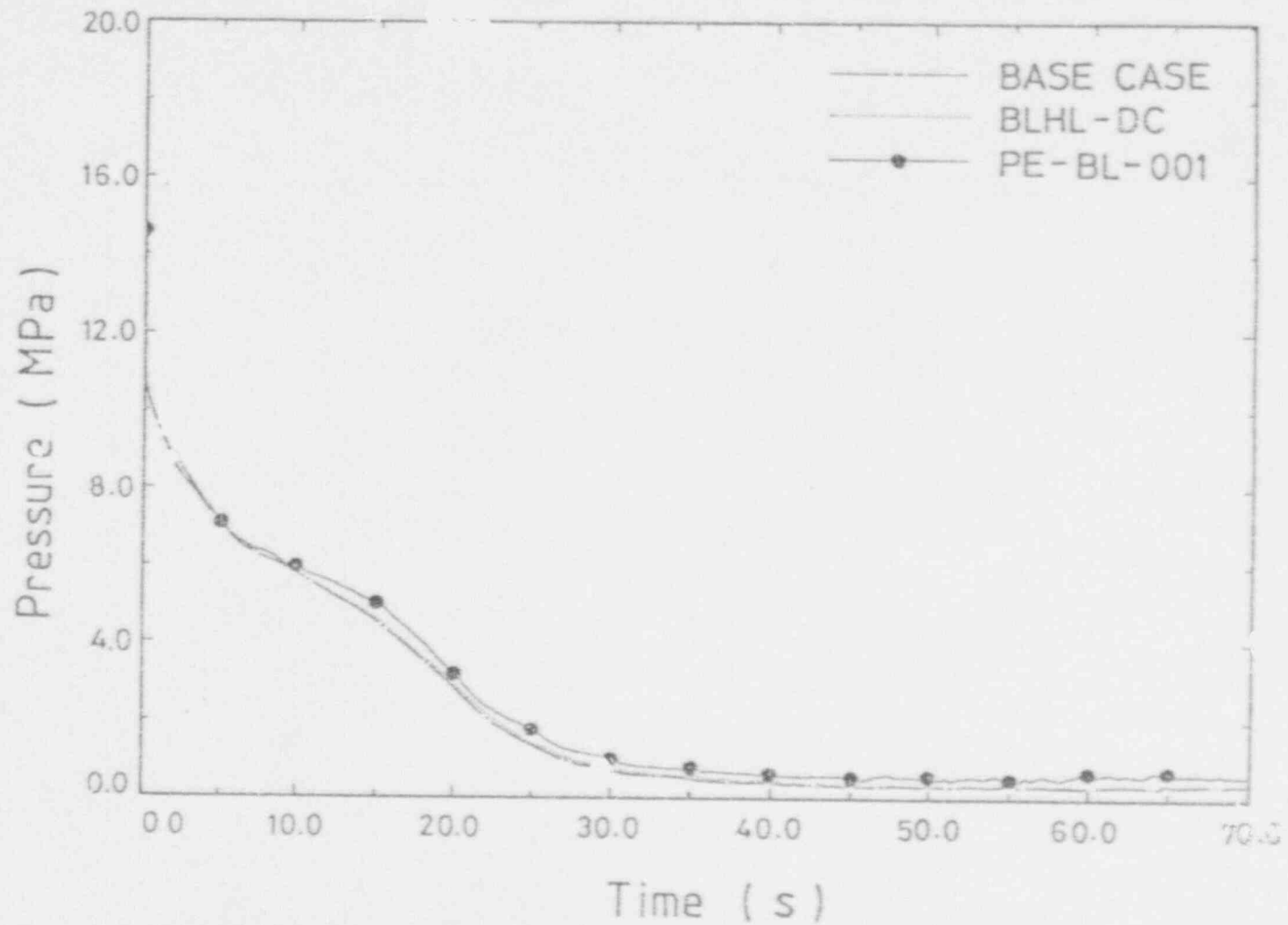


Figure 4.45 Comparison between Calculated Broken Loop Cold-Leg Pressures of the BASE and BLHL-DC Cases

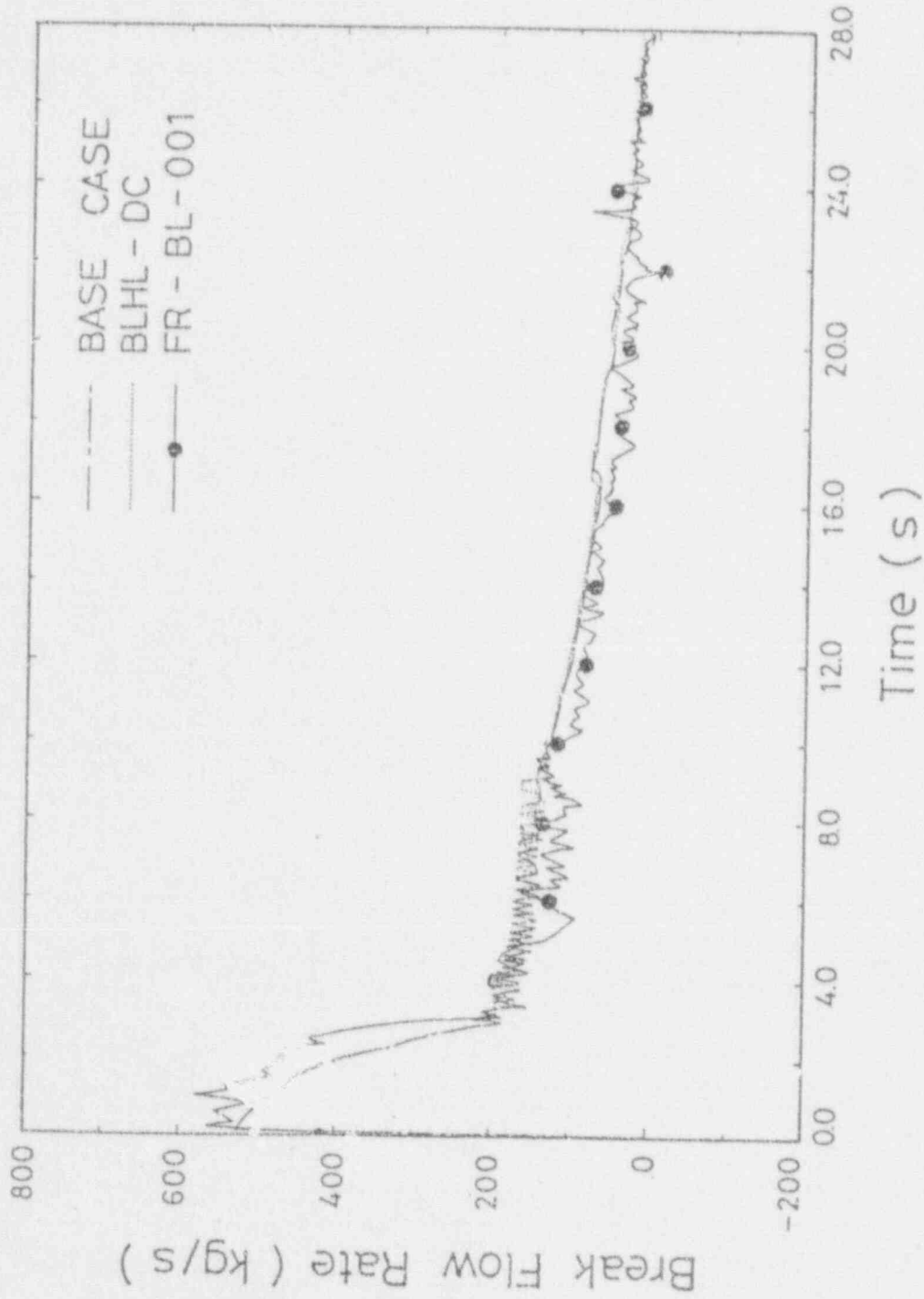


Figure 4.46 Comparison between Calculated Cold-Leg Break Flow Rates of the BASE and BLHL-DC Cases

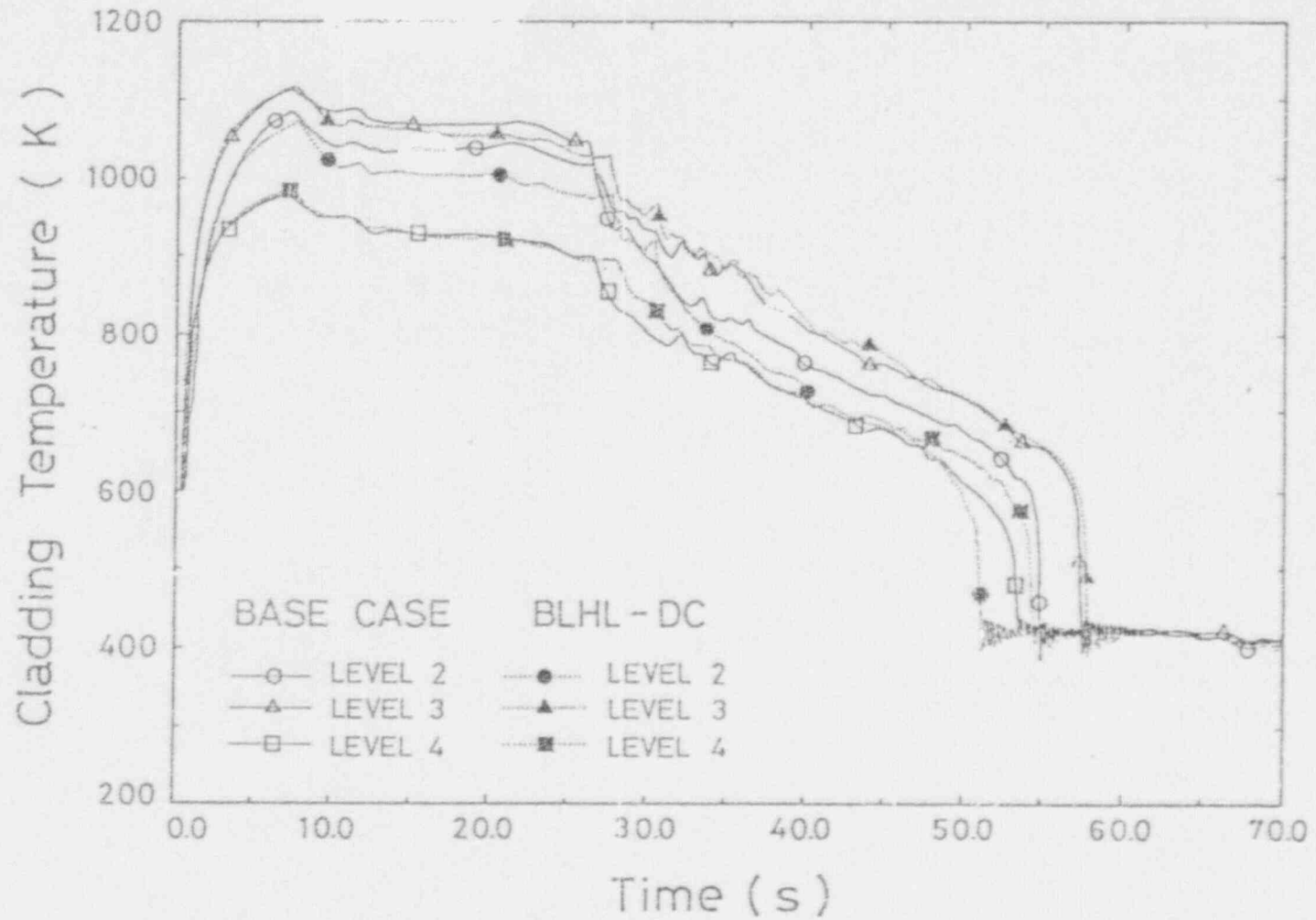


Figure 4.47 Comparison between Calculated Cladding Temperatures at Various Axial Locations of the BASE and BLHL-DC Cases

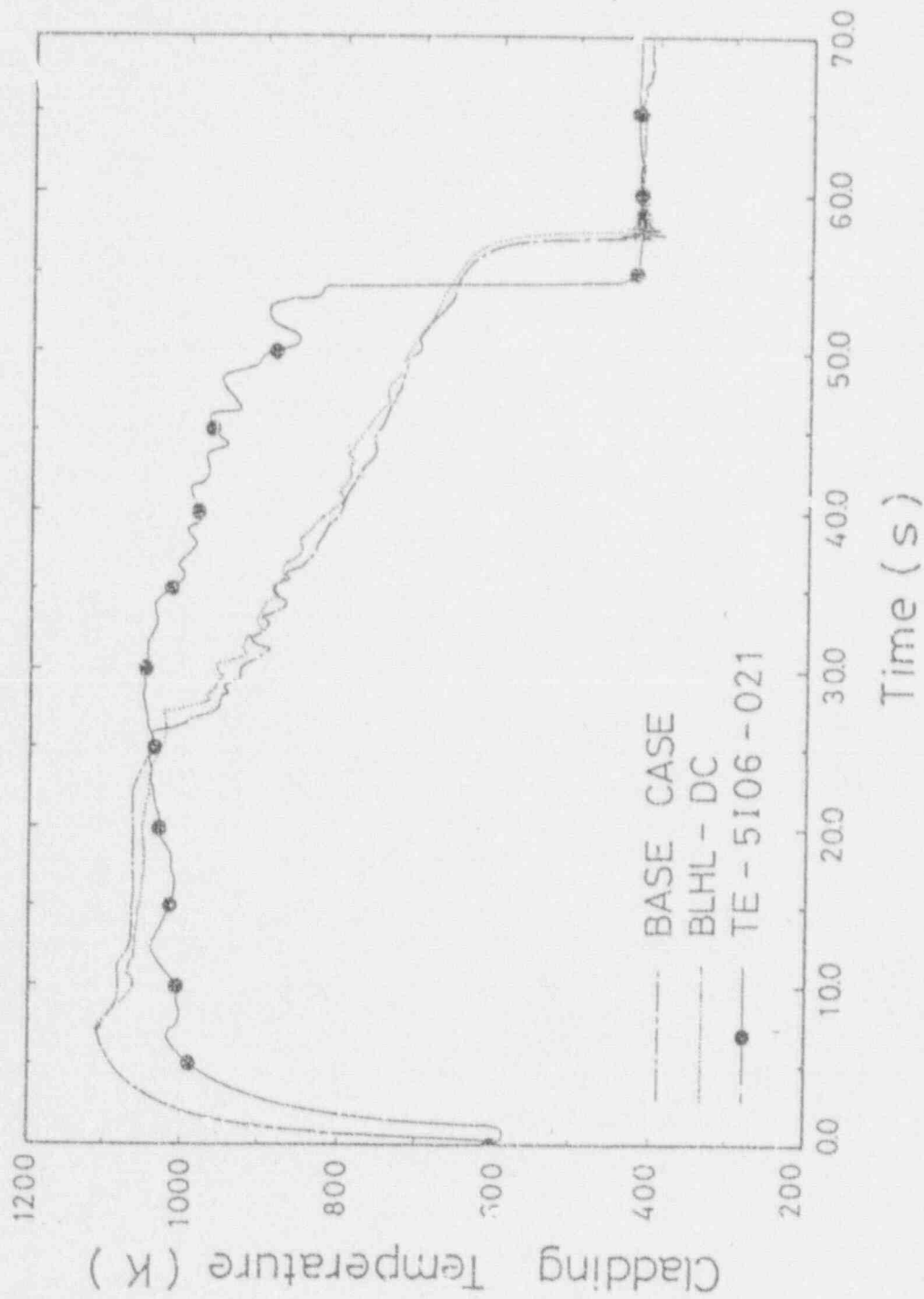


Figure 4.48 Comparison between Calculated Cladding Temperatures at Hottest Location of the BASE and BLHL-DC Cases

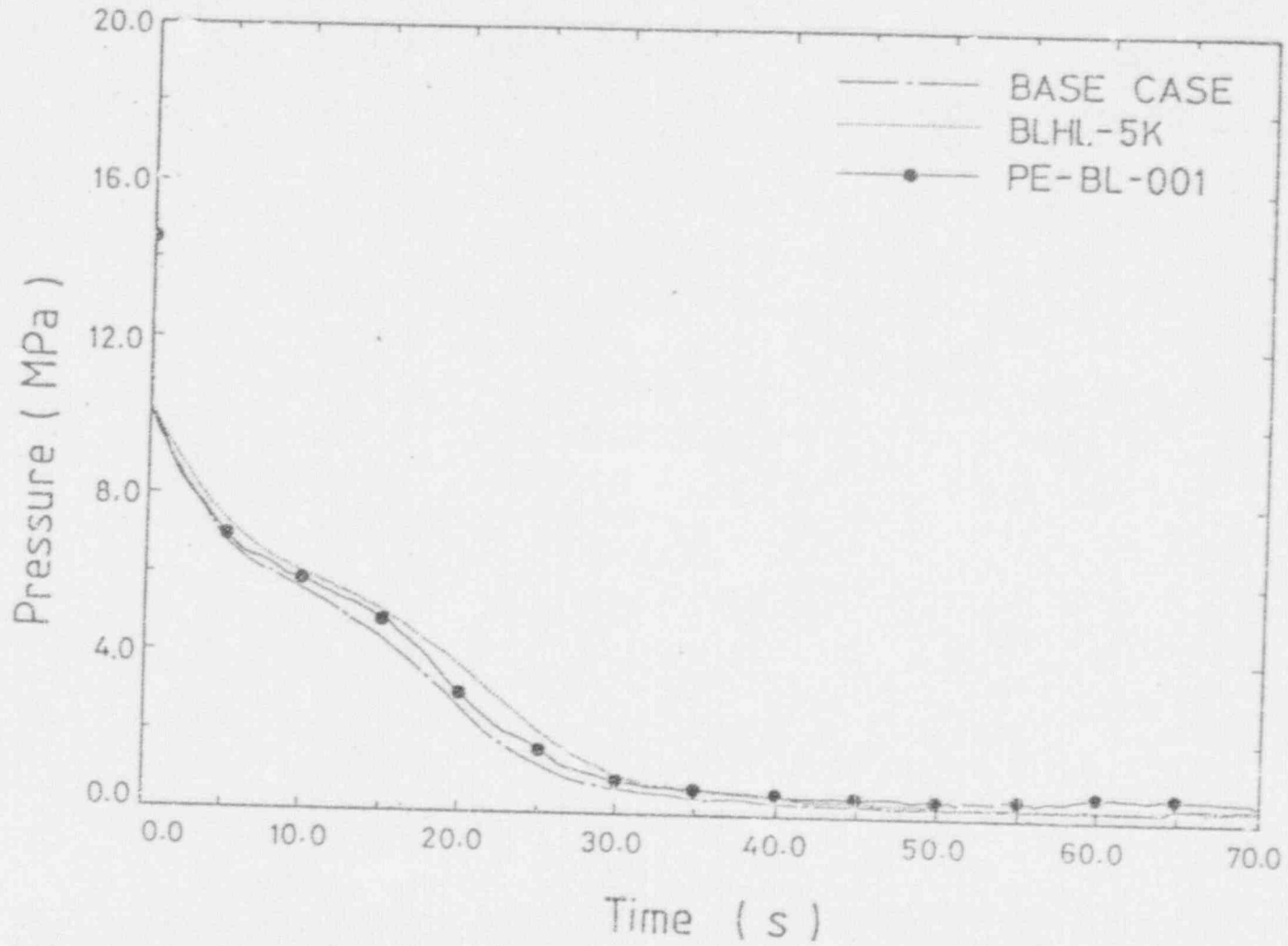


Figure 4.49 Comparison between Calculated Broken Loop Cold-Leg Pressures of the BASE and BLHL-5K Cases

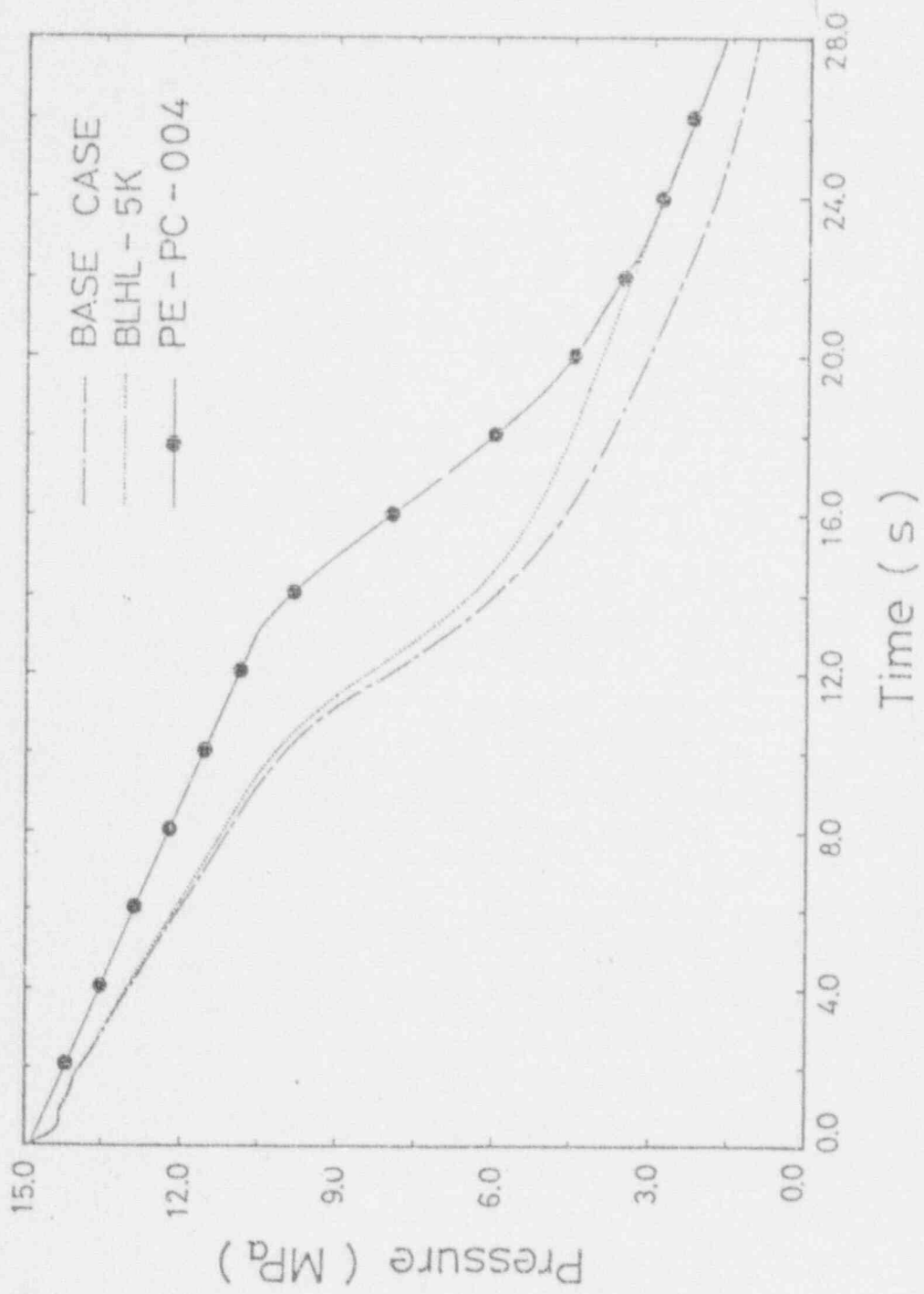


Figure 4.50 Comparison between Calculated Pressurizer Pressures of the BASE and BLHL-5K Cases

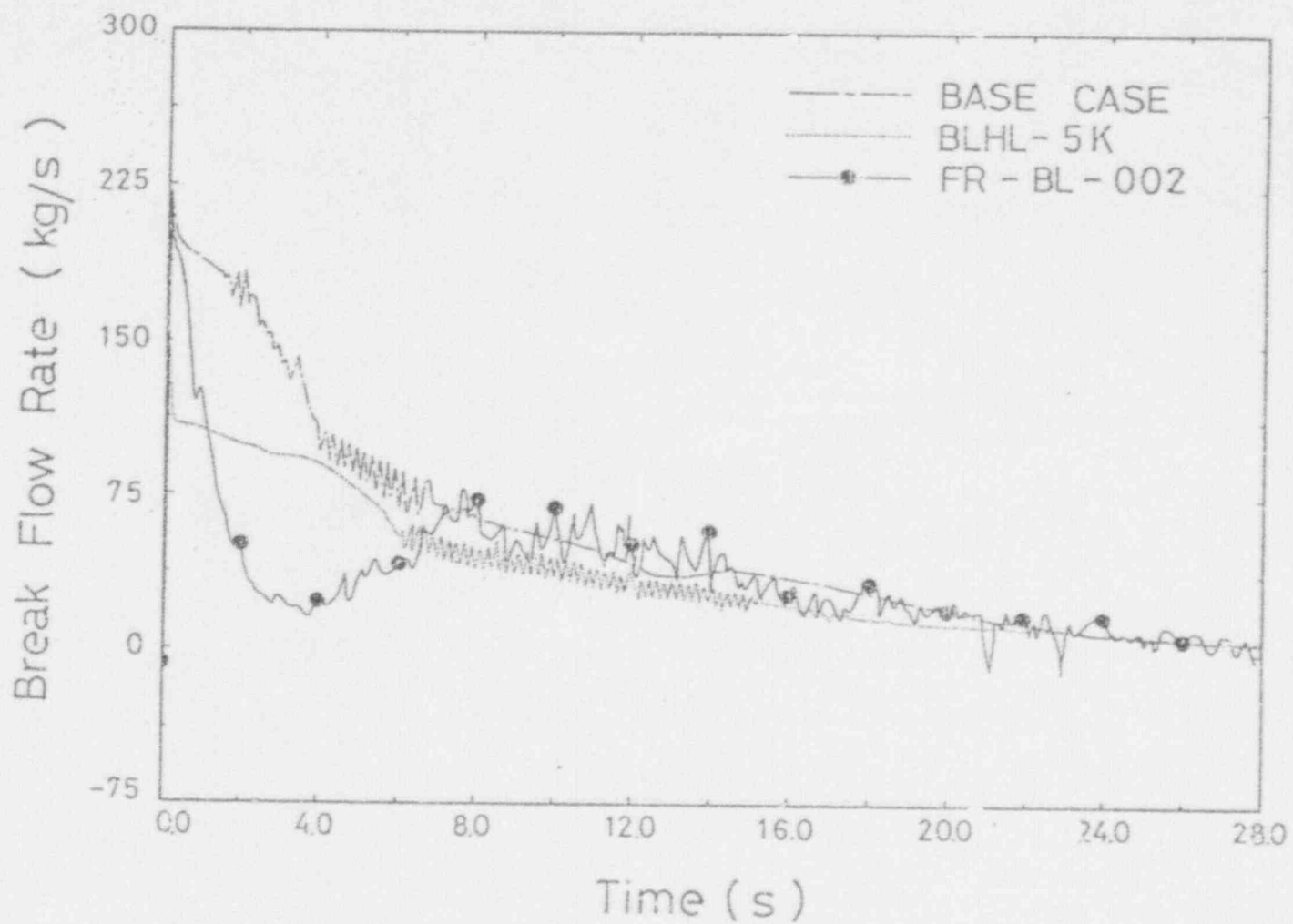


Figure 4.51 Comparison between Calculated Hot-Leg Break Flow Rates of the BASE and BLHL-5K Cases

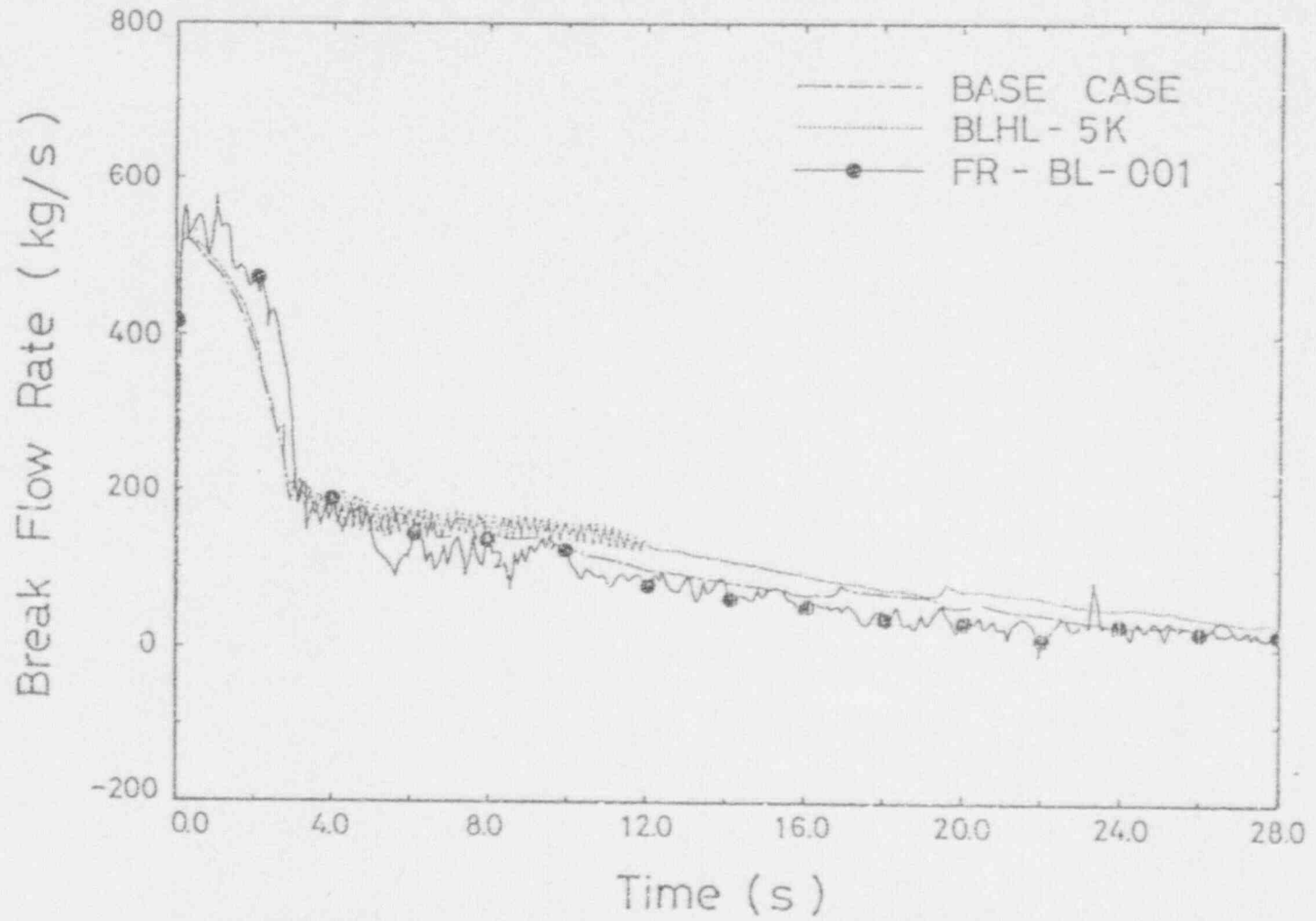


Figure 4.52 Comparison between Calculated Cold-Leg Break Flow Rates of the BASE and BLHL-5K Cases

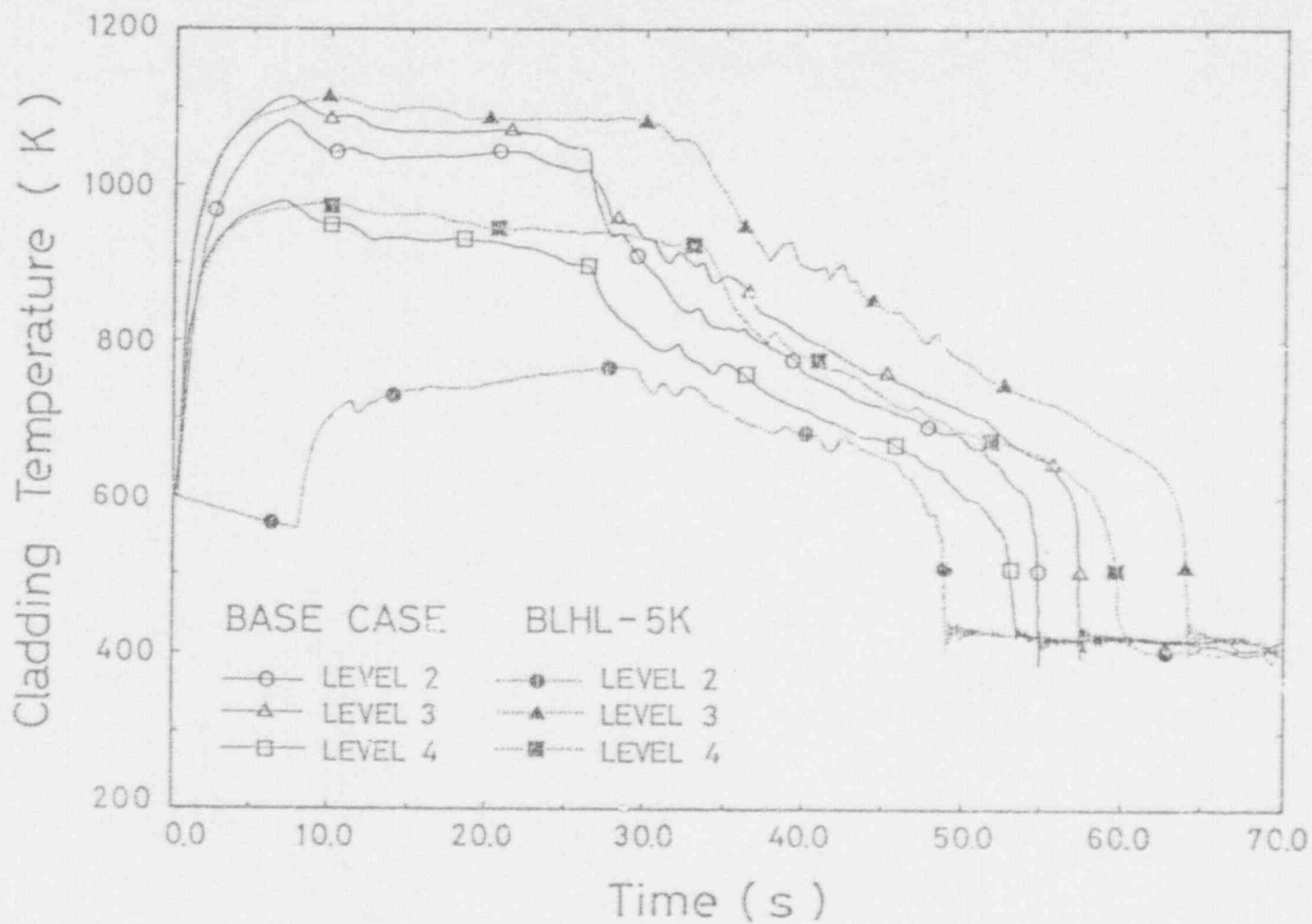


Figure 4.53 Comparison between Calculated Cladding Temperatures at Various Axial Locations of the BASE and BLHL-5K Cases

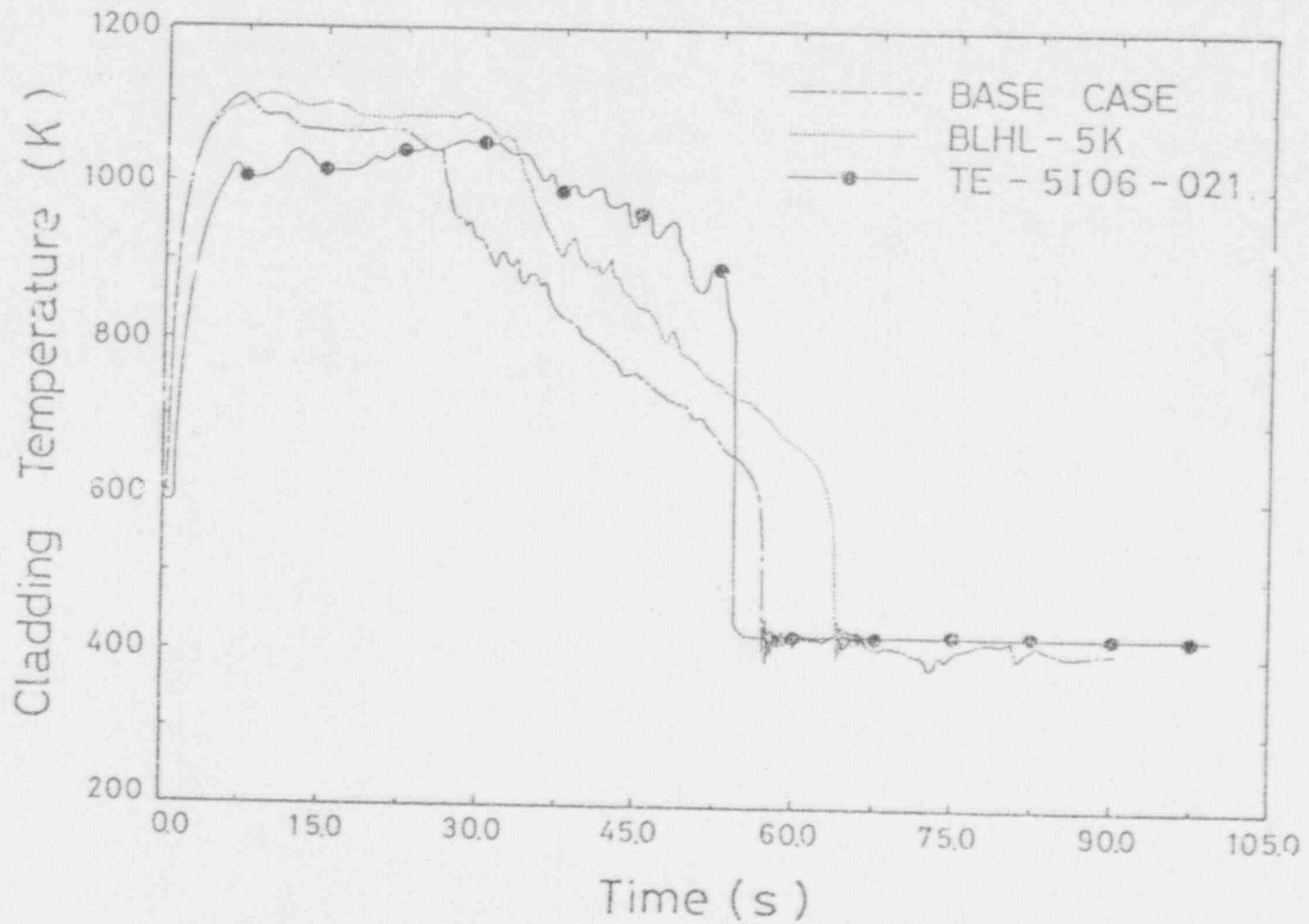


Figure 4.54 Comparison between Calculated Cladding Temperatures at Hottest Location of the BASE and BLHL-5K Cases

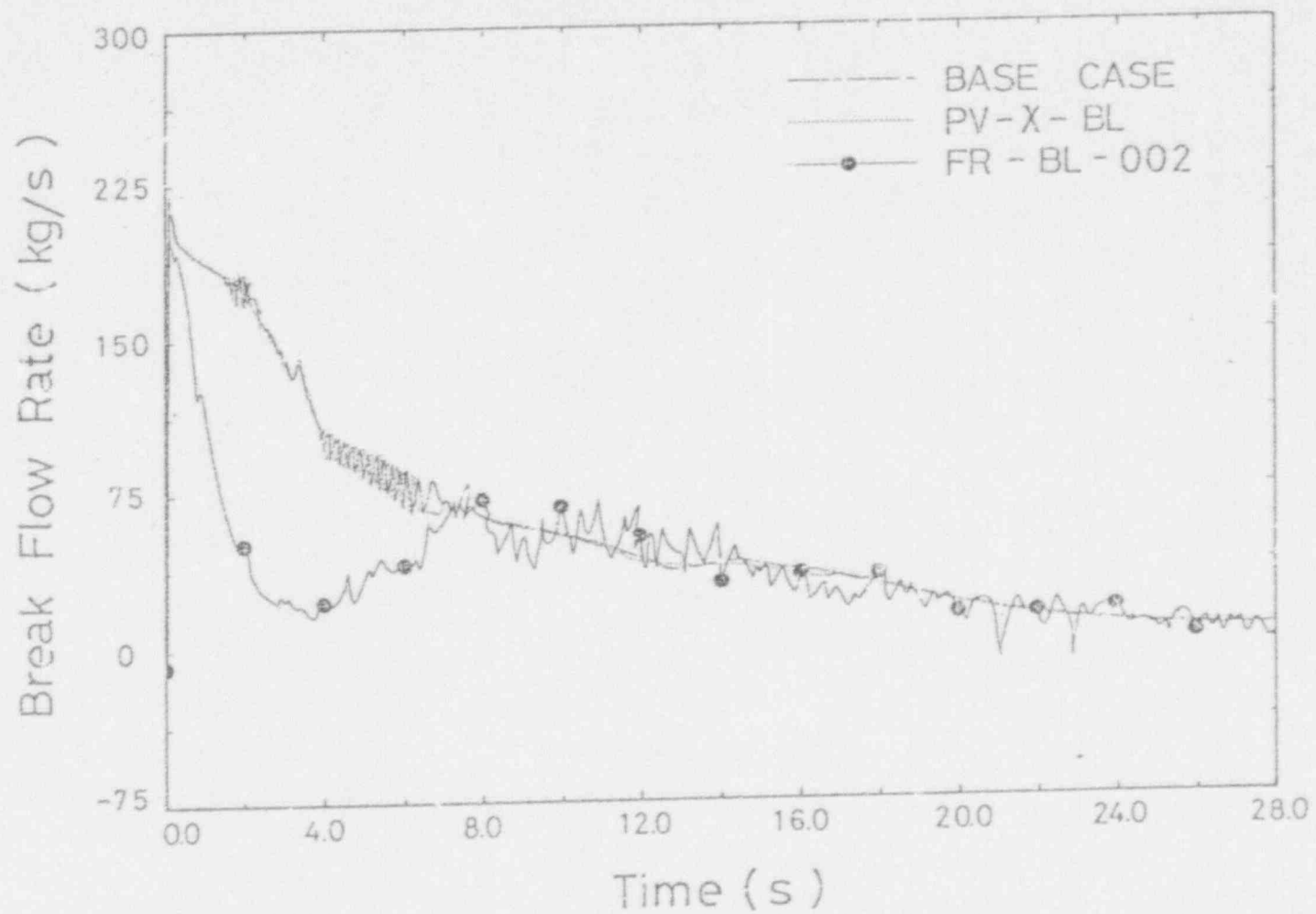


Figure 4.55 Comparison between Calculated Hot-Leg Break Flow Rates of the BASE and PV-X-BL Cases.

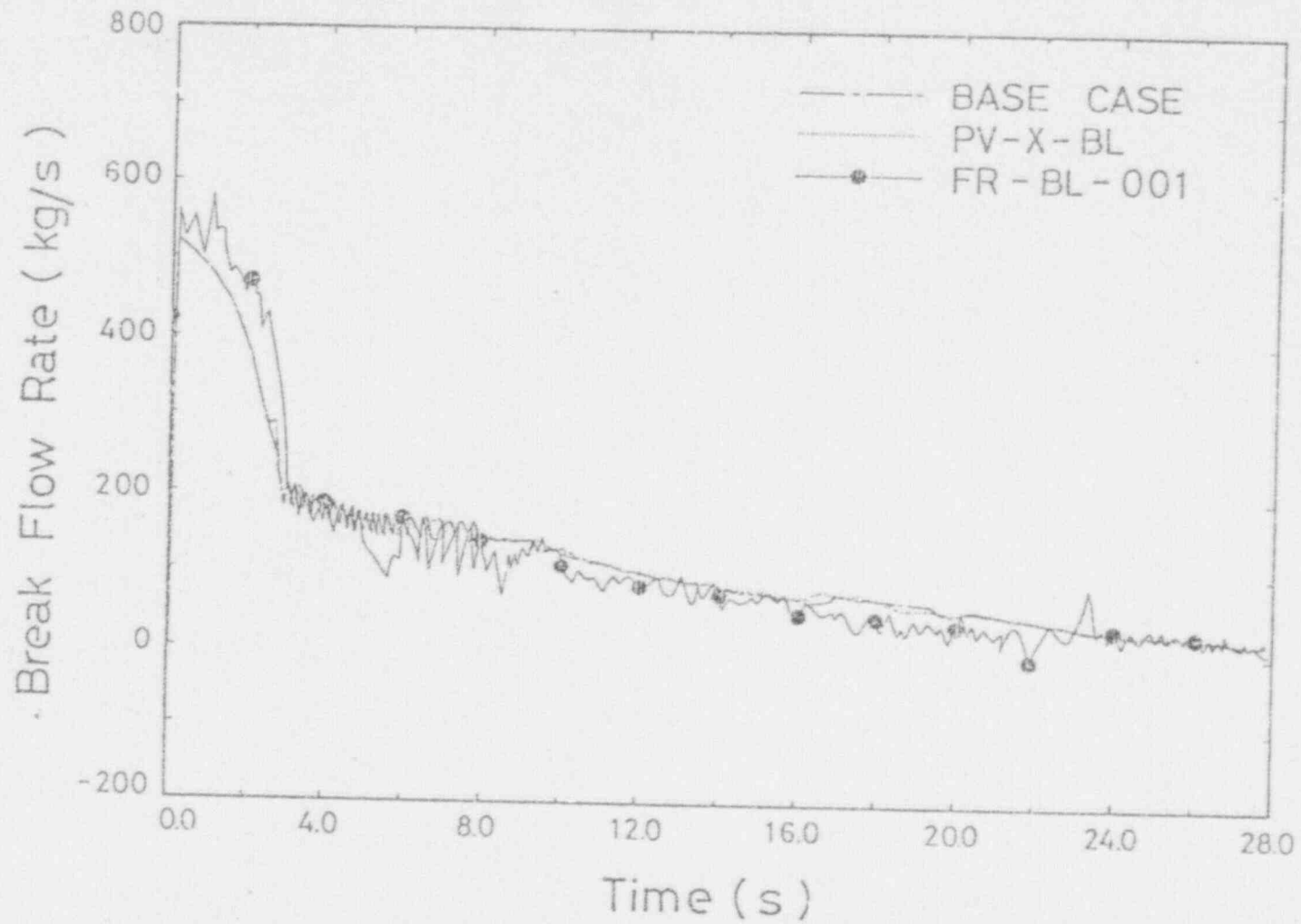


Figure 4.56 Comparison between Calculated Cold-Leg Break Flow Rates of the BASE and PV-X-BL Cases

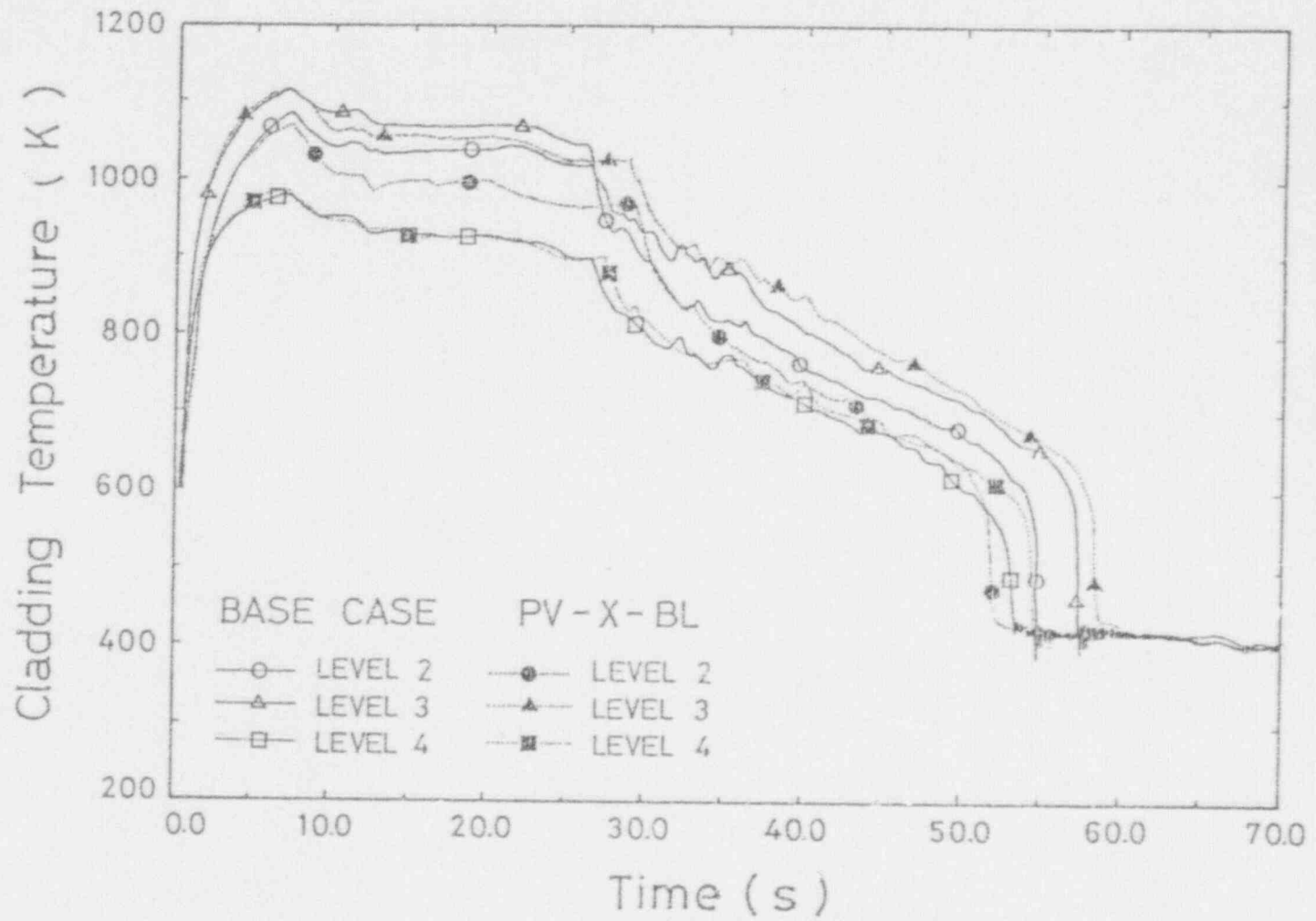


Figure 4.57 Comparison between Cladding Temperatures at Various Axial Locations of the BASE and PV-X-BL Cases

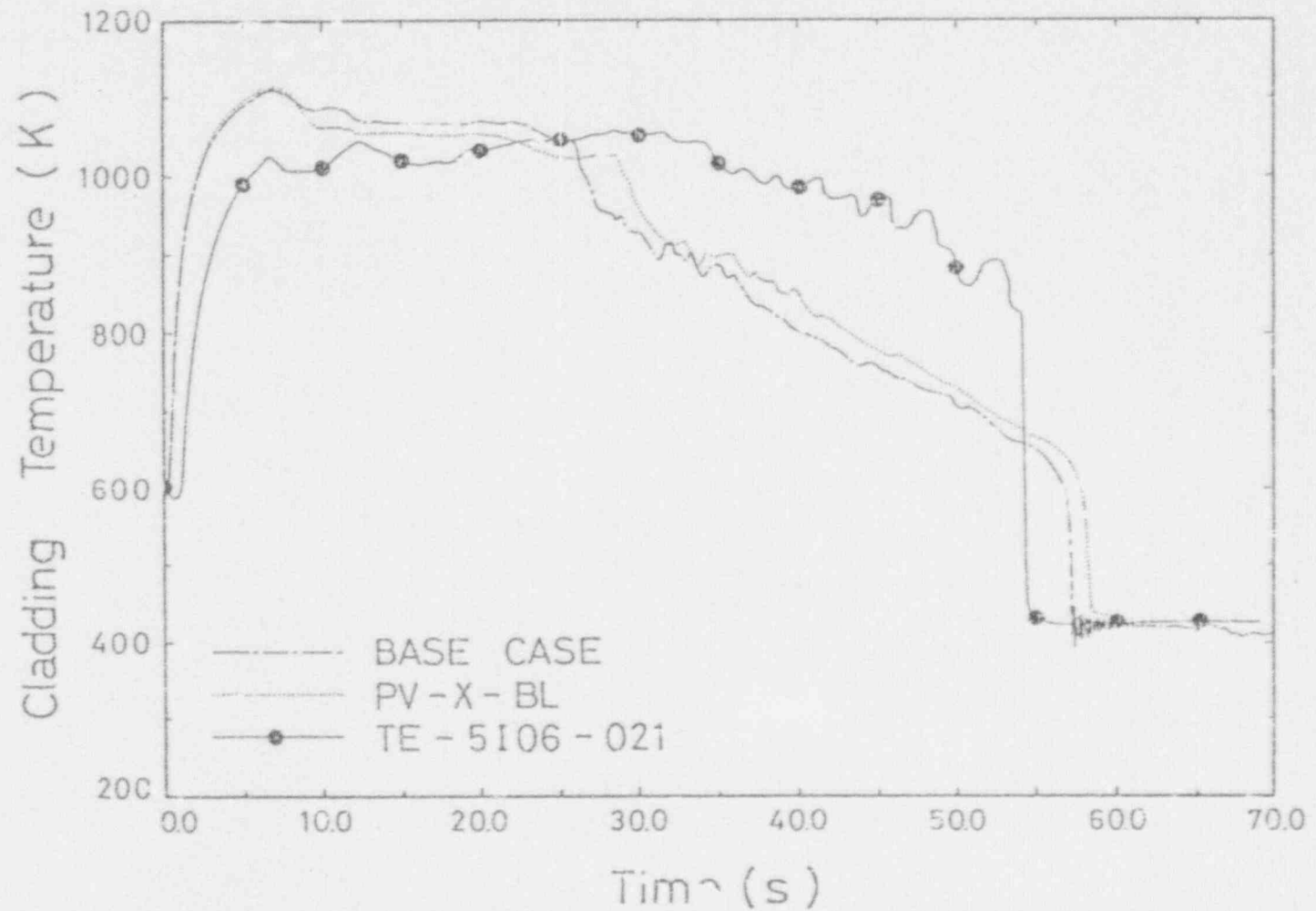


Figure 4.58 Comparison between Cladding Temperatures at Hottest Location of the BASE and PV-X-BL Cases

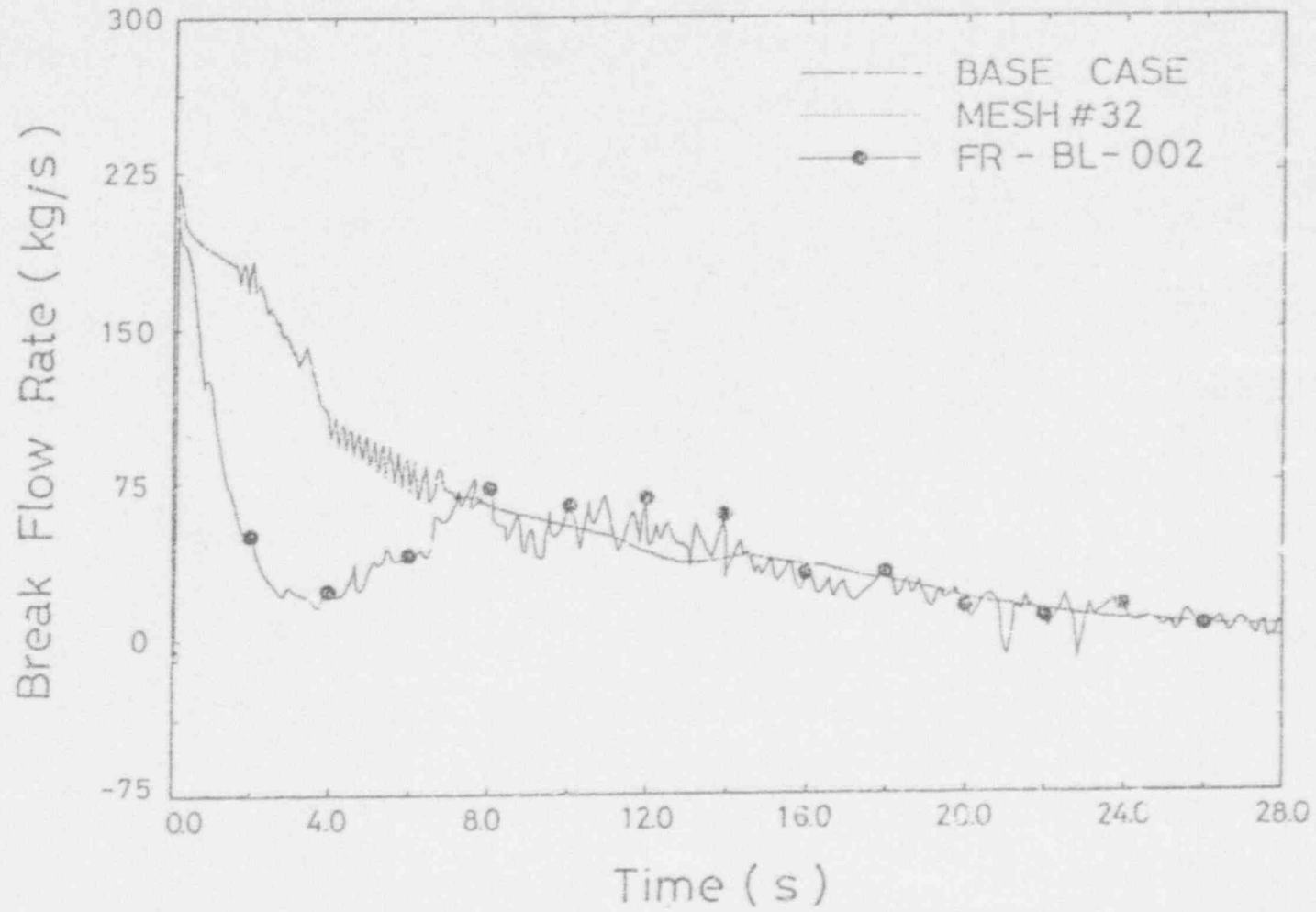


Figure 4.59 Comparison between Calculated Hot-Leg Break Flow of the BASE and MESH#32 Cases

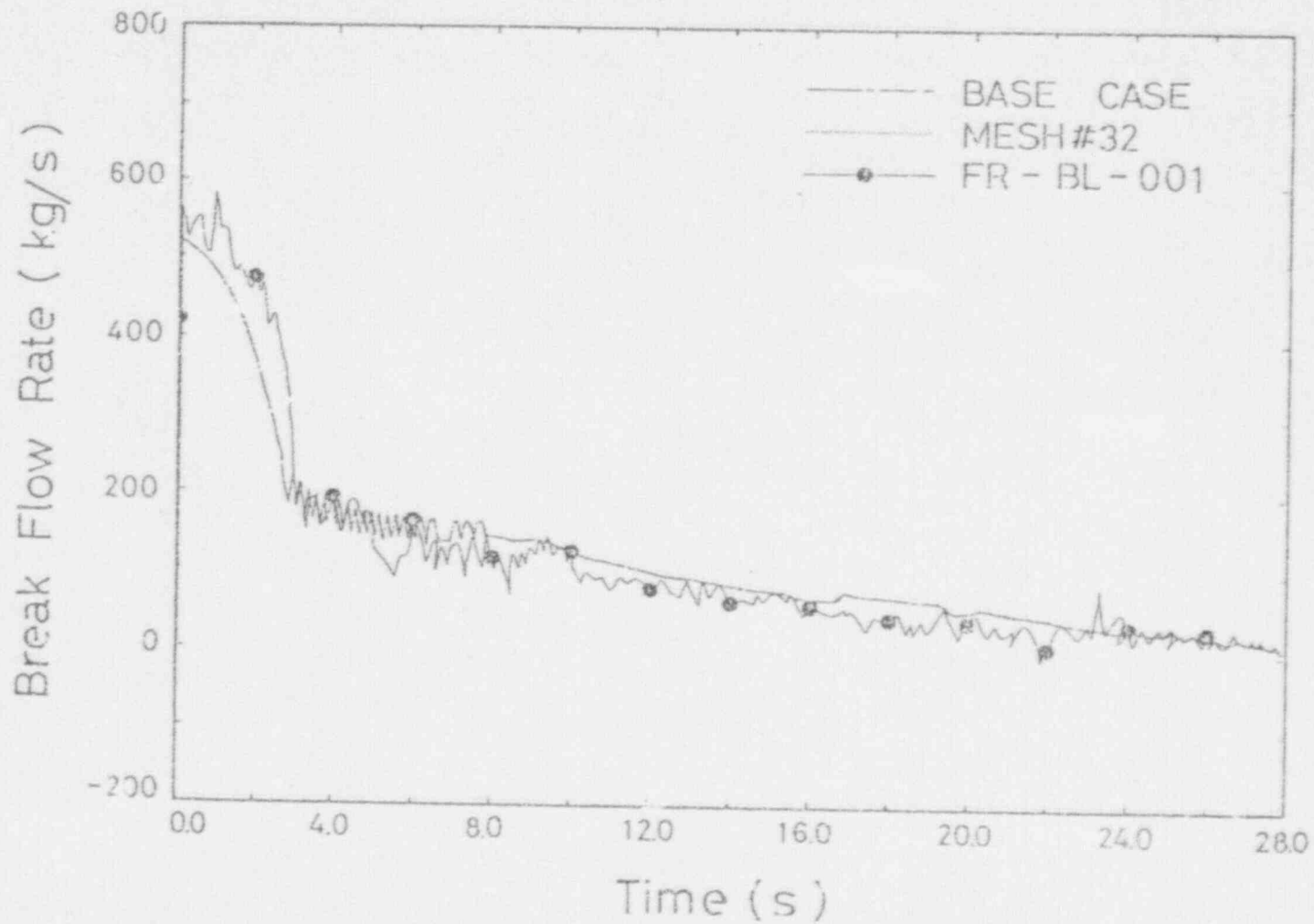


Figure 4.60 Comparison between Calculated Cold-Leg Break Flow Rates of the BASE and MESH#32 Cases

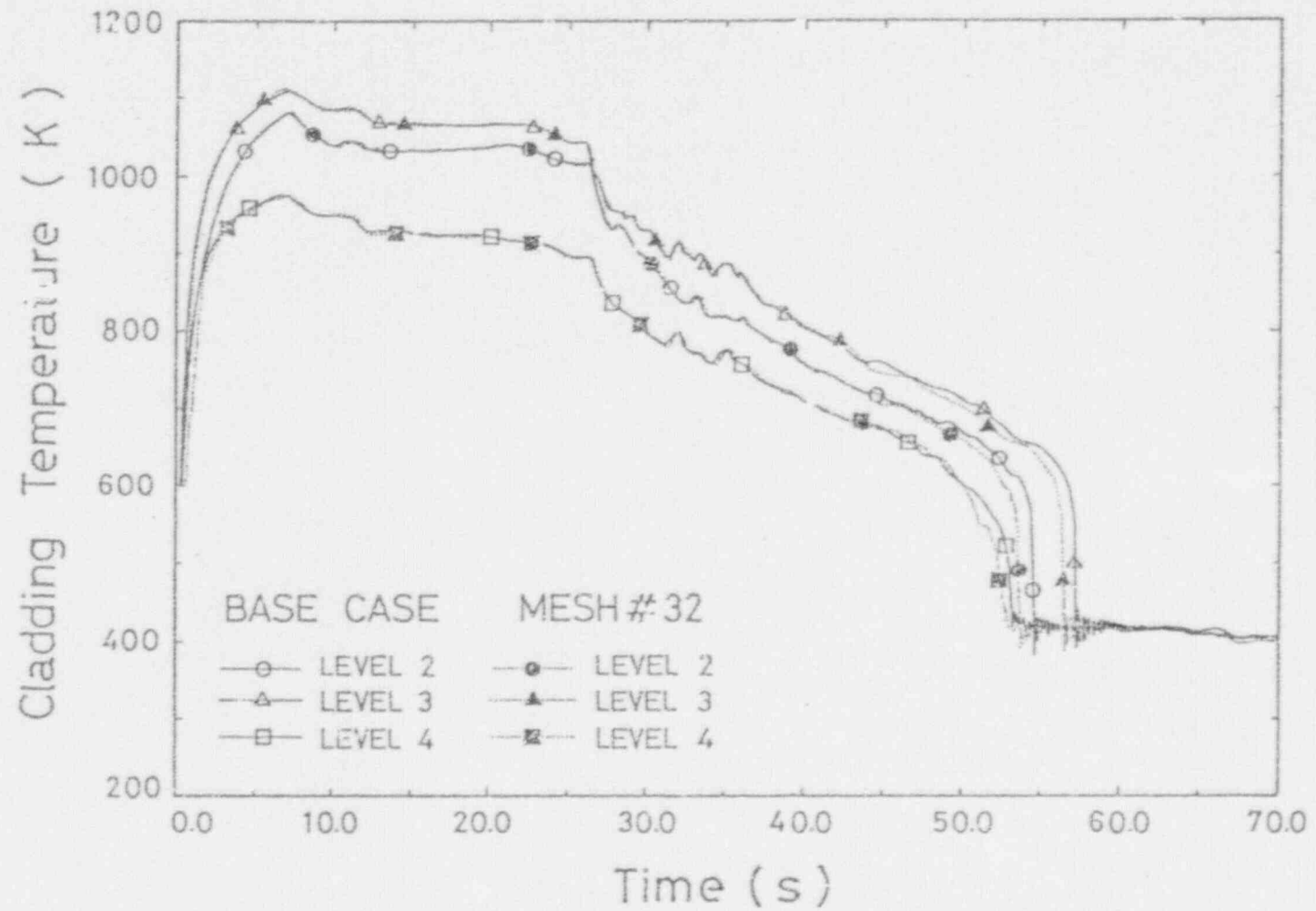


Figure 4.61 Comparison between Calculated Cladding Temperatures at Various Axial Locations of the BASE and MESH#32 Cases

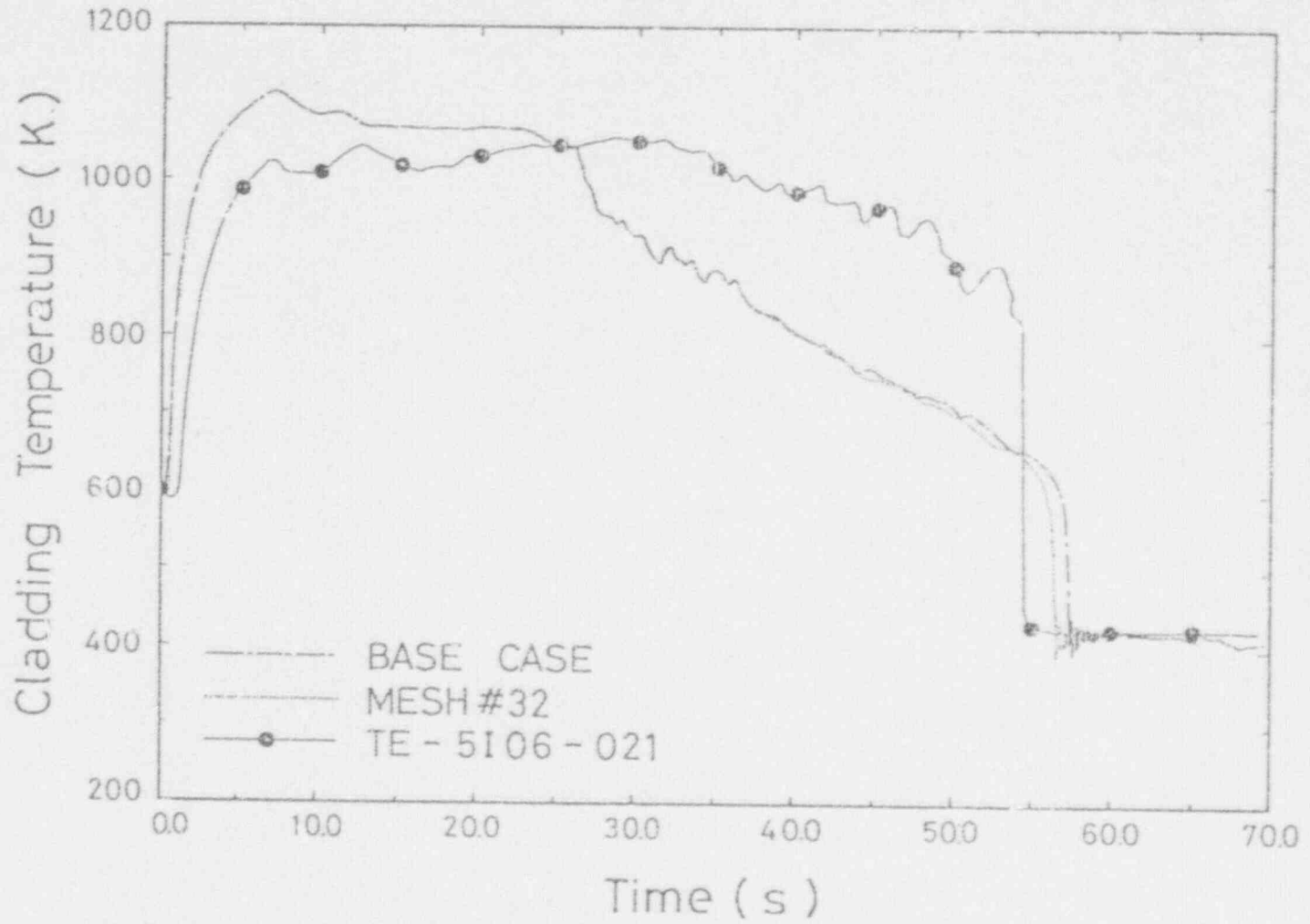


Figure 4.62 Comparison between Calculated Cladding Temperatures at Hottest Location of the BASE and MESH#32 Cases

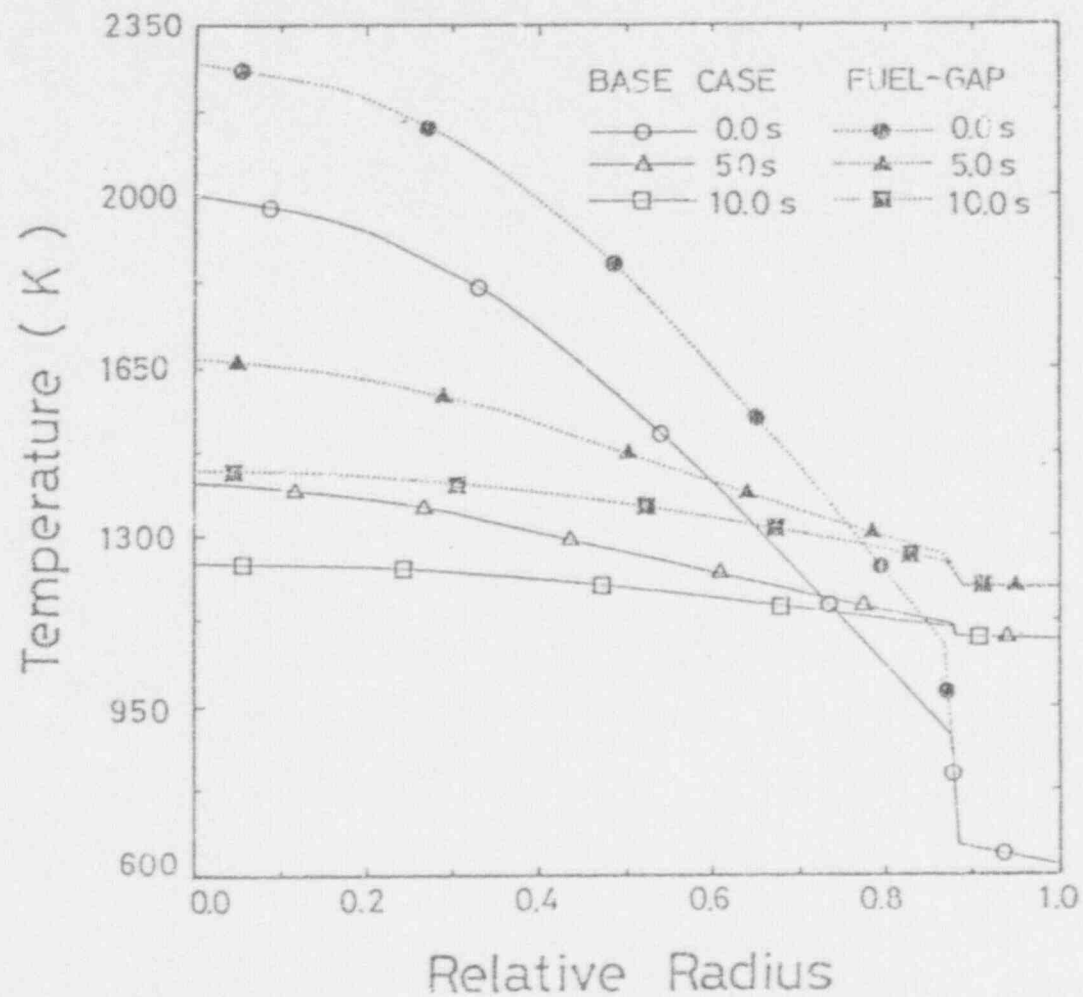


Figure 4.63 Comparison between Calculated Radial Temperature Distributions in Fuel Rod of the BASE and FUEL-GAP Cases

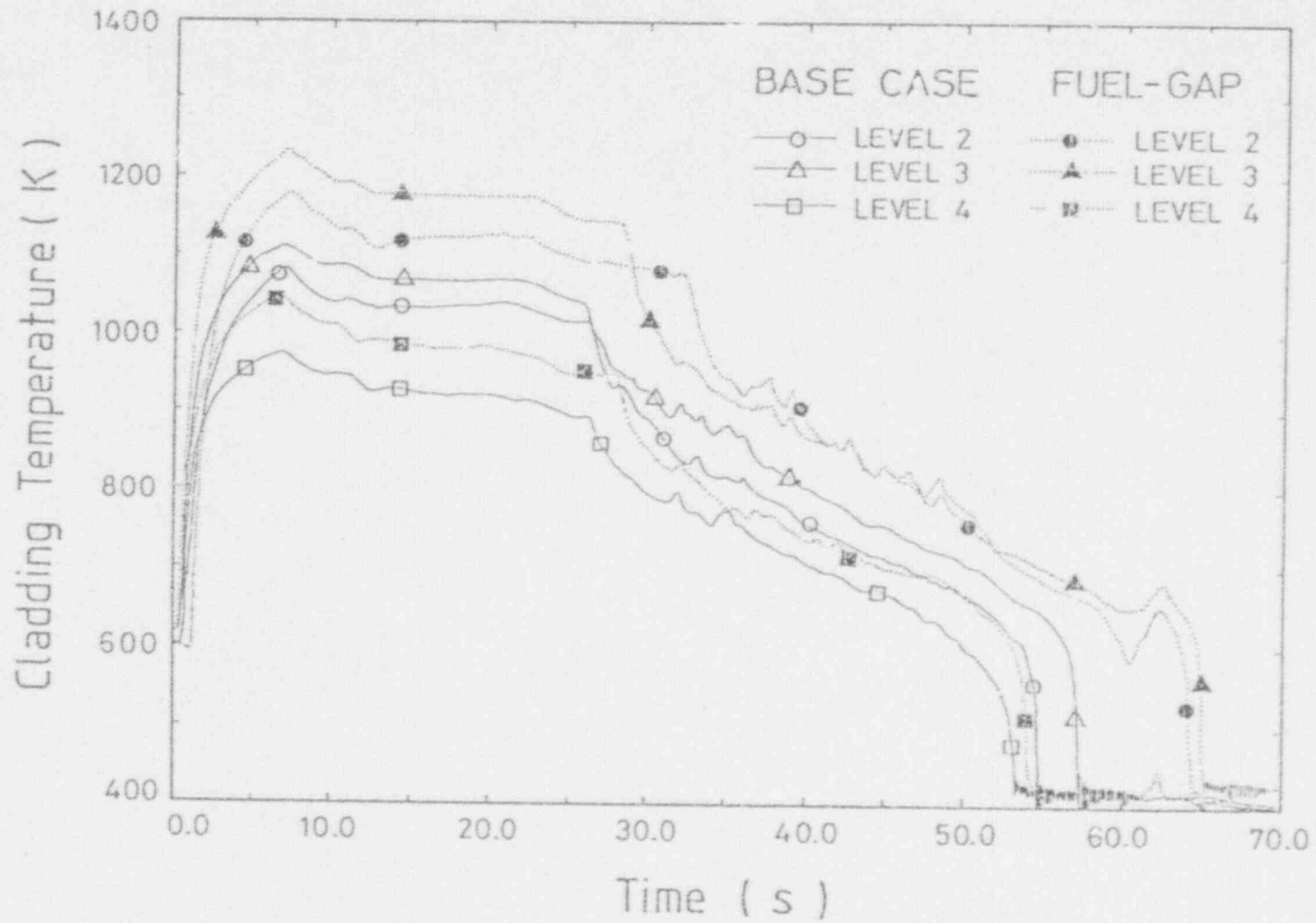


Figure 4.64 Comparison between Calculated Cladding Temperatures at Various Axial Locations of the BASE and FUEL-GAP Cases

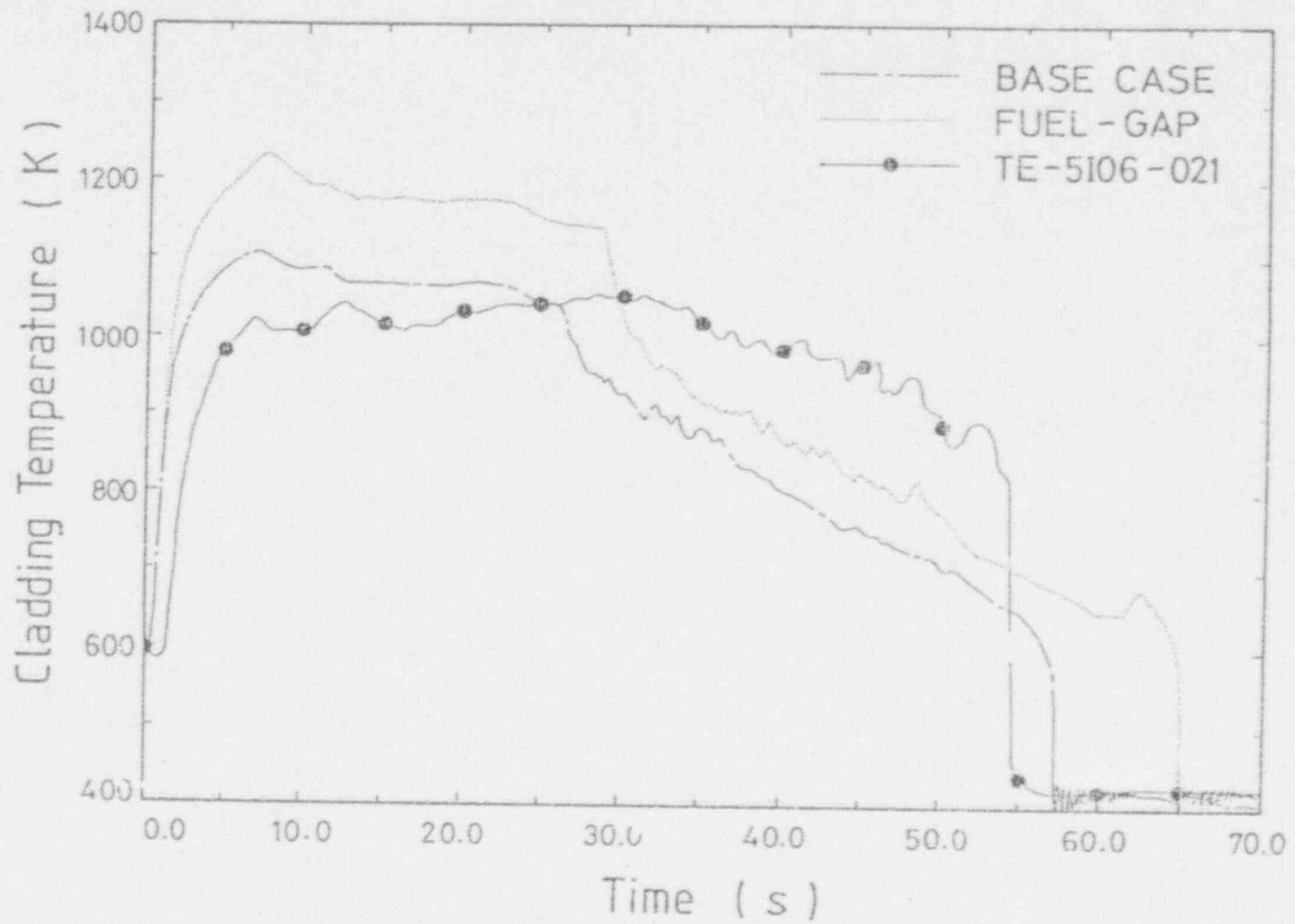


Figure 4.65 Comparison between Calculated Cladding Temperatures at Hottest Location of the BASE and FUEL-GAP Cases

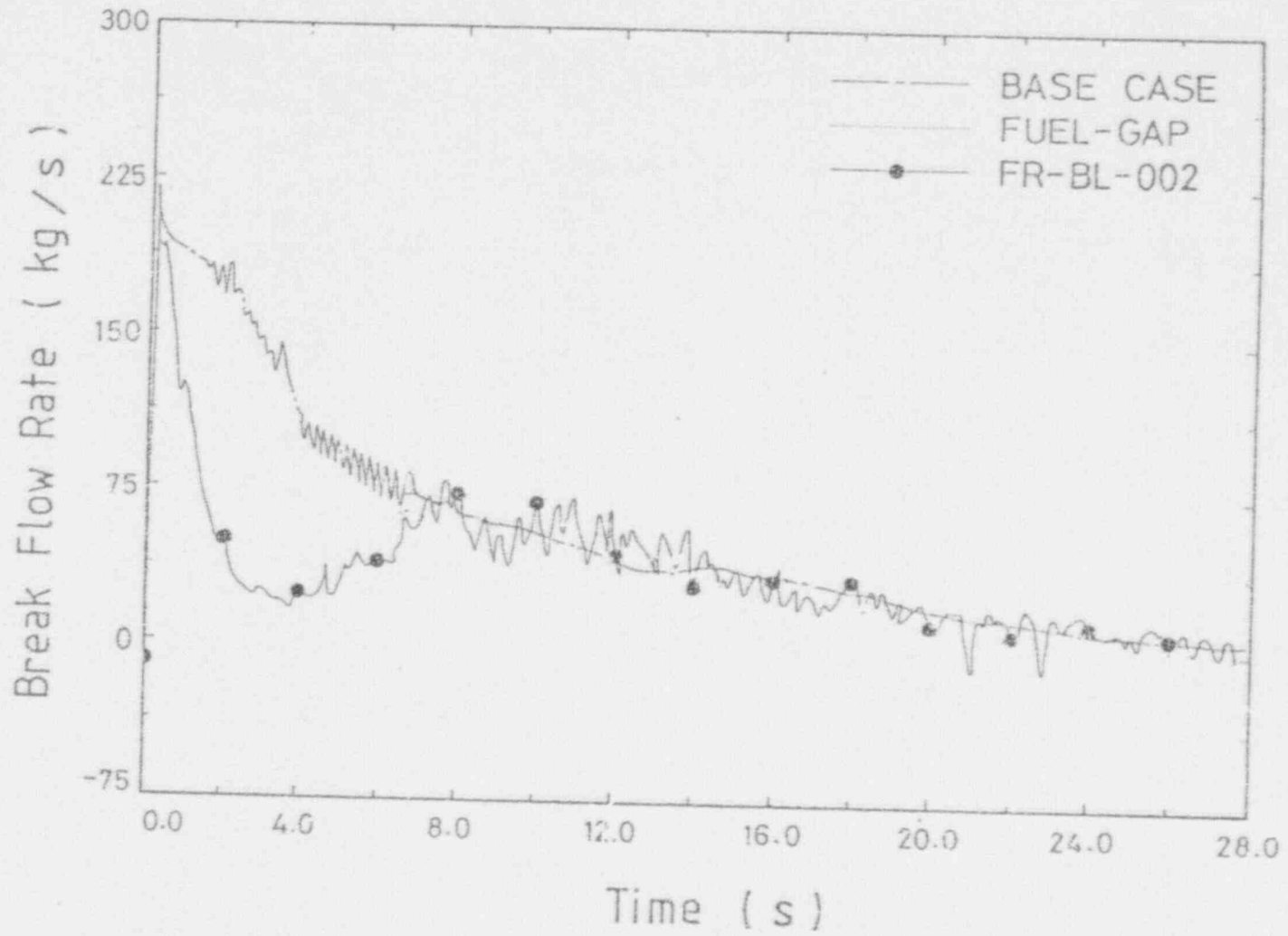


Figure 4.66 Comparison between Calculated Hot-Leg Break Flow Rates of the BASE and FUEL-GAP Cases

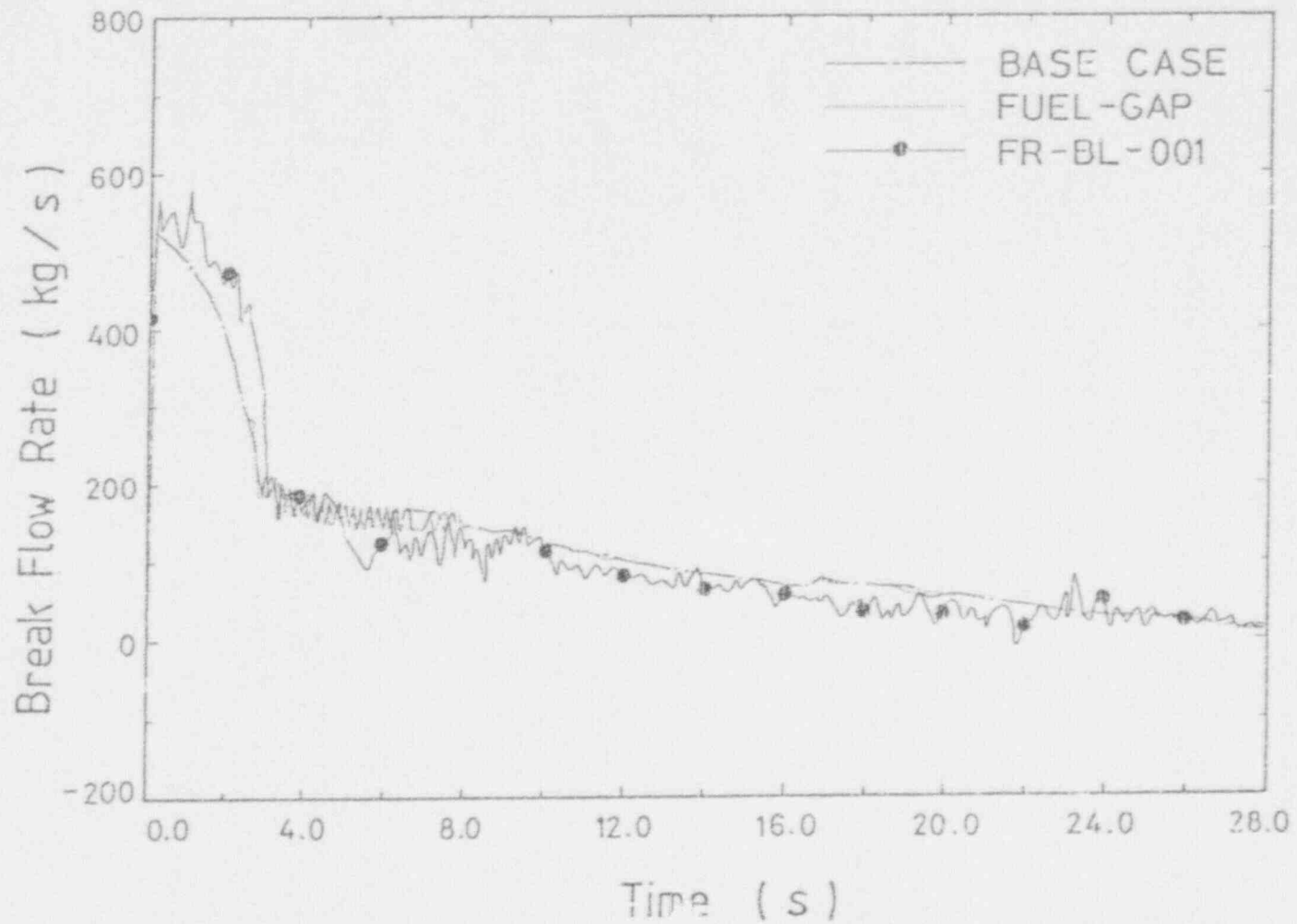


Figure 4.67 Comparison between Calculated Cold-Leg Break Flow Rates of the BASE and FUEL-Gap Cases

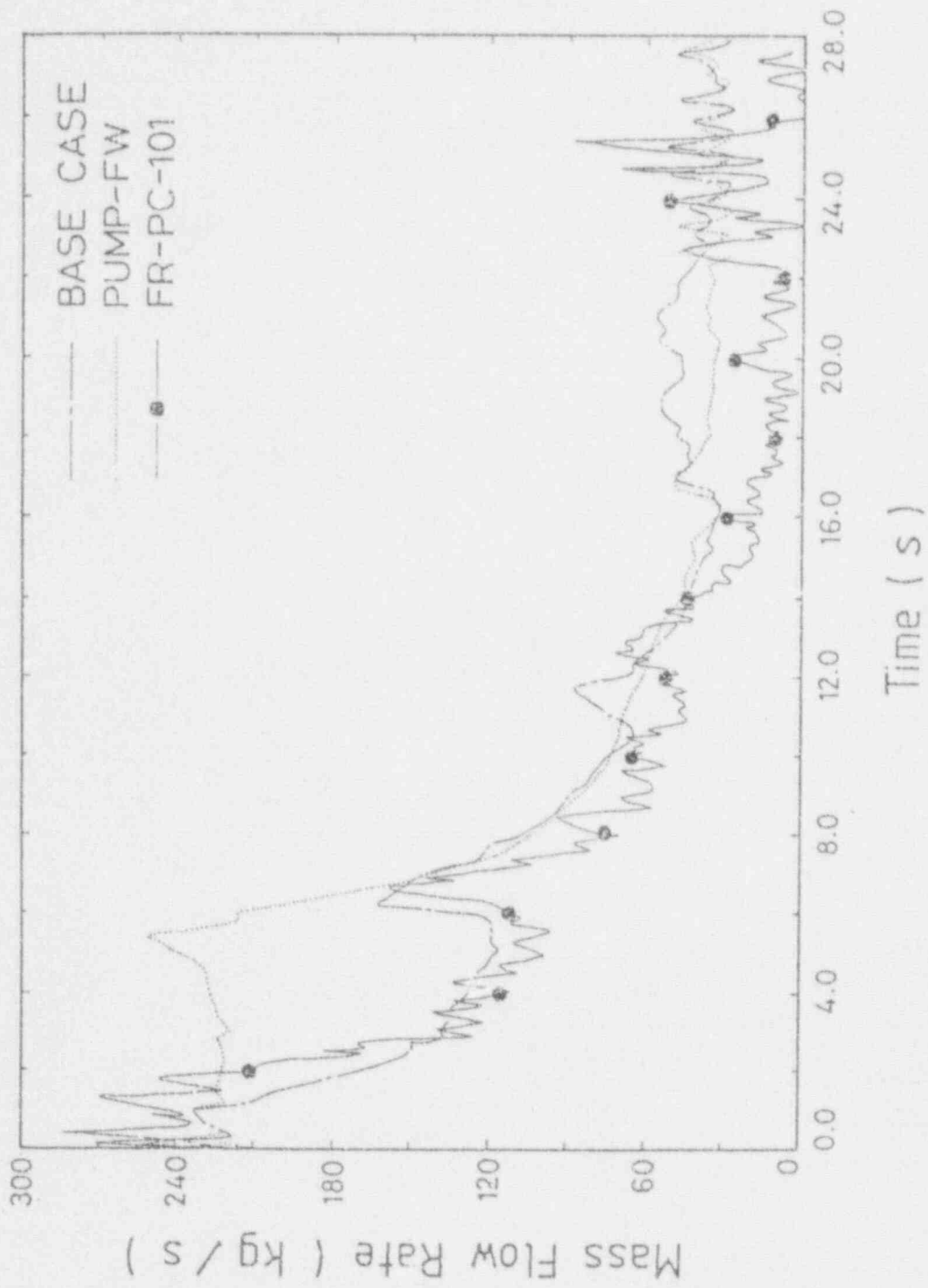


Figure 4.58 Comparison between Calculated Intact Loop Cold-Leg Flow Rates of the BASE and PUMP-FW Cases

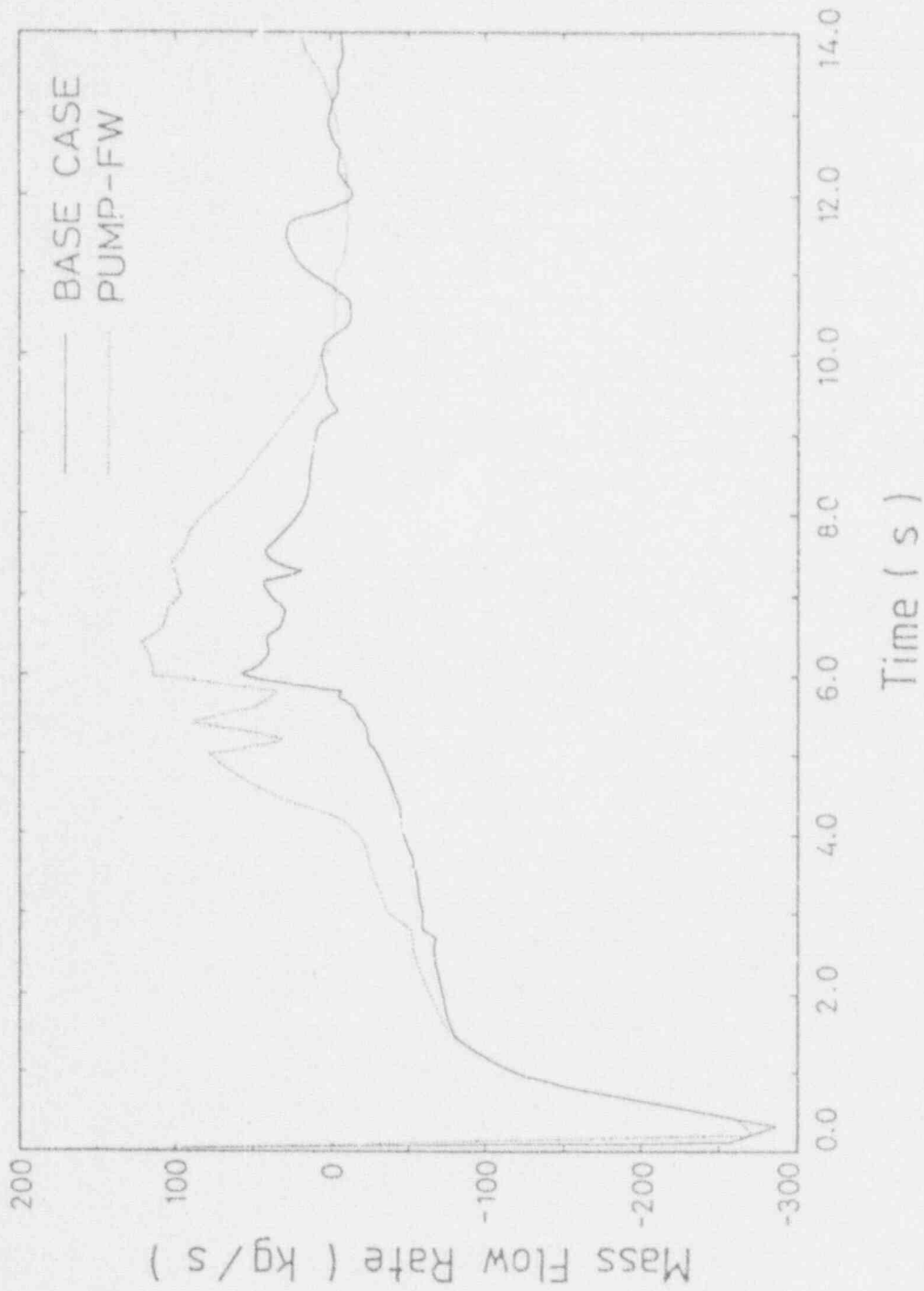


Figure 4.69 Comparison between Calculated Core Inlet Flow Rates of the BASE and PUMP-FW Cases

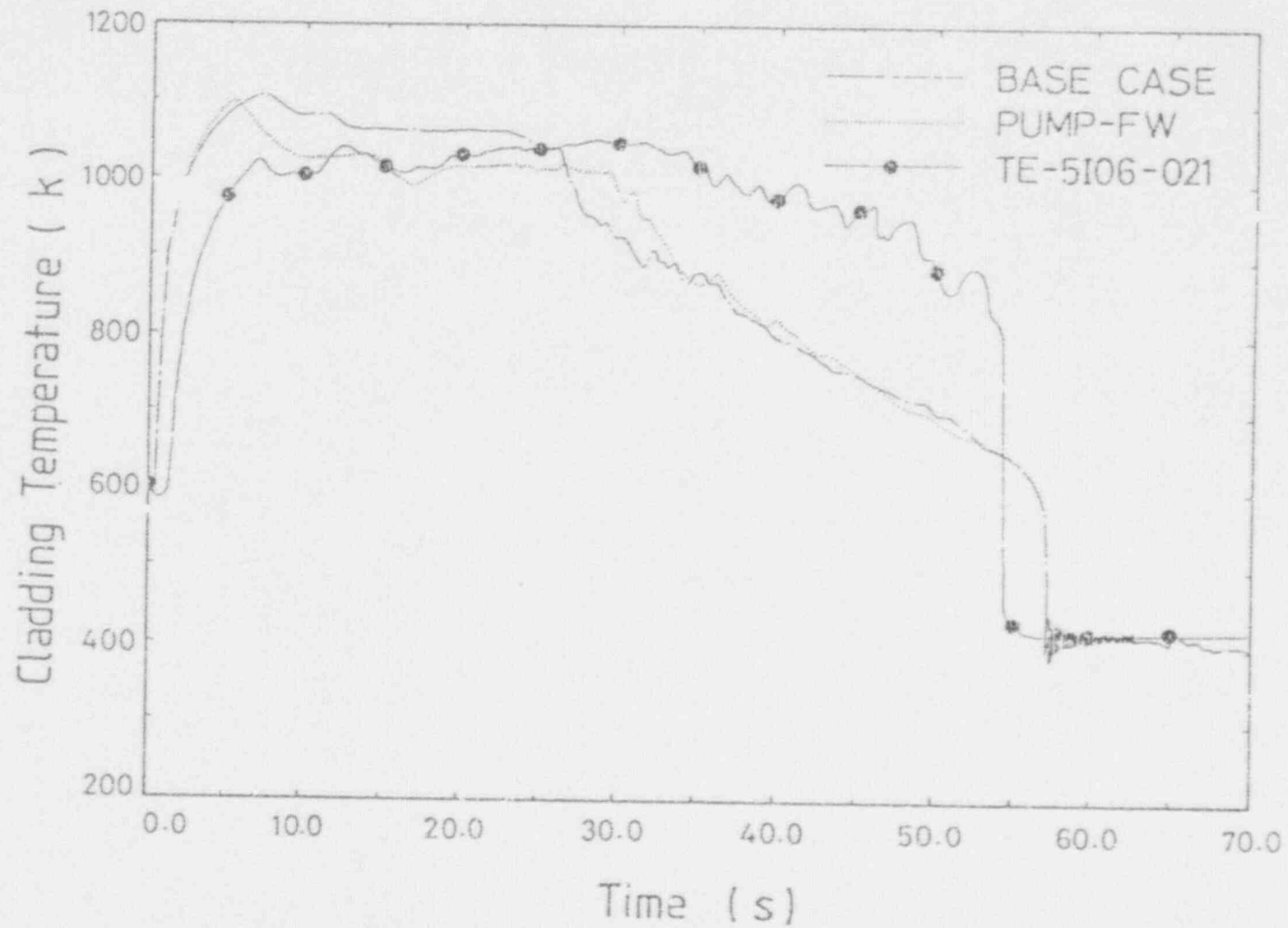


Figure 4.70 Comparison between Calculated Cladding Temperatures at Hottest Location of the BASE and PUMP-FW Cases

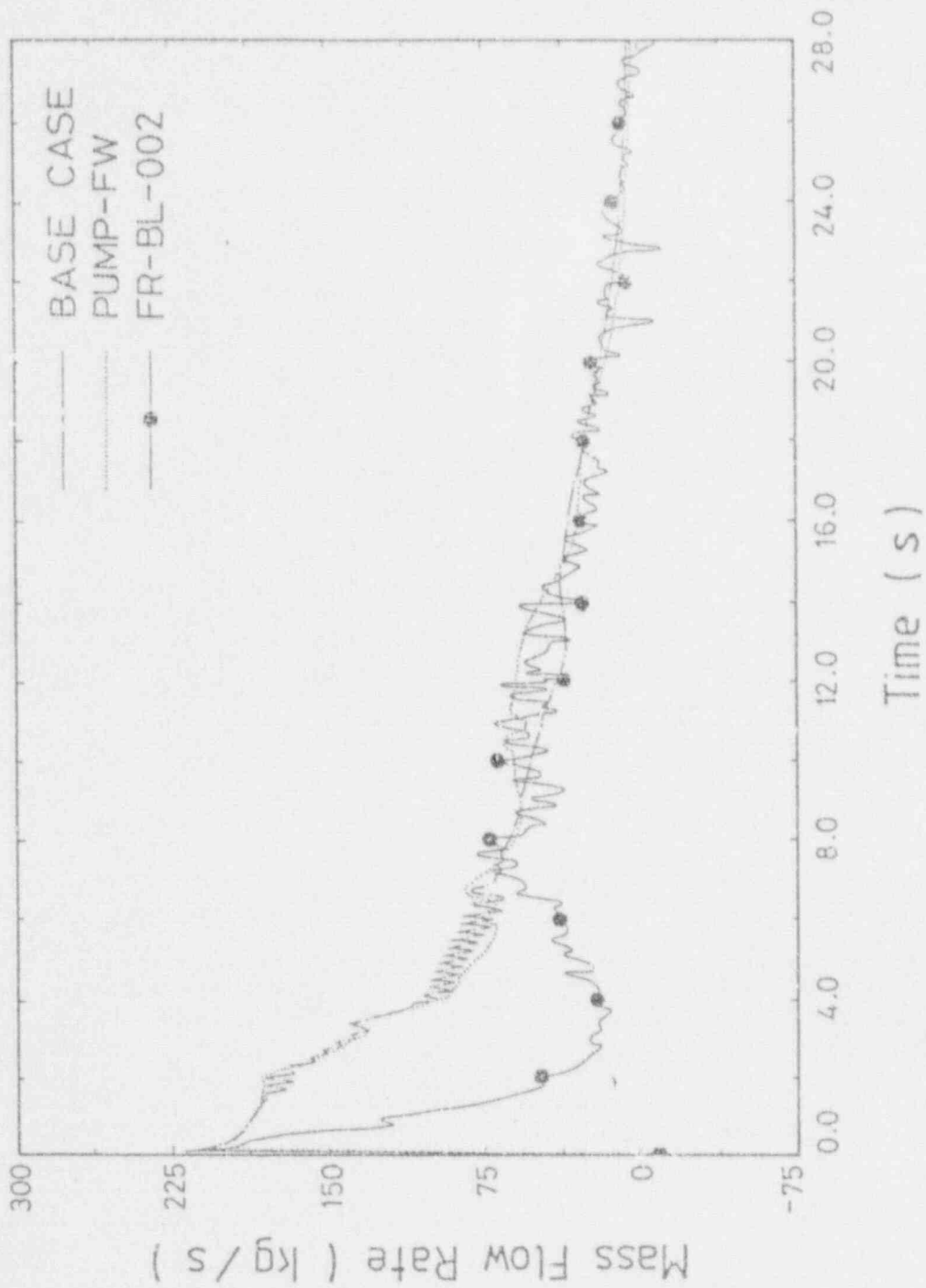


Figure 4.71 Comparison between Calculated Hot-L & Brak Flow Rates of the BASE and PUMP-FW Cases

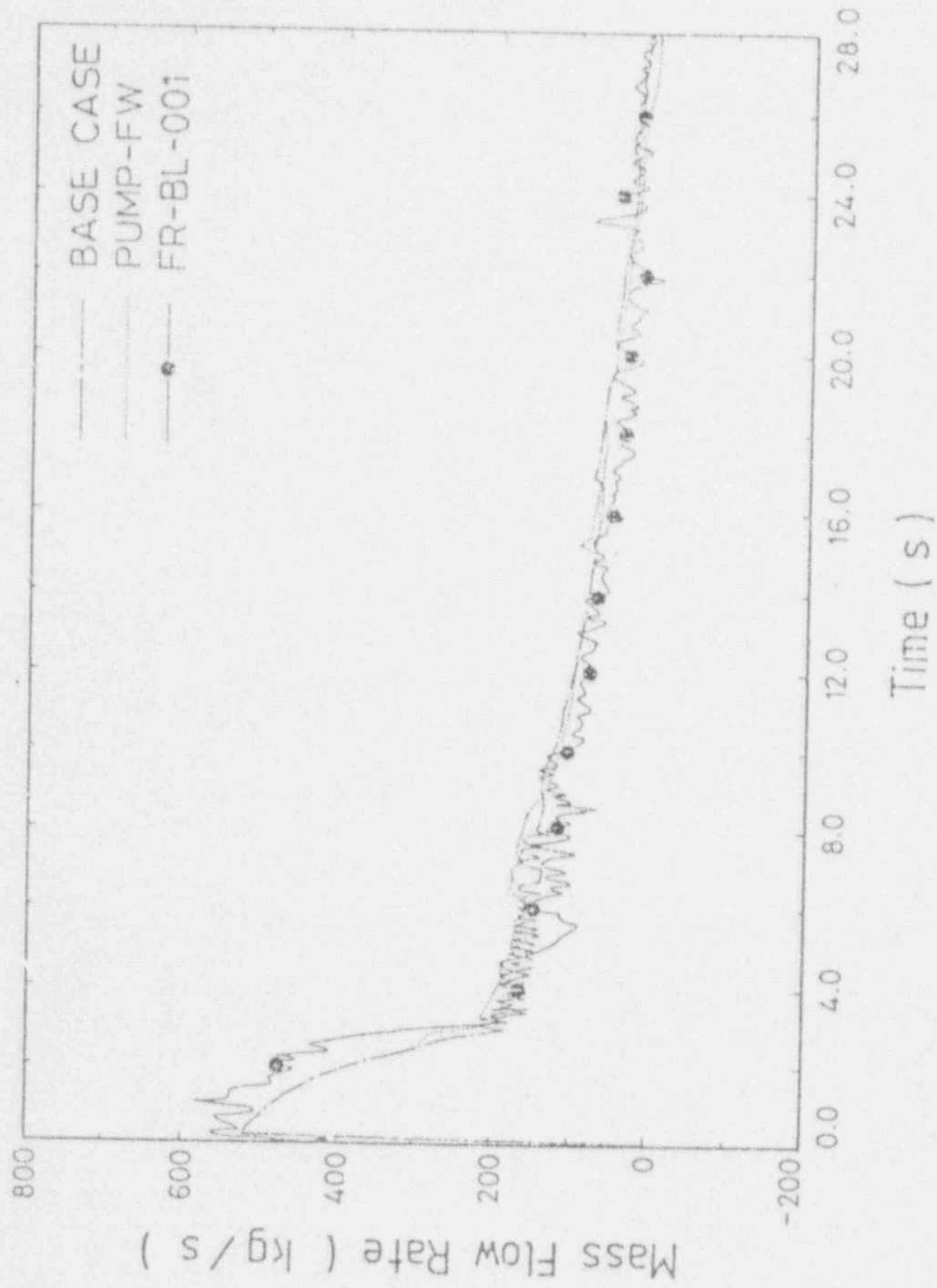


Figure 4.72 Comparison between Calculated Cold-Leg Break Flow Rates of the BASE and PUMP-FW Cases

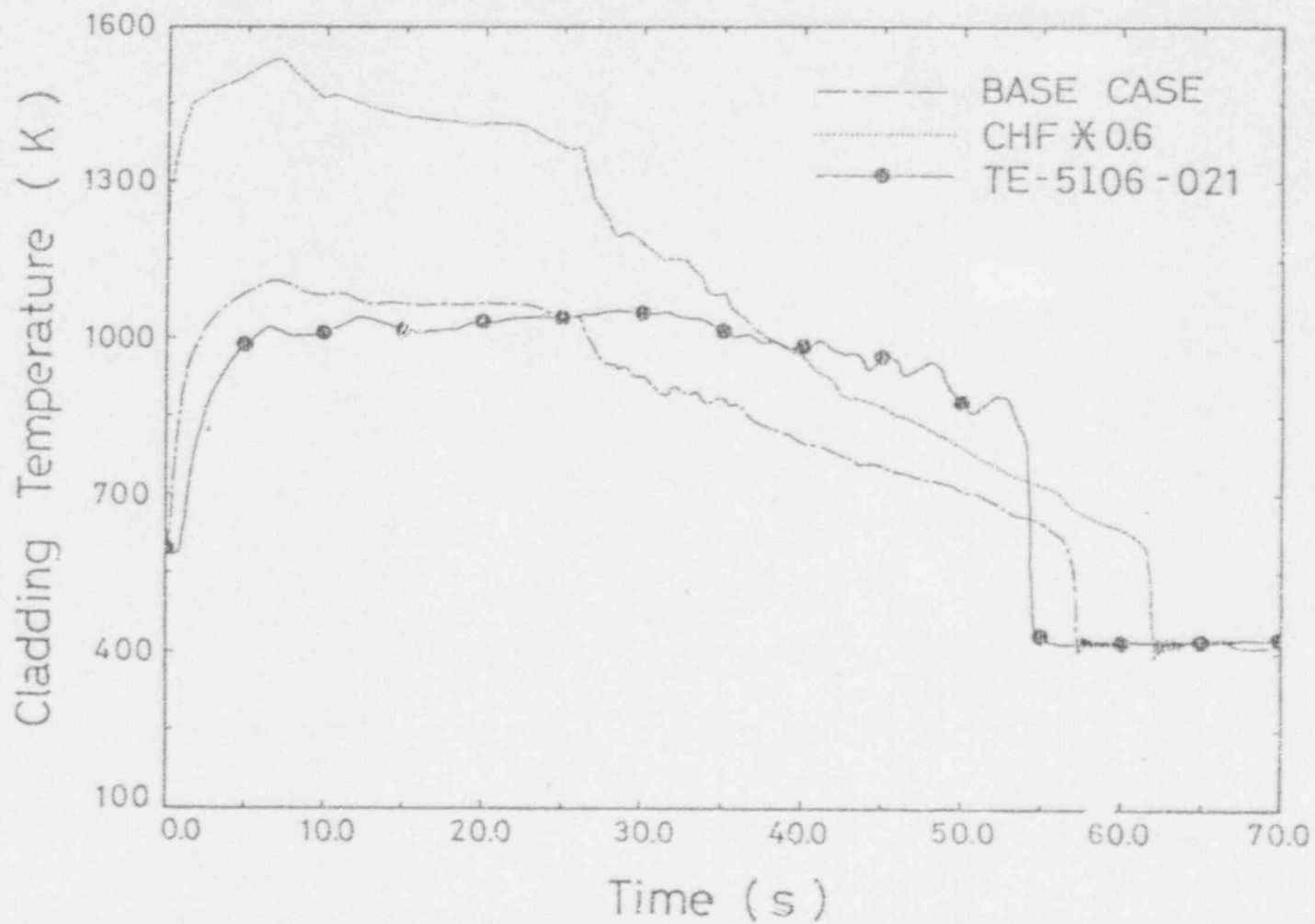


Figure 4.73 Comparison between Calculated Cladding Temperatures at Axial Level 3 of the BASE and CHF*0.6 Cases

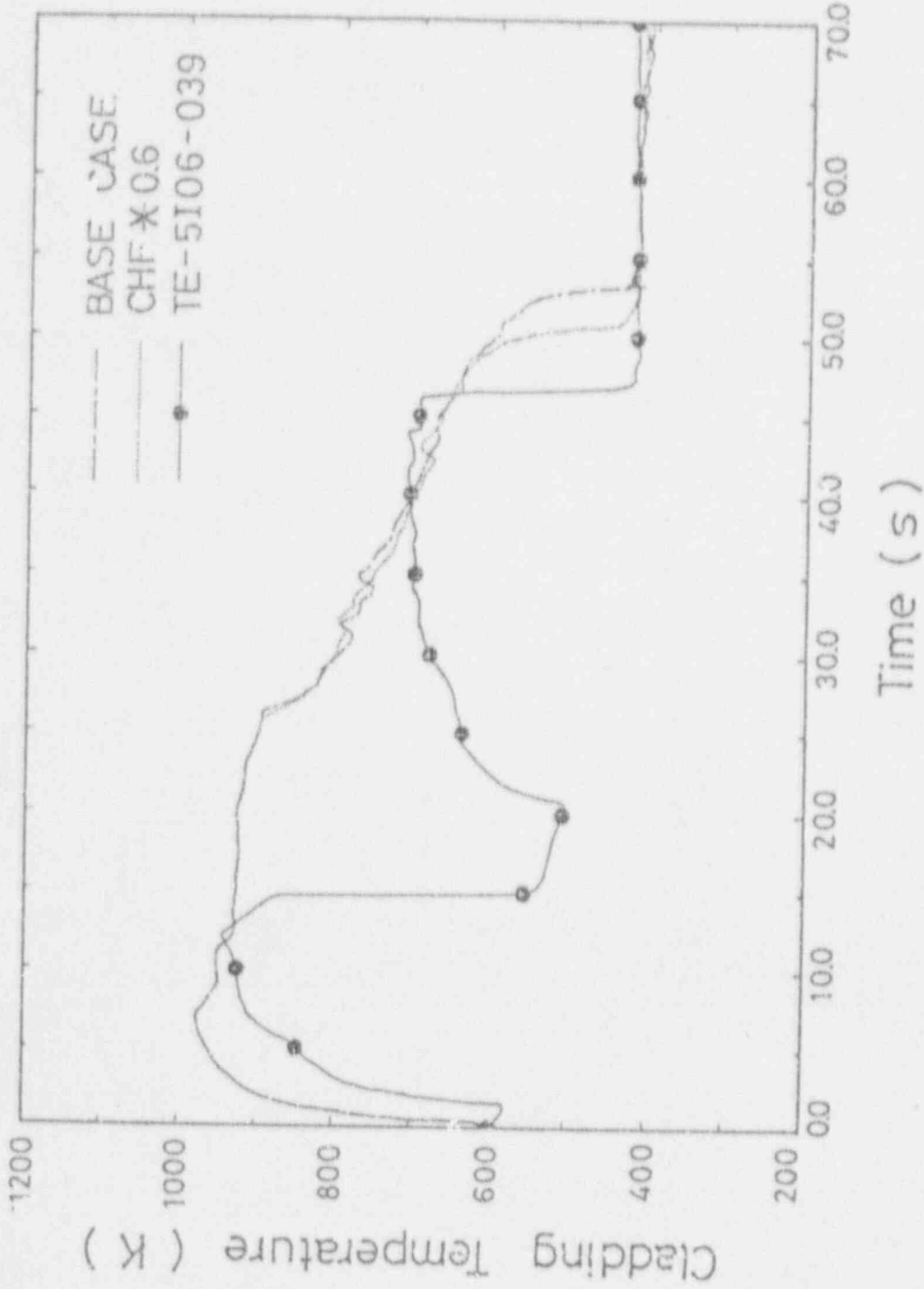


Figure 4.74 Comparison between Calculated Cladding Temperatures at Axial Level 4 of the BASE and CHF*0.6 Cases

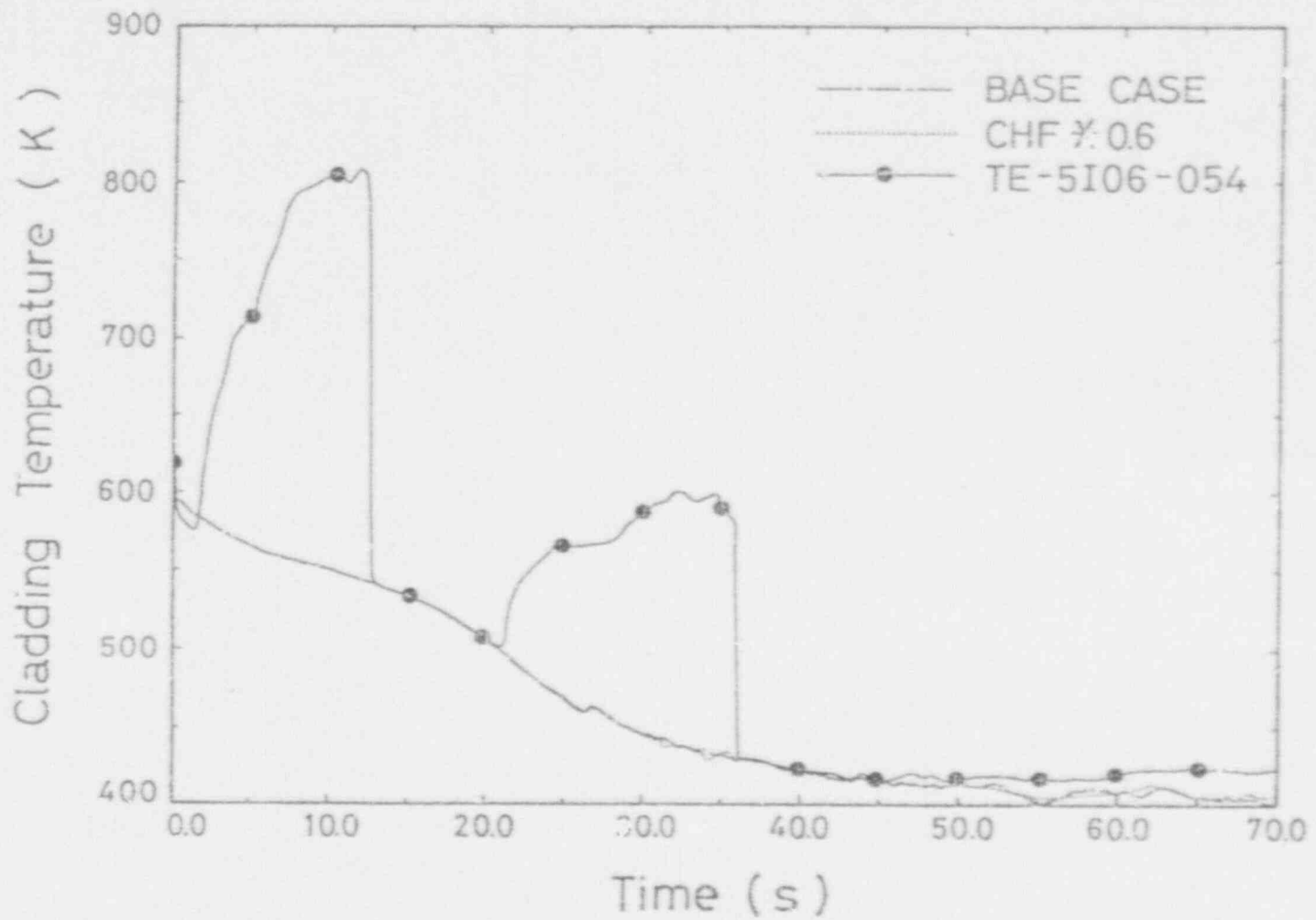


Figure 4.75 Comparison between Calculated Cladding Temperatures at Axial Level 5 of the BASE and CHF*0.6 Cases

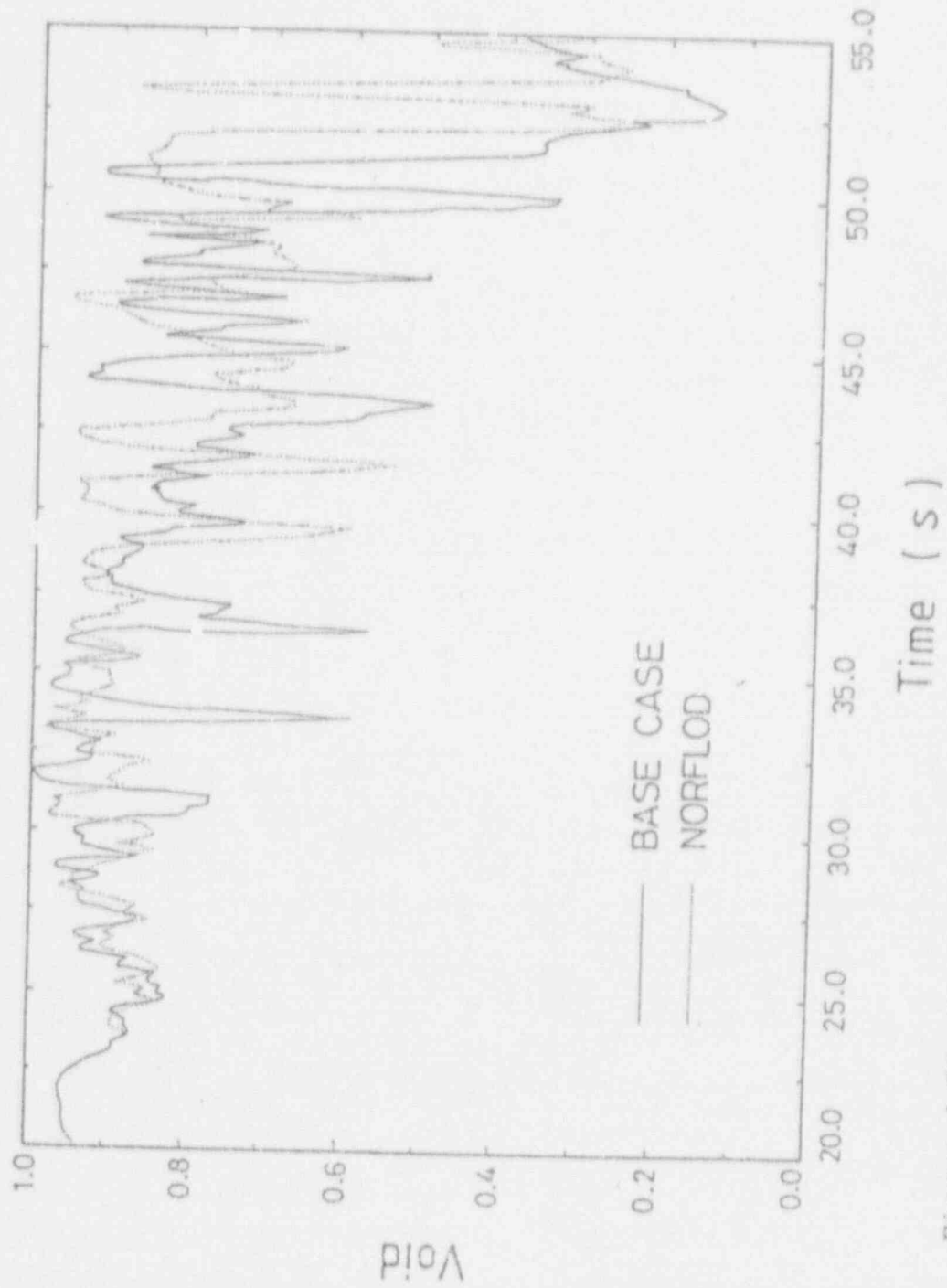


Figure 4.76 Comparison between Calculated Voids in Core Region of the BASE and NORFLOD Cases

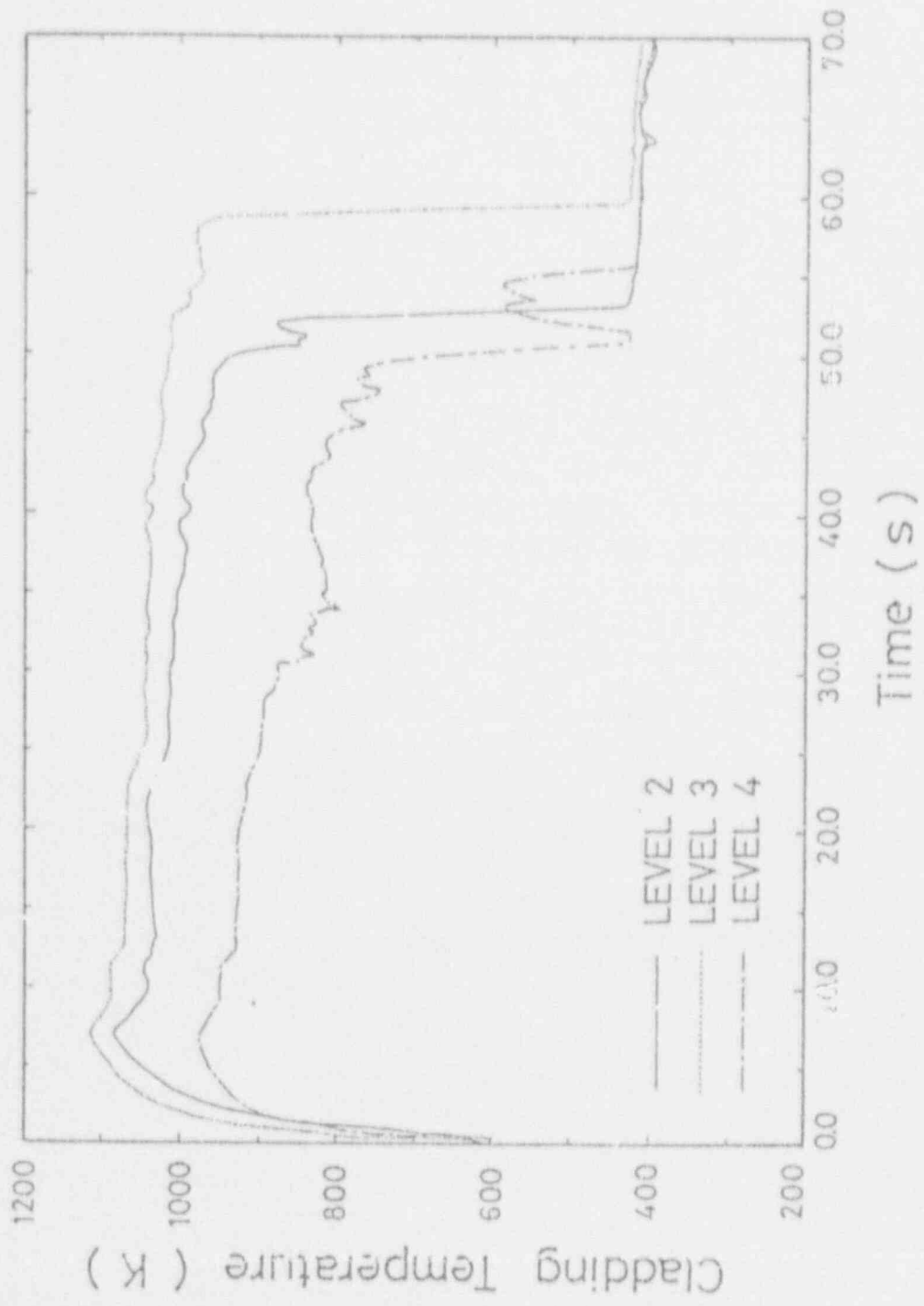


Figure 4.77 Calculated Cladding Temperatures at Hot Channel Hot Rod of the NORFLOD Case

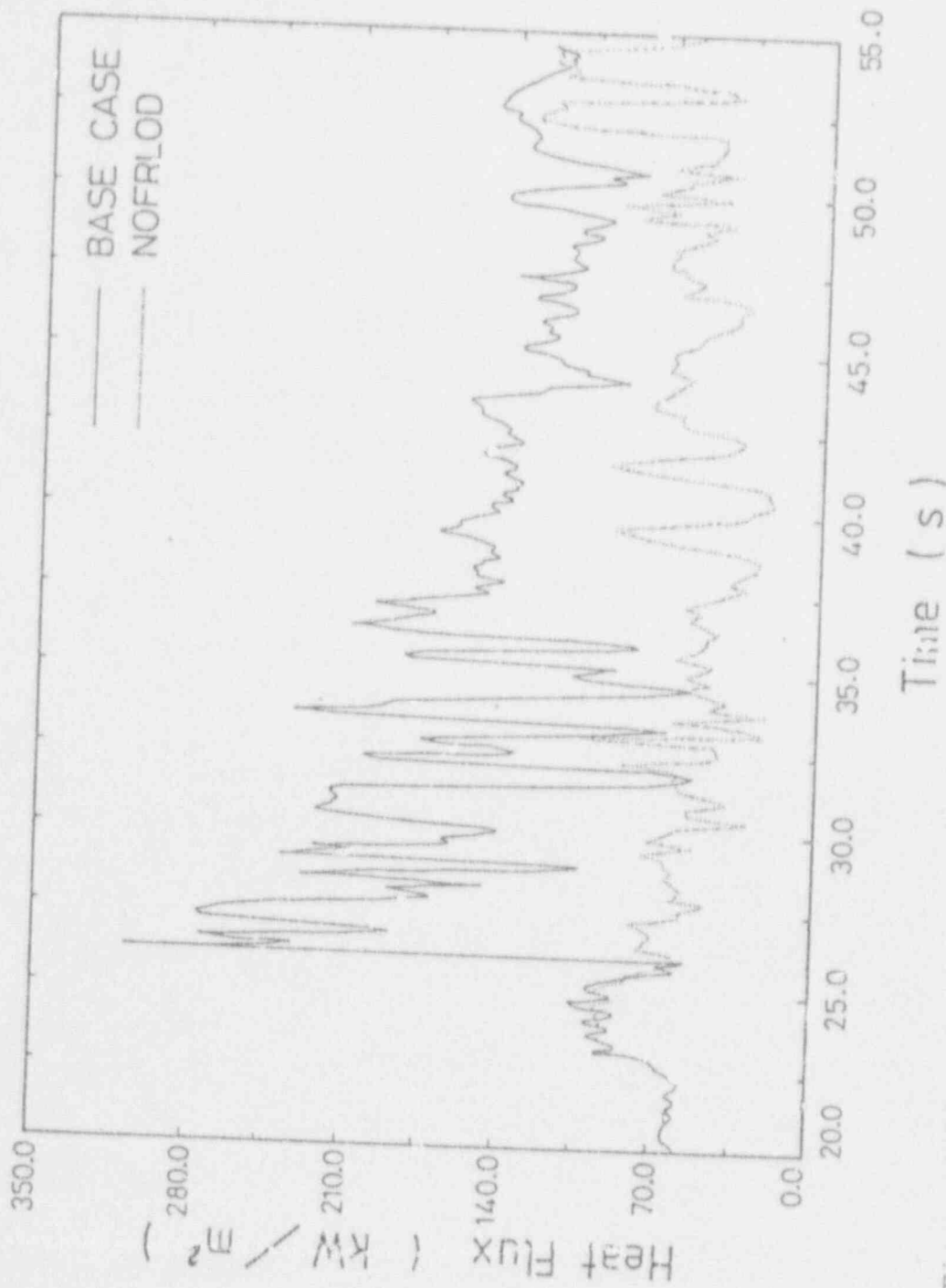


Figure 4.78 Comparison between Calculated Cladding Surface Heat Fluxes of the BASE and NOFRLOD Cases

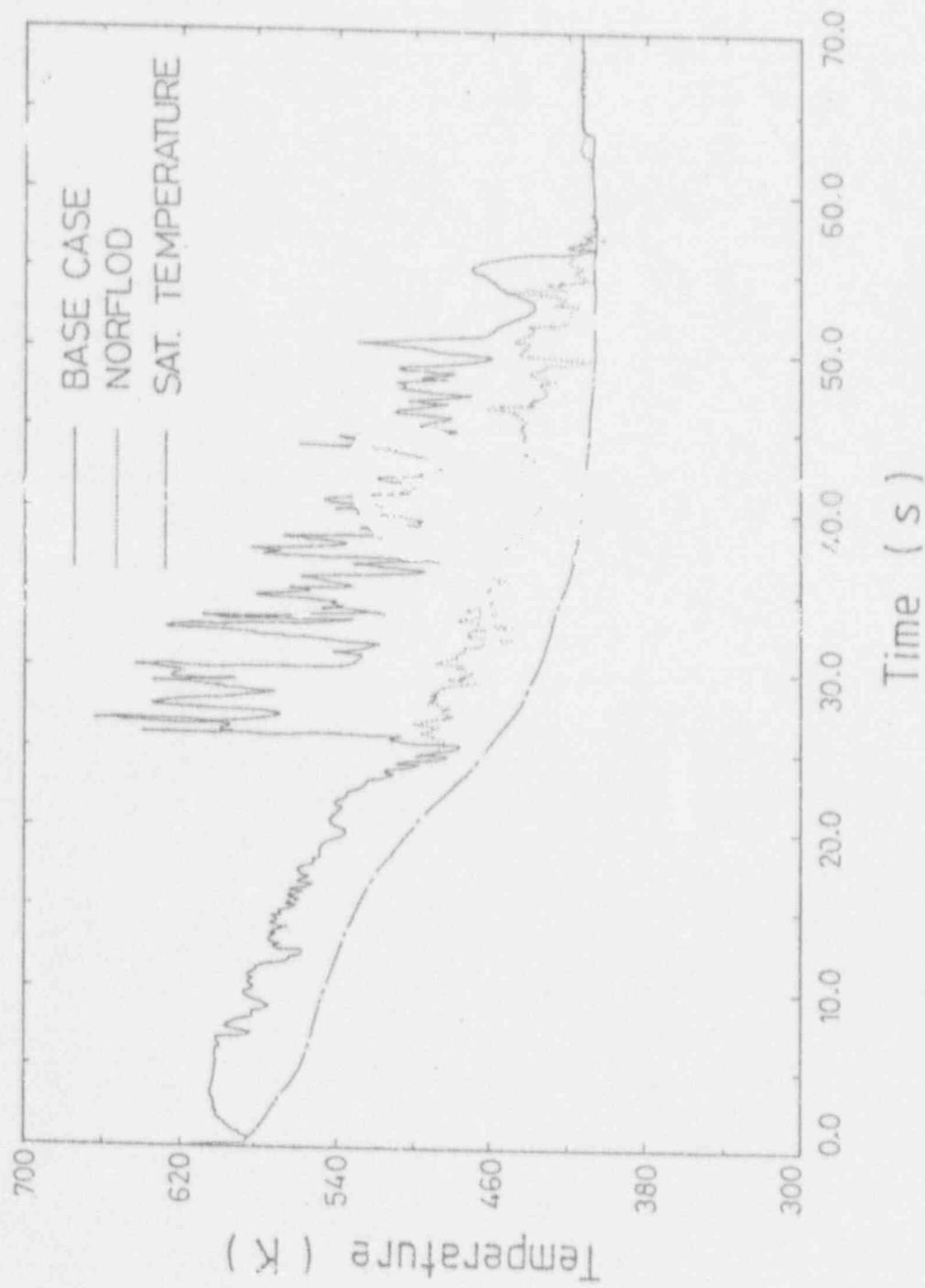


Figure 4.79 Comparison between Calculated Vapor Temperatures in Core Region of the BASE and NORFLOD Cases

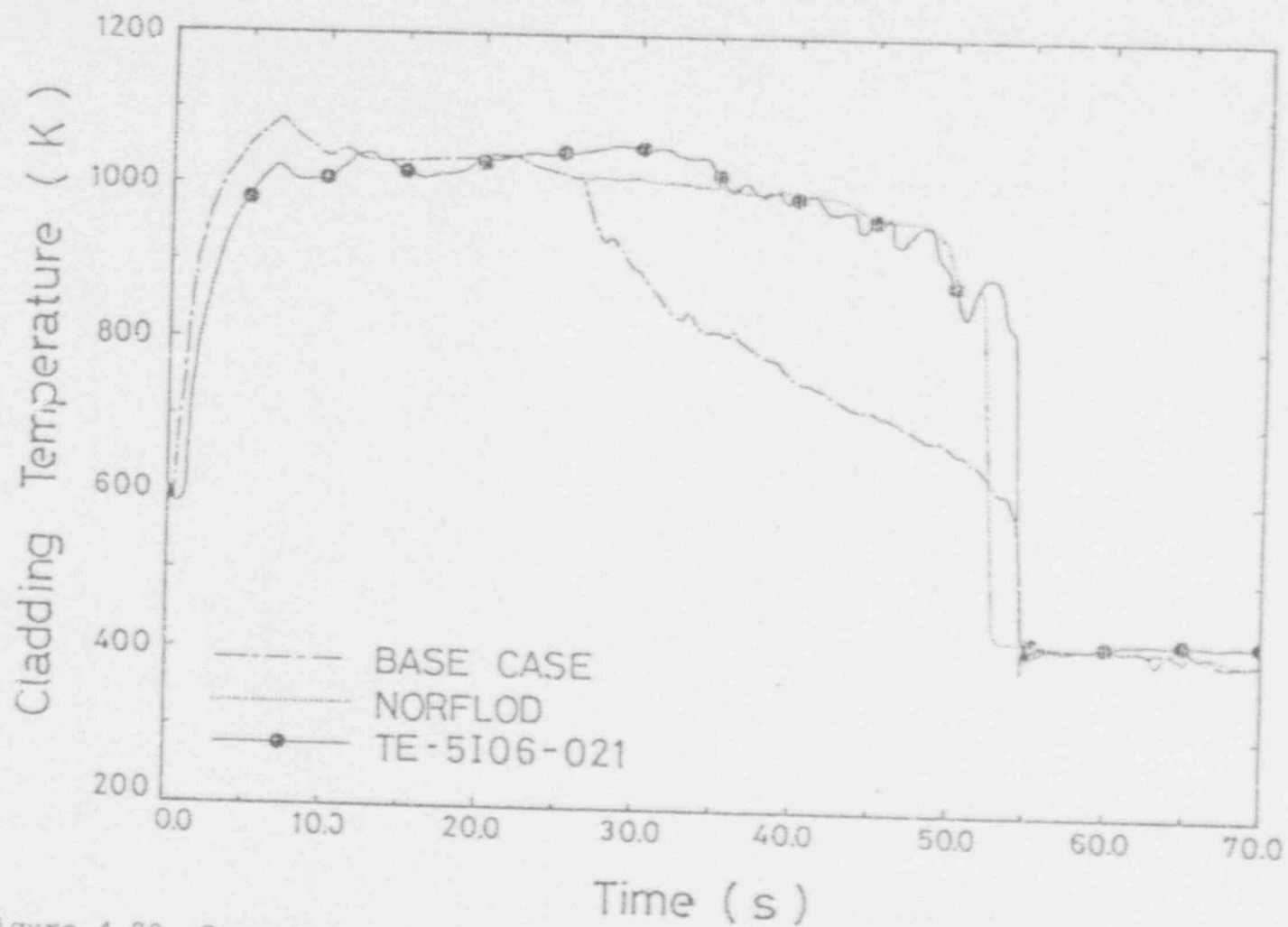


Figure 4.80 Comparison between Calculated Cladding Temperatures at Axial Level 2 of the BASE and NORFLOD Cases

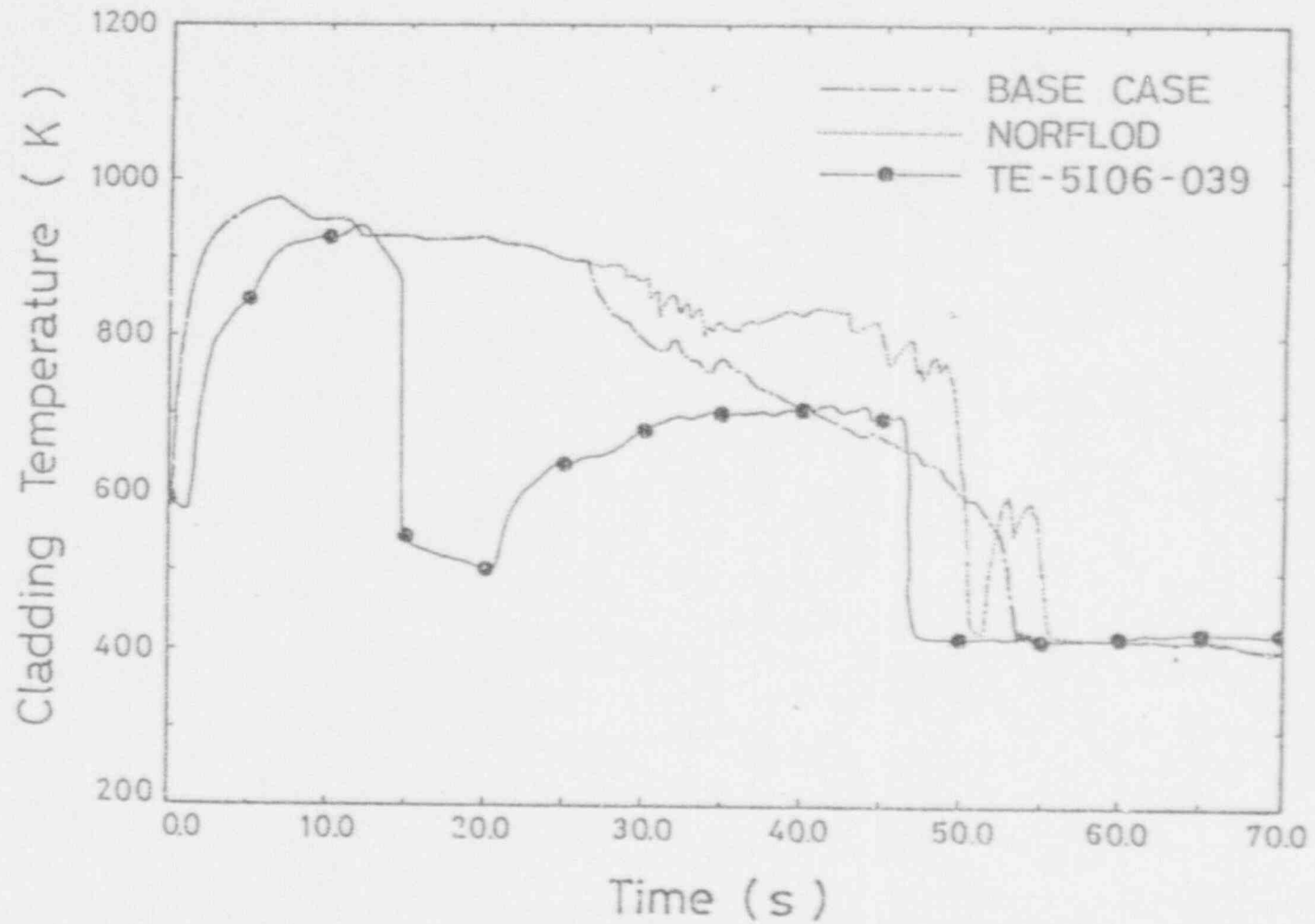


Figure 4.81 Comparison between Calculated Cladding Temperatures at Axial Level 4 of the BASE and NORFLOD Cases

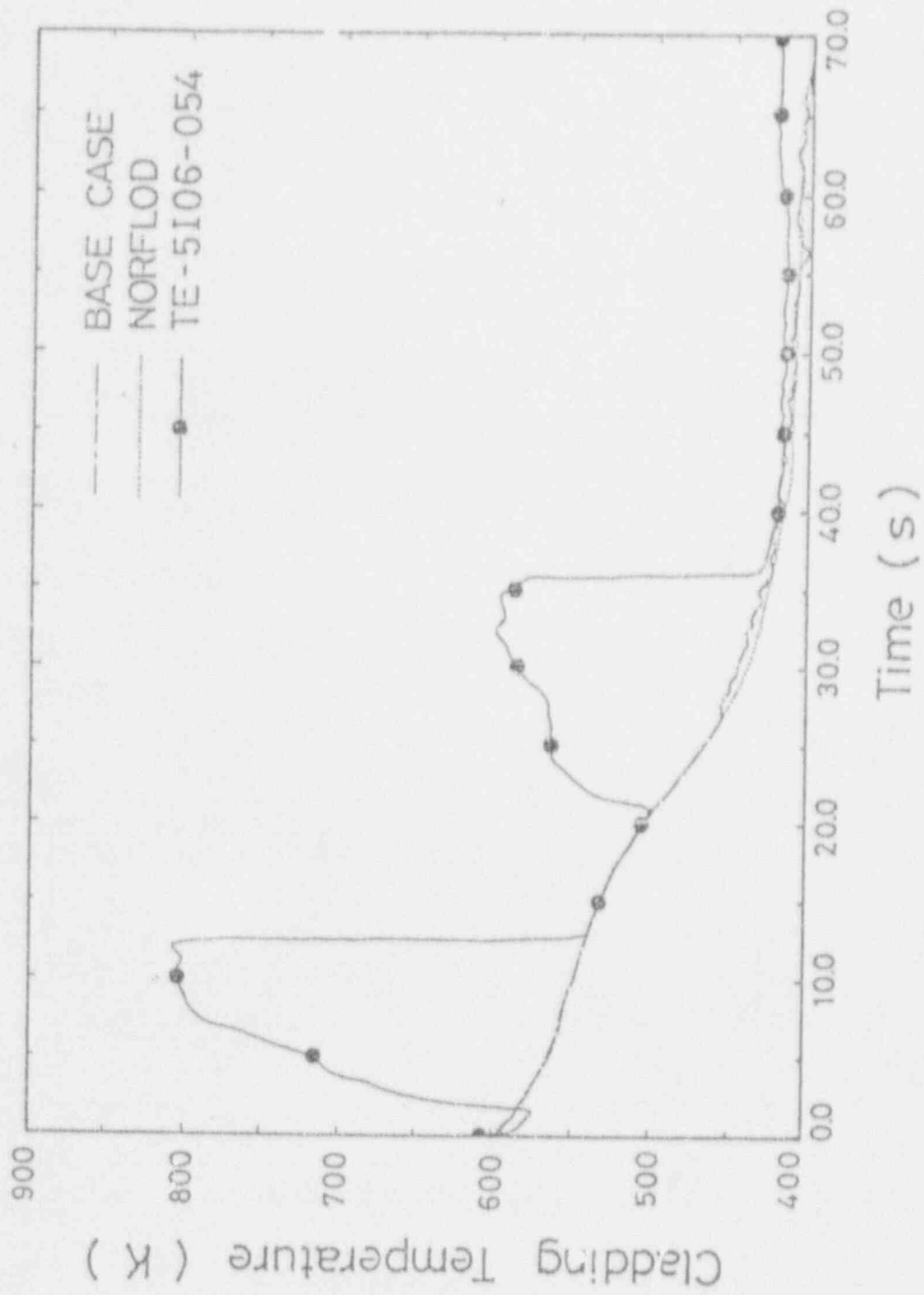


Figure 4.82 Comparison between Calculated Cladding Temperatures at Axial Level 5 of the BASE and NORFLOD Cases

REFERENCE

- [1] V. Ransom et. al., "RELAP5/MOD2 Code Manual," NUREG/CR-4312, EGG-2396, August 1985.
- [2] D. L. Reeder, "LOFT System and Test Description (5.5-ft Nuclear Core 1 LOCEs)," NUREG/CR-0247, TREE-1208, July 1978.
- [3] R.S. Semken, "LOFT Experiment Operating Specification LOFT Power Ascension Experiment Series L2 Nuclear Experiment L2-5," EGG-LOFT-5696, June 2, 1982.
- [4] P. N. Demmie, T. H. Chen, and S. R. Behling, "Best Estimate Prediction for LOFT Nuclear Experiment L2-5," EGG-LOFT-5869, May 1982.
- [5] P. D. Bayless and J. M. Divine, "Experiment Data Report for LOFT Large Break Loss-of-Coolant Experiment L2-5," NUREG/CR-2826, EGG-2210, August 1982.
- [6] D. G. Hall, "Empirically Based Modeling Techniques for Predicting Critical Flow Rates in Nozzles, Tubes, and Orifices," CVAP-TR-78-010, EG&G Idaho, Inc., NTIS, May 1978.
- [7] J. R. Travis, C.W. Hirt, and W. C. Rivard, "Multidimensional Effects in Critical Two-Phase Flow," Nucl. Sci. Eng., Vol. 68, December 1978.
- [8] A. Sjoberg and D. Caraher, "Assessment of RELAP5/MOD2 Against 25 Dryout Experiments Conducted at the Royal Institute of Technology," NUREG/IA-0009, October 1986.
- [9] Y. A. Hassan, "Modifications and Assessment of Rewetting Correlations for Light Water Reactor System Analysis," Trans. ANS, Vol. 53, PP. 537, November 1986.
- [10] D. G. Morris et. al., "An Experimental Study of Rod Bundle Dispersed-Flow Film Boiling with High-Pressure Water," Nucl. Technol., Vol. 69, 1985.
- [11] Y. A. Hassan, "Analysis of FLECHT and FLECHT-SEASET Reflood Tests with RELAP5/MOD2," Nucl. Technol., Vol. 74, August 1986.
- [12] J. Dreier, G. Analytis, and R. Chawla, "NEPTUN-III Reflooding and Boiloff Experiments with an LWHCR Fuel Bundle Simulator: Experimental Results and Initial Code Assessment Efforts," Nucl. Technol., Vol. 80, Jan. 1988.

- [13] G. Analytis, "An Experimental Version of RELAP5/MOD2/36.02: Model Changes Assessment Efforts and Numerical Problems," ICAP Meeting, Grenoble, France, March 1-3, 1988.
- [14] Y. A. Hassan, "Dispersed-Flow Heat Transfer During Reflood in a Pressurized Water Reactor After a Large-Break Loss-of-Coolant Accident," Trans. ANS, Vol. 53, November 1986.
- [15] Private Communication, "Code Improvement Plan for TRAC-PF1 and RELAP5," U. S. NRC, November 1987.
- [16] M. Dillistone and C. G. Richards, "Counter-Current Flow Modelling in RELAP5," ICAP Meeting, Grenoble, France, March 1-3, 1988.

APPENDIX


```

*****
* LOFT MODEL FOR EXPERIMENT L2-5
*****
* TWO-CHANNEL CORE AND SPLIT INLET ANNULUS AND DOWNCOMER
*****
0000100 NEW TRANSNT
*000101 INP-CHK
0000105 5.0 10.0
0000110 NITROGEN
*****
* TIME STEP CONTROL CARDS * REQUIRED
*****
0000201 60.0 1.0-8 0.02 00002 10 500 500
*****
* MINOR EDIT VARIABLES
*****
* PRESSURES
*****
0000301 P 345010000 * PE-BL-001
0000302 P 310010000 * PE-BL-002
0000303 P 185010000 * PE-PC-001
0000304 P 100010000 * PE-PC-002
0000305 P 250010000 * PE-1UP-001A
0000306 P 215010000 * PE-1ST-001A
0000307 P 415060000 * PE-PC-004
0000308 P 510010000 * S.G.
*****
* TEMPERATURES
*****
0000310 TEMPF 345010000 * TE-BL-001A,001B,001C
0000311 TEMPF 310010000 * TE-BL-002B
0000312 TEMPF 100010000 * TE-PC-002A,002B,002C
0000313 TEMPF 185010000 * TE-PC-001A,001B,001C
0000314 TEMPF 215010000 * TE-1ST-010
0000315 TEMPF 250010000 * TE-1UP-006
*
0000316 TEMPG 345010000 * TE-BL-001A,001B,001C
0000317 TEMPG 310010000 * TE-BL-002B
0000318 TEMPG 100010000 * TE-PC-002A,002B,002C
0000319 TEMPG 185010000 * TE-PC-001A,001B,001C
0000320 TEMPG 215010000 * TE-1ST-010
0000321 TEMPG 250010000 * TE-1UP-006
*****
* DENSITIES
*****
0000322 RHO 345010000 * DE-BL-105
0000323 RHO 310010000 * DE-BL-002A,002C
0000324 RHO 180010000 * DE-PC-105
0000325 RHO 100010000 * DE-PC-205
*****
* MASS FLOW RATES
*****
0000330 MFLOWJ 365000000 * BREAK PLANE BLCL: FR-BL-001
0000331 MFLOWJ 330000000 * BREAK PLANE BLHL: FR-BL-002
0000332 MFLOWJ 345020000 * DTT-RAKE BLCL
0000333 MFLOWJ 310020000 * DTT-RAKE BLHL
0000334 MFLOWJ 185020000 * DTT-RAKE ILCL
0000335 MFLOWJ 100020000 * DTT-RAKE ILHL
0000336 MFLOWJ 400010000 * PRES. SURGE LINE FLOW
0000337 MFLOWJ 500010000 * SEPR. STEAM OUTLET
0000338 MFLOWJ 550000000 * STEAM FLOW
*****

```

* CLADDING TEMPERATURES CONTROL MODULE

```

*****
0000340  HTTEMP  236100110      * AVG ROD AVG CH LEV 1
0000341  HTTEMP  236200110      * AVG ROD AVG CH LEV 2
0000342  HTTEMP  236300110      * AVG ROD AVG CH LEV 3
0000343  HTTEMP  236400110      * AVG ROD AVG CH LEV 4
0000344  HTTEMP  236500110      * AVG ROD AVG CH LEV 5
0000345  HTTEMP  236600110      * AVG ROD AVG CH LEV 6
*
0000346  HTTEMP  237100110      * AVG ROD HOT CH LEV 1
0000347  HTTEMP  237200110      * AVG ROD HOT CH LEV 2
0000348  HTTEMP  237300110      * AVG ROD HOT CH LEV 3
0000349  HTTEMP  237400110      * AVG ROD HOT CH LEV 4
0000350  HTTEMP  237500110      * AVG ROD HOT CH LEV 5
0000351  HTTEMP  237600110      * AVG ROD HOT CH LEV 6
*
0000352  HTTEMP  238100110      * HOT ROD HOT CH LEV 1
0000353  HTTEMP  238200110      * HOT ROD HOT CH LEV 2
0000354  HTTEMP  238300110      * HOT ROD HOT CH LEV 3
0000355  HTTEMP  238400110      * HOT ROD HOT CH LEV 4
0000356  HTTEMP  238500110      * HOT ROD HOT CH LEV 5
0000357  HTTEMP  238600110      * HOT ROD HOT CH LEV 6
*****

```

* CORE HOT CHANNEL DENSITIES AND VOID FRACTIONS

```

*****
0000360  RHO      233010000
0000361  RHO      234010000
0000362  RHO      235010000
0000363  RHO      236010000
0000364  RHO      237010000
0000365  RHO      238010000
0000366  VOIDG    233010000
0000367  VOIDG    234010000
0000368  VOIDG    235010000
0000369  VOIDG    236010000
0000370  VOIDG    237010000
0000371  VOIDG    238010000
*****

```

* CORE HOT SPOT MASS FLOWS

```

*****
0000375  MFLOWJ  228010000      * AVERAGE CHANNEL HOT SPOT
0000376  MFLOWJ  228020000      * CROSSFLOW
0000377  MFLOWJ  234010000      * HOT CHANNEL HOT SPOT
*****

```

* ECC SYSTEM MASS FLOWS

```

*****
0000380  MFLOWJ  635000000      * LPIS FLOW
0000381  MFLOWJ  640000000      * HPIS FLOW
0000382  MFLOWJ  603000000      * ACCUMULATOR FLOW
0000383  MFLOWJ  630000000      * ECC FLOW INJECTED INTO 185
0000384  MFLOWJ  631000000      * ECC FLOW INJECTED INTO 180
*****

```

* LIQUID LEVELS

```

*****
0000385  CNTRLVAR 3      * REACTOR VESSEL
0000386  CNTRLVAR 4      * DOWNCOMER 1
0000387  CNTRLVAR 7      * DOWNCOMER 2
0000388  CNTRLVAR 2      * PRESSURIZER
0000389  CNTRLVAR 100    * PRZR WATER LEVEL DEVIATION
0000390  MFLOWJ  910000000  * PRZR WATER LEVEL CONTROL
*****

```

* DOWNCOMER MASS FLOWS

```

*****
0000391 MFLOWJ 203000000 * DOWNCOMER 1 ENTRANCE
0000392 MFLOWJ 283000000 * DOWNCOMER 2 ENTRANCE
0000393 MFLOWJ 270000000 * CROSSFLOW UPPER IN ANN
0000394 MFLOWJ 272000000 * CROSSFLOW LOWER IN ANN
0000395 MFLOWJ 273000000 * CROSSFLOW DWM 1 AND 2
*
*****
* TRIPS
*****
*****
* ALWAYS TRUE
*****
0000501 TIME 0 GE NULL 0 -1.0 L -1.0
*****
* ALWAYS FALSE
*****
0000502 TIME 0 LT NULL 0 -1.0 N -1.0
*****
* BREAK INITIATION
*****
0000510 TIME 0 GE NULL 0 0.0 L -1.0
*****
* HPIS INITIATION
*****
0000513 TIME 0 GE TIMEOF 510 23.9 L -1.0
0000514 TIME 0 GE TIMEOF 510 144.0 L -1.0
0000614 515 AND -514 N -1.0
*****
* LPIS INITIATION
*****
0000535 TIME 0 GE TIMEOF 510 37.32 L -1.0
0000536 TIME 0 GE TIMEOF 510 107.1 L -1.0
0000615 535 AND -535 N -1.0
*****
* PCP TRIP
*****
0000516 TIME 0 GE TIMEOF 510 0.94 L -1.0# 2-5
*****
* LT 660 ACCUMULATOR VALVE CARD 6120301
*****
0000517 P 185010000 LT NULL 0 4.2+6 L -1.0
0000518 VOIDF 615010000 LE NULL 0 0.00001 L -1.0
0000519 MFLOWJ 615010000 GE NULL 0 0.0 N -1.0
0000520 VOIDF 605010000 LE NULL 0 0.00001 L -1.0
0000521 MFLOWJ 603000000 GE NULL 0 0.0 N -1.0
0000659 517 AND 519 N -1.0
0000660 -518 AND 659 N -1.0
0000661 517 AND 521 N -1.0
0000662 -520 AND 661 N -1.0
*****
* LT 580 ECC CHECK VALVE CARD 6300301
*****
0000580 P 600010000 GE P 185010000 1.0+3 L -1.0
*****
* LT 691 PORV CARD 4250301
*****
0000581 P 420010000 GT NULL 0 1.620058+7 N -1.
0000582 P 420010000 LT NULL 0 1.606269+7 N -1.
0000664 581 OR 691 N -1.0
0000691 -582 AND 664 N -1.0

```

 ***** HYDRAULIC COMPONENTS SIMULATION *****

* INTACT LOOP

* REACTOR VESSEL NOZZLE - INTACT LOOP HOT LEG

1000000	RUN=ILHL	BRANCH					
1000001	2	0					
1000101	0.0634	1.5373	0.0	0.0	0.0	0.0	
1000102	4.0-5	0.0	00				
1000200	000	14.935E6	1.4117E6	2.4613E6	1.7880-5		
1001101	250010000	100000000	0.0634	1.10264	0.66160	00000	
1002101	100010000	105000000	0.0	0.1	0.1	00000	
1001201	4.4738	4.5765	0.0				
1002201	4.4737	4.4863	0.0				

* PRESSURIZER CONNECTION TEE REACTOR VESSEL SIDE

1050000	PZRT-RUS	BRANCH					
1050001	1	0					
1050101	0.0634	1.634	0.0	0.0	0.0	0.0	
1050102	4.0-5	0.0	00				
1050200	000	14.934E6	1.4117E6	2.4614E6	4.1779-6		
1051101	105010000	110000000	0.0	0.1	0.1	00000	
1051201	5.8318	5.8637	0.0				

* PRESSURIZER CONNECTION TEE STEAM GENERATOR SIDE

1100000	PZRT-SGS	BRANCH					
1100001	1	0					
1100101	0.0	0.623	0.0303	0.0	0.0	0.0	
1100102	4.0-5	0.0	00				
1100200	000	14.928E6	1.4118E6	2.4615E6	2.1446-6		
1101101	110010000	112000000	0.0	0.1	0.1	00000	
1101201	5.8320	5.8242	0.0				

* HOT LEG PIPING

1120000	HOTLEGPP	PIPE					
1120001	2						
1120101	0.0	2					
1120201	0.0	1					
1120301	1.4385	1					
1120302	0.708	2					
1120401	0.09	1					
1120402	0.057	2					
1120501	0.0	2					
1120601	0.0	1					
1120602	90.0	2					
1120701	0.0	1					
1120702	0.246	2					
1120801	4.0-5	0.0	2				
1120901	0.15	0.15	1				
1121001	00	2					
1121101	00000	1					
1121201	000	14.931E6	1.4118E6	2.4615E6	5.5532-7	0.0	1
1121202	000	14.931E6	1.4118E6	2.4615E6	1.9745-7	0.0	2

```

1121300 0
1121301 4.5335 4.5325 0.0 01
*****
* SG INLET PLENUM
*****
1140000 SGINPLNM BRANCH
1140001 2 0
1140101 0.0 0.63 0.335 0.0 90.0 0.513
1140102 4.0-5 0.0 00
1140200 000 14.921E6 1.4118E6 2.4617E6 1.7048-8
1141101 112010000 114000000 0.0512 1.10000 1.10000 00000
1142101 114010000 115000000 0.0 0.20000 0.20000 00000
1141201 5.5399 5.5567 0.0
1142201 1.8785 1.8792 0.0
*****
* SG U-TUBES
*****
1150000 SG-TUBES PIPE
1150001 8
1150101 0.151 8
1150201 0.151 7
1150301 0.902 1
1150302 0.6096 3
1150303 0.4612 5
1150304 0.6096 7
1150305 0.902 8
1150401 0.0 8
1150501 0.0 8
1150601 90.0 4
1150602 -90.0 8
1150701 0.902 1
1150702 0.6096 3
1150703 0.3048 4
1150704 -0.3048 5
1150705 -0.6096 7
1150706 -0.902 8
1150801 1.27-7 0.01022 8
1150901 0.0 0.0 7
1151001 00 8
1151101 00000 7
1151201 000 14.914E6 1.3694E6 2.4618E6 3.2232-9 0.0 1
1151202 000 14.907E6 1.3352E6 2.4620E6 8.1280-10 0.0 2
1151203 000 14.901E6 1.3074E6 2.4621E6 2.0175-10 0.0 3
1151204 003 14.897E6 567.83 0.0 0.0 0.0 4
1151205 003 14.896E6 564.85 0.0 0.0 0.0 5
1151206 003 14.898E6 561.53 0.0 0.0 0.0 6
1151207 003 14.901E6 558.68 0.0 0.0 0.0 7
1151208 003 14.905E6 556.21 0.0 0.0 0.0 8
1151300 0
1151301 1.8310 1.8310 0.0 01
1151302 1.7961 1.7961 0.0 02
1151303 1.7698 1.7698 0.0 03
1151304 1.7534 1.7534 0.0 04
1151305 1.7396 1.7396 0.0 05
1151306 1.7249 1.7249 0.0 06
1151307 1.7128 1.7128 0.0 07
*****
* SG OUTLET PLENUM
*****
1160000 SGOPLNM BRANCH
1160001 2 0
1160101 0.0 0.63 0.335 0.0 -90.0 -0.513

```

```

1160102 4.0-5 0.0 00
1160200 003 14.910E6 556.21
1161101 116010000 116000000 0.0 0.20000 0.20000 00000
1162101 116010000 118000000 0.0512 1.10000 1.10000 00000
1161201 1.7026 1.7026 0.0
1162201 5.0213 5.0213 0.0

```

```

*****
* PUMP SUCTION PIPING
*****

```

```

1180000 PMSUCPP PIPE
1180001 3
1180101 0.0 2
1180102 0.0634 3
1180201 0.0 2
1180301 0.547 1
1180302 0.689 2
1180303 0.559 3
1180401 0.0437 1
1180402 0.0462 2
1180403 0.0 3
1180501 0.0 3
1180601 -90. 3
1180701 -0.498 1
1180702 -0.689 2
1180703 -0.356 3
1180801 4.0-5 0.0 3
1180901 0.083 0.083 1
1180902 0.104 0.104 2
1181001 00 3
1181101 00000 2
1181201 003 14.900E6 556.21 0.0 0.0 0.0 1
1181202 003 14.902E6 556.21 0.0 0.0 0.0 2
1181203 003 14.904E6 556.21 0.0 0.0 0.0 3
1181300 0
1181301 3.8342 3.8342 0.0 01
1181302 4.0551 4.0551 0.0 02

```

```

*****
* PUMP SUCTION TEE
*****

```

```

1200000 PMSUCTE BRANCH
1200001 3 0
1200101 0.0634 0.76 0.0 0.0 0.0 0.0
1200102 4.0-5 0.0 00
1200200 003 14.904E6 556.21
1201101 118010000 120000000 0.0 0.20000 0.20000 00000
1202101 120010000 125000000 0.0 0.5 0.5 00000
1203101 120010000 155000000 0.0 0.5 0.5 00000
1201201 4.0551 4.0551 0.0
1202201 2.1013 2.1013 0.0
1203201 2.1053 2.1053 0.0

```

```

*****
* PUMP 1 SUCTION TEE OUTLET
*****

```

```

1250000 PMSUCTE BRANCH
1250001 1 0
1250101 0.0 1.003 0.0613 0.0 90.0 0.521
1250102 4.0-5 0.0 00
1250200 003 14.906E6 556.21
1251101 125010000 130000000 0.0 0.0 0.0 00000
1251201 3.1053 3.1053 0.0

```

```

*****
* PUMP 1 INLET

```

```

*****
1300000 PIPINLET          SNGLVOL
1300101 0.0          0.457          0.0189          0.0          90.0          0.457
1300102 4.0-5          0.0          00
1300200 003          14.900E6          556.21
*****
* PRIMARY COOLANT PUMP 1
*****
1350000 PCPUMP1          PUMP
1350101 0.0366          0.0          0.039          0.0          90.0          0.319
1350102 0
1350103 130010000 0.0          0.1          0.1          00000
1350109 140000000 0.0          0.1          0.1          00000
1350200 003          14.934E6          556.23
1350201 0          3.5087          3.5089          0.0
1350202 0          3.5088          3.5088          0.0
1350301 0 0          0          -1          -1          516          0
1350302 369.7          0.3541          0.3155          96.0          500.6          1.431
1350303 613.6          0.0          207.433          0.0444          19.5987          0.0
1350310 0.0          0.0          0.0
*****
* PUMP 1 OUTLET PUMP SIDE
*****
1400000 PMPOUTLT          SNGLVOL
1400101 0.0366          0.502          0.0          0.0          0.0          0.0
1400102 4.0-5          0.0          00
1400200 003          14.971E6          556.24
*****
* PUMP 1 OUTLET PIPE TEE SIDE
*****
1450000 PMP1OUT          BRANCH
1450001 2          0
1450101 0.0          1.4084          0.0633          0.0          0.0          0.0
1450102 4.0-5          0.0          00
1450200 003          14.972E6          556.24
1451101 140010000 145000000 0.0          0.0          0.0          00000
1452101 145010000 150000000 0.0366          0.40000          0.40000          00000
1451201 3.5086          3.5086          0.0
1452201 3.5086          3.5036          0.0
*****
* PUMP OULET TEE
*****
1500000 PMPOUT-T          BRANCH
1500001 2          0
1500101 0.0634          0.4966          0.0          0.0          0.0          0.0
1500102 4.0-5          0.0          00
1500200 003          14.967E6          556.24
1501101 170010000 150000000 0.0366          0.40000          0.40000          00000
1502101 150010000 175000000 0.0          0.0          0.0          00000
1501201 3.5154          3.5154          0.0
1502201 4.0549          4.0549          0.0
*****
* PUMP 2 SUCTION TEE OUTLET
*****
1550000 PUMP2SCT          BRANCH
1550001 1          0
1550101 0.0          1.003          0.0613          0.0          90.0          0.521
1550102 4.0-5          0.0          00
1550200 003          14.906E6          556.21
1551101 155010000 160000000 0.0          0.0          0.0          00000
1551201 3.1112          3.1112          0.0
*****

```

* PUMP 2 INLET PIPE

```

*****
1600000 PMP2INLT          SNGLVOL
1600101 0.0            0.457      0.0189    0.0        90.0        0.457
1600102 4.0-5            0.0            00
1600200 003             14.900E6      556.21
*****

```

* PRIMARY COOLANT PUMP 2

```

*****
1650000 PCPUMP2          PUMP
1650101 0.0366          0.0            0.099     0.0        90.0        0.319
1650102 0
1650108 160010000      0.0            0.1        0.1        00000
1650109 1700000000     0.0            0.1        0.1        00000
1650200 003             14.934E6      556.23
1650201 0                3.5156        3.5156     0.0
1650202 0                3.5155        3.5155     0.0
1650301 135 135        135           -1          -1          516         0
1650302 369.7          0.3541        0.3155     96.0       500.6       1.431
1650303 613.6          0.0            207.433    0.0444     19.5967     0.0
1650310 0.0            0.0            0.0
*****

```

* PUMP 2 OUTLET

```

*****
1700000 PMP2OUTT        BRANCH
1700001 0                0
1700101 0.0366          0.514          0.0         0.0         0.0         0.0
1700102 4.0-5            0.0            00
1700200 003             14.971E6      556.24
*****

```

* INTACT LOOP COLD LEG PIPE

```

*****
1750000 ILCLP1          BRANCH
1750001 1                0
1750101 0.0634          0.559          0.0         0.0         0.0         0.0
1750102 4.0-5            0.0            00
1750200 003             14.967E6      556.24
1751101 175010000      176000000     0.0         0.0         0.0         00000
1751201 4.0549          4.0549         0.0
*****

```

* ILCLP2 BRANCH

```

1760000 ILCLP2          BRANCH
1760001 0                0
1760101 0.0634          0.613          0.0         0.0         0.0         0.0
1760102 4.0-5            0.0            00
1760200 003             14.967E6      556.24
*****

```

* ECC CONNECTION TEE

```

*****
1800000 ECC-T          BRANCH
1800001 1                0
1800101 0.0634          1.152          0.0         0.0         0.0         0.0
1800102 4.0-5            0.0            00
1800200 003             14.965E6      556.24
1801101 176010000      180000000     0.0         0.20700    0.20700    00000
1801201 4.0549          4.0549         0.0
*****

```

* REACTOR VESSEL NOZZLE-INTACT LOOP COLD LEG

```

*****
1850000 RVN-ILCL        BRANCH
1850001 2                0
1850101 0.0634          1.01           0.0         0.0         0.0         0.0
1850102 4.0-5            0.0            00
*****

```



```

1850200 003 14.964E6 556.24
1851101 185010000 202000000 0.0634 1.43960 0.60400 00000
1852101 180010000 185000000 0.0 0.20700 0.20700 00000
1851201 4.0549 4.0549 0.0
1852201 4.0549 4.0549 0.0

```

```

*****
* REACTOR VESSEL
*****

```

```

* INLET ANNULUS TOP VOL 'E 1
*****

```

```

2000000 INANTOP1 ANNULUS
2000001 1
2000101 0.0 1
2000301 0.33 1
2000401 0.0428 1
2000501 0.0 1
2000601 90.0 1
2000701 0.33 1
2000801 3.81-6 0.178 1
2001001 00 1
2001201 003 14.960E6 556.25 0.0 0.0 0.0 1

```

```

*****
* JUNCTION BETWEEN UPPER INLET ANNULUS 1 AND BOTTOM VOLUME 1
*****

```

```

2010000 J200-202 SNGLJUN
2010101 200000000 202000000 0.0 0.0 0.0 00000
2010201 0 -0.15613 -0.15613 0.0

```

```

*****
* INLET ANNULUS BOTTOM VOLUME 1
*****

```

```

2020000 INANBOT1 ANNULUS
2020001 1
2020101 0.0 1
2020301 0.424 1
2020401 0.055 1
2020501 0.0 1
2020601 -90.0 1
2020701 -0.424 1
2020801 3.81-6 0.172 1
2021001 00 1
2021201 003 14.961E6 556.24 0.0 0.0 0.0 1

```

```

*****
* JUNCTION BETWEEN INLET ANNULUS BOTTOM VOLUME 1 AND DOWNCOMER 1
*****

```

```

2030000 J202-204 SNGLJUN
2030101 202010000 204000000 0.0 0.22632 0.20400 00000
2030201 0 3.0332 3.0332 0.0

```

```

*****
* DOWNCOMER 1
*****

```

```

* DOWNCOMER 1.1

```

```

2040000 DWNCR1.1 ANNULUS
2040001 1
2040101 0.071 1
2040301 0.958 1
2040401 0.0 1
2040501 0.0 1
2040601 -90. 1
2040701 -0.958 1
2040801 3.81-6 0.102 1

```

2041001	00	1						
2041201	003	14.963E6	556.24	0.0	0.0	0.0	1	
* JUNCTION BETWEEN DOWNCOMER 1.1 AND 1.2								
2050000	J1.1-1.2		SNGLJUN					
2050101	204010000	206000000	0.0	0.0	0.0	00000		
2050201	0	2.9165	2.9165	0.0				
* DOWNCOMER 1.2								
2060000	DWNCR1.2		ANNULUS					
2060001	1							
2060101	0.071	1						
2060301	0.958	1						
2060401	0.0	1						
2060501	0.0	1						
2060601	-90.0	1						
2060701	-0.958	1						
2060801	3.81-6	0.102	1					
2061001	00	1						
2061201	003	14.970E6	556.24	0.0	0.0	0.0	1	
* JUNCTION BETWEEN DOWNCOMER 1.2 AND 1.3								
2070000	J1.2-1.3		SNGLJUN					
2070101	206010000	208000000	0.0	0.0	0.0	00000		
2070201	0	2.8162	2.8162	0.0				
* DOWNCOMER 1.3								
2080000	DWNCR1.3		ANNULUS					
2080001	1							
2080101	0.071	1						
2080301	0.958	1						
2080401	0.0	1						
2080501	0.0	1						
2080601	-90.0	1						
2080701	-0.958	1						
2080801	3.81-6	0.102	1					
2081001	00	1						
2081201	003	14.977E6	556.23	0.0	0.0	0.0	1	
* JUNCTION BETWEEN DOWNCOMER 1.3 AND 1.4								
2090000	J1.3-1.4		SNGLJUN					
2090101	208010000	210000000	0.0	0.0	0.0	00000		
2090201	0	2.7403	2.7403	0.0				
* DOWNCOMER 1.4								
2100000	DWNCR1.4		ANNULUS					
2100001	1							
2100101	0.071	1						
2100301	0.958	1						
2100401	0.0	1						
2100501	0.0	1						
2100601	-90.0	1						
2100701	-0.958	1						
2100801	3.81-6	0.102	1					
2101001	00	1						
2101201	003	14.984E6	556.23	0.0	0.0	0.0	1	

```

*****
* LOWER PLENUM TOP VOLUME
*****
2150000  LWRPLTOP          BRANCH
2150001  4                    0
2150101  0.740                0.360      0.0      0.0      -90.      -0.360
2150102  3.81-6                0.0      00
2150200  003                   14.989E6  55.23
2151101  210010000 215000000 0.0      0.72650  0.17160  00000
2152101  215010000 220000000 0.0      0.0      0.0      00000
2153101  215000000 225000000 0.15     1.40372  1.14100  00000
2154101  290010000 215000000 0.0      0.72650  0.17160  00000
2151201  2.9689                2.9689      0.0
2152201  2.7292-6             2.7292-6     0.0
2153201  1.7138                1.7138      0.0
2154201  0.65179              0.65179     0.0
*****
* LOWER PLENUM BOTTOM VOLUME
*****
2200000  LWRPLBOT          SNG_VOL
2200101  0.790                0.370      0.0      0.0      -90.      -0.370
2200102  3.81-6                0.0      00
2200200  003                   14.992E6  559.38
*****
* LOWER CORE SUPPORT STRUCTURE
*****
2250000  LCORESUP          BRANCH
2250001  3                    0
2250101  0.25                 0.52        0.0      0.0      90.      0.52
2250102  3.81-6                0.095      00
2250200  003                   14.984E6  556.23
2251101  225010000 226000000 0.0      1.46961  1.46961  00000
2252101  225010000 227000000 8.23260-2 0.60800  0.71330  00000
2253101  225010000 233000000 1.53281-2 0.69015  0.75490  00000
2251201  0.66670              0.66670     0.0
2252201  2.5488                2.5488      0.0
2253201  2.4289                2.7226      0.0
*****
* CORE BYPASS VOLUME
*****
2260000  COREBYP          PIPE
2260001  3
2260101  0.015                3
2260201  0.0                   2
2260301  0.559                 2
2260302  0.657                 3
2260401  0.0                   3
2260501  0.0                   3
2260601  90.                   3
2260801  4.0-5                 0.003      3
2260901  0.0                   0.0        2
2261001  00                    3
2261101  00000                 2
2261201  003                   14.979E6  556.23  0.0      0.0      0.0      1
2261202  003                   14.973E6  556.23  0.0      0.0      0.0      2
2261203  003                   14.967E6  556.23  0.0      0.0      0.0      3
2261300  0
2261301  0.66671              0.66671     0.0      01
2261302  0.66671              0.66671     0.0      02
*
*****
* ACTIVE CURVE
*****

```

***** CORE AVERAGE CHANNEL (227,228,229,230,231,232)

* BRANCH (227)

AVCORE1	BRANCH					
2270000	2	0				
2270101	0.138436	0.27950	0.0	0.0	90.0	
2270102	0.27950	1.27-7	0.012	00		
2270200	003	14.979E6	561.80			
2271101	227010000	228000000	0.121430	0.05320	0.05320	00000
2272101	233000000	227000000	0.239275	4.69	4.69	00003
2271201	1.7456	1.8880	0.0			
2272201	-3.1096-3	-3.4875-3	0.0			

* BRANCH (228)

AVCORE2	BRANCH					
2280000	2	0				
2280101	0.138436	0.27950	0.0	0.0	90.0	
2280102	0.27950	1.27-7	0.012	00		
2280200	000	14.976E6	1.3019E6	2.4605E6	6.7600-4	
2281101	228010000	229000000	0.121430	0.05320	0.05320	00000
2282101	234000000	228000000	0.239275	4.69	4.69	00003
2281201	1.7869	1.9737	0.0			
2282201	5.5703-4	8.2698-4	0.0			

* BRANCH (229)

AVCORE3	BRANCH					
2290000	2	0				
2290101	0.138436	0.27950	0.0	0.0	90.0	
2290102	0.27950	1.27-7	0.012	00		
2290200	000	14.974E6	1.3467E6	2.4605E6	3.0013-3	
2291101	229010000	230000000	0.121430	0.05320	0.05320	00000
2292101	235000000	229000000	0.239275	4.69	4.69	00003
2291201	1.8079	2.0028	0.0			
2292201	-1.3281-2	-2.7326-2	0.0			

* BRANCH (230)

AVCORE4	BRANCH					
2300000	2	0				
2300101	0.138436	0.27950	0.0	0.0	90.0	
2300102	0.27950	1.27-7	0.012	00		
2300200	000	14.971E6	1.3817E6	2.4605E6	3.2853-3	
2301101	230010000	231000000	0.121430	0.05320	0.05320	00000
2302101	236000000	230000000	0.239275	4.69	4.69	00003
2301201	1.8661	2.0884	0.0			
2302201	1.1899-2	1.8866-2	0.0			

* BRANCH (231)

AVCORE5	BRANCH					
2310000	2	0				
2310101	0.138436	0.27950	0.0	0.0	90.0	
2310102	0.27950	1.27-7	0.012	00		
2310200	000	14.969E6	1.4010E6	2.4606E6	1.3774-3	
2311101	231010000	232000000	0.121430	0.05320	0.05320	00000
2312101	237000000	231000000	0.239275	4.69	4.69	00003
2311201	1.8398	2.0123	0.0			

```

2312201 -2.2904-2 -5.1744-2 0.0
*
* BRANCH (232)
*
2320000 AVCORE6 BRANCH
2320001 2 0
2320101 0.138436 0.37750 0.0 0.0 90.0
2320102 0.37750 1.27-7 0.012 00
2320200 000 14.966E6 1.4093E6 2.4607E6 1.4438-3
2321101 232010000 240000000 9.78055-2 0.887340 0.887205 00000
2322101 238000000 232000000 0.239275 4.69 4.69 00003
2321201 2.4159 2.5666 0.0
2322201 5.2195-2 8.2698-2 0.0
*
***** CORE HOT CHANNEL ( 233,234,235,236,237,238)
*
* BRANCH (233)
*
2330000 HTCORE1 BRANCH
2330001 1 0
2330101 2.50439-2 0.27950 0.0 0.0 90.0
2330102 0.27950 1.27-7 0.012 00
2330200 000 14.979E6 1.2744E6 2.4604E6 3.5939-5
2331101 233010000 234000000 2.21109-2 0.04981 0.04981 00000
2331201 1.7548 1.9930 0.0
*
* BRANCH (234)
*
2340000 HTCORE2 BRANCH
2340001 1 0
2340101 2.50439-2 0.27950 0.0 0.0 90.0
2340102 0.27950 1.27-7 0.012 00
2340200 000 14.976E6 1.3399E6 2.4605E6 1.7943-2
2341101 234010000 235000000 2.21109-2 0.04981 0.04981 00000
2341201 1.8382 2.0253 0.0
*
* BRANCH (235)
*
2350000 HTCORE3 BRANCH
2350001 1 0
2350101 2.50439-2 0.27950 0.0 0.0 90.0
2350102 0.27950 1.27-7 0.012 00
2350200 000 14.974E6 1.3985E6 2.4605E6 4.9742-2
2351101 235010000 236000000 2.21109-2 0.04981 0.04981 00000
2351201 2.1092 2.3011 0.0
*
* BRANCH (236)
*
2360000 HTCORE4 BRANCH
2360001 1 0
2360101 2.62243-2 0.27950 0.0 0.0 90.0
2360102 0.27950 1.27-7 0.012 00
2360200 000 14.971E6 1.4401E6 2.4606E6 6.8761-2
2361101 236010000 237000000 2.21109-2 0.04981 0.04981 00000
2361201 2.0708 2.4552 0.0
*
* BRANCH (237)
*
2370000 HTCORE5 BRANCH
2370001 1 0
2370101 2.50439-2 0.27950 0.0 0.0 90.0
2370102 0.27950 1.27-7 0.012 00

```

2370200	000	14.969E6	1.4603E6	2.4606E6	6.0046-2	
2371101	237010000	238000000	2.21109-2	0.04981	0.04981	00000
2371201	2.3519	2.9438	0.0			

*
* BRANCH (238)
*

2380000	HTCORE6	BRANCH				
2380001	1	0				
2380101	2.62243-2	0.37750	0.0	0.0	90.0	
2380102	0.37750	1.7-7	0.012	00		
2380200	000	14.966E6	1.4705E6	2.4606E6	3.5	
2381101	238010000	240000000	1.50001-2	0.99580	0.9467	00000
2381201	2.5789	4.6181	0.0			

* UPPER END BOXES AND SUPPORT STRUCTURE

2400000	UPRENDX	BRANCH				
2400001	1	0				
2400101	0.297	0.559	0.0	0.0	90.	0.559
2400102	3.81-6	0.145	00			
2400200	000	14.961E6	1.4114E6	2.4608E6	1.5489-3	
2401101	226010000	240000000	0.0	2.93767	2.93767	00000
2401201	0.66672	0.74886	0.0			

* UPPER CORE SUPPORT STRUCTURE - CROSS FLOW REGION

2450000	UPRCRSUP	BRANCH				
2450001	2	0				
2450101	0.297	0.559	0.0	0.0	90.	0.559
2450102	3.81-6	0.145	00			
2450200	000	14.958E6	1.4117E6	2.4609E6	2.6155-4	
2451101	240010000	245000000	0.0	0.0	0.0	00000
2452101	245010000	251000000	0.0	0.0	0.0	00000
2451201	0.95598	1.1248	0.0			
2452201	4.5990-6	0.24995	0.0			

* UPPER FLOW SKIRT REGION

2500000	UFLWSKRT	BRANCH				
2500001	1	0				
2500101	0.114	0.843	0.0	0.0	90.0	0.843
2500102	3.81-6	0.131	00			
2500200	000	14.951E6	1.4117E6	2.4610E6	7.1467-5	
2501101	245010000	250000000	0.0	0.0	0.0	00000
2501201	2.4884	2.6192	0.0			

* DEAD END OF FUEL MODULES

2510000	DEFLMDS	SNGLVOL				
2510101	0.183	0.700	0.0	0.0	90.0	0.700
2510102	3.81-6	0.214	00			
2510200	000	14.954E6	1.4313E6	2.4610E6	2.6921-2	

* COMBINED UPPER PLENUM BOTTOM VOLUME

2550000	UPRPLBOT	BRANCH				
2550001	1	0				
2550101	0.268	1.566	0.0	0.0	90.0	1.566
2550102	3.81-6	0.0	00			
2550200	000	14.945E6	1.4156E6	2.4612E6	1.7143-3	
2551101	250010000	255000000	0.0	0.006	0.006	00000

```

*****
2820000  INANBOT2          ANNULUS
2820001  1
2820101  0.0          1
2820301  0.424        1
2820401  0.0550       1
2820501  0.0          1
2820601  -90.0         1
2820701  -0.424        1
2820801  3.81-6       0.172    1
2821001  00           1
2821201  003         14.958E6  556.25    0.0    0.0    0.0    1
*****
* JUNCTION BETWEEN INLET ANNULUS BOTTOM VOLUME 2 AND DOWNCOMER 2
*****
2830000  J282-284      SNGLJUN
2830101  282010000 284000000 0.0    0.22632  0.20490  00000
2830201  0          0.58777  0.58777  0.0
*****
* DOWNCOMER 2
*****
*
* DOWNCOMER 2.1
*
2840000  DWNCR2.1      ANNULUS
2840001  1
2840101  0.071        1
2840301  0.958        1
2840401  0.0          1
2840501  0.0          1
2840601  -90.0        1
2840701  -0.958       1
2840801  3.81-6       0.102    1
2841001  00           1
2841201  003         14.963E6  556.24    0.0    0.0    0.0    1
*
* JUNCTION BETWEEN DOWNCOMER 2.1 AND 2.2
*
2850000  J2.1-2.2      SNGLJUN
2850101  284010000 286000000 0.0    0.0    0.0    00000
2850201  0          0.70438  0.70438  0.0
*
* DOWNCOMER 2.2
*
2860000  DWNCR2.2      ANNULUS
2860001  1
2860101  0.071        1
2860301  0.958        1
2860401  0.0          1
2860501  0.0          1
2860601  -90.0        1
2860701  -0.958       1
2860801  3.81-6       0.102    1
2861001  00           1
2861201  003         14.970E6  556.23    0.0    0.0    0.0    1
*
* JUNCTION BETWEEN DOWNCOMER 2.2 AND 2.3
*
2870000  J2.2-2.3      SNGLJUN
2870101  286010000 288000000 0.0    0.0    0.0    00000
2870201  0          0.80458  0.80458  0.0
*

```

```

2551201 1.0411-6 0.17006 0.0
*****
* CROSSFLOW JUNCTION BETWEEN UPPER INLET ANNULUS 1 AND 2
*****
2700000 UINCR-FL SNGLJUN
2700101 200010000 280010000 5.86740-2 98.0000 18.0000 00003
2700201 0 0.34514 0.34514 0.0
*****
* CROSSFLOW JUNCTION BETWEEN LOWER INLET ANNULUS 1 AND 2
*****
2720000 LINCR-FL SNGLJUN
2720101 202000000 282000000 7.27937-2 98.0000 18.0000 00003
2720201 0 0.29508 0.29508 0.0
*****
* CROSSFLOW JUNCTION BETWEEN DOWNCOMERS 1&2
*****
*
* JUNCTION BETWEEN DOWNCOMER 1.1 AND 2.1
*
2730000 CROSFLW1 SNGLJUN
2730101 204000000 284000000 9.73328-2 98.0000 18.0000 00003
2730201 0 8.5077-2 8.5077-2 0.0
*
* JUNCTION BETWEEN DOWNCOMER 1.2 AND 2.2
*
2750000 CROSFLW2 SNGLJUN
2750101 206000000 286000000 9.73328-2 98.0000 18.0000 00003
2750201 0 7.3113-2 7.3113-2 0.0
*
* JUNCTION BETWEEN DOWNCOMER 1.3 AND 2.3
*
2770000 CROSFLW3 SNGLJUN
2770101 208000000 288000000 9.73328-2 98.0000 18.0000 00003
2770201 0 5.5365-2 5.5365-2 0.0
*
* JUNCTION BETWEEN DOWNCOMER 1.4 AND 2.4
*
2790000 CROSFLW4 SNGLJUN
2790101 210000000 290000000 9.73328-2 98.0000 18.0000 00003
2790201 0 -0.16678 -0.16678 0.0
*****
* INLET ANNULUS TOP VOLUME 2
*****
2800000 INANTOP2 ANNULUS
2800001 1
2800101 0.0 1
2800301 0.33 1
2800401 0.0428 1
2800501 0.0 1
2800601 90.0 1
2800701 0.33 1
2800801 3.81-6 0.178 1
2801001 00 1
2801201 003 14.955E6 556.26 0.0 0.0 0.0 1
*****
* JUNCTION BETWEEN UPPER INLET ANNULUS 2 AND BOTTOM VOLUME 2
*****
2810000 J280-282 SNGLJUN
2810101 280000000 282000000 0.0 0.0 0.0 00000
2810201 0 0.15614 0.15614 0.0
*****
* INLET ANNULUS BOTTOM VOLUME 2

```


* DOWNCOMER 2.3

```

*
2880000  DWNCR2.3          ANNULUS
2880001  1
2880101  0.071      1
2880301  0.958      1
2880401  0.0         1
2880501  0.0         1
2880601  -90.0       1
2880701  -0.958      1
2880801  3.81-6     0.102    1
2881001  00          1
2881201  003        14.977E6  556.23    0.0      0.0      0.0      1

```

* JUNCTION BETWEEN DOWNCOMER 2.3 AND 2.4

```

*
2890000  J2.3-2.4          SINGLJUN
2890101  288010000 290000000 0.0      0.0      0.0      00000
2890201  0          0.88045  0.88045  0.0

```

* DOWNCOMER 2.4

```

*
2900000  DWNCR2.5          ANNULUS
2900001  1
2900101  0.071      1
2900301  0.958      1
2900401  0.0         1
2900501  0.0         1
2900601  -90.0       1
2900701  -0.958      1
2900801  3.81-6     0.102    1
2901001  00          1
2901201  003        14.984E6  556.22    0.0      0.0      0.0      1

```

 * BROKEN LOOP

* REACTOR VESSEL NOZZLE - BROKEN LOOP HOT LEG

```

*****
* REACTOR VESSEL NOZZLE - BROKEN LOOP HOT LEG
*****
3000000  RVN-BLWL          BRANCH
3000001  2                0
3000101  0.0634          0.876    0.0      0.0      0.0      0.0
3000102  4.0-5           0.0      00
3000200  003             14.950E6  1.2768E6  2.4611E6  3.8315-7
3001101  250010000 300000000 0.0634    1.10264  0.66160  00000
3002101  300010000 305000000 0.0        0.10050  0.10050  00000
3001201  -6.4728-7 4.2262-2 0.0
3002201  1.6459-10 3.5352-7 0.0

```

* HOT LEG PIPE TO REFLOOD ASSIST BYPASS TEE

```

*****
* HOT LEG PIPE TO REFLOOD ASSIST BYPASS TEE
*****
3050000  HLP-RAPT          BRANCH
3050001  1                0
3050101  0.134           0.698    0.0      0.0      0.0      0.0
3050102  4.0-5           0.0      00
3050200  003             14.950E6  365.45
3051101  305010000 310000000 0.0        0.10050  0.10050  00000
3051201  2.1220-10 2.1220-10 0.0

```

* BROKEN LOOP HOT LEG CONTRACTION -1.0

```

*****
* BROKEN LOOP HOT LEG CONTRACTION -1.0
*****
3100000  BLH-CNTR          BRANCH
3100001  2                0

```

3100101	0.0	1.424	0.0668	0.0	0.0	0.0
3100102	4.0-5	0.0	00			
3100200	003	14.950E6	564.96			
3101101	380010000	310000000	0.0328	1.24700	0.45760	00000
3102101	310010000	315000000	0.0	0.39605	0.75363	00000
3101201	-5.566-11	-6.503-11	0.0			
3102201	8.4236-10	8.7407-10	0.0			

 * STEAM GENERATOR AND PUMP SIMULATOR

3150000 SG-PUMP PIPE

3150001	8						
3150101	0.0	8					
3150201	8.365-3	1					
3150202	3.260-2	2					
3150203	1.056-1	3					
3150204	3.260-2	4					
3150205	8.365-3	7					
3150301	0.93100	1					
3150302	2.05100	2					
3150303	0.84950	4					
3150304	2.05100	5					
3150305	1.47300	6					
3150306	1.03200	7					
3150307	1.84200	8					
3150401	7.788-3	1					
3150402	1.725-1	2					
3150403	8.980-2	4					
3150404	1.725-1	5					
3150405	2.030-2	6					
3150406	4.560-2	7					
3150407	1.980-2	8					
3150601	90.0	3					
3150602	-90.0	7					
3150603	90.0	8					
3150701	0.6150	1					
3150702	2.0510	2					
3150703	0.4570	3					
3150704	-0.4570	4					
3150705	-2.0510	5					
3150706	-1.1143	6					
3150707	-0.6860	7					
3150708	1.2140	8					
3150801	4.0-5	0.0	8				
3150901	0.93596	0.93596	1				
3150902	16.8777	16.8777	2				
3150903	0.50000	0.50000	3				
3150904	16.8777	16.8777	4				
3150905	0.23025	0.23025	5				
3150906	2.53400	2.53400	6				
3150907	5.06900	5.06900	7				
3151001	00	8					
3151101	00000	7					
3151201	003	14.948E6	564.86	0.0	0.0	0.0	1
3151202	003	14.9J8E6	560.98	0.0	0.0	0.0	2
3151203	003	14.929E6	560.98	0.0	0.0	0.0	3
3151204	003	14.929E6	559.98	0.0	0.0	0.0	4
3151205	003	14.938E6	558.98	0.0	0.0	0.0	5
3151206	003	14.950E6	556.98	0.0	0.0	0.0	6
3151207	003	14.957E6	556.98	0.0	0.0	0.0	7
3151208	003	14.955E6	556.98	0.0	0.0	0.0	8
3151300	0						

```

3151301  8.3150-10 1.0084-9  0.0      01
3151302  1.5261-10 3.3970-10 0.0      02
3151303  3.7289-11 3.7270-11 0.0      03
3151304  8.9420-11 -9.763-11 0.0      04
3151305  1.1480-10 -1.511-10 0.0      05
3151306  8.7688-11 -2.121-11 0.0      06
3151307  2.6580-11 -2.2972-11 0.0      07
*****
* HJT LEG BREAK PLANE
*****
3300000  HLBRKPL          VALVE
3300101  315010000 800000000 8.3650-3  0.95883  1.0+6  00100
3300102  1.00      1.00
3300201  0          ,000000000 ,000000000 0.0
3300300  TRPVLV
3300301  510
*****
* REACTOR VESSEL NOZZLE - BROKEN LOOP COLD LEG
*****
3350000  RVN=3LPL          BRANCH
3350001  2          0
3350101  0.0634    0.0000    0.0      0.0      0.0      0.0
3350102  4.0-5     0.0      00
3350200  003      14.956E6  554.31
3351101  282700000 335000000 0.0634    0.80400  1.43960  00000
3352101  335110000 340000000 0.0      0.10050  0.10050  00000
3351201  -1.732-10 -1.483-10 0.0
3352201  -1.528-10 -1.528-10 0.0
*****
* COLD LEG PIPE TO REFLOOD ASSIST BYPASS TEE
*****
3400000  CLP-RABT          BRANCH
3400001  1          0
3400101  0.0634    0.698     0.0      0.0      0.0      0.0
3400102  4.0-5     0.0      00
3400200  003      14.956E6  554.09
3401101  340010000 345000000 0.0      0.10050  0.10050  00000
3401201  -1.338-10 -1.338-10 0.0
*****
* BROKEN LOOP COLD LEG CONTRACTION -1.0
*****
3450000  BLC-CNTR          BRANCH
3450001  2          0
3450101  0.0634    0.700     0.0      0.0      0.0      0.0
3450102  4.0-5     0.0      00
3450200  003      14.956E6  553.99
3451101  345000000 370000000 0.0388    0.45760  1.24700  00000
3452101  345010000 350000000 0.0634    9.01672  19.3560  00000
3451201  -1.719-10 -1.501-10 0.0
3452201  -9.748-12 -1.115-11 0.0
*****
* BREAK SPOOL PIECE
*****
3500000  BRK-SP          SNGLVOL
3500101  0.0      0.762     0.023360 0.0      0.0      0.0
3500102  4.0-5     0.0      00
3500200  003      14.956E6  552.47
*****
* COLD LEG BREAK PLANE
*****
3650000  CLBRKPL          VALVE
3650101  350010000 805000000 8.3650-3  0.41500  1.0+6  00100

```

3650102 0.84 0.84
3650201 0 .00000000 .00000000 0.0
3650300 TRPVLV
3650301 510

* REFLOOD ASSIST BYPASS PIPING--COLD LEG SIDE

3700000 RABS-C-L PIPE
3700001 3
3700101 0.0388 2
3700102 0.0776 3
3700201 0.0388 2
3700301 0.0 3
3700401 0.0279 1
3700402 0.070 2
3700403 0.1165 3
3700601 90. 1
3700602 0.0 3
3700701 0.64 1
3700702 0.0 3
3700801 4.0-5 0.0 3
3700901 0.28 0.28 1
3700902 0.84 0.84 2
3701001 00 3
3701101 00000 2
3701201 003 14.954E6 565.96 0.0 0.0 0.0 1
3701202 003 14.952E6 565.96 0.0 0.0 0.0 2
3701203 003 14.952E6 565.97 0.0 0.0 0.0 3
3701300 0
3701301 -1.491-10 -1.393-10 0.0 01
3701302 -9.301-11 -9.301-11 0.0 02

* REFLOOD ASSIST BYPASS VALVE

3750000 RAB-VLV VALVE
3750101 370C10000 380000000 0. 0.0 0.0 00000
3750201 0 .00000000 .00000000 0.0
3750300 TRPVLV
3750301 502

* REFLOOD ASSIST BYPASS PIPING - HOT LEG SIDE

3800000 RABS-H-L PIPE
3800001 3
3800101 0.0776 1
3800102 0.0388 3
3800201 0.0388 2
3800301 0.0 3
3800401 0.1165 1
3800402 0.023 2
3800403 0.0489 3
3800601 0.0 1
3800602 0.0 2
3800603 -90. 3
3800701 0.0 1
3800702 0.0 2
3800703 -0.64 3
3800801 4.0-5 0.0 3
3800901 0.84 0.84 1
3800902 0.28 0.28 2
3801001 00 3
3801101 00000 2

```

3801201 003 14.946E6 565.97 0.0 0.0 0.0 1
3801202 003 14.946E6 565.97 0.0 0.0 0.0 2
3801203 003 14.948E6 565.96 0.0 0.0 0.0 3
3801300 0
3801301 -3.448-11 -3.448-11 0.0 01
3801302 -4.128-11 -5.256-11 0.0 02

```

* PRESSURIZER

* SURGE LINE PCS SIDE

```

4000000 SRGLPCS BRANCH
4000001 2 0
4000101 0.00145 2.300 0.0 0.0 90.0 0.54
4000102 4.0-5 0.0 00
4000200 003 14.938E6 614.60
4001101 110000000 400000000 0.0 0.93000 0.93000 00100
4002101 400010000 405000000 0.0 0.93000 0.93000 00000
4001201 -5.9858-3 -8.8060-3 0.0
4002201 -5.9860-3 -5.9860-3 0.0

```

* PRESSURIZER SURGE LINE

4050000 SRG-PZR PIPE

```

4050001 2
4050101 0.00145 2
4050201 0.00145 1
4050301 2.30 2
4050401 0.0 2
4050601 90.0 2
4050701 0.30 2
4050801 4.0-5 0.0 2
4050901 0.930000 0.930000 1
4051001 00 2
4051101 00000 1
4051201 003 14.935E6 614.41 0.0 0.0 0.0 1
4051202 003 14.934E6 614.42 0.0 0.0 0.0 2
4051300 0
4051301 -5.9860-3 -5.9860-3 0.0 01

```

* PRESSURIZER SURGE LINE VALVE

```

4100000 PZR-VLV VALVE
4100101 405010000 415000000 0.0 0.93000 0.93000 00100
4100201 0 -5.9861-3 -5.9861-3 0.0
4100300 TRPVLV
4100301 501

```

* PRESSURIZER VESSEL

4150000 PZRVESEL PIPE

```

4150001 7
4150101 0.0 2
4150102 0.5653 5
4150103 0.0 7
4150201 0.0 6
4150301 0.1815 1
4150302 0.1524 2
4150303 0.3967 3
4150304 0.5289 4
4150305 0.3967 5
4150306 0.1943 6

```

4150307	0.1029	7						
4150401	0.0684	1						
4150402	0.0838	2						
4150403	0.0	5						
4150404	0.0732	6						
4150405	0.0142	7						
4150501	0.0	7						
4150601	90.0	7						
4150801	4.0-5	0.0	7					
4151001	00	7						
4151101	00000	6						
4151201	003	14.932E6	614.42	0.0	0.0	0.0	1	
4151202	000	14.931E6	1.5833E6	2.4615E6	1.6479-9	0.0	2	
4151203	000	14.930E6	1.5837E6	2.4615E6	5.5001-7	0.0	3	
4151204	000	14.927E6	1.5836E6	2.4616E6	0.22596	0.0	4	
4151205	000	14.926E6	1.5834E6	2.4616E6	1.0	0.0	5	
4151206	000	14.925E6	1.5834E6	2.4616E6	1.0	0.0	6	
4151207	000	14.925E6	1.5834E6	2.4616E6	1.0	0.0	7	
4151300	0							
4151301	1.0230-6	3.0885-5	0.0	01				
4151302	7.0120-7	7.0512-3	0.0	02				
4151303	6.2771-7	0.32550	0.0	03				
4151304	-0.23616	9.3043-6	0.0	04				
4151305	-1.1303-3	3.1549-6	0.0	05				
4151306	-3.4390-3	8.6127-6	0.0	06				

 * TOP VOLUME PRESSURIZER

 4200000 TOPV-PZR BRANCH
 4200001 1 0
 4200101 0.0 0.1029 0.0142 0.0 90.0 0.1029
 4200102 4.0-5 0.0 00
 4200200 000 14.925E6 1.5834E6 2.4616E6 1.0
 4201101 415010000 420000000 0.0 0.0 0.0 00000
 4201201 -6.7300-4 8.6127-6 0.0

 * PORV

 4250000 POR-VLV VALVE
 4250101 420010000 810000000 9.0-5 0.0 0.0 00100
 4250201 0 .00000000 .00000000 0.0
 4250300 TRPVLV
 4250301 691

 * STEAM GENERATOR SECONDARY SIDE

 * TOP OF DOWNCOMER (OUTLET OF PRIMARY SEPARATOR)

 5000000 SPR-OUT SEPARATR
 5000001 3 0
 5000101 0.0 0.8288 1.0277 0.0 90.0 0.8288
 5000102 4.0-5 0.7697 00
 5000200 000 5.5192E6 1.1789E6 2.5936E6 0.95637
 5001101 500010000 520000000 0.0 0.0 0.0 00100
 5002101 500000000 505000000 0.0 0.0 0.0 00100
 5003101 515010000 500000000 0.196 0.0 0.0 00100
 5001201 0.88915 2.4000 0.0
 5002201 0.45877 -0.77061 0.0
 5003201 2.4507 2.9618 0.0

 * LOWER SEPARATOR SECTION -1.0

```

*****
5050000 LWR-SEPR BRANCH
5050001 1 0
5050101 0.0 0.8288 1.0085 0.0 -90.0 -0.8288
5050102 4.0-5 0.72845 00
5050200 003 5.5227E6 543.31
5051101 505010000 507000000 0.0 0.0 0.0 00100
5051201 0.13345 0.13345 0.0
*****
5070000 LWR-SEPR BRANCH
5070001 1 0
5070101 0.0 0.8288 1.0085 0.0 -90.0 -0.8288
5070102 4.0-5 0.72845 00
5070200 003 5.5290E6 543.31
5071101 507010000 508000000 0.0 0.0 0.0 00100
5071201 0.44778 0.44778 0.0
*****
* FEED INLET VOLUME
*****
5080000 FEIN-VOL BRANCH
5080001 1 0
5080101 0.0 0.6096 0.22107 0.0 -90.0 -0.6096
5080102 4.0-5 0.163697 00
5080200 003 5.5343E6 535.37
5081101 508010000 510000000 0.0 0.0 0.0 00100
5081201 0.79141 0.79141 0.0
*****
* STEAM GENERATOR DOWNCOMER
*****
5100000 SGTR-DMR ANNULUS
5100001 3
5100101 0.232 3
5100201 0.0 2
5100301 0.6096 3
5100401 0.0 3
5100601 -90.0 3
5100701 -0.6096 3
5100801 4.0-5 0.10793 3
5100901 0.0 0.0 2
5100001 00 3
5101101 00000 2
5101201 003 5.5388E6 535.41 0.0 0.0 0.0 1
5101202 003 5.5434E6 535.46 0.0 0.0 0.0 2
5101203 003 5.5481E6 535.50 0.0 0.0 0.0 3
5101300 0
5101301 0.79148 0.79148 0.0 01
5101302 0.79155 0.79155 0.0 02
*****
* JUNCTION FROM DOWNCOMER TO BOILER
*****
5130000 DNMR-BLR SNGLJUN
5130101 510010000 515000000 0.0 17.5 17.5 00000
5130201 0 0.79161 1.0727 0.0
*****
* STEAM GENERATOR BOILER
*****
5150000 BOILER PIPE
5150001 6
5150101 0.2776 4
5150102 0.31299 5
5150103 0.291864 6
5150201 0.0 5

```

5150301	1.8288	4					
5150302	0.8288	6					
5150401	0.0	6					
5150601	60.0	4					
5150602	90.0	6					
5150701	0.6096	4					
5150702	0.8288	6					
5150801	4.0-5	0.0234	4				
5150802	4.0-5	0.587423	5				
5150803	4.0-5	0.6096	6				
5150901	4.05	4.05	4				
5150902	0.0	0.0	5				
5151001	00	6					
5151101	00000	5					
5151201	000	5.5443E6	1.1728E6	2.5934E6	0.36177	0.0	1
5151202	000	5.5397E6	1.1790E6	2.5935E6	0.57486	0.0	2
5151203	000	5.5347E6	1.1797E6	2.5935E6	0.68895	0.0	3
5151204	000	5.5289E6	1.1795E6	2.5936E6	0.74821	0.0	4
5151205	000	5.5237E6	1.1792E6	2.5936E6	0.76686	0.0	5
5151206	000	5.5219E6	1.1791E6	2.5936E6	0.77299	0.0	6
5151300	0						
5151301	1.0245	1.3191	0.0	01			
5151302	1.4999	2.0197	0.0	02			
5151303	1.9438	2.7519	0.0	03			
5151304	2.3241	3.2080	0.0	04			
5151305	2.4073	2.9755	0.0	05			

 * TOP OF RISER(INSIDE SHROUD, ABOVE TUBES)

5200000	SEPAR-IN		BRANCH				
5200001	1	0					
5200101	0.27871	0.718	0.0	0.0	90.0	0.718	
5200102	4.0-5	1.0827	00				
5200200	002	5.5189E6	1.0				
5201101	520010000	525000000	0.0	0.0	0.0	00100	
5201201	2.2848	2.4001	0.0				

 * BELOW MIST EXTRACTOR , ABOVE TOP OF SHROUD IN STEAM DOME

5250000	BOTSTMDM		BRANCH				
5250001	1	0					
5250101	1.5886	0.762	0.0	0.0	90.0	0.762	
5250102	4.0-5	0.64417	00				
5250200	002	5.5187E6	1.0				
5251101	525010000	530000000	0.0	0.8	0.8	00000	
5251201	7.8662	14.433	0.0				

 * MIST EXTRACTOR AND STEAM GEN OUTLET PIPE TO SCV

5300000	STDM/PIP		SNGLVOL				
5300101	0.04635	25.07	0.0	0.0	0.0	0.0	
5300102	4.0-5	0.0	00				
5300200	000	5.5111E6	1.1785E6	2.5936E6	0.99999		

 *** STEAM CONTROL VALVE ***

5500000	STCVVA		SNGLVOL				
5500101	530010000	555000000	0.003667	0.0	0.0	01000	
5500201	0	69.717	182.67	0.0			

 *** PIPE DOWNSTREAM OF SCV ***

```

5550000  CND-INLT  SNGLVOL
5550101  0.06557  54.44      0.0      0.0      0.0      0.0
5550102  4.E-5     0.0         00
5550200  000       5.5085E6   1.1783E6  2.5937E6  0.99960
*****
*** FLOW PATH TO THE AIR COOLED CONDENSER ***
*****
5600000  CDACCO    SNGLJUN
5600101  555010000 565000000 0.0      0.0      0.0      01100
5600201  0         0.87374   10.225   0.0
*****
*** AIR COOLED CONDENSER ***
*****
5650000  CONDNR    TMDPVOL
5650101  0.21677  17.67      0.0      0.0      0.0      0.0
5650102  4.E-5     0.02      00
5650200  002       510
5650201  -0.0      5.5072E6  1.0
5650202  0.0       5.5072E6  1.0
5650203  0.51724  5.5104E6  1.0
5650204  0.68966  5.5234E6  1.0
5650205  1.03448  5.5364E6  1.0
5650206  1.55172  5.5559E6  1.0
5650207  1.89655  5.5657E6  1.0
5650208  2.41379  5.5754E6  1.0
5650209  2.75362  5.5754E6  1.0
5650210  2.93103  5.5722E6  1.0
5650211  3.10345  5.5657E6  1.0
5650212  3.62069  5.5527E6  1.0
5650213  4.13793  5.5364E6  1.0
5650214  4.82759  5.5104E6  1.0
5650215  5.17241  5.4909E6  1.0
5650216  5.68966  5.4779E6  1.0
5650217  6.37931  5.4421E6  1.0
5650218  6.89655  5.4226E6  1.0
5650219  7.58621  5.4096E6  1.0
5650220  8.44828  5.3966E6  1.0
5650221  9.31034  5.3933E6  1.0
5650222  10.6897  5.4031E6  1.0
5650223  11.2069  5.3998E6  1.0
5650224  12.5862  5.3901E6  1.0
5650225  13.6207  5.3803E6  1.0
5650226  15.0000  5.3706E6  1.0
5650227  17.5862  5.3673E6  1.0
5650228  20.0000  5.3608E6  1.0
5650229  22.5862  5.3576E6  1.0
5650230  25.0000  5.3511E6  1.0
5650231  27.4138  5.3478E6  1.0
5650232  30.0000  5.3446E6  1.0
5650233  120.000  5.2196E6  1.0
*****
*** MAIN FEED WATER VALVE ***
*****
5700000  MAINFWVA  TMDPJUN
5700101  575000000 508000000 0.05
5700200  1         510
5700201  -0.0      18.824    0.0      0.0
5700202  0.0       18.824    0.0      0.0
5700203  0.17341  18.824    0.0      0.0
5700204  0.34682  14.743    0.0      0.0
5700205  0.52023  9.6836    0.0      0.0
5700206  0.69364  7.2827    0.0      0.0

```

5700207	0.86705	3.7906	0.0	0.0
5700208	1.04046	3.1557	0.0	0.0
5700209	1.21387	2.2033	0.0	0.0
5700210	1.38728	1.5684	0.0	0.0
5700211	1.73410	0.93349	0.0	0.0
5700212	2.08092	0.77476	0.0	0.0
5700213	2.60116	0.61603	0.0	0.0
5700214	5.02890	0.45730	0.0	0.0
5700215	7.63006	0.45730	0.0	0.0
5700216	120.000	0.45730	0.0	0.0

 *** MAKE UP FEED STORAGE TANK ***

5750000	FED-TANK	TMDPVOL				
5750101	29.81	3.048	0.0	0.0	0.0	0.0
5750102	4.E-5	0.0	00			
5750200	001	510				
5750201	-0.0	478.0	0.0			
5750202	0.0	478.0	0.0			
5750203	120.0	478.0	0.0			

 * ECCS SYSTEM

* ECCS PIPING TO PCS

6000000	ECCS-PCS	BRANCH				
6000001	0	1				
6000101	9.009-3	8.8776	0.0	0.0	-90.0	-3.2
6000102	4.0-5	0.0	00			
6000200	003	4.7738E6	307.22			

 ^ ACCUMULATOR CHECK VALVE

6030000	ACCHKVLV	VALVE				
6030101	605010000	600000000	1.93221-3	2.98310	2.98310	00000
6030201	0	0.0	0.0	0.0		
6030300	TRPVLV					
6030301	662					

 * ACCUMULATOR PIPE 1

6050000	ACCP1PE1	BRANCH				
6050001	1	0				
6050101	0.014582	9.4891	0.0	0.0	0.0	0.0
6050102	4.0-5	0.0	00			
6050200	003	4.2190E6	307.20			
6051101	610010000	605000000	0.0	0.7	0.7	00000
6051201	0.0	0.0	0.0			

 * ACCUMULATOR PIPE 2

6100000	ACCP1PE2	SNGLVOL				
6100101	0.018608	7.55998	0.0	0.0	0.0	0.0
6100102	4.0-5	0.0	00			
6100200	003	4.2190E6	307.21			

 *** ACCUMULATOR VESSEL ***

6150000	ACCUMTOR	ACCUM				
6150101	1.0905	1.8041	0.0	0.0	90.0	1.8041
6150102	4.0E-5	0.0	10			

```

*6150200 4.20E6 306.0 0.0
*6151101 610000000 0.003167 1.6 1.6 00000
*6152200 0.0 1.20 60.0 0.0 0.04445 0 0 0
*
6150101 1.613734 2.33 0.0 0.0 90.0 2.33
6150102 4.0E-5 0.0 10
6150200 4.20E6 306.0 0.0
6151101 610000000 0.003167 1.6 1.6 00000
6152200 2.85 0.0 60.0 0.0 0.04445 0 0 0
*****
* BWST LPIS
*****
6200000 BWST-LP TMDPVOL
6200101 20.44 5.0 0.0 0.0 90. 5.0
6200102 4.0-5 0.0 00
6200200 003
6200201 0.0 1.00+5 303.0
*****
* BWST HPIS
*****
6250000 BWST-HP TMDPVOL
6250101 20.44 5.0 0.0 0.0 90. 5.0
6250102 4.0-5 0.0 00
6250200 003
6250201 0.0 1.00+5 303.0
*****
* ECC SYSTEM VALVE
*****
6300000 ECCALVE1 VALVE
6300101 600010000 185000000 5.989-3 0.0 0.0 00100
6300201 0 .00000000 .00000000 0.0
6300300 TRPVLV
6300301 580
*
6310000 ECCALVE2 VALVE
6310101 600010000 180010000 5.989-3 0.0 0.0 00100
6310201 0 .00000000 .00000000 0.0
6310300 TRPVLV
6310301 580
*****
* LOW PRESSURE INJECTION SYSTEM
*****
6350000 LPIS TMDPJUN
6350101 620000000 600000000 0.0
6350200 1 615 P 185010000
6350201 -1.0 0.0 0.0 0.0
6350202 0.0 7.500 0.0 0.0
6350203 8.483+4 7.045 0.0 0.0
6350204 4.297+5 6.091 0.0 0.0
6350205 7.745+5 5.045 0.0 0.0
6350206 9.443+5 4.313 0.0 0.0
6350207 1.119+6 3.454 0.0 0.0
6350208 1.186+6 3.173 0.0 0.0
6350209 1.257+6 2.673 0.0 0.0
6350210 1.326+6 2.159 0.0 0.0
6350211 1.395+6 1.536 0.0 0.0
6350212 1.464+6 0.718 0.0 0.0
6350213 1.517+6 0.000 0.0 0.0
*****
* HIGH PRESSURE INJECTION SYSTEM
*****
6400000 HPIS TMDPJUN

```

6400101	625000000	600000000	0.0		
6400200	1	614	P	1.0010000	
6400201	-1.0	0.0	0.0	0.0	
6400202	0.0	1.58528	0.0	0.0	
6400203	0.9000+6	1.58528	0.0	0.0	
6400204	5.0000+6	1.30435	0.0	0.0	
6400205	15.060+6	0.31533	0.0	0.0	
6400206	50.000+6	0.00000	0.0	0.0	

 * CONTAINMENT

 * CONTAINMENT BROKEN LOOP HOT LEG

8000000	CONTRLHL		TMDPVOL			
8000101	0.05200	0.0	3.15005	0.0	0.0	0.0
8000102	0.0	0.0	00			
8000200	003	510				
8000201	-1.0	1.00000+5	293.000			
8000202	0.0	1.00000+5	293.000			
8000203	2.0	1.24110+5	359.111			
8000204	7.0	1.55827+5	365.222			
8000205	17.7	2.36499+5	398.556			
8000206	20.	2.52357+5	400.222			
8000207	22.5	2.62700+5	401.889			
8000208	25.	2.72353+5	403.000			
8000209	30.	2.81316+5	404.111			
8000210	32.5	2.84074+5	404.667			
8000211	35.	2.86143+5	404.667			
8000212	37.5	2.86832+5	404.667			
8000213	40.	2.86832+5	404.667			
8000214	45.	2.86143+5	404.667			
8000215	50.	2.83385+5	404.111			
8000216	70.	3.50000+5	404.111			
8000217	100.	3.10000+5	404.111			
8000218	150.	3.10000+5	404.111			
8000219	1.0+5	1.00000+5	293.000			

 * CONTAINMENT BROKEN LOOP COLD LEG

8050000	CONTRLHL		TMDPVOL			
8050101	0.05200	0.0	4.08155	0.0	0.0	0.0
8050102	0.0	0.0	00			
8050200	003	510				
8050201	-1.0	1.00000+5	293.000			
8050202	0.0	1.00000+5	293.000			
8050203	2.0	1.24110+5	359.111			
8050204	7.0	1.55827+5	365.222			
8050205	17.7	2.36499+5	398.556			
8050206	20.	2.52357+5	400.222			
8050207	22.5	2.62700+5	401.889			
8050208	25.	2.72353+5	403.000			
8050209	30.	2.81316+5	404.111			
8050210	32.5	2.84074+5	404.667			
8050211	35.	2.86143+5	404.667			
8050212	37.5	2.86832+5	404.667			
8050213	40.	2.86832+5	404.667			
8050214	45.	2.86143+5	404.667			
8050215	50.	2.83385+5	404.111			
8050216	70.	3.50000+5	404.111			
8050217	100.	3.10000+5	404.111			
8050218	150.	3.10000+5	404.111			
8050219	1.0+5	1.00000+5	293.000			

```

*****
* CONTAINMENT POWER OPERATED RELIEF VALVE
*****
8100000  CONTPRV          TNDPVOL
8100101  0.0          1.0          0.1          0.0          0.0          0.0
8100102  0.0          0.0          00
8100200  003          510
8100201  -1.0         1.00000+5  293.000
8100202  0.0          1.00000+5  293.000
8100203  1000.0       1.00000+5  293.000
*****
* BOUNDARY VALVE INTACT LOOP HOT LEG
*****
*9000000  BOUNDVLV          VALVE
*9000101  420010000  905000000  0.0          0.0          0.0          00100
*9000201  0          0.0          0.0          0.0
*9000300  TRPVLV
*9000301  501
*****
* BOUNDARY VOLUME INTACT LOOP HOT LEG
*****
*9050000  BOUNDVOL          TNDPVOL
*9050101  0.0          1.0          0.1          0.0          0.0          0.0
*9050102  0.0          0.0          00
*9050200  001
*9050201  0.0          614.88       1.0
*9050202  1000.0       614.88       1.0
*****
* BOUNDARY JUNCTION FOR PREZ WATER LEVEL
*****
*9100000  BOUNDTJ          TNDPJUN
*9100101  915000000  415000000  0.0
*9100200  1          501          CNTRLVAR    100
*9100201  -10.0        0.0          0.0          0.0
*9100202  -10.0        -500.0       0.0          0.0
*9100203  0.0          0.0          0.0          0.0
*9100204  10.0         500.0       0.0          0.0
*****
* BOUNDARY VOLUME FOR PREZ WATER LEVEL
*****
*9150000  BOUNDTV          TNDPVOL
*9150101  0.0          1.0          0.1          0.0          0.0          0.0
*9150102  0.0          0.0          00
*9150200  001          501          TEMPF       415010000
*9150201  -0.0         613.55       0.0
*9150202  0.0          0.0          0.0
*9150203  700.0        700.0       0.0
*****
* REACTOR VESSEL HEAT STRUCTURE
*****
* REACTOR VESSEL WALL HEAT STRUCTURES
*****
* REACTOR VESSEL FILLER BLOCKS HEAT STRUCTURES
*****
* INLET ANNULUS TOP VOLUME 1
* STATION 264 TO 2 77
*****
12000000  1          21          2          1          0.508
12000100  0          1
12000101  20         0.7264
12000201  4          20
12000301  0.0        20

```

```

12000401 559.75 21
12000501 200010000 0 1 1 0.165 1
12000601 0 0 0 1 0.165 1
12000701 0 0.0 0.0 0.0 1
12000801 0 0.1524 0.3245 0.33 1
*****
* INLET ANNULUS TOP VOLUME 2
* STATION 264 TO 277
*****
12001000 1 21 2 1 0.505
12001100 0 1
12001101 20 0.7264
12001201 4 20
12001301 0.0 20
12001401 559.77 21
12001501 280010000 0 1 1 0.165 1
12001601 0 0 0 1 0.165 1
12001701 0 0.0 0.0 0.0 1
12001801 0 0.1524 0.3245 0.33 1
*****
* INLET ANNULUS LOWER VOLUME 1
* STATION 247.3 TO 264.0
*****
12020000 1 21 2 1 0.501
12020100 0 1
12020101 20 0.7264
12020201 4 20
12020301 0.0 20
12020401 559.68 21
12020501 202010000 0 1 1 0.212 1
12020601 0 0 0 1 0.212 1
12020701 0 0.0 0.0 0.0 1
12020801 0 0.1524 0.3245 0.424 1
*****
* INLET ANNULUS LOWER VOLUME 2
* STATION 247.3 TO 264.0
*****
12021000 1 21 2 1 0.501
12021100 0 1
12021101 20 0.7264
12021201 4 20
12021301 0.0 20
12021401 559.75 21
12021501 282010000 0 1 1 0.212 1
12021601 0 0 0 1 0.212 1
12021701 0 0.0 0.0 0.0 1
12021801 0 0.1524 0.3245 0.424 1
*****
* DOWNCOMER 1 AND LOW PLENUM
* STATION 67.7 TO 247.3
*****
12100000 6 21 2 1 0.47
12100100 0 1
12100101 20 0.7264
12100201 4 20
12100301 0.0 20
12100401 545.0 21
12100501 204010000 2000000 1 1 0.479 4
12100502 215010000 0 1 1 0.36 5
12100503 220010000 0 1 1 0.37 6
12100601 -939 0 3949 1 0.479 4
12100602 -939 0 3949 1 0.36 5

```

```

12100603 -939      0      3949      1      0.37      6
12100701  0      0.0      0.0      0.0      6
12100801  0      0.1016    0.2155    0.958    4
12100802  0      0.1016    0.2155    0.36     5
12100803  0      0.1016    0.2155    5.00     6
*****
* DOWNCOMER 2
*****
12101000  4      21      2      1      0.47
12101100  0      1
12101101  20     0.7264
12101201  4      20
12101301  0.0    20
12101401  545.0  21
12101501  284010000 2000000  1      1      0.479    4
12101601 -939    0      3949    1      0.479    4
12101701  0      0.0      0.0      0.0      4
12101801  0      0.1016    0.2155    0.958    4
*****
* CORE SUPPORT BARREL (SECTION 1)
* STATION 96.44 TO 277
*****
12150000  6      11      2      1      0.381
12150100  0      1
12150101  10     0.419
12150201  4      10
12150301  0.0    10
12150401  559.60 11
12150501  0      0      0      1      0.165    1
12150502  0      0      0      1      0.212    2
12150503  0      0      0      1      0.479    6
12150601  200010000 0      1      1      0.165    1
12150602  202010000 0      1      1      0.212    2
12150603  204010000 2000000  1      1      0.479    6
12150701  0      0.0      0.0      0.0      6
12150901  0      0.1016    0.2155    0.330    1
12150902  0      0.1016    0.2155    0.424    2
12150903  0      0.1016    0.2155    0.958    6
*****
* CORE SUPPORT BARREL (SECTION 2)
* STATION 96.44 TO 277
*****
12151000  6      11      2      1      0.381
12151100  0      1
12151101  10     0.419
12151201  4      10
12151301  0.0    10
12151401  559.65 11
12151501  0      0      0      1      0.165    1
12151502  0      0      0      1      0.212    2
12151503  0      0      0      1      0.479    6
12151601  280010000 0      1      1      0.165    1
12151602  282010000 0      1      1      0.212    2
12151603  284010000 2000000  1      1      0.479    6
12151701  0      0.0      0.0      0.0      6
12151901  0      0.1016    0.2155    0.330    1
12151902  0      0.1016    0.2155    0.424    2
12151903  0      0.1016    0.2155    0.958    6
*****
* FLOW SKIRT - CORE FILLER ASSEMBLY
* STATION 96.44 TO 261.13
*****

```

12250000	10	5	2		0.3	
12250100	0	1				
12250101	4	0.38				
12250201	4	4				
12250301	0.0	4				
12250401	575.0	5				
12250501	225010000	0	1	1	0.5200	1
12250502	227010000	1000000	1	1	0.2795	6
12250503	232010000	0	1	1	0.3775	7
12250504	240010000	5000000	1	1	0.5590	9
12250505	250010000	0	1	1	0.8430	10
12250601	0	0	0	1	0.5200	1
12250602	0	0	0	1	0.2795	6
12250603	0	0	0	1	0.3775	7
12250604	0	0	0	1	0.5590	9
12250605	0	0	0	1	0.8430	10
12250701	0	0.0	0.0	0.0	10	
12250801	0	0.6	0.0	0.520	1	
12250802	0	0.6	0.0	0.2795	6	
12250803	0	0.6	0.0	0.3775	7	
12250804	0	0.6	0.0	0.5590	9	
12250805	0	0.6	0.0	0.8430	10	

 > LOWER CORE SUPPORT STRUCTURE

* STATION 96.44 TO 116.91
 * INCLUDES CORE SUPPORT BARREL LIP, LOWER CORE SUPPORT
 * STRUCTURE AND FUEL MODULE LOWER END BOXES

12251000	1	7	2	1	0.282	
12251100	0	1				
12251101	6	0.3				
12251201	4	6				
12251301	0.0	6				
12251401	559.64	7				
12251501	225010000	0	1	1	0.52	1
12251601	0	0	0	1	0.52	1
12251701	0	0.0	0.0	0.0	1	
12251801	0	0.095	0.095	0.52	1	

 * ACTIVE CORE

* STATION 116.91 TO 182.94

* AVERAGE FUEL RODS IN AVERAGE CHANNEL (AXIAL LEVEL 1)

12361000	1	10	2	1	0.0	
+	1	1	8			
12361100	0	1				
12361101	5	4.66893-3				
12361102	1	4.74351-3				
12361103	3	5.36265-3				
12361201	1	5				
12361202	-2	6				
12361203	-3	9				
12361301	1.0	5				
12361302	0.0	9				
12361401	1080.3	1				
12361402	1065.4	2				
12361403	1022.3	3				
12361404	954.05	4				
12361405	864.85	5				
12361406	760.66	6				
12361407	616.54	7				

12361408	610.30	8				
12361409	604.29	9				
12361410	598.48	10				
12361501	0	0	0	1	306.222	1
12361601	227010000	0	1	1	306.222	1
12361701	900	0.127545	0.0	0.0	1	
12361901	0	0.013633	0.0	0.2795	1	

* AVERAGE FUEL RODS IN AVERAGE CHANNEL (AXIAL LEVEL 2)

12362000	1	10	2	1	0.0	
+	1	1	8			
12362100	0	1				
12362101	5	4.68060-3				
12362102	1	4.74415-3				
12362103	3	5.36341-3				
12362201	1	5				
12362202	-2	6				
12362203	-3	9				
12362301	1.0	5				
12362302	0.0	9				
12362401	1402.1	1				
12362402	1374.7	2				
12362403	1294.5	3				
12362404	1168.5	4				
12362405	1005.1	5				
12362406	826.87	6				
12362407	644.72	7				
12362408	635.29	8				
12362409	626.18	9				
12362410	617.36	10				
12362501	0	0	0	1	306.222	1
12362601	228010000	0	1	1	306.222	1
12362701	900	0.197174	0.0	0.0	1	
12362901	0	0.013633	0.0	0.2795	1	

* AVERAGE FUEL RODS IN AVERAGE CHANNEL (AXIAL LEVEL 3)

12363000	1	10	2	1	0.0	
+	1	1	8			
12363100	0	1				
12363101	5	4.68112-3				
12363102	1	4.74424-3				
12363103	3	5.36350-3				
12363201	1	5				
12363202	-2	6				
12363203	-3	9				
12363301	1.0	5				
12363302	0.0	9				
12363401	1424.6	1				
12363402	1396.2	2				
12363403	1313.2	3				
12363404	1183.0	4				
12363405	1014.6	5				
12363406	831.04	6				
12363407	646.30	7				
12363408	636.66	8				
12363409	627.34	9				
12363410	618.32	10				
12363501	0	0	0	1	306.222	1
12363601	229010000	0	1	1	306.222	1
12363701	900	0.201827	0.0	0.0	1	

```

12363901 0 0.013633 0.0 0.2795 1
*
* AVERAGE FUEL RODS IN AVERAGE CHANNEL (AXIAL LEVEL 4)
*
12364000 1 10 2 1 0.0
+ 1 1 8
12364100 0 1
12364101 5 4.67304-3
12364102 1 4.74412-3
12364103 3 5.36335-3
12364201 1 5
12364202 -2 6
12364203 -3 9
12364301 1.0 5
12364302 0.0 9
12364401 1199.4 1
12364402 1180.6 2
12364403 1125.4 3
12364404 1037.1 4
12364405 925.42 5
12364406 795.98 6
12364407 638.27 7
12364408 622.06 8
12364409 624.10 9
12364410 617.38 10
12364501 0 0 1 306.222 1
12364601 230010000 0 1 1 306.222 1
12364701 900 0.150138 0.0 0.0 1
12364901 0 0.013633 0.0 0.2795 1

```

```

*
* AVERAGE FUEL RODS IN AVERAGE CHANNEL (AXIAL LEVEL 5)

```

```

*
12365000 1 10 2 1 0.0
+ 1 1 8
12365100 0 1
12365101 5 4.66378-3
12365102 1 4.74379-3
12365103 3 5.36299-3
12365201 1 5
12365202 -2 6
12365203 -3 9
12365301 1.0 5
12365302 0.0 9
12365401 920.10 1
12365402 911.62 2
12365403 886.56 3
12365404 845.91 4
12365405 791.96 5
12365406 726.87 6
12365407 623.37 7
12365408 619.27 8
12365409 615.33 9
12365410 611.53 10
12365501 0 0 1 306.222 1
12365601 231010000 0 1 1 306.222 1
12365701 900 0.084338 0.0 0.0 1
12365901 0 0.013633 0.0 0.2795 1

```

```

*
* AVERAGE FUEL RODS IN AVERAGE CHANNEL (AXIAL LEVEL 6)

```

```

*
12366000 1 10 2 1 0.0
+ 1 1 8

```

12366100	0	1				
12366101	5	4.65917-3				
12366102	1	4.74339-3				
12366103	3	5.36250-3				
12366201	1	5				
12366202	-2	6				
12366203	-3	9				
12366301	1.0	5				
12366302	0.0	9				
12366401	665.18	1				
12366402	663.63	2				
12366403	658.99	3				
12366404	651.33	4				
12366405	640.74	5				
12366406	627.34	6				
12366407	599.70	7				
12366408	598.70	8				
12366409	597.74	9				
12366410	596.81	10				
12366501	0	0	0	1	306.222	1
12366601	232010000	0	1	1	306.222	1
12366701	900	0.020229	0.0	0.0	1	
12366901	0	0.013633	0.0	0.2795	1	

* AVERAGE FUEL RODS IN HOT CHANNEL (AXIAL LEVEL 1)

12371000	1	10	2	1	0.0	
+	1	1	8			
12371100	0	1				
12371101	5	4.67914-3				
12371102	1	4.74659-3				
12371103	3	5.36552-3				
12371201	1	5				
12371202	-2	6				
12371203	-3	9				
12371301	1.0	5				
12371302	0.0	9				
12371401	1396.3	1				
12371402	1369.4	2				
12371403	1291.0	3				
12371404	1167.7	4				
12371405	1007.5	5				
12371406	832.22	6				
12371407	643.06	7				
12371408	633.82	8				
12371409	624.88	9				
12371410	616.24	10				
12371501	0	0	0	1	54.7624	1
12371601	233010000	0	1	1	54.7624	1
12371701	900	3.45563-2	0.0	0.0	1	
12371901	0	0.013633	0.0	0.2795	1	

* AVERAGE FUEL RODS IN HOT CHANNEL (AXIAL LEVEL 2)

12372000	1	10	2	1	0.0	
+	1	1	8			
12372100	0	1				
12372101	5	4.69746-3				
12372102	1	4.74708-3				
12372103	3	5.36610-3				
12372201	1	5				
12372202	-2	6				

12372203	-3	9					
12372301	1.0	5					
12372302	0.0	9					
12372401	1855.5	1					
12372402	1807.9	2					
12372403	1667.1	3					
12372404	1444.1	4					
12372405	1165.5	5					
12372406	870.55	6					
12372407	661.11	7					
12372408	647.03	8					
12372409	633.36	9					
12372410	620.08	10					
12372501	0	0	0	1	54.7624	1	
12372601	234010000	0	1	1	54.7624	1	
12372701	900	5.33355-2	0.0	0.0	1		
12372901	0	0.013633	0.0	0.2795	1		

* AVERAGE FUEL RODS IN HOT CHANNEL (AXIAL LEVEL 3)

12373000	1	10	2	1	0.0		
+	1	1	8				
12373100	0	1					
12373101	5	4.69770-3					
12373102	1	4.74714-3					
12373103	3	5.36616-3					
12373201	1	5					
12373202	-2	6					
12373203	-3	9					
12373301	1.0	5					
12373302	0.0	9					
12373401	1861.3	1					
12373402	1813.5	2					
12373403	1672.0	3					
12373404	1447.8	4					
12373405	1167.7	5					
12373406	871.21	6					
12373407	661.84	7					
12373408	647.72	8					
12373409	634.01	9					
12373410	620.70	10					
12373501	0	0	0	1	54.7624	1	
12373601	235010000	0	1	1	54.7624	1	
12373701	900	5.35414-2	0.0	0.0	1		
12373901	0	0.013633	0.0	0.2795	1		

* AVERAGE FUEL RODS IN HOT CHANNEL (AXIAL LEVEL 4)

12374000	1	10	2	1	0.0		
+	1	1	8				
12374100	0	1					
12374101	5	4.68411-3					
12374102	1	4.74696-3					
12374103	3	5.36594-3					
12374201	1	5					
12374202	-2	6					
12374203	-3	9					
12374301	1.0	5					
12374302	0.0	9					
12374401	1504.5	1					
12374402	1472.8	2					
12374403	1380.4	3					

12374404	1234.8	4					
12374405	1049.2	5					
12374406	846.83	6					
12374407	650.05	7					
12374408	639.69	8					
12374409	629.67	9					
12374410	619.95	10					
12374501	0	0	0	1	54.7624	1	
12374601	236010000	0	1	1	54.7624	1	
12374701	900	3.89479-2	0.0	0.0	1		
12374901	0	0.013633	0.0	0.2795	1		

* AVERAGE FUEL RODS IN HOT CHANNEL (AXIAL LEVEL 5)

12375000	1	10	2	1	0.0		
+	1	1	8				
12375100	0	1					
12375101	5	4.66963-3					
12375102	1	4.74674-3					
12375103	3	5.36570-3					
12375201	1	5					
12375202	-2	6					
12375203	-3	9					
12375301	1.0	5					
12375302	0.0	9					
12375401	1094.0	1					
12375402	1079.3	2					
12375403	1036.7	3					
12375404	969.44	4					
12375405	881.49	5					
12375406	778.20	6					
12375407	635.57	7					
12375408	629.61	8					
12375409	623.86	9					
12375410	618.32	10					
12375501	0	0	0	1	54.7624	1	
12375601	237010000	0	1	1	54.7624	1	
12375701	900	2.21880-2	0.0	0.0	1		
12375901	0	0.013633	0.0	0.2795	1		

* AVERAGE FUEL RODS IN HOT CHANNEL (AXIAL LEVEL 6)

12376000	1	10	2	1	0.0		
+	1	1	8				
12376100	0	1					
12376101	5	4.66100-3					
12376102	1	4.74638-3					
12376103	3	5.36527-3					
12376201	1	5					
12376202	-2	6					
12376203	-3	9					
12376301	1.0	5					
12376302	0.0	9					
12376401	750.24	1					
12376402	746.98	2					
12376403	737.27	3					
12376404	721.29	4					
12376405	699.34	5					
12376406	671.97	6					
12376407	620.33	7					
12376408	618.47	8					
12376409	616.67	9					

12376410	614.94	10					
12376501	0	0	0	1	54.7624	1	
12376601	238010000	0	1	1	54.7624	1	
12376701	900	0.68731-2	0.0	0.0	1		
12376901	0	0.013633	0.0	0.2795	1		

*

* HOT FUEL RODS IN HOT CHANNEL (AXIAL LEVEL 1)

*

12381000	1	10	2	1	0.0	
+	1	1	8			
12381100	0	1				
12381101	5	4.67914-3				
12381102	1	4.74659-3				
12381103	3	5.36552-3				
12381201	1	5				
12381202	-2	6				
12381203	-3	9				
12381301	1.0	5				
12381302	0.0	9				
12381401	1501.4	1				
12381402	1470.3	2				
12381403	1379.6	3				
12381404	1236.6	4				
12381405	1053.9	5				
12381406	854.07	6				
12381407	646.82	7				
12381408	636.62	8				
12381409	626.75	9				
12381410	617.18	10				
12381501	0	0	0	1	2.23520	1
12381601	233010000	0	1	1	2.23520	1
12381701	900	1.56176-3	0.0	0.0	1	
12381901	0	0.013633	0.0	0.2795	1	

*

* HOT FUEL RODS IN HOT CHANNEL (AXIAL LEVEL 2)

*

12382000	1	10	2	1	0.0	
+	1	1	8			
12382100	0	1				
12382101	5	4.69746-3				
12382102	1	4.74008-3				
12382103	3	5.36610-3				
12382201	1	5				
12382202	-2	6				
12382203	-3	9				
12382301	1.0	5				
12382302	0.0	9				
12382401	2006.5	1				
12382402	1953.3	2				
12382403	1796.4	3				
12382404	1544.0	4				
12382405	1227.3	5				
12382406	891.39	6				
12382407	665.18	7				
12382408	649.86	8				
12382409	634.98	9				
12382410	620.51	10				
12382501	0	0	0	1	2.23520	1
12382601	234010000	0	1	1	2.23520	1
12382701	900	2.37504-3	0.0	0.0	1	
12382901	0	0.013633	0.0	0.2795	1	

*

* HDT	FUEL RODS IN HDT	CHANNEL	(AXIAL LEVEL 3)
12383000	1	10	2 1 0.0
+	1	1	8
12383100	0	1	
12383101	5	4.69770-3	
12383102	1	4.74714-3	
12383103	3	5.36616-3	
12383201	1	5	
12383202	-2	6	
12383203	-3	9	
12383301	1.0	5	
12383302	0.0	9	
12383401	2002.1	1	
12383402	1949.0	2	
12383403	1792.5	3	
12383404	1540.9	4	
12383405	1225.2	5	
12383406	890.56	6	
12383407	665.60	7	
12383408	650.32	8	
12383409	635.48	9	
12383410	621.06	10	
12383501	0	0	0 1 2.23520 1
12383601	235010000	0	1 1 2.23520 1
12383701	900	2.37012-3	0.0 0.0 1
12383901	0	0.013633	0.0 0.2795 1

* HOT	FUEL RODS IN HOT	CHANNEL	(AXIAL LEVEL 4)
12384000	1	10	2 1 0.0
+	1	1	8
12384100	0	1	
12384101	5	4.68411-3	
12384102	1	4.74696-3	
12384103	3	5.36594-3	
12384201	1	5	
12384202	-2	6	
12384203	-3	9	
12384301	1.0	5	
12384302	0.0	9	
12384401	1593.1	1	
12384402	1557.7	2	
12384403	1454.4	3	
12384404	1291.9	4	
12384405	1086.8	5	
12384406	863.28	6	
12384407	652.66	7	
12384408	641.51	8	
12384409	630.71	9	
12384410	620.23	10	
12384501	0	0	0 1 2.23520 1
12384601	236010000	0	1 1 2.23520 1
12384701	900	1.71484-3	0.0 0.0 1
12384901	0	0.013633	0.0 0.2795 1

* HOT FUEL ROD IN HOT CHANNEL (AXIAL LEVELS)

12385000	1	10	2 1 0.0
+	1	1	8
12385100	0	1	
12385101	5	4.66963-3	

12385102	1	4.74674-3					
12385103	3	5.36570-3					
12385201	1	5					
12385202	-2	6					
12385203	-3	9					
12385301	1.0	5					
12385302	0.0	9					
12385401	1139.7	1					
12385402	1123.5	2					
12385403	1075.6	3					
12385404	1000.7	4					
12385405	903.61	5					
12385406	790.08	6					
12385407	637.14	7					
12385408	630.72	8					
12385409	624.53	5					
12385410	618.55	10					
12385501	0	0	0	1	2.23520	1	
12385601	237010000	0	1	1	2.23520	1	
12385701	900	0.97663-3	0.0	0.0	1		
12385901	0	0.013633	0.0	0.2795	1		

*

* HOT FUEL ROD IN HOT CHANNEL (AXIAL LEVEL 6)

*

12386000	1	10	2	1	0.0		
+	1	1	8				

12386100	0	1					
12386101	5	4.66100-3					
12386102	1	4.74638-3					
12386103	3	5.36527-3					
12386201	1	5					
12386202	-2	6					
12386203	-3	9					
12386301	1.0	5					
12386302	0.0	9					
12386401	771.60	1					
12386402	767.79	2					
12386403	756.45	3					
12386404	737.83	4					
12386405	712.35	5					
12386406	680.55	6					
12386407	621.74	7					
12386408	619.61	8					
12386409	617.56	9					
12386410	615.58	10					
12386501	0	0	0	1	2.23520	1	
12386601	237010000	0	1	1	2.23520	1	
12386701	900	0.32091-3	0.0	0.0	1		
12386901	0	0.013633	0.0	0.2795	1		

* UPPER CORE SUPPORT STRUCTURE

* STATION 190.5 TO 234.5

12400000	2	7	2	1	0.282		
12400100	0	1					
12400101	6	0.31					
12400201	4	6					
12400301	0.0	6					
12400401	592.68	7					
12400501	240010000	5000000	1	1	0.559	2	
12400601	0	0	0	1	0.559	2	
12400701	0	0.0	0.0	0.0	2		

12400801 0 0.56 0.0 1.118 2

* FUEL MODULES

* STATION 187.6 TO 258.4

12510000 1 5 1 1 0.0
12510100 0 1
12510101 4 0.01
12510201 4 4
12510301 0.0 4
12510401 592.73 5
12510501 250010000 0 1 1 1.8 1
12510601 251010000 0 1 1 1.8 1
12510701 0 0.0 0.0 0.0 1
12510801 0 0.0 0.0 1.8 1
12510901 0 0.0 0.0 1.8 1

* UPPER PLENUM INTERNALS

12551000 2 5 1 1 0.0
12551100 0 1
12551101 4 0.005
12551201 4 4
12551301 0.0 4
12551401 590.62 5
12551501 255010000 0 1 1 1.0 2
12551601 0 0 1 1.0 2
12551701 0 0.0 0.0 0.0 2
12551801 0 0.0 0.0 1.0 2

* CORE SUPPORT BARREL - UPPER PLENUM LOWER VOLUME

* STATION 264 TO 297.6

12552000 1 11 2 1 0.381
12552100 0 1
12552101 10 0.419
12552201 5 10
12552301 0.0 10
12552401 590.62 11
12552501 255010000 0 1 1 0.854 1
12552601 0 0 1 0.854 1
12552701 0 0.0 0.0 0.0 1
12552801 0 0.762 0.0 0.854 1

* CORE SUPPORT BARREL - UPPER PLENUM TOP VOLUME

* STATION 297.6 TO 325

12601000 1 21 2 1 0.381
12601100 0 1
12601101 20 0.728
12601201 5 20
12601301 0.0 20
12601401 590.62 21
12601501 255010000 0 1 1 0.712 1
12601601 0 0 1 0.712 1
12601701 0 0.0 0.0 0.0 1
12601801 0 0.762 0.0 0.712 1

* UPPER HEAD TOP PLATE

* STATION 325

12602000 1 21 1 1 0.0

12602100	0		1				
12602101	20		0.474				
12602201	5		20				
12602301	0.0		20				
12602401	575.50		21				
12602501	255010000	0		1	1	0.712	1
12602601	-939	0		3949	1	0.712	1
12602701	0	0.0	0.0	0.0	0.0	1	
12602801	0	0.0	0.0	0.0	0.712	1	

* STEAM GENERATOR HEAT STRUCTURES

* TUBING

10060000	8	8	2	1		0.0051054	
10060100	0	1					
10060101	7		6.348984-3				
10060201	6	7					
10060301	0.0	7					
10060401	559.65	1					
10060402	558.37	2					
10060403	557.09	3					
10060404	556.16	4					
10060405	555.12	5					
10060406	553.83	6					
10060407	552.68	7					
10060408	551.56	8					
10060501	115010000	10000	1	1		1124.71	3
10060502	115040000	10000	1	1		849.063	5
10060503	115060000	10000	1	1		1124.71	8
10060601	515010000	10000	1	1		1124.71	3
10060602	515040000	0	1	1		849.063	4
10060603	515040000	0	1	1		849.063	5
10060604	515030000	-10000	1	1		1124.71	8
10060701	0	0.0	0.0	0.0		8	
10060801	0	0.0468	0.0	0.0		8	
10060901	0	0.0	0.0	0.0		8	

* SHROUD - UPPER SECTION -1.0

15000000	2	4	2	1		0.3048	
15000100	0	1					
15000101	3		0.3143				
15000201	5	3					
15000301	0.0	3					
15000401	546.76	4					
15000501	515060000	0	1	0		1.58726	1
15000502	515050000	0	1	1		0.92736	2
15000601	505010000	0	1	0		1.63672	1
15000602	507010000	0	1	1		0.92736	2
15000701	0	0.0	0.0	0.0		2	
15000801	0	0.0	0.0	0.0		2	
15000901	0	0.0	0.0	0.0		2	

* SHROUD - LOWER SECTION -1.0

15100000	4	4	2	1		0.6445	
15100100	0	1					
15100101	3		0.6572				
15100201	5	3					

15100301	0.0	3					
15100401	542.5	4					
15100501	515040000	0	1	1	0.646354	1	
15100502	515030000	-10000	1	0	2.46893	4	
15100601	508010000	0	1	1	0.646354	1	
15100602	510010000	10000	1	0	2.51723	4	
15100701	0	0.0	0.0	0.0	4		
15100801	0	0.0	0.0	0.0	4		
15100901	0	0.0	0.0	0.0	4		

 * HEAT STRUCTURE THERMAL PROPERTY DATA

20100100	TBL/FCTN	1	1	* UO2
20100200	TBL/FCTN	1	1	* GAP
20100300	TBL/FCTN	1	1	* ZR
20100400	TBL/FCTN	1	1	* S-STELL
20100500	C-STEEL			
20100600	TBL/FCTN	1	1	* INCONEL 600
20100700	TBL/FCTN	1	1	* NGO
20100800	TBL/FCTN	1	1	* NICR

 * UO2 - THERMAL CONDUCTIVITY

20100101	2.7315E2	8.44
20100102	4.1667E2	6.46
20100103	5.3315E2	5.782785
20100104	6.99817E2	4.633177
20100105	8.66483E2	3.880307
20100106	1.03315E3	3.351625
20100107	1.08871E3	3.155129
20100108	1.19982E3	2.983787
20100109	1.28315E3	2.836674
20100110	1.36648E3	2.713792
20100111	1.53315E3	2.521680
20100112	1.61648E3	2.448990
20100113	1.69982E3	2.391875
20100114	1.97759E3	2.289762
20100115	2.25537E3	2.307069
20100116	2.53315E3	2.433413
20100117	2.81093E3	2.661870
20100118	3.08871E3	2.994171

 * UO2 - VOLUMETRIC HEAT CAPACITY

20100151	2.73150E2	2.310427E6
20100152	3.23150E2	2.571985E6
20100153	3.73150E2	2.746357E6
20100154	6.73150E2	3.138694E6
20100155	1.37315E3	3.443844E6
20100156	1.77315E3	3.531030E6
20100157	1.97315E3	3.792588E6
20100158	2.17315E3	4.228518E6
20100159	2.37315E3	4.882412E6
20100160	2.67315E3	6.015829E6
20100161	2.77315E3	6.320980E6
20100162	2.87315E3	6.582538E6
20100163	2.97315E3	6.713317E6
20100164	3.11315E3	6.800503E6
20100165	4.69982E3	6.800503E6

* GAP--THERMAL CONDUCTIVITY

```

*****
20100201  273.15   0.14
20100202  590.0     0.24
20100203  810.0     0.29
20100204  1090.0    0.36
20100205  1370.0    0.42
20100206  3260.0    0.75
*****

```

* GAP - VOLUMETRIC HEAT CAPACITY

```

*****
20100251  273.15   5.1
20100252  3260.0   5.4
*****

```

* ZIRCALOY-4 - THERMAL CONDUCTIVITY FROM MATPRO

```

*****
20100301  300.0     12.7
20100302  380.4     13.6
20100303  469.3     14.6
20100304  577.6     15.8
20100305  685.9     17.3
20100306  774.8     18.4
20100307  872.0     19.8
20100308  973.2     21.8
20100309  1073.2    23.2
20100310  1123.2    25.4
20100311  1152.3    24.2
20100312  1232.2    25.5
20100313  1331.2    26.6
20100314  1404.2    28.2
20100315  1576.2    33.0
20100316  1625.2    36.7
20100317  1755.2    41.2
20100318  2273.2    55.0
*****

```

* ZIRCALOY-4 VOLUMETRIC HEAT CAPACITY FROM MATPRO

```

*****
20100351  300.0     1.841E6
20100352  400.0     1.978+6
20100353  640.0     2.168E6
20100354  1090.0    2.456E6
20100355  1093.0    3.288E6
20100356  1113.0    3.865E6
20100357  1133.0    4.028E6
20100358  1153.0    4.709E6
20100359  1173.0    5.345E6
20100360  1193.0    5.044E6
20100361  1213.0    4.054E6
20100362  1233.0    3.072E6
20100363  1243.0    2.332E6
20100364  3000.0    2.332E6
*****

```

* S-STEEL - THERMAL CONDUCTIVITY

```

*****
20100401  273.15    12.98
20100402  1199.82   25.1
*****

```

* S-STEEL - VOLUMETRIC HEAT CAPACITY

```

*****
20100451  273.15    3.83E6
20100452  366.5     3.93E6
20100453  477.59    4.190E6
*****

```

20100454	588.59	4.336E6
20100455	699.82	4.504E6
20100456	810.93	4.639E6
20100457	922.04	4.773E6
20100458	1144.26	5.076E6
20100459	1477.59	5.376E6
20100460	1477.59	5.541E6

 * INCONEL-600 - THERMAL CONDUCTIVITY

20100601	366.5	13.85
20100602	477.6	15.92
20100603	588.7	18.17
20100604	700.0	20.42
20100605	810.9	22.50
20100606	922.0	24.92
20100607	1033.2	26.83
20100608	1144.3	29.42
20100609	1477.6	36.06

 * INCONEL-600 - VOLUMETRIC HEAT CAPACITY

20100651	366.5	7.908+6
20100652	477.6	4.084+6
20100653	588.7	4.260+6
20100654	700.0	4.436+6
20100655	810.9	4.665+6
20100657	922.0	4.929+6
20100658	1033.2	5.105+6
20100659	1477.6	5.727+6

 * MAGNESIUM OXIDE - THERMAL CONDUCTIVITY

20100701	373.15	0.2451
20100702	422.04	0.2405
20100703	477.59	0.2352
20100704	533.15	0.2300
20100705	588.71	0.2249
20100706	644.26	0.2196
20100707	699.82	0.2143
20100708	755.37	0.2091
20100709	810.93	0.2039
20100710	866.48	0.1987
20100711	922.04	0.1934
20100712	977.59	0.1882
20100713	1033.15	0.1830
20100714	1088.71	0.1777
20100715	1144.26	0.1725
20100716	1199.82	0.1673
20100717	1255.37	0.1621
20100718	1310.93	0.1568
20100719	1366.48	0.1516
20100720	1422.04	0.1464
20100721	1477.59	0.1412
20100722	1533.15	0.1359
20100723	1588.71	0.1307
20100724	1644.26	0.1255
20100725	1699.82	0.1203
20100726	1755.37	0.1150
20100727	1810.93	0.1098
20100728	1866.48	0.1046
20100729	1922.04	0.0993

```

20100730 5000.00 0.0993
*****
* MAGNESIUM OXIDE - VOLUMETRIC HEAT CAPACITY
*****
20100731 373.15 2033.52
20100752 422.04 2004.59
20100753 477.59 1971.74
20100754 533.15 1938.87
20100755 588.71 1906.01
20100756 644.26 1873.15
20100757 699.82 1840.29
20100758 755.37 1807.43
20100759 810.93 1774.56
20100760 866.48 1741.70
20100761 922.04 1708.84
20100762 977.59 1675.96
20100763 1033.15 1643.11
20100764 1088.71 1610.25
20100765 1144.26 1577.39
20100766 1199.82 1544.53
20100767 1255.37 1511.67
20100768 1310.93 1478.80
20100769 1366.48 1445.94
20100770 1422.04 1413.08
20100771 1477.59 1380.22
20100772 1533.15 1347.35
20100773 1588.71 1314.49
20100774 1644.26 1281.63
20100775 1699.82 1248.77
20100776 1755.37 1215.90
20100777 1810.93 1183.04
20100778 1866.48 1150.18
20100779 1922.04 1117.32
20100780 5000.00 1117.32

```

```

*****
* NICHROME - THERMAL CONDUCTIVITY
*****

```

```

20100801 373.15 1.1163
20100802 1922.04 1.1163
20100803 5000.00 1.1163

```

```

*****
* NICHROME - VOLUMETRIC HEAT CAPACITY
*****

```

```

20100851 373.15 2180.80
20100852 1922.04 2180.80
20100853 5000.00 2180.80

```

```

*****
* GENERAL TABLE DATA
*****

```

```

* TABLE

```

```

* NUMBER DESCRIPTION -1.0

```

```

* 900 REACTOR POWER VS. TIME AFTER SCRAM

```

```

*****
20290000 POWER 510 1.0 36.0+6 L2-5
20290001 0.0 1.0
20290002 0.1 0.900689 * FROM L2-3 POSTTEST
20290003 0.2 0.74300
20290004 0.3 0.153171
20290005 0.4 0.110821
20290006 0.5 0.091625
20290007 0.6 0.083212

```

```

20290008 0.8 0.073556
20290009 1.0 0.044777
20290010 1.5 0.033089
20290011 2.0 0.059854
20290012 3.0 0.037265
20290013 4.0 0.055204
20290014 6.0 0.052085
20290015 8.0 0.049776
20290016 10.0 0.047947
20290017 15.0 0.044575
20290018 20.0 0.042176
20290019 30.0 0.038783
20290020 40.0 0.036348
20290021 60.0 0.031546
20290022 1.+5 0.001460 * FROM LTR LD-06-81-173

```

```

*****
* ENVIRONMENTAL HEAT LOSS BOUNDARY TEMPERATURE
*****

```

```

20293900 TEMP
20293901 0.0 311.00

```

```

*****
* REACTOR VESSEL ENVIRONMENTAL LOSS HEATXFER COEFFICIENT
*****

```

```

20294900 HTC-T
20294901 0.0 10.0

```

```

*****
* PUMP DATA

```

```

*****
* SINGLE PHASE HEAD CURVES

```

```

*****
* HEAD CURVE NO. 1

```

```

*****
1351100 1 1
1351101 0.000000E+00 1.403600+00
1351102 1.906100E-01 1.363600+00
1351103 3.896300E-01 1.318600+00
1351104 5.939600E-01 1.232800+00
1351105 7.902000E-01 1.133600+00
1351106 1.000000E+00 1.000000+00

```

```

*****
* HEAD CURVE NO.2

```

```

*****
1351200 1 2
1351201 0.000000E+00 -6.700000E-01
1351202 2.000000E-01 -5.000000E-01
1351203 4.000000E-01 -2.500000E-01
1351204 5.755400E-01 0.000000E+00
1351205 7.443200E-01 2.583000E-01
1351206 7.734800E-01 3.778000E-01
1351207 8.631300E-01 6.326000E-01
1351208 1.000000E+00 1.000000E+00

```

```

*****
* HEAD CURVE NO.3

```

```

*****
1351300 1 3
1351301 -1.000000E+00 2.472200E+00
1351302 -8.057400E-01 2.047400E+00
1351303 -7.069000E-01 1.831000E+00
1351304 -4.068300E-01 1.624000E+00
1351305 -2.001710E-01 1.470500E+00
1351306 0.000000E+00 1.403600E+00

```

```

* HEAD CURVE NO.4
*****
1351400      1      4
1351401     -1.000000E+00      2.472200E+00
1351402     -8.229700E-01      1.996900E+00
1351403     -6.333200E-01      1.589700E+00
1351404     -4.553400E-01      1.327900E+00
1351405     -2.710900E-01      1.194900E+00
1351406     -1.771600E-01      1.300500E+00
1351407     -9.073000E-02      1.015600E+00
1351408      0.000000E+00      9.342790E-01
*****
* HEAD CURVE NO.5
*****
1351500      1      5
1351501      0.000000E+00      2.500000E-01
1351502      2.000000E-01      2.300000E-01
1351503      4.000000E-01      3.400000E-01
1351504      4.113000E-01      2.769000E-01
1351505      5.976300E-01      4.584000E-01
1351506      7.934670E-01      6.892000E-01
1351507      1.000000E+00      1.000000E+00
*****
* HEAD CURVE NO.6
*****
1351600      1      6
1351601      0.000000E+00      9.342790E-01
1351602      9.109900E-02      8.229000E-01
1351603      1.865090E-01      8.963000E-01
1351604      2.717620E-01      8.750000E-01
1351605      4.553720E-01      8.433000E-01
1351606      5.744060E-01      8.355000E-01
1351607      7.409760E-01      8.466000E-01
1351608      7.666190E-01      8.469000E-01
1351609      8.714710E-01      8.838000E-01
1351610      1.000000E+00      1.000000E+00
*****
* HEAD CURVE NO.7
*****
1351700      1      7
1351701     -1.000000E+00     -1.000000E+00
1351702     -8.000000E-01     -6.000000E-01
1351703     -6.000000E-01     -3.000000E-01
1351704     -4.000000E-01     -5.000000E-02
1351705     -2.000000E-01      1.500000E-01
1351706      0.000000E+00      2.500000E-01
*****
* HEAD CURVE NO.8
*****
1351800      1      8
1351801     -1.000000E+00     -1.000000E+00
1351802     -8.000000E-01     -9.700000E-01
1351803     -6.000000E-01     -9.500000E-01
1351804     -4.000000E-01     -8.800000E-01
1351805     -2.000000E-01     -8.000000E-01
1351806      0.000000E+00     -6.700000E-01
*****
* SINGLE PHASE TORQUE DATA
*****
* TORQUE CURVE NO.1
*****
1351900      2      1

```


1351901	0.000000E+00	6.032000E-01
1351902	1.930000E-01	6.325000E-01
1351903	3.930000E-01	7.369000E-01
1351904	5.955200E-01	8.331000E-01
1351905	7.978200E-01	9.229000E-01
1351906	1.000000E+00	1.000000E+00

 * TORQUE CURVE NO.2

1352000	2	2
1352001	0.000000E+00	-6.700000E-01
1352002	4.000000E-01	-2.500000E-01
1352003	5.000000E-01	1.500000E-01
1352004	7.372550E-01	5.265860E-01
1352005	7.660490E-01	6.065940E-01
1352006	8.672300E-01	7.436600E-01
1352007	1.000000E+00	1.000000E+00

 * TORQUE CURVE NO.3

1352100	2	3
1352101	-1.000000E+00	1.984300E+00
1352102	-8.009600E-01	1.394000E+00
1352103	-6.063800E-01	1.097500E+00
1352104	-0.40686	0.82200
1352105	-1.992800E-01	6.648000E-01
1352106	0.000000E+00	6.032000E-01

 * TORQUE CURVE NO.4

1352200	2	4
1352201	-1.000000E+00	1.984300E+00
1352202	-8.223400E-01	1.830800E+00
1352203	-6.337100E-01	1.682400E+00
1352204	-4.585300E-01	1.557000E+00
1352205	-2.670230E-01	1.406200E+00
1352206	-1.761070E-01	1.387900E+00
1352207	-8.931000E-02	1.348100E+00
1352208	0.000000E+01	1.233610E+00

 * TORQUE CURVE NO.5

1352300	2	5
1352301	0.000000E+00	-4.500000E-01
1352302	4.000000E-01	-2.500000E-01
1352303	5.000000E-01	0.000000E+00
1352304	1.000000E+00	3.569000E-01

 * TORQUE CURVE NO.6

1352400	2	6
1352401	0.000000E+00	1.233610E+00
1352402	9.064300E-02	1.196500E+00
1352403	1.885690E-01	1.109600E+00
1352404	2.734700E-01	1.041600E+00
1352405	4.586690E-01	8.958000E-01
1352406	5.744800E-01	7.807000E-01
1352407	7.361600E-01	6.134000E-01
1352408	7.685200E-01	5.849000E-01
1352409	8.700570E-01	4.877000E-01
1352410	1.000000E+00	3.569000E-01

```

* TORQUE CURVE NO.7
*****
1352500 2 7
1352501 -1.000000E+00 -1.000000E+00
1352502 -3.000000E-01 -9.000000E-01
1352503 -1.000000E-01 -5.000000E-01
1352504 0.000000E+00 -4.500000E-01
*****
* TORQUE CURVE NO.8
*****
1352600 2 8
1352601 -1.000000E+00 -1.000000E+00
1352602 -2.500000E-01 -9.000000E-01
1352603 -8.000000E-02 -8.000000E-01
1352604 0.000000E+00 -6.700000E-01
*****
* TWO-PHASE MULTIPLIER DATA L 3-6 TEST DATA
*****
* HEAD CURVE
*****
1353000 0
1353001 0.000000E+00 0.000000E+00
1353002 1.000000E-01 0.000000E+00
1353003 2.000000E-01 1.000000E-01
1353004 3.000000E-01 2.000000E-01
1353005 3.500000E-01 3.000000E-01
1353006 4.000000E-01 6.000000E-01
1353007 5.000000E-01 6.000000E-01
1353008 6.000000E-01 6.000000E-01
1353009 7.000000E-01 6.000000E-01
1353010 8.000000E-01 5.000000E-01
1353011 9.000000E-01 3.000000E-01
1353012 1.000000E+00 0.000000E+00
*****
* TORQUE CURVE
*****
1353100 0
1353101 0.000000E+00 0.000000E+00
1353102 1.000000E-01 0.000000E+00
1353103 2.000000E-01 1.000000E-01
1353104 3.000000E-01 3.000000E-01
1353105 3.500000E-01 5.000000E-01
1353106 4.000000E-01 7.500000E-01
1353107 5.000000E-01 7.500000E-01
1353108 6.000000E-01 7.500000E-01
1353109 7.000000E-01 7.500000E-01
1353110 8.000000E-01 7.500000E-01
1353111 9.000000E-01 5.000000E-01
1353112 1.000000E+00 0.000000E+00
*****
* PUMP TWO-PHASE DIFFERENCE DATA
*****
* HEAD CURVE NO. 1
*****
1354100 1 1
1354101 0.000000E+00 1.000000+00
1354102 1.000000E+00 1.000000+00
*****
* HEAD CURVE NO. 2
*****
1354200 1 2
1354201 0.000000E+00 1.000000+00

```

```

1354202 1.000000E+00 1.000000+00
*****
* HEAD CURVE NO. 3
*****
1354300 1 3
1354301 -.000000E+00 -1.160000+00
1354302 -9.000000E-01 -1.240000+00
1354303 -8.000000E-01 -1.770000+00
1354304 -7.000000E-01 -2.360000+00
1354305 -6.000000E-01 -2.790000+00
1354306 -5.000000E-01 -2.910000+00
1354307 -4.000000E-01 -2.670000+00
1354308 -2.500000E-01 -1.690000+00
1354309 -1.000000E-01 -5.000000-01
1354310 0.000000E+00 0.000000+00
*****
* HEAD CURVE NO. 4
*****
1354400 1 4
1354401 -1.000000E+00 -1.160000+00
1354402 -9.000000E-01 -7.800000-01
1354403 -8.000000E-01 -5.000000-01
1354404 -7.000000E-01 -3.100000-01
1354405 -6.000000E-01 -1.700000-01
1354406 -5.000000E-01 -8.000000-02
1354407 -3.500000E-01 0.000000+00
1354408 -2.000000E-01 5.000000-02
1354409 -1.000000E-01 8.000000-02
1354410 0.000000E+00 1.100000-01
*****
* HEAD CURVE NO. 5
*****
1354500 1 5
1354501 0.000000E+00 0.000000E+00
1354502 2.000000E-01 -3.400000E-01
1354503 4.000000E-01 -6.500000E-01
1354504 6.000000E-01 -9.300000E-01
1354505 8.000000E-01 -1.190000E+00
1354506 1.000000E+00 -1.470000E+00
*****
* HEAD CURVE NO. 6
*****
1354600 1 6
1354601 0.000000E+00 1.100000E-01
1354602 1.000000E-01 1.300000E-01
1354603 2.500000E-01 1.500000E-01
1354604 4.000000E-01 1.300000E-01
1354605 5.000000E-01 7.000000E-02
1354606 6.000000E-01 -4.000000E-02
1354607 7.000000E-01 -2.300000E-01
1354608 8.000000E-01 -5.100000E-01
1354609 9.000000E-01 -9.100000E-01
1354610 1.000000E+00 -1.470000E+00
*****
* HEAD CURVE NO. 7
*****
1354700 1 7
1354701 -1.000000E+00 0.000000E+00
1354702 0.000000E+00 0.000000E+00
*****
* HEAD CURVE NO. 8
*****

```

```

1354800 1 8
1354801 -1.000000E+00 0.000000E+00
1354802 0.000000E+00 0.000000E+00
*****
* TORQUE CURVE NO. 1
*****
1354900 2 1
1354901 0.000000E+00 1.000000E+00
1354902 1.000000E+00 1.000000E+00
*****
* TORQUE CURVE NO. 2
*****
1355000 2 2
1355001 0.000000E+00 1.000000E+00
1355002 1.000000E+00 1.000000E+00
*****
* TORQUE CURVE NO. 3
*****
1355100 2 3
1355101 -1.000000E+00 1.984300E+00
1355102 -8.009600E-01 1.394000E+00
1355103 -6.063800E-01 1.097500E+00
1355104 -0.40686 0.82200
1355105 -1.992800E-01 6.648000E-01
1355106 0.000000E+00 6.032000E-01
*****
* TORQUE CURVE NO. 4
*****
1355200 2 4
1355201 -1.000000E+00 1.984300E+00
1355202 -8.223400E-01 1.830800E+00
1355203 -6.337100E-01 1.682400E+00
1355204 -4.585300E-01 1.557000E+00
1355205 -2.670230E-01 1.436200E+00
1355206 -1.761070E-01 1.387900E+00
1355207 -8.931000E-02 1.348100E+00
1355208 0.000000E+00 1.233610E+00
*****
* TORQUE CURVE NO. 5
*****
1355300 2 5
1355301 0.000000E+00 -4.500000E-01
1355302 4.000000E-01 -2.500000E-01
1355303 5.000000E-01 0.000000E+00
1355304 1.000000E+00 3.569000E-01
*****
* TORQUE CURVE NO. 6
*****
1355400 2 6
1355401 0.000000E+00 1.233610E+00
1355402 9.064300E-02 1.196500E+00
1355403 1.885690E-01 1.109600E+00
1355404 2.734700E-01 1.041600E+00
1355405 4.586690E-01 8.958000E-01
1355406 5.744800E-01 7.807000E-01
1355407 7.381600E-01 6.134000E-01
1355408 7.685200E-01 5.849000E-01
1355409 8.700570E-01 4.877000E-01
1355410 1.000000E+00 3.569000E-01
*****
* TORQUE CURVE NO. 7
*****

```

```

1355500      2              7
1355501      -1.000000E+00      -1.000000E+00
1355502      -3.000000E-01      -9.000000E-01
1355503      -1.000000E-01      -5.000000E-01
1355504      0.000000E+00      -4.500000E-01
*****
* TORQUE CURVE NO. 8
*****
1355600      2              8
1355601      -1.000000E+00      -1.000000E+00
1355602      -2.500000E-01      -9.000000E-01
1355603      -8.000000E-02      -8.000000E-01
1355604      0.000000E+00      -6.700000E-01
*****
* CONTROL VARIABLES
*****
* 001 - 007 LEVEL CALCULATORS
*****
* 001 STEAM GENERATOR LEVEL
*****
20500100  SGLVL      SUM      1.0      0.0      1
20500101  0.0      0.8288      VOIDF      500010000
20500102      0.8288      VOIDF      505010000
20500103      0.8288      VOIDF      507010000
20500104      0.6096      VOIDF      508010000
20500105      0.6096      VOIDF      510010000
20500106      0.6096      VOIDF      510020000
20500107      0.6096      VOIDF      510030000
*****
* 002 PRESSURIZER LEVEL
*****
20500200  PZRLVL      SUM      1.0      0.0      1
20500201  0.0      0.1815      VOIDF      415010000
20500202      0.1524      VOIDF      415020000
20500203      0.3967      VOIDF      415030000
20500204      0.5289      VOIDF      415040000
20500205      0.3967      VOIDF      415050000
20500206      0.1943      VOIDF      415060000
20500207      0.1029      VOIDF      415070000
20500208      0.1029      VOIDF      420010000
*****
* 003 REACTOR VESSEL LEVEL
*****
20500300  RXCLVL      SUM      1.0      0.0      1
20500301  0.0      1.566      VOIDF      255010000
20500302      0.843      VOIDF      250010000
20500303      0.559      VOIDF      245010000
20500304      0.559      VOIDF      240010000
20500305      0.375      VOIDF      232010000
20500306      0.2795      VOIDF      231010000
20500307      0.2795      VOIDF      230010000
20500308      0.2795      VOIDF      229010000
20500309      0.2795      VOIDF      228010000
20500310      0.2795      VOIDF      227010000
20500311      0.520      VOIDF      225010000
20500312      0.360      VOIDF      215010000
20500313      0.370      VOIDF      220010000
*****
* 004 REACTOR VESSEL DOWNCOMER 1 LEVEL
*****
20500400  DCMR1LVL      SUM      1.0      0.0      1
20500401  0.0      0.330      VOIDF      200010000

```

```

20500402      0.424      VOIDF      202010000
20500403      0.958      VOIDF      204010000
20500404      0.958      VOIDF      206010000
20500405      0.958      VOIDF      208010000
20500406      0.958      VOIDF      210010000
20500407      0.360      VOIDF      215010000
20500408      0.370      VOIDF      220010000
*****
* 005      LOOP SEAL      UPSTREAM      LEVEL
*****
20500500      LPSLUP      SUM      1.0      0.0      1
20500501      0.0      0.284175      VOIDF      120010000
20500502      0.356      VOIDF      118030000
20500503      0.689      VOIDF      118020000
20500504      0.498      VOIDF      118010000
*****
* 006      LOOP SEAL      DOWNSTREAM      LEVEL
*****
20500600      LPSLDWN      SUM      1.0      0.0      1
20500601      0.0      0.284175      VOIDF      120010000
20500602      0.2605      VOIDF      125010000
20500603      0.2285      VOIDF      130010000
20500604      0.2605      VOIDF      155010000
20500605      0.2285      VOIDF      160010000
*****
* 007      REACTOR VESSEL DOWNCOMER 2 LEVEL
*****
20500700      DCMR2LVL      SUM      1.0      0.0      1
20500701      0.0      0.330      VOIDF      280010000
20500702      0.424      VOIDF      282010000
20500703      0.958      VOIDF      284010000
20500704      0.958      VOIDF      286010000
20500705      0.958      VOIDF      288010000
20500706      0.958      VOIDF      290010000
20500707      0.360      VOIDF      215010000
20500708      0.370      VOIDF      220010000
*****
* 061-075      PRIMARY SYSTEM MASS CALCULATOR
*****
* 061      INTACT LOOP HOT LEG      MASS
*****
20506100      ILHLMASS      SUM      1.0      0.0      1
20506101      0.0      9.74648-2      RHO      100010000
20506102      0.1035956      RHO      105010000
20506103      3.03000-2      RHO      110010000
20506104      9.00000-2      RHO      112010000
20506105      5.70000-2      RHO      112020000
*****
* 062      STEAM GENERATOR PRIMARY MASS
*****
20506200      SGPRIASS      SUM      1.0      0.0      1
20506201      0.0      0.335000      RHO      114010000
20506202      0.136202      RHO      115010000
20506203      9.20496-2      RHO      115020000
20506204      9.20496-2      RHO      115030000
20506205      6.96412-2      RHO      115040000
20506206      6.96412-2      RHO      115050000
20506207      9.20496-2      RHO      115060000
20506208      9.20496-2      RHO      115070000
20506209      0.136202      RHO      115080000
20506210      0.335000      RHO      116010000
*****

```

```

* 063      PUMP SUCTION PIPING      MASS
*****
20506300  PMPSUASS  SUM      1.0      0.0      1
20506301  0.0      4.37000-2  RHO      118010000
20506302      4.62000-2  RHO      118020000
20506303      3.54406-2  RHO      118030000
20506304      4.81840-2  RHO      120010000
20506305      6.13000-2  RHO      125010000
20506306      1.89000-2  RHO      130010000
20506307      6.13000-2  RHO      155010000
20506308      1.89000-2  RHO      160010000
*****
* 064      INTACT LOOP COLD LEG      MASS
*****
20506400  ILCLMASS  SUM      1.0      0.0      1
20506401  0.0      9.90000-2  RHO      135010000
20506402      1.83732-2  RHO      140010000
20506403      6.33000-2  RHO      145010000
20506404      3.14844-2  RHO      150010000
20506405      9.90000-2  RHO      165010000
20506406      1.88124-2  RHO      170010000
20506407      3.54406-2  RHO      175010000
20506408      3.88642-2  RHO      176010000
20506409      7.30368-2  RHO      180010000
20506410      6.40340-2  RHO      185010000
*****
* 065      DOWNCOMER/LOWER PLENUM      MASS
*****
20506500  DCLPMASS  SUM      1.0      0.0      1
20506501  0.0      4.28000-2  RHO      200010000
20506502      4.28000-2  RHO      280010000
20506503      5.50000-2  RHO      202010000
20506504      5.50000-2  RHO      282010000
20506505      6.80180-2  RHO      204010000
20506506      6.80180-2  RHO      284010000
20506507      6.80180-2  RHO      206010000
20506508      6.80180-2  RHO      286010000
20506509      6.80180-2  RHO      208010000
20506510      6.80180-2  RHO      288010000
20506511      6.80180-2  RHO      210010000
20506512      6.80180-2  RHO      290010000
20506513      2.66400-1  RHO      215010000
20506514      2.92300-1  RHO      220010000
*****
* 067      AVERAGE/CORE UPPER PLENUM      MASS
*****
20506700  ACUPMASS  SUM      1.0      0.0      1
20506701  0.0      1.30000-1  RHO      225010000
20506702      3.86929-2  RHO      227010000
20506703      3.86929-2  RHO      228010000
20506704      3.86929-2  RHO      229010000
20506705      3.86929-2  RHO      230010000
20506706      3.86929-2  RHO      231010000
20506707      5.22596-2  RHO      232010000
20506708      8.38500-3  RHO      226010000
20506709      8.38500-3  RHO      226020000
20506710      9.85500-3  RHO      226030000
20506711      1.66023-1  RHO      240010000
20506712      1.66023-1  RHO      245010000
20506713      9.61020-2  RHO      250010000
20506714      1.28100-1  RHO      251010000
20506715      4.19680-1  RHO      255010000

```

```

*****
* 068      BROKEN LOOP HOT LEG  MASS(TO BREAK PLANE)
*****
20506800  BLHLMASS  SUM      1.0      0.0      1
20506801  0.0      5.55384-2  RHO      300010000
20506802  4.42532-2  RHO      305010000
20506803  6.68000-2  RHO      310010000
20506804  7.78800-3  RHO      315010000
20506805  1.72500-1  RHO      315020000
20506806  8.98000-2  RHO      315030000
20506807  8.98000-2  RHO      315040000
20506808  1.72500-1  RHO      315050000
20506809  2.00000-2  RHO      315060000
20506810  4.56000-2  RHO      315070000
20506811  1.98000-2  RHO      315080000
20506812  1.16500-1  RHO      380010000
20506813  2.30000-2  RHO      380020000
20506814  4.89000-2  RHO      380030000
*****
* 069      BROKEN LOOP COLD LEG  MASS(TO BREAK PLANE)
*****
20506900  BLCLMASS  SUM      1.0      0.0      1
20506901  0.0      4.75183-2  RHO      335010000
20506902  4.42532-2  RHO      340010000
20506903  4.43800-2  RHO      345010000
20506904  2.33600-2  RHO      350010000
20506905  2.79000-2  RHO      370010000
20506906  7.00000-2  RHO      370020000
20506907  1.16500-1  RHO      370030000
*****
* 070      PRESSURIZ ER          MASS
*****
20507000  PZERMMASS SUM      1.0      0.0      1
20507001  0.0      3.33500-3  RHO      400010000
20507002  3.33500-3  RHO      405010000
20507003  3.33500-3  RHO      405020000
20507004  6.84000-2  RHO      415010000
20507005  8.38000-2  RHO      415020000
20507006  2.24255-1  RHO      415030000
20507007  2.98987-1  RHO      415040000
20507008  2.24255-1  RHO      415050000
20507009  7.32000-2  RHO      415060000
20507010  1.42000-2  RHO      415070000
20507011  1.42000-2  RHO      420010000
*****
* 077      TOTAL COR E/UPPER PLE NUM MASS
*****
20507700  TCUPMASS  SUM      1.0      0.0      1
20507701  0.0      6.99977-3  RHO      233010000
20507702  6.99977-3  RHO      234010000
20507703  6.99977-3  RHO      235010000
20507704  6.99977-3  RHO      236010000
20507705  6.99977-3  RHO      237010000
20507706  9.45407-3  RHO      238010000
20507707  1.0      CNTRLVAR  067
*****
* 078      REACTOR VESSEL TOTAL MASS
*****
20507800  RCVEMASS  SUM      1.0      0.0      1
20507801  0.0      1.0      CNTRLVAR  65
20507802  1.0      CNTRLVAR  67
* 079      PCS TOTAL MASS

```



```

20507900 PCSTMASS SUM 1.0 0.0 1
20507901 0.0 1.0 CNTRLVAR 61
20507902 1.0 CNTRLVAR 62
20507903 1.0 CNTRLVAR 63
20507904 1.0 CNTRLVAR 64
20507905 1.0 CNTRLVAR 68
20507906 1.0 CNTRLVAR 69
20507907 1.0 CNTRLVAR 70
20507908 1.0 CNTRLVAR 78
*****
* 073-076 STEAM GENERATOR MASS CALCULATOR *****
*****
* 073 STEAM GENERATOR DOWNCOMER MASS *****
20507300 CGDCMASS SUM 1.0 0.0 1
20507301 0.0 1.02770 RHO 500010000
20507302 1.00850 RHO 505010000
20507303 1.00850 RHO 507010000
20507304 2.21070-1 RHO 508010000
20507305 1.41427-1 RHO 510010000
20507306 1.41427-1 RHO 510020000
20507307 1.41427-1 RHO 510030000
*****
* 074 STEAM GENERATOR BOILER MASS *****
20507400 CGBLMASS SUM 1.0 0.0 1
20507401 0.0 5.07675-1 RHO 515010000
20507402 5.07675-1 RHO 515020000
20507403 5.07675-1 RHO 515030000
20507404 5.07675-1 RHO 515040000
20507405 2.59406-1 RHO 515050000
20507406 2.41897-1 RHO 515060000
20507407 2.00114-1 RHO 520010000
*****
* 075 STEAM GENERATOR DOME MASS *****
20507500 SGDMMASS SUM 1.0 0.0 1
20507501 0.0 1.210513 RHO 525010000
20507502 1.162180 RHO 527010000
*****
* 076 STEAM GENERATOR TOTAL MASS *****
20507600 SGTLMASS SUM 1.0 0.0 1
20507601 0.0 1.0 CNTRLVAR 73
20507602 1.0 CNTRLVAR 74
20507603 1.0 CNTRLVAR 75
* 100 PRESSURE *****
*****
* 0510000 PZRLCNTL LEVEL CONTROL *****
* 0510001 -1.14 1.0 -1.0 0.0 1
*****
* * * * * RELAP END * * * * *

```

```

20507900  PCSTMASS  SUM      1.0      0.0      1
20507901  0.0          1.0      CNTRLVAR 61
20507902  1.0          1.0      CNTRLVAR 62
20507903  1.0          1.0      CNTRLVAR 63
20507904  1.0          1.0      CNTRLVAR 64
20507905  1.0          1.0      CNTRLVAR 68
20507906  1.0          1.0      CNTRLVAR 69
20507907  1.0          1.0      CNTRLVAR 70
20507908  1.0          1.0      CNTRLVAR 78
*****
* 073-076 STEAM GENERATOR MASS CALCULATOR
*****
* 073 STEAM GENERATOR DOWNCOMER MASS
20507300  CGDCMASS  SUM      1.0      0.0      1
20507301  0.0          1.02770  RHO      500010000
20507302  1.00850     1.00850  RHO      505010000
20507303  1.00850     1.00850  RHO      507010000
20507304  2.21070-1   2.21070  RHO      508010000
20507305  1.41427-1   1.41427  RHO      510010000
20507306  1.41427-1   1.41427  RHO      510020000
20507307  1.41427-1   1.41427  RHO      510030000
*****
* 074 STEAM GENERATOR BOILER MASS
*****
20507400  CGBLMASS  SUM      1.0      0.0      1
20507401  0.0          5.07675-1 RHO      515010000
20507402  5.07675-1   5.07675-1 RHO      515020000
20507403  5.07675-1   5.07675-1 RHO      515030000
20507404  5.07675-1   5.07675-1 RHO      515040000
20507405  2.59406-1   2.59406-1 RHO      515050000
20507406  2.41897-1   2.41897-1 RHO      515060000
20507407  2.00114-1   2.00114-1 RHO      520010000
*****
* 075 STEAM GENERATOR DOME MASS
*****
20507500  SGDMMASS  SUM      1.0      0.0      1
20507501  0.0          1.210513  RHO      525010000
20507502  1.162180    1.162180  RHO      530010000
*****
* 076 STEAM GENERATOR TOTAL MASS
*****
20507600  SGTLMASS  SUM      1.0      0.0      1
20507601  0.0          1.0      CNTRLVAR 73
20507602  1.0          1.0      CNTRLVAR 74
20507603  1.0          1.0      CNTRLVAR 75
*****
* 100 PRESSURIZED LEVEL CONTROL
*****
*0510000  PZRLCNTL  SUM      -1.0     0.0      1
*0510001  -1.14      1.0      CNTRLVAR 2
*****
* * * * * RELAP END CARD * * * * *

```

NRC FORM 335
(2-89)
NRCM-1102
5001-1007

U.S. NUCLEAR REGULATORY COMMISSION

BIBLIOGRAPHIC DATA SHEET

(See instructions on the reverse.)

1. REPORT NUMBER
(Assigned by NRC. Add Vol., Supp., Rev.
and Addendum Numbers, if any.)

NUREG/IA-0045

2. TITLE AND SUBTITLE

Assessment of RELAP5/MOD2 Using LOCE Large Break Loss-of-Coolant
Experiment L2-5

3. DATE REPORT PUBLISHED

MONTH YEAR
April 1992

4. PIN OR GRANT NUMBER

A4682

5. AUTHOR(S)

Lainsu Kao, Kuo-Shing Liang, Jeng-Lang Chiou, Lih-Yih Liao,
Song-Feng Wang, Yi-Bin Chen

6. TYPE OF REPORT

Technical

7. PERIOD COVERED (Inclusive Dates)

8. PERFORMING ORGANIZATION - NAME AND ADDRESS (If NRC, provide Division, Office or Region, U.S. Nuclear Regulatory Commission, and mailing address; if contractor, provide
name and mailing address.)

Institute of Nuclear Energy Research
P. O. Box 3, Lung-Tan 32500
Taiwan, Republic of China

9. SPONSORING ORGANIZATION - NAME AND ADDRESS (If NRC, type "Same as above"; if contractor, provide NRC Division, Office or Region, U.S. Nuclear Regulatory Commission
and mailing address.)

Office of Nuclear Regulatory Research
U. S. Nuclear Regulatory Commission
Washington, DC 20555

10. SUPPLEMENTARY NOTES

11. ABSTRACT (200 words or less)

This report documents the results and conclusions of the RELAP5/MOD2 code assessment in the analysis of LOCE Test L2-5. The objective of this assessment study is to provide systematic assessment of RELAP5/MOD2 Code relative to code development, code improvement and the enhancement of user guidelines.

12. KEY WORDS (DESCRIPTORS) (List words or phrases that will assist researchers in locating the report.)

ICAP Program, RELAP5/MOD2, L2-5

13. AVAILABILITY STATEMENT

Unlimited

14. SECURITY CLASSIFICATION

(This Page)
Unclassified

(This Report)

Unclassified

15. NUMBER OF PAGES

16. PRICE

THIS DOCUMENT WAS PRINTED USING RECYCLED PAPER

UNITED STATES
NUCLEAR REGULATORY COMMISSION
WASHINGTON, D.C. 20555

SPECIAL FOURTH-CLASS RATE
POSTAGE AND FEES PAID
USNRC
PERMIT NO. G-67

OFFICIAL BUSINESS
PENALTY FOR PRIVATE USE, \$300

120555139531 1 IANICI
US NRC-CADM
DIV FOIA & PUBLICATIONS SVCS
TPS-PDR-NUREG
P-211
WASHINGTON DC 20555